



OTTO VON GUERICKE  
UNIVERSITÄT  
MAGDEBURG

FACULTY OF  
PROCESS & SYSTEMS  
ENGINEERING

# **Investigation of integrated crystallization methods for the biocatalytic preparation of pharmaceutically relevant compounds and fine chemicals**

## **Dissertation**

zur Erlangung des akademischen Grades

**Doctor rerum naturalium**

**(Dr. rer. nat.)**

von

**M. Sc. Feodor Belov**

geb. am **26.03.1997** in **Moskau**

genehmigt durch die Fakultät für Verfahrens- und Systemtechnik der  
Otto-von-Guericke-Universität Magdeburg

Gutachter/innen:

Prof. Dr. Jan von Langermann

Prof. Dr. Udo Kragl

Prof. Dr. Annett Schallmeyer

Promotionskolloquium am **23.06.2025**

**Feodor Belov**

Investigation of integrated crystallization methods for the biocatalytic preparation of pharmaceutically relevant compounds and fine chemicals

Betreuer: Prof. Dr. Jan von Langermann

Eingereicht: 26.02.2025

Promotionskolloquium: 23.06.2025

**Otto-von-Guericke-Universität Magdeburg**

Fakultät für Verfahrens- und Systemtechnik

Institut für Chemie

**Arbeitskreis Biokatalytische Synthese**

Universitätsplatz 2, 39106 Magdeburg

**Feodor Belov**

Investigation of integrated crystallization methods for the biocatalytic preparation of pharmaceutically relevant compounds and fine chemicals

Supervisor: Prof. Dr. Jan von Langermann

**Otto von Guericke University Magdeburg**

Faculty of Process and System Engineering

Institute of Chemistry

**Biocatalytic Synthesis Group**

Universitätsplatz 2, 39106 Magdeburg

Submitted: 26.02.2025

Defense: 23.06.2025

**“Omne tulit punctum, qui miscuit utile dulci”**

*Horace, Ars Poetica*





# Abstract

Throughout the last three decades, the transition towards a sustainable and “green” approach to chemistry has been set as a future goal for many states and industrial players. In pursuit of this goal, the research on enzymes as biocatalysts and on enzymatically driven synthesis of industrially relevant compounds has intensified. During that time, first industrial-scale applications containing enzymatic reaction steps have been adopted by pharmaceutical and agrochemical manufacturers. Enzymatic catalysis possesses many advantages compared to conventional organic chemistry synthesis pathways, yet it also has its drawbacks, which often prevents enzymes from replacing their conventional counterparts in the manufacturing process. Nevertheless, some of those drawbacks, like product inhibitions and unfavorable reaction equilibria, can be circumvented by reaction engineering towards combining the reaction with a simultaneous separation process, removing the product to another phase. This process is called *in situ* product removal (ISPR). This work investigates ISPR approaches based on product removal to the solid phase, namely reactive crystallization, focusing on their application for the (chemo)enzymatic synthesis of the compound classes of chiral amines and chiral carboxylic acids.

In the first part, a previously developed concept for the reactive crystallization of chiral amines from transaminase-catalyzed reactions is reverted to a simple downstream processing concept to test its selectivity towards the high molecular weight amino products compared to low molecular weight amino donors. A model compound is crystallized selectively as an ammonium-carboxylate salt with very high purity and high yield recovered from the reaction mixtures. In the process, this crystallization technique is further adopted for another class of enzymatic reaction systems (amine dehydrogenases), broadening the application field for this separation method to other enzymatic methods of amine synthesis. The selectivity of this product crystallization system is tested under duress with varying crystallization parameters and surpluses of low molecular weight amino donors, showing robustness and reproducibility of high purities and yields of the crystallized amino product salts.

In the second part of this work, the amine product salt crystallization concept, previously developed for reactive crystallization of primary  $\alpha$ -chiral amines, is adopted for the transaminase-catalyzed synthesis of  $\beta$ -chiral amines. As a representative  $\beta$ -chiral amine model compound, (*R*)- $\beta$ -methylphenethylamine is chosen. A dynamic kinetic resolution of its precursor, 2-phenylpropanal, is performed, using a highly stereoselective transaminase as the enzymatic catalyst. Reactions, which are augmented by the described reactive amine product salt crystallization concept, show much higher yields, than the controls without reactive crystallization, reaching productivities of 16 g/(l·d) on preparative scale. Therefore, in the second part of this work, the concept for continuous reactive crystallization of amino product salts from transaminase-catalyzed reactions is proven to be applicable in the synthesis of  $\beta$ -chiral amines, a compound class represented among important pharmaceuticals.

In the third part of this work, a novel reactive crystallization concept is established for the (chemo)enzymatic dynamic kinetic resolution of chiral racemic compounds. On the basis of mandelic acid as a model substrate, enzymatically driven racemization (via a mandelate racemase) was successfully combined with diastereomeric salt crystallization. The resolution of the racemic mandelic acid towards (*R*)-mandelic acid was achieved via diastereomeric salt crystallization with an enantiopure ammonium counterion. On preparative scale, the developed concept led to yields of up to 60 % (based on the total amount of the racemate) and a very high enantiomeric excess of 95 % for the isolated mandelic acid enantiomer, underlining the enantioselectivity of the crystallization. Remarkably, this concept was realized in an aqueous medium, although the initial solubility of mandelic acid in water is fairly high (1 M).

# Zusammenfassung

In den letzten 30 Jahren wurde der Übergang zur nachhaltigen und „grünen“ Chemie zum Zukunftsziel vieler Staaten und Industriespieler deklariert. Als eines der Mittel zum Erreichen dieses Ziels, nahm unter anderem die Forschung am Einsatz von Enzymen als Biokatalysatoren und enzymatischer Synthese industriell relevanter Chemikalien deutlich zu. In dieser Zeit fanden die ersten Prozesse mit Einsatz von Enzymen ihre Anwendung im industriellen Großmaßstab in der pharmazeutischen und agrochemischen Industrie. Enzymatische Katalyse hat viele Vorteile gegenüber klassischen organisch-chemischen Syntheserouten. Dennoch hat sie auch Nachteile, welche den Einsatz von Biokatalysatoren anstatt klassischer Techniken verhindern. Manche dieser Nachteile, wie z.B. Produktinhibitionen und ungünstige Reaktionsgleichgewichtslagen, können mithilfe von *in situ* Produktentfernung (ISPR) überwunden werden, welche die Kombination der Reaktion mit einem simultanen Trennverfahren darstellt, wobei das Reaktionsprodukt in eine andere Phase entfernt wird. In dieser Arbeit werden ISPR-Methoden basierend auf der reaktiven Kristallisation von Reaktionsprodukten (Entfernung in die feste Phase) untersucht. Dabei liegt der Fokus auf der Anwendbarkeit dieser in (chemo)enzymatischen Reaktionssystemen zur Synthese von chiralen Aminen und chiralen Carboxylsäuren.

Im ersten Teil der Arbeit wird ein bereits entwickeltes Reaktivkristallisationskonzept für chirale Amine aus Transaminase-katalysierten Reaktionen in einen einfachen Separationsprozess umgewandelt, um dessen Selektivität für die hochmolekularen Aminoprodukte gegenüber niedermolekularen Aminodonoren zu untersuchen. Eine Modellverbindung wird selektiv als Ammonium-Carboxylat-Salz kristallisiert, wobei sehr hohe Reinheit und hohe Ausbeuten des Produktsalzes erzielt werden. Dabei wird das Konzept auch auf ein weiteres enzymatisches System, die Aminoaldehyddehydrogenasen, erweitert, was den Anwendungsbereich der Kristallisationsmethode in der chiralen Aminsynthese vergrößert. Die Selektivität der Kristallisation wird auf verschiedene Parametereinflüsse und Konzentrationsüberschuss der Aminodonoren geprüft. Hierbei zeigt das Kristallisationskonzept Beständigkeit und Reproduzierbarkeit, sowie hohe Reinheit und Ausbeuten der kristallisierten Aminoproduktsalze.

Im weiteren Verlauf dieser Arbeit wird das Reaktivkristallisationskonzept, welches ursprünglich für primäre  $\alpha$ -chirale Amine entwickelt worden ist, auf die Transaminase-katalysierte Synthese von  $\beta$ -chiralen Aminen angewandt. Als  $\beta$ -chirale Modellverbindung wird dabei (*R*)- $\beta$ -Methylphenethylamin durch eine dynamisch-kinetische Racematspaltung aus 2-Phenylpropanal mittels einer stereoselektiven Transaminase hergestellt. Reaktionen, welche mit dem Reaktivkristallisationskonzept von Aminoproduktsalzen kombiniert werden, erzielen deutlich höhere Produktausbeuten, als Kontrollversuche ohne Kristallisation, und Produktivitäten von bis zu 16 g/(L·d) im präparativen Maßstab. Demnach wird im zweiten Teil dieser Arbeit die Anwendung des Konzepts der selektiven kontinuierlichen Reaktivkristallisation von Aminoproduktsalzen aus Transaminase-katalysierten

Reaktionen auf die Stoffklasse der  $\beta$ -chiralen Amine übertragen, wessen Vertreter unter wichtigen Pharmazeutika vorzufinden sind.

Als letzter Teil dieser Arbeit wird ein neu erarbeitetes Reaktivkristallisationskonzept vorgestellt, welches durch Kombination von enzymatischer Racemisierung und diastereomerer Salzkristallisation eine neue Route zur dynamisch-kinetischen Racematspaltung bietet. Mandelsäure, welche als racemische Modellverbindung festgelegt wurde, wird kontinuierlich durch das Enzym Mandelatracemase racemisiert und parallel wird (*R*)-Mandelsäure mit einem enantiomerenreinen Ammoniumgegenion als diastereomeres Salz herauskristallisiert. So wird im präparativen Maßstab eine Ausbeute von 60 % (bezogen auf die gesamte Racematstoffmenge) und ein sehr hoher Enantiomerenüberschuss der isolierten (*R*)-Mandelsäure von 95 % erreicht, was die Enantioselektivität des Prozesses unterstreicht. Dabei ist bemerkenswert, dass der Vorgang im wässrigen Medium abläuft und solch hohe Ausbeuten trotz der hohen Löslichkeit von reiner Mandelsäure in Wasser (1 M) aufzeigt.

# Abbreviations

<b>1PEA</b>	1-Phenylethylamine	<b>HFCS</b>	High-fructose corn syrup
<b>2BPA</b>	2-Biphenylcarboxylic acid	<b>HIV</b>	Human immunodeficiency virus
<b>2DPPA</b>	2,2-Diphenylpropionic acid	<b>IPA</b>	Isopropylamine
<b>25CNA</b>	2-Chloro-5-nitrobenzoic acid	<b>IRED</b>	Imine reductase
<b>3D</b>	Three-dimensional	<b>IScPR</b>	<i>In situ</i> co-product removal
<b>3DPPA</b>	3,3-Diphenylpropionic acid	<b>ISPC</b>	<i>In situ</i> product crystallization
<b>34CA</b>	3,4-Dichlorobenzoic acid	<b>ISPR</b>	<i>In situ</i> product removal
<b>4BPA</b>	4-Biphenylacetic acid	<b>IUBMB</b>	International Union of Biochemistry and Molecular Biology
<b>43CNA</b>	4-Chloro-3-nitrobenzoic acid		Kinetic resolution
<b>AADH</b>	Amino acid dehydrogenase		
<b>ACE</b>	Angiotensin converting enzyme	<b>KR</b>	
<b>ADH</b>	Alcohol dehydrogenase	<b>LE-AmDH-v1</b>	L-lysine dehydrogenase from <i>Geobacillus stearothermophilus</i> F137A mutant
<b>ADP</b>	Adenosine diphosphate		
<b>ADPE</b>	2-Amino-1,2-diphenylethanol	<b>MA</b>	Mandelic acid
<b>AmDH</b>	Amine dehydrogenase	<b>MAO</b>	Monoamine oxidase
<b>AMP</b>	Adenosine monophosphate		
<b>API</b>	Active pharmaceutical ingredient	<b>MIO</b>	3,5-dihydro-5-methyldiene-4H-imidazol-4-one
<b>ATA</b>	Amine transaminase		
<b>ATP</b>	Adenosine triphosphate	<b>β-MPEA</b>	β-Methylphenethylamine
<b>BPA</b>	Biphenyl-4-carboxylic acid	<b>NAD<sup>+</sup>/NADH</b>	Nicotinamide adenine dinucleotide
<b>CAL-B</b>	<i>Candida antarctica</i> lipase B	<b>NADP<sup>+</sup>/NADP</b>	Nicotinamide adenine dinucleotide phosphate
<b>CR</b>	Chiral resolution	<b>H</b>	NADH-oxidase
<b>DKR</b>	Dynamic kinetic resolution	<b>NO<sub>x</sub></b>	1-
<b>DNA</b>	Deoxyribonucleic acid	<b>PCPA</b>	Phenylcyclopentanecarboxylic acid
<b>DPAA</b>	Diphenylacetic acid		
<b>DPEN</b>	1,2-Diphenylethanediamine	<b>PFA</b>	5-Phenyl-2-furoic acid
<b>E<sub>A</sub></b>	Activation energy	<b>PGA</b>	Penicillin G acylase
<b>EC</b>	Enzyme commission	<b>PLP</b>	Pyridoxal 5'-phosphate
<b>ee</b>	Enantiomeric excess	<b>PMP</b>	Pyridoxamine 5'-phosphate
<b>e.g.</b>	Example given		
<b>EI</b>	Enzyme-inhibitor complex	<b>RNA</b>	Ribonucleic acid
<b>EP</b>	Enzyme-product complex	<b>Rpo-ATA</b>	ATA from <i>Ruegeria pomeroyi</i>
<b>er</b>	Enantiomeric ratio		
<b>ES</b>	Enzyme-substrate complex	<b>TPEA</b>	1,2,2-Triphenylethylamine
<b>ESI</b>	Enzyme-substrate-inhibitor complex	<b>TTQ</b>	Tryptophan
<b>FAD/FADH<sub>2</sub></b>	Flavin adenine dinucleotide		tryptophylquinone
<b>FDH</b>	Formate dehydrogenase		
<b>GABA</b>	γ-aminobutyric acid		
<b>GDH</b>	Glucose dehydrogenase		

# Table of Contents

Abstract.....	v
Zusammenfassung .....	vii
Abbreviations .....	ix
Table of Figures .....	xii
Table of Tables.....	xiii
1. Introduction.....	1
1.1 Catalysis and biocatalysis.....	1
1.2 Enzymes: Classification, structural elements and their function.....	2
1.3 Advantages and disadvantages of enzymatic catalysis .....	8
1.4 Enzyme inhibition.....	10
1.5 Chirality and optically active compounds.....	12
1.5.1 Resolutions of stereoisomers: classical, kinetic and dynamic kinetic resolutions .....	14
1.6 Chiral amines.....	16
1.7 Chemical synthesis of amines .....	17
1.8 Enzymatic amine synthesis .....	21
1.8.1 Transaminases.....	22
1.8.2 Amine dehydrogenases.....	26
1.9 Beta-chiral amines .....	28
1.10 Isomerases, racemases, mandelate racemase.....	30
1.11 Circumvention of limitations in enzymatic catalysis.....	31
1.11.1 Enzyme engineering.....	32
1.11.2 Le Chatelier's principle .....	33
1.11.3 Enzymatic cascades.....	33
1.11.4 Reaction engineering towards <i>in situ</i> product removal (ISPR) and <i>in situ</i> co-product removal (IScPR).....	34
1.12 Crystallization as a separation process.....	38
1.12.1 <i>In situ</i> product crystallization (ISPC).....	44
1.12.2 ISPC of amines .....	46
1.12.3 Crystallization and ISPR approaches for the production of enantiopure mandelic acid.....	47
2. Objectives of this work.....	49
3. Case study I: Crystallization for selective post-reaction downstream processing of amines from enzymatic reactions.....	51

4. Case study II: Broadening the product scope of pharmaceutically relevant amine classes for reactive crystallization .....	57
5. Case study III: Combining diastereomeric salt crystallization with enzymatic racemization for the resolution of chiral carboxylic acids .....	63
6. Conclusion and Outlook .....	67
Bibliography .....	71
List of publications .....	87
Appendix .....	88
Publication 1: Crystallization-based downstream processing of $\omega$ -transaminase- and amine dehydrogenase-catalyzed reactions .....	89
Publication 2: Crystallization Assisted Dynamic Kinetic Resolution for the Synthesis of ( <i>R</i> )- $\beta$ -Methylphenethylamine .....	103
Publication 3: Crystallization-integrated mandelate racemase-catalyzed dynamic kinetic resolution of racemic mandelic acid .....	113
Ehrenerklärung .....	123
Declaration of Honor .....	124

# Table of Figures

<b>Figure 1</b> Activation energy comparison for catalytic reactions .....	1
<b>Figure 2</b> Subdivision of protein structure types .....	4
<b>Figure 3</b> Enzymatic catalytic cycle following the induced fit theory .....	5
<b>Figure 4</b> The catalytic triade of a serine protease .....	6
<b>Figure 5</b> Examples of organic cofactors .....	7
<b>Figure 6</b> Different enzyme inhibition mechanisms .....	10
<b>Figure 7</b> CIP-rule and Fischer projection for chiral molecules .....	12
<b>Figure 8</b> Exemplary stereochemical configuration of diastereomers .....	13
<b>Figure 9</b> Principles of kinetic and dynamic kinetic resolutions .....	14
<b>Figure 10</b> Activation energy profile of an enzymatic kinetic resolution .....	15
<b>Figure 11</b> Chiral amines in important pharmaceuticals .....	16
<b>Figure 12</b> Enantiomers of thyroxine and thalidomide in comparison .....	17
<b>Figure 13</b> Classical chemical synthesis routes towards amines .....	19
<b>Figure 14</b> Main asymmetric chemical synthesis routes for chiral amines .....	20
<b>Figure 15</b> Different enzyme classes for stereoselective chiral amine synthesis .....	21
<b>Figure 16</b> Mechanism of transaminase-catalyzed reactions .....	23
<b>Figure 17</b> Examples of the industrial application of transaminases .....	26
<b>Figure 18</b> Mechanism and cofactor regeneration of amine dehydrogenases .....	28
<b>Figure 19</b> Examples for $\beta$ -chiral amines as pharmaceuticals .....	29
<b>Figure 20</b> Synthesis pathways for obtainment of $\beta$ -chiral amines .....	29
<b>Figure 21</b> Mechanism of mandelate racemase from <i>Pseudomonas putida</i> .....	31
<b>Figure 22</b> Types of enzymatic cascades .....	34
<b>Figure 23</b> Selection of ISPR separation methods .....	35
<b>Figure 24</b> ISPR configurations and operation modes .....	36
<b>Figure 25</b> Different nucleation models .....	40
<b>Figure 26</b> Binary phase diagrams for a two-component system .....	41
<b>Figure 27</b> Ternary phase diagrams for a three-component system .....	43
<b>Figure 28</b> Ternary phase diagrams for racemic mixtures .....	43
<b>Figure 29</b> Examples for direct, salt and compound ISPC .....	45
<b>Figure 30</b> Concept of salt ISPC for the asymmetric synthesis of chiral amines .....	47
<b>Figure 31</b> Concept of diastereomeric salt crystallization .....	48
<b>Figure 32</b> Counterions for ( <i>S</i> )-1-phenylethylamine salt crystallization .....	53
<b>Figure 33</b> Phase diagram of the IPA-( <i>S</i> )-1PEA-43CNA salt pair .....	55
<b>Figure 34</b> Transaminase-catalyzed DKR-synthesis of $\beta$ -chiral amines .....	57
<b>Figure 35</b> The influence of oxygen and light on the formation of acetophenone .....	58
<b>Figure 36</b> Screening for inhibitions and beneficial counterion concentrations .....	60
<b>Figure 37</b> Yields and enantiomeric excesses of the DKR-based mandelate crystallization experiments .....	66



# Table of Tables

<b>Table 1</b> Classification of enzymes .....	3
<b>Table 2</b> Seven crystal systems and their defining properties .....	39
<b>Table 3</b> Solubility screening of ammonium salts for post-reaction ( <i>S</i> )-1-phenylethylamine salt crystallization .....	53
<b>Table 4</b> Crystallization yields and purities of the preparative-scale enzymatic synthesis of 1-phenylethylamine .....	55
<b>Table 5</b> Amino donor and product salt solubilities for chosen counterions .....	59
<b>Table 6</b> Yields and enantiomeric excesses of the preparative-scale $\beta$ -methylphenethylamine synthesis .....	60
<b>Table 7</b> Solubility screening of the diastereomeric mandelate salt pairs .....	64
<b>Table 8</b> Results of the diastereomeric crystallization screening of potential resolving agents for racemic mandelic acid .....	65



# 1. Introduction

## 1.1 Catalysis and biocatalysis

Chemical reactions require a certain amount of energy to occur. According to the Arrhenius equation, the minimum amount of energy required for a reaction is called activation energy ( $E_A$ ). Without providing this amount of activation energy, the reaction encounters a thermodynamic barrier and cannot proceed. Naturally, for some reactions the activation energy can be quite high, hindering conventional synthesis.<sup>1-4</sup> A common way to provide the needed activation energy is to elevate the reaction temperature, thus essentially flooding the reaction system with energy from the outside. However, although it is an efficient method to circumvent this thermodynamic barrier, not all substances may remain stable and intact with rising temperatures, leading to unwanted by-products and side reactions. Thus, another approach may be chosen, lowering the required reaction energy. This is achieved by the process called catalysis. A catalyst is, per definition, a substance, which modifies the transition state of the reaction by forming a complex with the reaction substrates, thus lowering the activation energy. After the reaction is finished, the reaction product dissociates from the catalyst, returning it to the reaction system in an unchanged form. Thus, a catalyst cannot be consumed during the reaction.<sup>5</sup> Although it alters the activation energy of a reaction system, a catalyst does not alter the energies of the reaction substrates and products, meaning, that the reaction equilibrium is not altered as well (see Figure 1 I.). Consequently, a catalyst simply accelerates the reaction, although, with no effect being induced in the reaction equilibrium, the reaction can still run both ways, it is reversible.

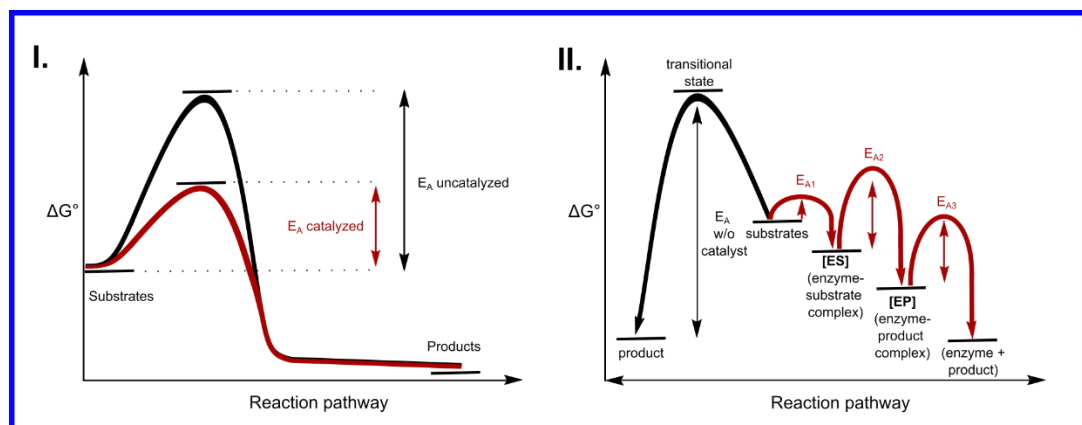


Figure 1: Comparison of activation energy for catalyzed and uncatalyzed reactions. I. The utilization of a catalyst (red curve) significantly decreases the required amount of activation energy ( $E_A$ ) to reach the transitional state of the reaction. II. Activation energy of the catalytic steps in enzymatic catalysis (red curve) compared to an uncatalyzed reaction (black curve). Adapted from Faber 2018.<sup>6</sup>

A special subdivision of catalysis is biocatalysis. As the name suggests, biocatalysis makes use of biocatalysts, biological structures naturally occurring in living organisms for catalysis of chemical reactions under their respective hosts physiological

conditions.<sup>6,7</sup> Most of the variety of biocatalysts is made up of catalytic proteins called enzymes (either in a free form or within living organisms, so-called whole cells)<sup>6</sup>, although other biocatalysts, such as ribozymes (catalytic RNA)<sup>8</sup> and deoxyribozymes (catalytic DNA)<sup>9</sup> exist. This work will focus on enzymes, thus only enzymes will be discussed in detail. Since enzymes catalyze reactions of the hosts metabolism within the confined space of a single cell, most of them were shaped by evolution to have high regio- and stereoselectivities, as well high chemoselectivity allowing for high substrate specificities. This means, that enzymes are highly specialized on the formation of specific reaction products, making them very efficient for their respective chemical reaction.<sup>6,10</sup> This, however, does not imply, that a certain enzyme is highly specialized on only one “natural” substrate. While this may be true for highly conserved enzymes from the primary metabolism (energy provision for life) of organisms, most enzymes of the secondary metabolism exhibit a varying level of substrate promiscuity towards natural, non-natural and even artificially made substrates.<sup>6</sup> Enzymes follow the general principle of catalysis, forming an enzyme-substrate complex with the reactants, thus lowering their respective activation energy. The formed product is then briefly bound in the enzyme-product complex, which then dissociates yielding the freed product and unchanged enzymatic catalyst. All three steps require a certain amount of activation energy, however it is usually much lower, than the  $E_A$  of the uncatalyzed reaction (see Figure 1 II.).<sup>6,10</sup>

## 1.2 Enzymes: Classification, structural elements and their function

Enzymes are usually classified in accordance with the guidelines of the Nomenclature Committee of the International Union of Biochemistry and Molecular Biology (IUBMB). The guidelines produce an international system of codification called the “Enzyme Commission numbers” (EC-numbers) assigned to each enzyme individually. EC-numbers consist of main classes and following subcategories. With this nomenclature the enzymes are sorted by their respective catalyzed reaction types. Those are shown in Table 1 with their corresponding reaction type. The first six main classes of EC-numbers show the original classification as it was first proposed, while the 7<sup>th</sup> class of translocases was added only in 2018.<sup>11</sup>

Table 1: Classification of enzymes according to IUBMB guidelines into EC-classes.

Enzyme Class	EC-number	Catalyzed reaction	Examples
<b>Oxidoreductases</b>	EC 1.X	Redox (oxidation and reduction) reactions	Oxygenases, peroxidases, dehydrogenases
<b>Transferases</b>	EC 2.X	Transfer of functional groups between molecules	Methyltransferases, acyltransferases, kinases, transaminases
<b>Hydrolases</b>	EC 3.X	Hydrolysis of bonds under consumption of water	Esterases, proteases
<b>Lyases</b>	EC 4.X	Breaking or formation of bonds without the consumption of water	Decarboxylases, dehydratases, aldolases
<b>Isomerases</b>	EC 5.X	Isomerization of molecules, incl. racemization	Racemases, epimerases
<b>Ligases</b>	EC 6.X	Formation of bonds under consumption of energy (simultaneous breakdown of ATP)	Chelatases, DNA-ligases
<b>Translocases</b>	EC 7.X	Transport of compounds and ions across membranes	Transporter proteins

The latest release of the EXPASY-Database contains 6843 active entries for classified enzymes. However, the classification only ranges up to the catalyzed reaction. Thus, if enzymes from certain organisms follow the same reaction pattern, they are grouped under the same EC-number.<sup>11</sup> That is why the respective entries contain listings of enzymes from another database called UniProt/SwissProt. The UniProt database is a general protein database classifying proteins (thus also enzymes) via their unique protein sequences. In UniProt, a simple search query of “enzyme” shows over 64000 reviewed enzyme sequences, while the number of unreviewed enzymatic sequences is far over 11 000 000 for this query only.<sup>12</sup> With the assumption, that there are over 2.1 million described eukaryotic species on earth<sup>13</sup>, while bacteria and viruses (also possessing enzymes) have not been counted, the real number of existing unique enzymes is much higher.

As already mentioned above, enzymes are proteins. Proteins per definition are macromolecules composed of amino acids which are chained together via peptide (amide) bonds. In living organisms, proteins perform a variety of functions, ranging from catalysis (enzymes) to structural integrity and compound transportation. As with many biological concepts, with all proteins the structure-function relationship is important, as only a certain spatial structure allows the protein to perform its function properly. Generally, protein structures can be subdivided into four categories (see Figure 2). The primary structure of a protein is the simple chain of amino acids, essentially a polyamide (Figure 2 I.). Primary chains can however assume different

forms, coordinated through forces of intramolecular attraction between the side chains of the amino acids and the polar elements of the peptide bonds. These are subdivided into two types of secondary protein structures: the  $\alpha$ -helices and  $\beta$ -sheets (see Figure 2 II.). Since the primary amino acid chain of a protein can easily encompass 300 - 400 amino acids, several secondary structures can be formed sequentially within one protein. Those in turn form the tertiary structure of the protein (see Figure 2 III.), which is again held together by intramolecular attraction, like hydrogen bonds,  $\pi$ - $\pi$ -stacking and Van der Waals forces, as well as through covalent bonds between amino acid side chains (disulfide bonds). However, sometimes proteins aggregate into a quaternary structure, consisting of several tertiary protein molecules as subunits (see Figure 2 IV.). Those quaternary structures (also referred to as protein complexes) can be homogenous (consisting only of one type of protein) or heterogenous (several different types of subunits). Both tertiary and quaternary structures of the proteins are functional within organisms, the formation of quaternary structures being dependent on the organism of origin of the protein. Both can complex metal ions and organic molecules within a single tertiary structure or the quaternary conglomerate.<sup>14</sup>

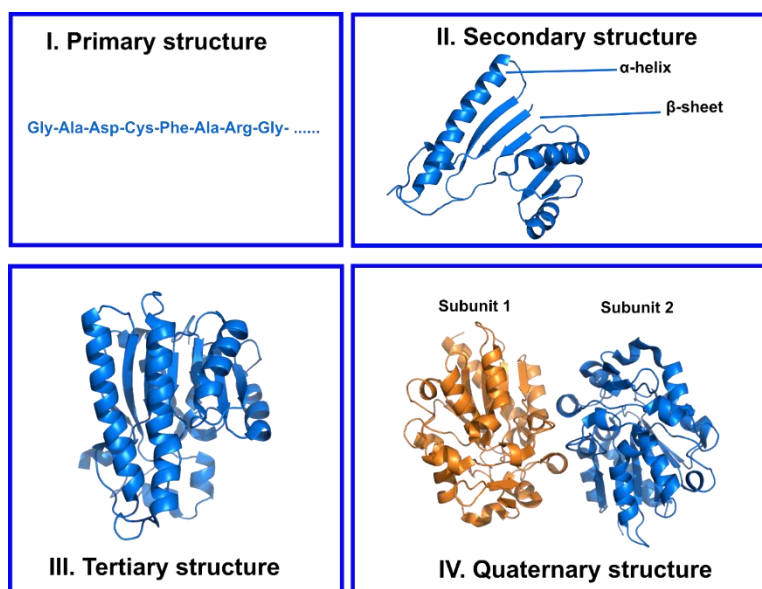


Figure 2: Subdivision of protein structure types. I. Primary structure, II. Secondary structure elements, III: Tertiary structure of a protein, IV. Quaternary structure. Adapted from Whitford 2005.<sup>14</sup>

Proper tertiary protein structure is achieved by a process called folding. It is estimated, that the functional tertiary structure, the so-called native form of a protein, represents a (local) minimum of the free energy level from all tertiary folding possibilities. However, since there are different minima in such a process, other (than the native) folding forms for the tertiary structure of the same protein can exist. Such misfolded forms usually are hindered in their function. Sometimes, such errors in folding, induced either by genetic mutations or outside factors, can cause disease in complex organisms.<sup>15-17</sup> That is why organisms even have specialized protein folding and “proofreading” machineries based on so-called chaperones. Those assist the folding and unfolding of tertiary structures both during and after protein synthesis.<sup>18</sup> Since within living cells an aqueous medium is predominant, most proteins are folded with

polar amino acid side-chains facing outwards, while hydrophobic non-polar side-chains face inward of the 3D-structure, greatly increasing the protein's stability.<sup>19</sup> However, through contact with non-optimal temperatures, pH-values or with organic solvents the tertiary structure is destabilized, those hydrophobic side chains can start facing outwards, prompting the molecule to quickly change its structure to a new free energy minimum. Through this, the functional structure is lost and the solubility in water greatly decreases. This state of the protein is called denatured.<sup>20,21</sup>

Within the enzyme, a region for substrate binding exists, which allows for the formation of the enzyme-substrate complex. This region also usually is the catalytic ground of the enzyme and is called an active site. Since only substrates with certain functional groups can form a catalyst-substrate complex with a specific enzyme (chemoselectivity), enzymatic catalysis can be described with the so-called “key-lock” principle, wherein both the substrates and the enzymatic active site follow the same geometry of their respective shape, allowing for an ideal fit for the reaction. The geometry of the active site hereby is generated by the residues of the amino acids forming the tertiary protein structure. However, since enzymes as proteins are dynamic structures, the “key-lock” principle was augmented in its description to yield the “induced fit” theory. It states, that an active site, while being specialized for a certain substrate, changes conformation by its binding, bending the side chains of its amino acids into shape. The same happens after product dissociation, restoring the active site to its pre-binding conformation (see Figure 3). This approach also explains the certain levels of substrate promiscuity within the borders of the same catalyzed reaction, which some enzymes are known to have.<sup>6,22,23</sup>

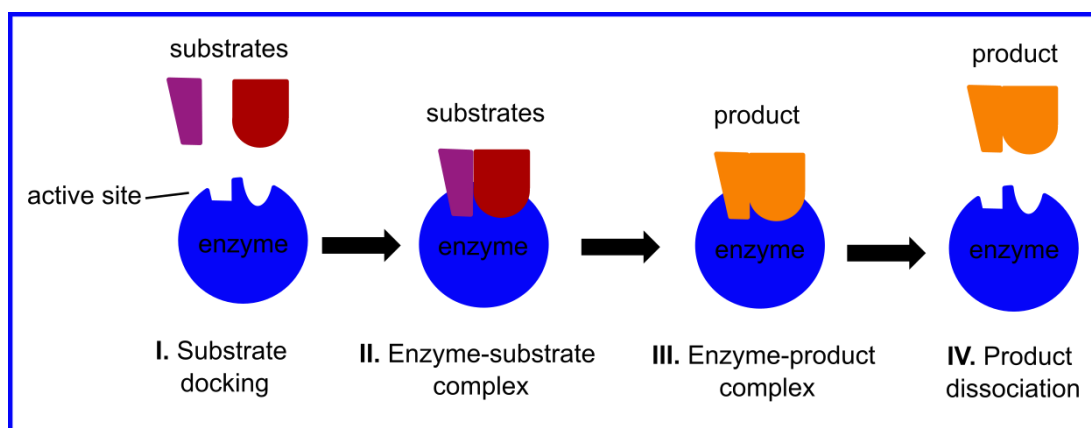


Figure 3: Visualization of an enzymatic catalytic cycle following the induced fit theory. The conformational change of the active site occurs for the binding of the substrates, forming the enzyme-substrate complex (I.-II.). After the catalytic step, the product dissociates from the active site, restoring its original shape and conformation (III.-IV.).

Only a small number of amino acid residues, mostly polar, act as the catalytic medium while the rest of active site-adjacent residues coordinate the substrate binding geometry and act as possible nucleophiles/electrophiles to accommodate possible charges of the substrate.<sup>6</sup> A prominent milestone, allowing for an insight into the mechanisms of enzymatic catalysis, was the discovery of the “catalytic triad”. The catalytic triad was first described for serine proteases (e.g. chymotrypsin), enzymes

catalyzing the hydrolysis of proteins.<sup>24</sup> Later, homologous catalytic motives were found predominantly in the enzyme classes of hydrolases and transferases (see Figure 4).<sup>6,25</sup>

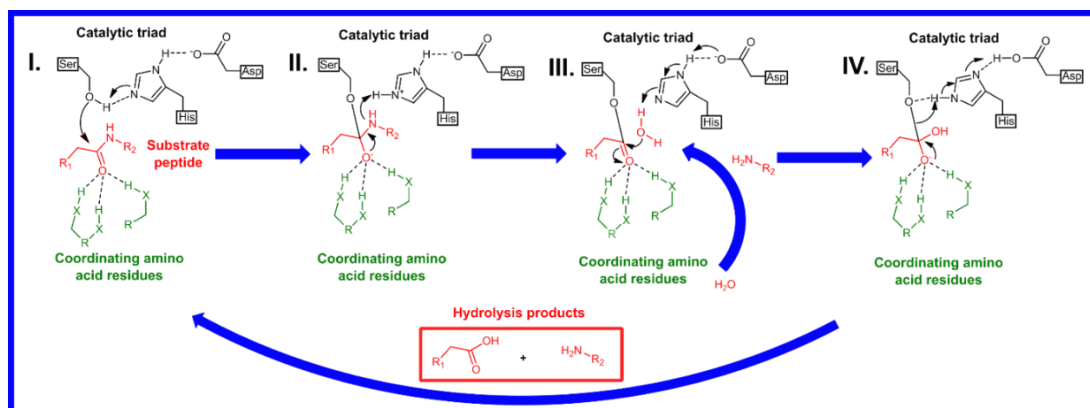


Figure 4: The catalytic triad of a serine protease (e.g. chymotrypsine). The mechanism of hydrolysis of a peptide (amide) bond is showcased in four separate steps through the charge relay within the catalytic triad. Adapted from *Wieczorek et al.* 2017<sup>26</sup> and *Rauwerdink et al.* 2015<sup>27</sup>.

A regional grouping of three amino acids allows for a creation of a charge relay system, which transfers electrons in the process of bond cleavage/formation. The nucleophile amino acid residue (serine) is polarized by the basic histidine, which in turn is coordinated and polarized by the sour aspartic acid. Hence, the activated serine nucleophile can attack the substrate, while the residual proton is accommodated by the histidine. Through the rearrangement of the peptide bond, the amine is cleaved, taking the previously deposited proton from the histidine. Then, the nucleophilic aspartic acid attacks the histidine residue's other electrophilic proton, rearranging the histidine's charge and turning it into a nucleophile, which in turn attacks a water molecule's proton. This prompts the oxygen of the water molecule to bind to the substrate-serine binding site. Through charge rearrangement, the serine is then cleaved and attacks the electrophilic proton of the histidine, which in turn returns its other electrophilic proton from the aspartic acid. This restores the catalytic triad to its starting form.<sup>6,24,25</sup> Depending on the enzyme class, mechanisms involving catalytic dyads (two active residues)<sup>28</sup> or tetrads (four active residues)<sup>29</sup> have also been described.

An alternative to the catalytic triad is a cofactor-based mechanism. Cofactors are small non-protein molecules or ions, that are required for the catalytic process of certain enzymes. They are divided into inorganic cofactors, which are represented by metal ions, and organic cofactors or coenzymes, which are represented by small organic molecules. Organic cofactors are further divided into prosthetic groups, which are permanently bound to the protein covalently or by intermolecular forces (e.g. heme group), and co-substrates, which are loosely associated to the enzyme and can dissociate and reattach at any time. Examples of organic cofactor molecules are shown in Figure 5.<sup>6,30</sup>



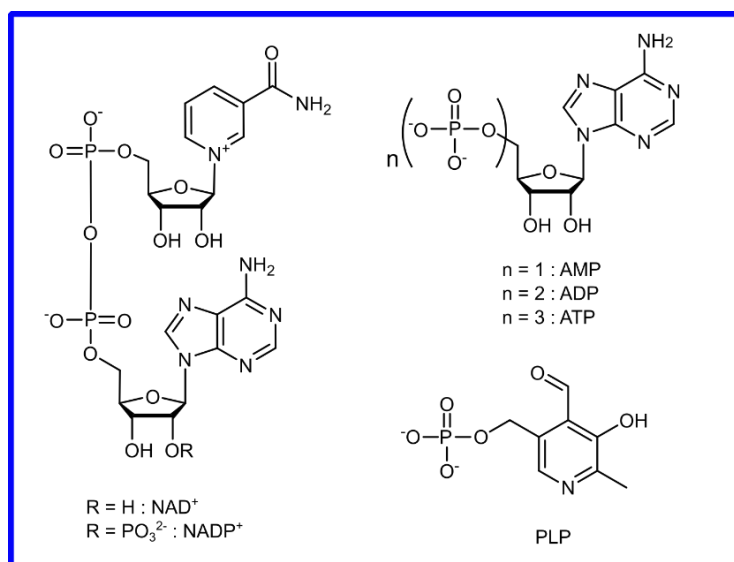


Figure 5: Examples of organic cofactors. The abbreviations mean the following: AMP/ADP/ATP – adenosine mono-/di-/triphosphate; PLP – pyridoxal phosphate; NAD<sup>+</sup>/NADP<sup>+</sup> – nicotianamide adenine dinucleotide/dinucleotide phosphate in its oxidized form.

Inorganic cofactors, such as metal ions, play a diverse role for enzyme activity. They augment the electron transfer and enzyme substrate complex stabilization, when they are a part of the active site. This happens due to the metal ion's ability to coordinate negative charges. However, this ability can also play a role in the stabilization of the enzymes tertiary structure while not participating directly in the catalytic process. Catalytically active metal ions, acting as Lewis acids or redox centers are also known.<sup>31,32</sup> Enzymatic structures accommodating different metal ions, ranging from simple alkaline earth metals, like Mg<sup>2+</sup> and finishing with heavy metals from the 4<sup>th</sup>-5<sup>th</sup> periods, like cobalt or molybdenum have been described in literature.<sup>31</sup>

Organic cofactors are also fairly common to be found in the active site or in its vicinity. A number of organic cofactors exist, covering different roles in the catalytic reactions of enzymes. As will be shown on the example of transaminases, cofactors like pyridoxal phosphate (PLP) can act as catalytic intermediates, transiently binding functional groups for transfer on other molecules, being regenerated to its original state after this process. Then again, cofactors like nicotianamide adenine dinucleotide (NAD<sup>+</sup>/NADH) or its phosphorylated form (NADP<sup>+</sup>/NADPH) act as electron donors or acceptors in enzymatically catalyzed redox reactions, thus also possessing an oxidized and a reduced form. If the enzymatic reaction requires additional activation energy, cofactors like adenosine triphosphate/diphosphate (ATP/ADP) commonly provide this energy through the hydrolysis of the pyrophosphate bond. Enzymes previous to cofactor binding are called apoenzyme, while enzymes with the bound cofactor are called holoenzyme.<sup>6,30,33</sup>

## 1.3 Advantages and disadvantages of enzymatic catalysis

Like any technique in chemical synthesis, the route using enzymatic catalysis has its advantages and disadvantages. Since enzymes exist in living organisms, one of their main advantages is their catalytic function in mild conditions. Enzymes usually have their catalytic optimum in aqueous media under the retainment of “physiological” conditions, such as narrow pH ranges of 5-8 (mostly pH 7) and temperature ranges of 20-40 °C. This has two subsequent advantages. Firstly, possibilities of side-reactions of the substrates and products, such as decompositions or rearrangements, are reduced. Secondly, mild reaction conditions combined with reaction processes in water reduce the environmental impact of those processes overall, contributing to sustainability. Although performing at low temperatures, the efficiency of enzymatic catalysis is very high. With reaction rates  $10^8$ - $10^{10}$ -fold higher than uncatalyzed reactions and employed catalyst loadings of 0.001-0.01 mol% (opposed to chemocatalyst loadings of 0.1-1 mol%), the efficiency of enzymatic catalysts can rival that of chemocatalysts quite comfortably. Then again, as previously mentioned, although enzymes possess high chemo- and regioselectivity, enzymes are known to show certain promiscuities in terms of their catalytic activity and specificity.<sup>34</sup> Literature describes three types of exhibited promiscuity, the first being condition promiscuity, allowing for the catalyzed reaction to occur in media not native for the enzyme (e.g. solvent other than water). Another possible variance in the enzyme’s activity is catalytic promiscuity, meaning the possibility of catalyzing different side reactions in addition to its main catalytic activity. Examples of the exploitation of such “accidental” catalytic side activities and even the intended induction of catalytic promiscuity have been also described in literature. The third type of catalytic deviation would be substrate promiscuity. Substrate promiscuity describes the phenomenon of possible (main) catalytic activity towards non-natural substrates, meaning that a range of different molecules can be accepted for the catalysis of the same reaction. Thus, substrate promiscuity allows for a certain degree of universal applicability of the same enzymatic catalyst to different substrates. All three promiscuity types combined elevate the universality factor of enzymes even further, allowing for some enzymes to be applied outside of their native conditions for catalysis of a broad substrate range, this fact, of course, being a major advantage.<sup>34,35</sup> All those advantages can then be combined with another major plus of enzymatic catalysis – its high stereoselectivity. Due to their biological origin, enzymes are composed of mainly L-amino acids (naturally most occurring form of amino acids in proteins), this fact already making them chiral catalysts. Adding the fact, that many biological processes also depend on only one enantiomer of a chiral compound, it becomes obvious, that the existence of a plethora of highly stereo- and enantiospecific enzymes in every organism is an evolutionary necessity. This pool of finely tuned biocatalysts can in turn be applied in asymmetric synthesis, since, depending on the organism, enzymes have been shown to exist for the catalysis of an overwhelming quantity of classic reactions of organic chemistry.<sup>6,10</sup>

Nevertheless, some advantages of enzymatic catalysis may also become its drawbacks. While mild reaction conditions may be environmentally sustainable, the changes in

those conditions may be critical to the enzyme's stability. Enzymes being proteins, an elevation of reaction temperature for the increase in reaction speed is risky beyond the 40 °C mark due to the risk of the enzyme's deactivation (e.g. through misfolding) or even denaturation of its tertiary structure and thus irreversible loss of catalytic activity. The same can be said about pH values, although exceptions exist in the form of enzymes from thermophilic or acidophilic organisms, which are naturally adapted to higher temperatures and/or pH values. Furthermore, while enzymes are highly stereoselective, this stereoselectivity only comes in one form. As naturally occurring proteins use L-amino acids as their backbone, an enzyme's other "enantiomer" consisting of D-amino acids is not obtainable, not allowing a simple change in chirality for the reaction products. Thus, another enzyme has to be found for synthesis of the product's other enantiomer. The stereopreference of an enzyme can usually only be modified through its artificial mutagenesis. While exhibiting substrate promiscuity, enzymes are known to be prone to inhibitions. For example, since a certain range of substrates can be bound in the active site of the enzyme, there is a possibility of binding a substrate, which cannot be converted by the enzyme. Such an inhibitor would then occupy the active site, blocking it for the desired substrate (competitive inhibition). The inhibition phenomena will be discussed in detail further. Finally, another disadvantage is the reliance on cofactors for some enzymes. Here, two factors come into play. Some organic cofactors can be unstable, e.g. ATP has a highly energetic yet unstable pyrophosphate bond and is prone to autohydrolyze into the more energetically balanced di- and monophosphate forms. Partially, such instability causes the second factor, namely the relatively high cost of organic cofactors, since those are difficult to replace, being essential to the enzyme's catalytic activity.<sup>6,10</sup>

A disputable point is the reliance of enzymes on water. While it is true, that enzymes are naturally specialized on reactions being performed in aqueous environments, in nature, plenty of enzymes are native to hydrophobic environments as well, e.g. bound to membranes. Hydrophobic substrates in organic synthesis possess very limited solubility in water, thus limiting substrate availability for a potential enzymatic reaction. Furthermore, enzymes have water molecules interspersed within their native tertiary structures, mediating hydrogen bonds and thus assisting in maintaining its stability. Nevertheless, it was found, that some enzymes require only trace amounts of water in their structure, sometimes referred to as "structural water" to remain catalytically active, while the remaining aqueous environment (so-called "bulk water") may be replaced by organic solvents.<sup>6</sup> A prominent example of such an enzyme is the lipase from *Candida antarctica* (CAL-B), of which plenty application examples in organic media exist throughout literature and industry.<sup>36,37</sup> As for the matter of substrate/product solubility, compromising and combinatorial approaches for enzymatic catalysis can be utilized. The former involves partially aqueous reaction media, which are obtained through addition of water-miscible organic solvents into the reaction mixture. With this approach, enzymes have been shown to tolerate fairly high percentages of organic solvents in their respective reaction media. For the latter, multiphasic systems have been adopted, combining an aqueous phase containing the enzymes with organic phases, accommodating the substrates and sometimes the products within the organic solvent layer, simultaneously benefiting product

separation. Enzymes were shown to survive on phase boundaries between organic and aqueous layers. In the matter of solvent choice for enzymatic reactions, the tolerance towards organic solvents has to be reviewed for each enzyme individually.<sup>6,10</sup>

## 1.4 Enzyme inhibition

As mentioned previously, enzymes are prone to several kinds of inhibition phenomena. An inhibitor for an enzyme can be defined as a molecule, that diminishes or eliminates the activity of an enzyme through binding to it. Several mechanisms of inhibition exist. They are divided into irreversible inhibition and reversible inhibition, while the reversible category also has several subcategories (see Figure 6).<sup>10,38</sup> As explained previously, following the “induced fit” theory, the substrate binds to an active site by being sterically positioned through intermolecular forces with the amino acid residues within the active site. However, if a molecule fitting into the active site was to covalently bind to one or several amino acid residues without the possibility to reverse this binding (e.g. through the proceeding reaction with the catalytic residue), then the active site is occupied and no reactions can proceed within the enzyme. Such a molecule, forming an irreversible covalent bond within the active site would then be called an irreversible inhibitor.<sup>39,40</sup>

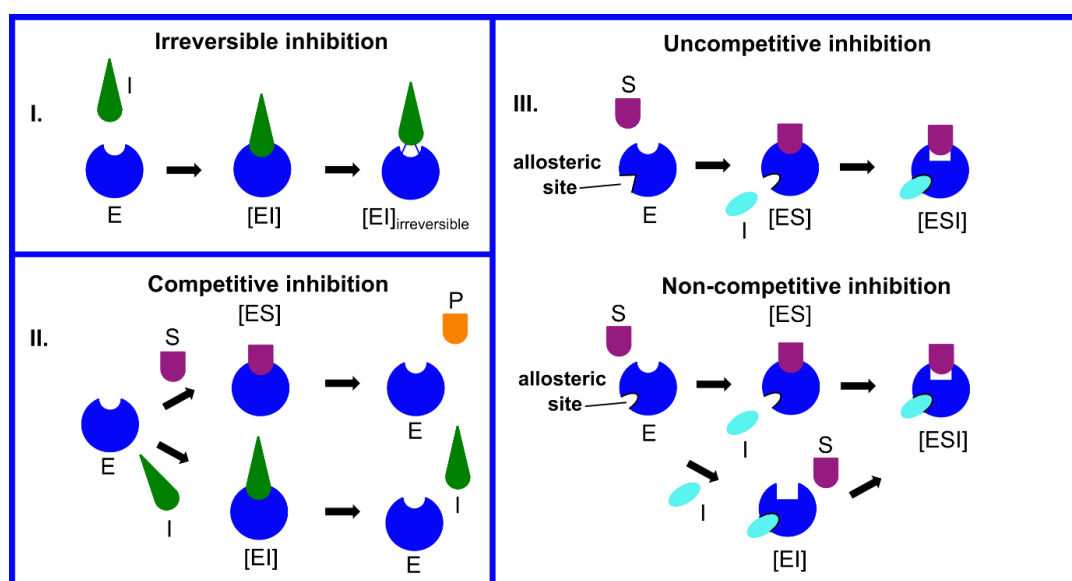


Figure 6: Graphical illustration of different enzyme inhibition mechanisms. **I.** Irreversible inhibition: An inhibitor is covalently irreversibly bound in the active site, not allowing further access to it for substrates. **II.** Competitive inhibition: The inhibitor competes with the substrate in the binding to the active site while not reacting with the enzyme itself. **III.** Allosteric inhibition: In uncompetitive inhibition, the allosteric site only becomes accessible to the inhibitor when the enzyme-substrate complex is formed. In non-competitive inhibition, the allosteric site can also be accessed by the inhibitor prior to substrate binding. As soon as the inhibitor is bound, the active site changes its conformation, impairing the reaction at the stage of an enzyme-substrate complex. E – enzyme, I – inhibitor, P – product, [ES] – enzyme-substrate complex, [EI] – enzyme-inhibitor complex, [ESI] – enzyme-substrate-inhibitor complex.

For reversible inhibition, as the name suggests, the inhibitor molecules only bind reversibly to the enzyme, impairing its function. Here, competitive and allosteric inhibition mechanisms exist. For competitive inhibition, the inhibitor is mostly a structurally similar molecule (possessing some degree of affinity to the active site) to the substrate, which cannot be converted to a product by the enzyme. Such a molecule then associates to the active site, occupying it and not allowing the real substrate to bind. With time, the competitive inhibitor then dissociates, freeing up the active site for the real substrate (reversible inhibition, see Figure 6 II.). This type of reversible inhibition thus slows the reaction not by altering the enzyme's reaction steps, but by competing with the substrate for binding at the active site. Thus, higher substrate concentrations are needed to statistically reach the same reaction velocities as with an uninhibited reaction.<sup>40,41</sup>

Opposed to competitive inhibition, allosteric inhibition does indeed alter the reaction steps of an enzyme by binding to the enzyme-substrate complex and not to an empty active site. With this type of reversible inhibition, an allosteric inhibitor binds to an allosteric site (distinctly other binding site than the active site), causing a conformational change within the enzyme-substrate complex, not allowing the reaction to proceed. Within allosteric inhibition, two mechanisms are distinguished: uncompetitive and non-competitive inhibitions (see Figure 6 III.) They vary in the mode of allosteric inhibitor binding. With uncompetitive inhibition, the inhibitor exclusively binds to the enzyme-substrate complex, thus not impairing the substrate binding at all. However, due to the deactivation of the enzyme-substrate complex, the velocity of the reaction is slowed (until dissociation of the inhibitor). Non-competitive inhibitors can bind to the allosteric site both when the active site is free (decrease in substrate binding affinity) and when it is occupied (deactivation of the enzyme-substrate complex).<sup>40,41</sup>

There is also another special type of reversible inhibition, called substrate or product inhibition, which can be observed in some enzyme classes (e.g. transaminases). Here, elevated concentrations of either the substrate or the product (or both) may influence the enzyme's activity. An exemplary explanation for the product inhibition would be for example, that due to similar structure, the product may act as a competitive inhibitor, when accumulated to a significant concentration. Exemplary for substrate inhibition would be the case, when multiple substrate molecules bind to the enzyme-substrate complex (due to high concentrations), thus not being able to be converted to a product.<sup>42-44</sup>

The mechanism of enzymatic inhibition is often exploited in pharmaceutical science, with over 100 different enzyme inhibitors being marketed.<sup>45</sup> The enzyme inhibitory market has been estimated to number 95 billion US dollars annually in 2007.<sup>46</sup> This is not unexpected since even though enzymes regulate almost all reactions in the human body, faulty enzymes also regulate reactions, that cause diseases, not even mentioning, that human pathogens have their own enzymes. Thus, enzymatic inhibitors can be found in therapy approaches ranging from high blood pressure (angiotensin-converting enzyme inhibitors – ACE inhibitors) to cancer therapy and treatment of HIV.<sup>45-48</sup>

## 1.5 Chirality and optically active compounds

Chirality is defined as a molecular property based on molecular asymmetry. Only when a molecule cannot be converted into itself by means of rotation or reflection in symmetry planes (asymmetry), but can be mirrored along its rotatory axis, it is considered chiral. Another term for chirality would be handedness. Said mirroring along its rotatory axis produces two enantiomers of a molecule. In practice, this means, that as soon a molecule assumes a non-planar three-dimensional form, it may produce enantiomers, if it shows asymmetry.<sup>49,50</sup> On the most widely spread example of a carbon atom, which forms 4 bonds and thus assumes a tetrahedral 3D-structure, that asymmetry is given only when all four bonds are formed with different substituents. Then the molecule can be mirrored along its rotatory axis, producing two enantiomers (see Figure 7), while the carbon atom acts as a so-called chirality center.

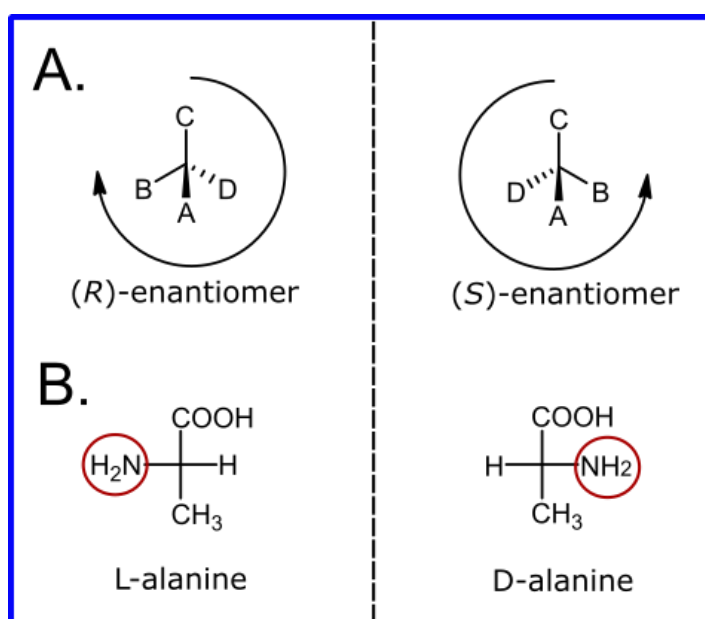


Figure 7: **A.** Two enantiomers of a molecule, formed from a quaternary substituted carbon atom. The nomenclature is determined by the CIP rule, placing A as highest priority and D as lowest. **B.** Two enantiomers of alanine in Fischer projection showing the nomenclature of the D-/L- enantiomeric nomenclature.<sup>50</sup>

The assignment of the correct nomenclature to the respective enantiomers is performed via the Cahn-Ingold-Prelog sequence rule (CIP rule). Here, possible substituents are sorted in a sequential priority. The substituent with the lowest priority is then positioned pointing away from the observer. If the priority of the remaining three substituents decreases clockwise, it constitutes an (*R*)-enantiomer, if it decreases counterclockwise, it is an (*S*)-enantiomer. Another version of stereochemical nomenclature used predominantly in sugars and amino acids is the D-/L- nomenclature based on their Fischer projection. Here, a molecule's D- or L- enantiomeric configuration is determined on the basis of its bottom placed stereocenter. If the higher prioritized substituent is facing right it constitutes a D-enantiomer, if it is facing left – an L-enantiomer (see Figure 7).<sup>51</sup>

The optical purity of a compound can be expressed via two different parameters – the enantiomeric excess (*ee*) and the enantiomeric ratio (*er*). Both show a degree of prevalence of one enantiomer over the other. Enantiomeric excess is calculated as the difference between the mole fractions (*x*) of both enantiomers in the mixture. The enantiomeric ratio is a quotient of the dominant enantiomer and the less dominant enantiomer. Both are interconvertible, as shown below (formula 1). A mixture of the two enantiomers in equal ratios is called a racemate. A racemate would have an *ee* of 0 and an *er* of 1.<sup>52</sup>

$$ee = \frac{x(R)-x(S)}{x(R)+x(S)} = \frac{er-1}{er+1} \quad er = \frac{x(R)}{x(S)} = \frac{1+ee}{1-ee} \quad (1)$$

Two enantiomers usually show the same physical properties and are only distinguishable by their optical characteristics of light polarization or by interaction with a chiral environment. However, a racemate can differ in its physical properties from a pure enantiomer, e.g. in solubility, melting point, density etc.<sup>53,54</sup> Another aspect to consider is the biological impact of the different enantiomers, which makes chirality especially important for pharmaceutical synthesis.<sup>55–57</sup>

If a molecule possesses more than one stereocenter, it can automatically produce two stereochemical variations at each stereocenter, increasing the number of optically active molecule variants (e.g. two stereocenters = 4 different stereochemical configurations). Such molecules, which are equal in constitution but different in stereochemical configuration are called diastereomers. Diastereomers usually consist of enantiomeric pairs (see Figure 8) and display different physical properties, thus allowing for separation methods based on those properties.<sup>58–61</sup>

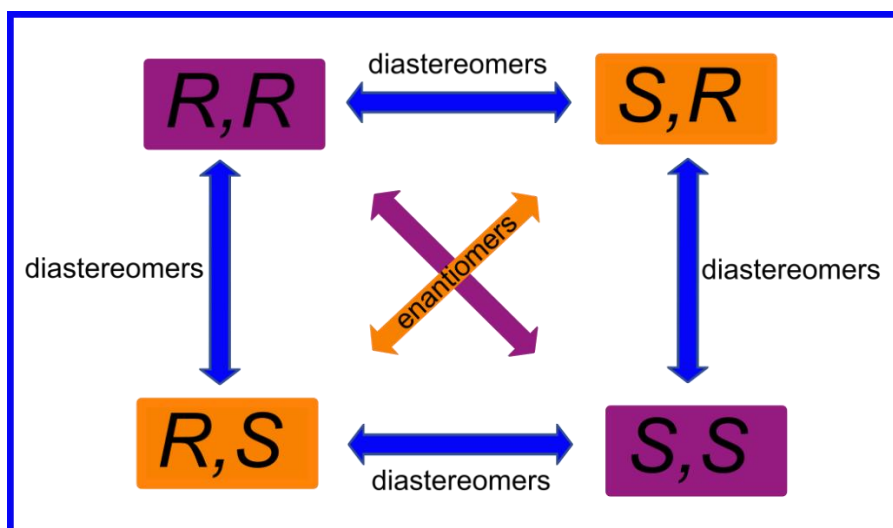


Figure 8: Exemplary stereochemical configuration of diastereomers with two stereocenters.

### 1.5.1 Resolutions of stereoisomers: classical, kinetic and dynamic kinetic resolutions

One of the broadly used pathways for obtainment of enantiopure compounds is called resolution. A racemic mixture is converted into a product by a resolving agent, which is stereoselective. Classical approaches are based on physical properties of the molecules in question, mostly involving chromatographic separation or diastereomeric crystallization (chiral resolution – CR).<sup>62,63</sup>

However, if a stereospecific catalyst (e.g. chemocatalyst or enzyme) is chosen as the resolving agent, the resolution is called a kinetic resolution (KR). Here, the catalyst converts both enantiomers of the racemic mixture at different reaction rates ( $k_R \gg k_S$ ). So, while over time one enantiomer is fully converted into the product with a total surplus, the other enantiomer remains essentially unchanged due to its very slow reaction rate (see Figure 9).<sup>64</sup>

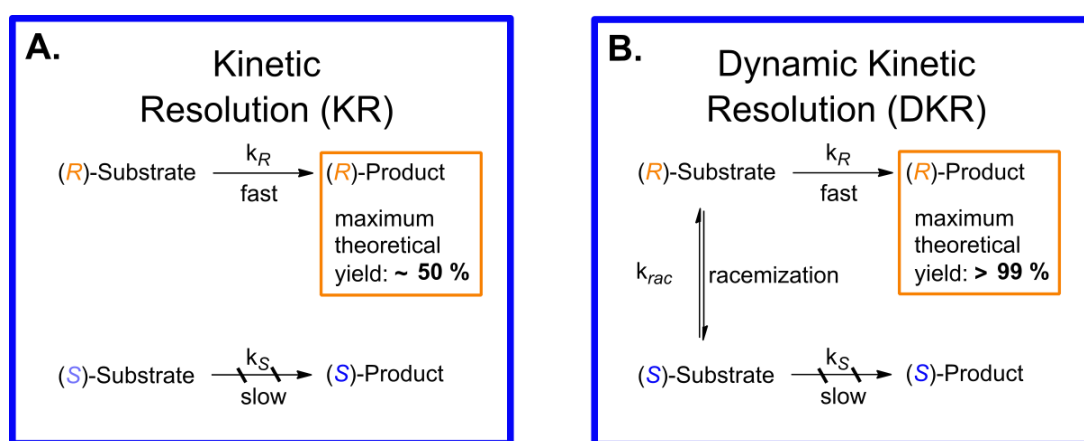


Figure 9: **A.** The main principle of a kinetic resolution. Due to the discrepancy in reaction rates for the enantiomers, only one enantiomerically pure product is accumulated in surplus. **B.** Principle of a dynamic kinetic resolution. The addition of a racemization step allows for yields of the desired enantiomerically pure product of up to 99 %.

Since many enzymes are naturally stereospecific catalysts, they often get employed as the resolving agent in kinetic resolutions. The ratio of asymmetric synthesis to kinetic resolution of racemic mixtures for enzymatic applications is estimated at 1:4.<sup>65</sup> Due to the structural conformation of the enzymes active site (allowing for the stereospecificity in the first place), the formation of an enzyme-substrate complex is energetically beneficial only with one of the enantiomers, thus mediating the discrepancy in the reaction rates between the respective enantiomers through the difference in activation energies (see Figure 10).



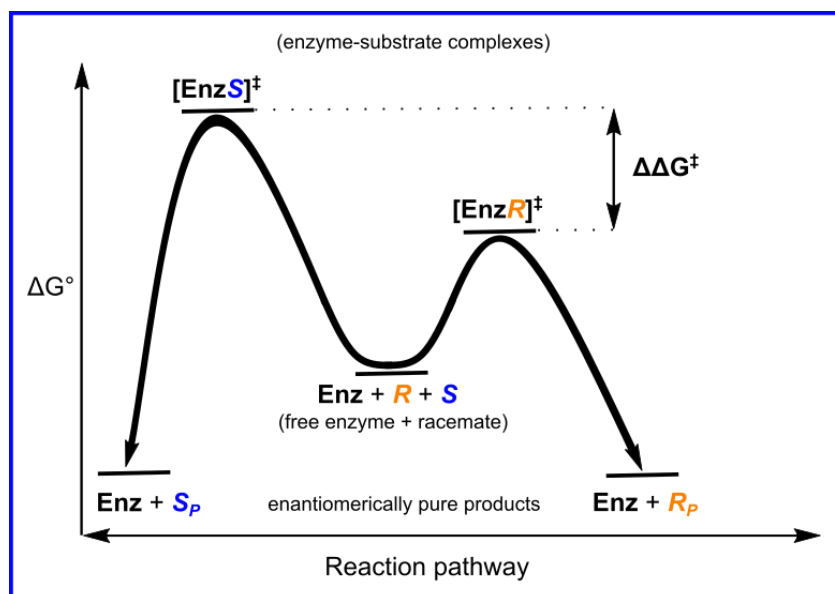


Figure 10: Activation energy profile of an enzymatic kinetic resolution. The difference in activation energy for the formation of the enzyme-substrate complex between the *R*- and *S*- enantiomers mediates the preferential formation of the *R<sub>P</sub>*-product. Adapted from Keith *et al.* 2001<sup>64</sup> and Faber 2018<sup>6</sup>.

Both classical and kinetic resolution approaches are limited in their maximum achievable yield, which is capped at 50 % of the racemic mixture due to preferentially converting only one enantiomer, while the other enantiomer frequently gets discarded. This challenge is addressed in the concept of dynamic kinetic resolution (DKR). A racemization step is added to the kinetic resolution approach, allowing for the interconversion of the unchanged enantiomer into a racemate. Thus, the supply of the converted enantiomer is replenished, allowing for yields of up to 99 % (see Figure 9 B.).<sup>64,66–69</sup> Said racemization step can be performed by various means. The substrate itself may be self-racemizing via tautomerism (e.g. keto-enol tautomerism) or a reaction equilibrium.<sup>70–72</sup> Alternatively, racemization may be performed through a catalyst, including the utilization of enzymes. In the enzyme class of isomerases, there exists a subgroup of racemases (EC 5.1.), enzymes, which are naturally trimmed for the interconversion of enantiomers into each other.<sup>65,73</sup> The broad possibilities for employment of enzymes as both a racemizing agent and a resolving agent has led to an increase in published chemoenzymatic<sup>74–77</sup> and purely enzymatically driven reaction cascades for dynamic kinetic resolutions of various compounds in the last two decades.<sup>78</sup> Thus, DKR represents an industrial tool for the production of optically pure compounds which is more sustainable, than classical resolutions and KRs, yet still simple in its realization, just like KR. With the progress achieved in the last 30 years for the discovery and development of robust and productive enzymes for industrial purposes, the sustainability factor of DKRs applying those is increased greatly on the path to a “greener” chemistry.

## 1.6 Chiral amines

An important compound class for chemical and pharmaceutical synthesis are chiral amines. Finding their use as building blocks in the assembly of more complex chemicals, the utilization of chiral amines ranges from pharmaceutical synthesis and agrochemical synthesis<sup>79–81</sup> to the application as chiral auxiliaries in analytical resolutions of other chiral molecules<sup>82–84</sup>. Furthermore, chiral amines can be applied as a part of stereoselective metalloorganic catalysts.<sup>85–87</sup> Especially relevant in the pharmaceutical sector, estimates suggest, that up to 40 % of APIs (active pharmaceutical ingredients) contain a chiral amine moiety as a structural element.<sup>79,88</sup> Some important chiral amine pharmaceuticals are shown in Figure 11.

As can be seen, all amine classes find usage in chiral pharmaceuticals. However, it is always important for those to possess the right stereochemical configuration, since the effect of a wrongfully employed enantiomer on the human organism may vary from no desired effect at all to a harmful impact with long-term consequences. A relatively harmless example for such a case would be the employment of thyroxine, also known as the hormone of the thyroid gland ( $T_4$ ). It possesses two enantiomers (see Figure 12), however only (*S*)-thyroxine (L-enantiomer) can act as the hormone, while (*R*)-thyroxine (D-enantiomer) has no such effect. (*R*)-thyroxine was employed as a commercial pharmaceutical due to its lowering effect on cholesterol levels, however this was discontinued due to its association with high mortality rates in cardiac patients and the general availability of more effective drugs.<sup>89,90</sup>

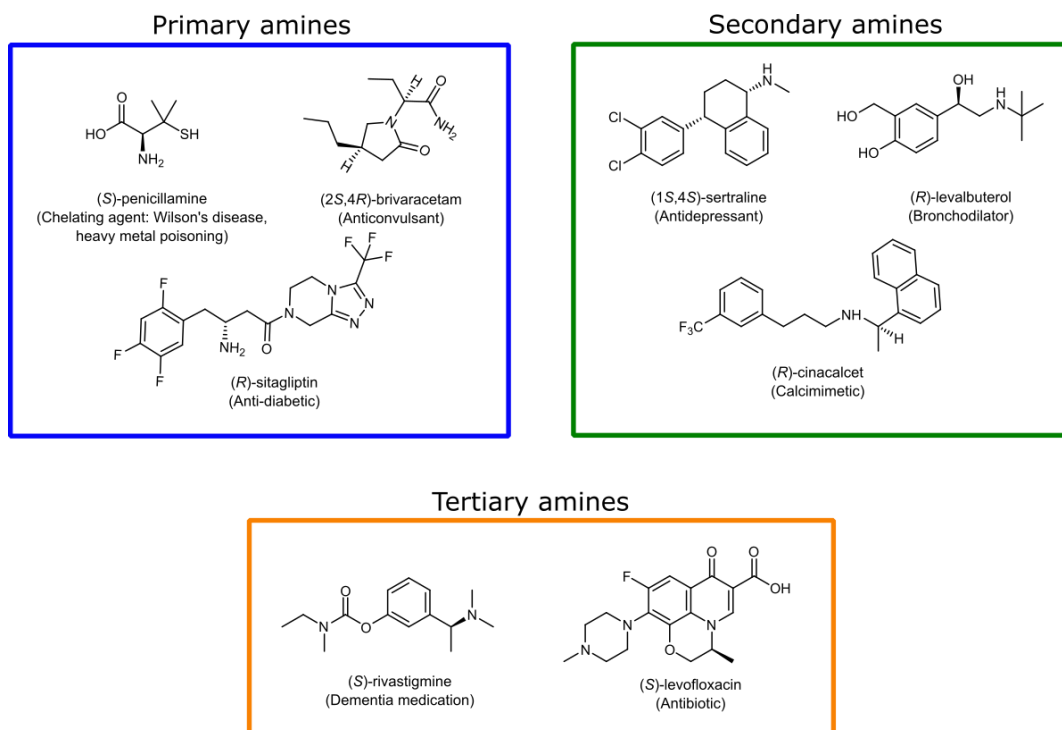


Figure 11: Important APIs containing chiral amine moieties. The pharmaceuticals are sorted by their respective amine classes into primary, secondary and tertiary amines.

Another example of an amine drugs, of which only one enantiomer actually produces a desired effect, would be sitagliptin<sup>91</sup> with only the (*R*)-enantiomer mediating the most therapeutic effect. However, in the case of the well-known pharmaceutical scandal involving thalidomide (also known as Contergan® scandal after the commercial name of the compound), the employment of a racemic mixture of this compound led to severe malformations in fetuses, whose mothers were prescribed Contergan® during pregnancy to relieve morning sickness or as a sleeping medication. While (*R*)-thalidomide was therapeutically active, (*S*)-thalidomide caused the described side effects (see Figure 12).<sup>92</sup> Hence, the development of efficient synthesis strategies for the stereoselective production of chiral amines is important to maximize the therapeutic efficacy and avoid harmful side effects.

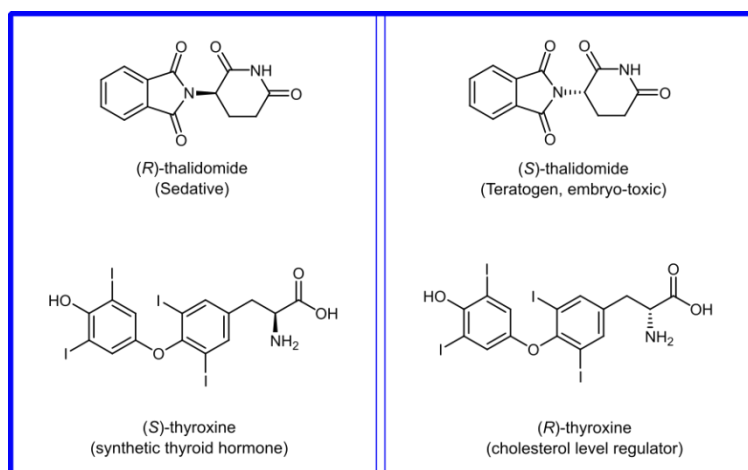


Figure 12: Structures of the enantiomers of thyroxine and thalidomide with their respective pharmaceutical effect.

## 1.7 Chemical synthesis of amines

Having established the importance of amines for industrial and pharmaceutical purposes, it is important to understand different synthesis pathways towards this compound class. In classic organic chemistry, a number of synthetic routes towards amines have been successfully established (see Figure 13).

The classic organic synthetic routes towards amines can be sorted according to the produced amine subgroup. For primary amines, the production pathways usually involve the obtainment of precursor functionalities, like azides, nitriles or nitro compounds, which are then reduced via a reducing agent (e.g.  $\text{LiAlH}_4$ ) or catalytically via hydrogenation. For aromatic compounds, an amino group can be attached through nucleophilic substitution. Furthermore, there are several pathways of rearrangement reactions starting from amides of carboxylic acids (like the Hofmann rearrangement), or less frequently utilized Curtius (from hydrazides/azides, not shown) or Lossen rearrangements (from hydroxamic acids, not shown).<sup>50</sup>  $\alpha,\beta$ -Unsaturated ketones possess the selectivity of forming primary amines (at the  $\beta$ -carbon) in reactions of conjugate additions with ammonia. However, for saturated ketones, imines would

form with the same reaction components due to the direct addition mechanism at the carbonyl C-atom being favored.<sup>50,93</sup> Finally, another prominent name reaction for the synthesis of primary amines is the Gabriel synthesis reaction. In its mechanism, it is essentially a nucleophilic substitution reaction of alkyl halides, where the nitrogen acts as the nucleophile. However, due to the possibility of multiple nucleophilic substitutions with one nitrogen atom (as its nucleophilicity is gradually increased with each subsequent substitution) and the resulting possibility of formation of secondary and tertiary amines, the N-nucleophile is introduced into the reaction in a “protected” form, being bound within a phthalimide moiety (with the two electron pulling carbonyl groups acidifying the nitrogen), thus only being able to react once. Having performed the substitution, the phthalimide moiety is separated using hydrazine, yielding a primary amine.<sup>50,94</sup>

Secondary and tertiary amines can also be produced via several synthesis strategies. The multiple nucleophilic substitution of alkyl halides, previously mentioned in the context of the Gabriel synthesis is one such strategy. Here, ammonia can act as the “unprotected” nucleophile, allowing for multiple substitutions towards secondary and tertiary amines. On this strategy, the so-called Hofmann elimination mechanism is based (also called exhaustive methylation). Here, a multiple nucleophilic substitution with a primary or secondary amine takes place, after which a quaternary ammonium hydroxide is formed with AgOH, dissociating from its initial compound as a tertiary amine through condensation.<sup>50</sup> The other important synthesis pathway for the obtainment of secondary and tertiary amines is reductive amination. Here, a carbonyl moiety reacts with an amine forming an imine. This imine can then be reduced to a secondary/tertiary amine. In practical applications, there is a challenge for this strategy, since the carbonyl group of the unreacted carbonyl is more likely to be reduced (due to higher reactivity) than an imine group, thus theoretically diminishing the possibility for a successful reduction of the imine.

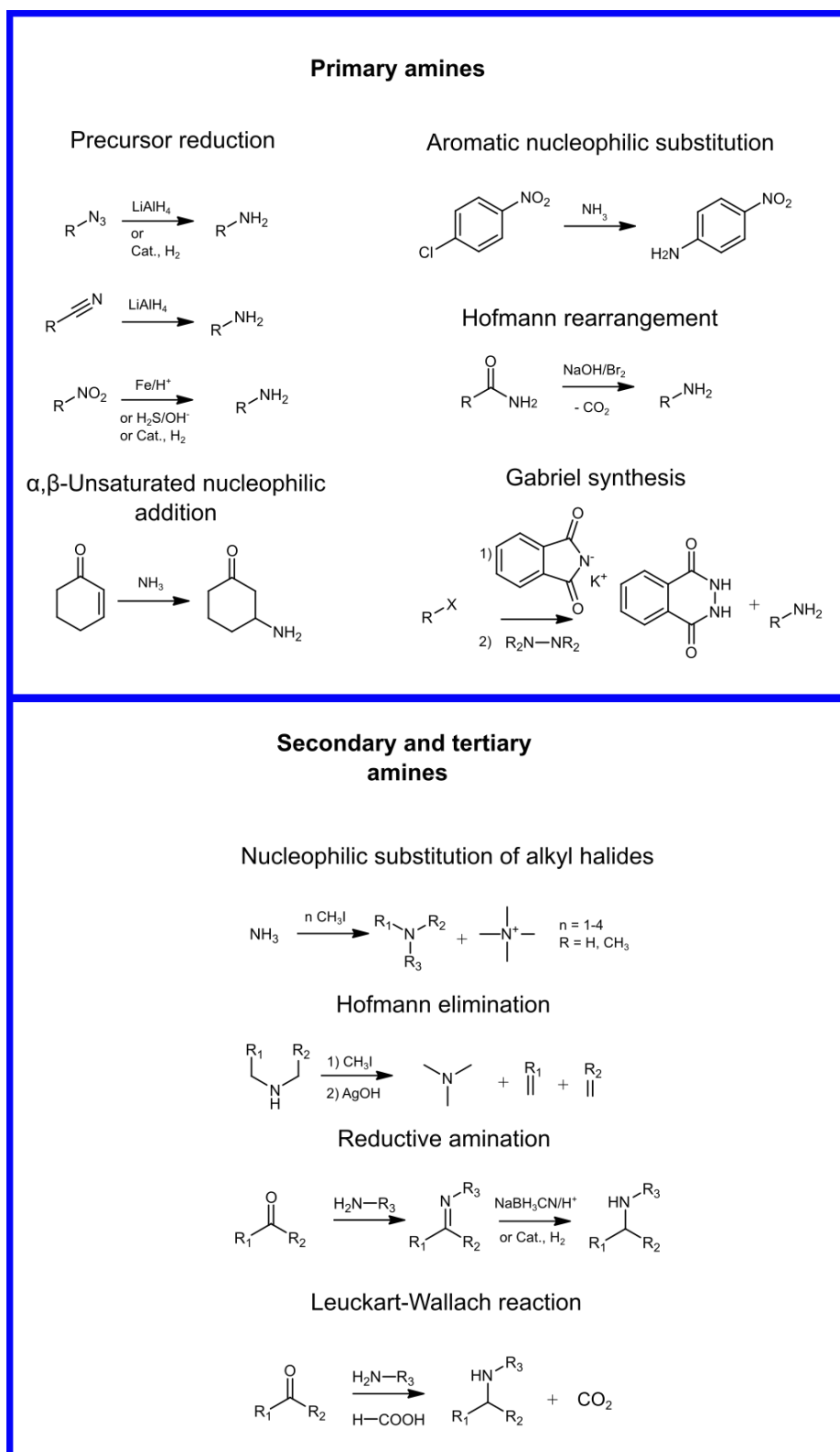


Figure 13: Scheme of established chemical synthesis routes towards primary, secondary and tertiary amines.<sup>50</sup>

This can be circumvented either by using tailored reductive agents in acidic conditions (protonating the imine to a more reactive iminium ion), which cannot react with carbonyl moieties (e.g.  $\text{NaBH}_3\text{CN}$ ) or catalytic (selective) hydrogenation.<sup>50</sup> Another pathway for reductive amination would be the Leuckart-Wallach reaction, where formic acid reduces the iminium ion under hydride transfer, allowing for the formation of an amine.<sup>95,96</sup> Similar mechanisms also work in the Eschweiler-Clarke and Pictet-Spengler reactions.<sup>97,98</sup>

However, the presented methods in most cases do not yield enantiopure compounds, mostly producing racemic mixtures of chiral amines. Thus, such racemic mixtures can be subjected to resolution processes (chiral, kinetic or dynamic kinetic resolution) to obtain the enantiopure amine compounds.<sup>99</sup> The other option for the production of chiral amines would in turn be asymmetric synthesis under employ of chiral catalysts (mostly metal-based or on the basis of chiral Brønsted acids). All corresponding approaches for this pathway can be summarized under two main routes.<sup>99,100</sup> The first is, again, reductive amination (including asymmetric addition and hydroamination). Prochiral imine/iminium/aldimine moieties are created through addition, after which a selective catalyst is applied, ensuring the reduction towards an amine product.<sup>99,101–107</sup> The second route is called asymmetric hydrogenation. Here, the prochiral precursor can also be an imine, but enamines and other forms of prochiral allylic amines can be employed as well. Those precursors can then be hydrogenated using a stereoselective catalyst (see Figure 14).<sup>100,104,108–111</sup> Chemical asymmetric synthesis of chiral amines can be challenging due to several factors. Firstly, imines and their amine products can act as ligands to the very metal ions employed in the selective catalysts or form metal-amine/amide complexes with them, thus deactivating those catalysts. Secondly, imines in acyclic configurations can assume E- and Z-isomeric forms, thus effectively inverting the stereoselectivity of the catalyst depending on the formed isomer. Furthermore, if multiple amine moieties are present on the desired molecule, the usually applied reaction conditions make the use of protective groups obsolete due to their easy dissociation. Thus, either the catalyst has to be highly selective towards only one amine moiety, or multiple undesired reductive aminations can happen within one reaction.<sup>101</sup>

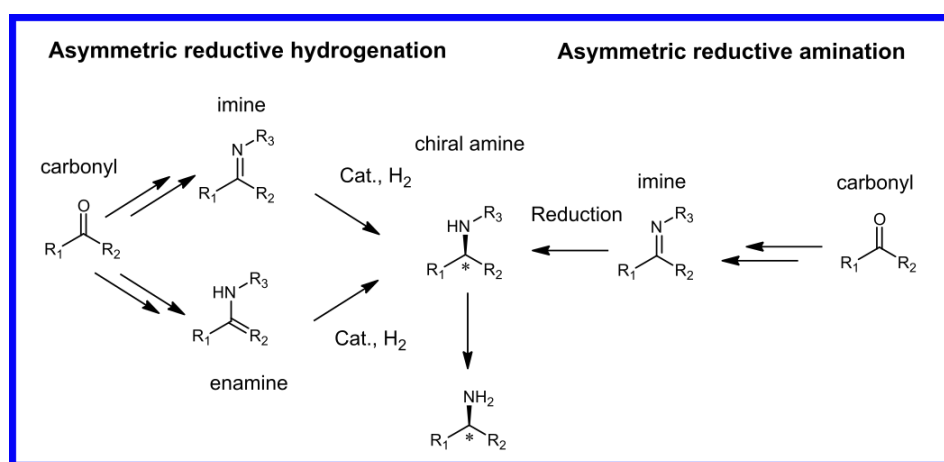


Figure 14: Reductive amination and asymmetric hydrogenation as main asymmetric chemical synthesis routes for chiral amines.

Although remarkable advances towards stereoselectivity and productivity of the described chiral amine synthesis strategies have been made in recent years, most of those synthesis approaches apply fairly harsh conditions, like high pressures or temperatures, although a trend towards milder temperatures of 20-50 °C can be observed.<sup>99,100</sup> Biocatalysis can help to avoid such downsides, while having the advantage of “built-in” stereoselectivity, which makes it a viable alternative to the classical synthesis routes.

## 1.8 Enzymatic amine synthesis

Some of the previously presented chemical amine synthesis methods can also be found in a natural setting, catalyzed by enzymes. Several of such enzyme classes have been shown in literature to catalyze amine formation outside of their natural setting, thus making them applicable in laboratory and industrial chiral amine synthesis. Those classes include ammonia lyases, monoamine oxidases (MAOs), imine reductases (IREDs), reductive aminases, amine/amino acid dehydrogenases (AmDHs/AADHs) and transaminases (see Figure 15).<sup>112</sup>

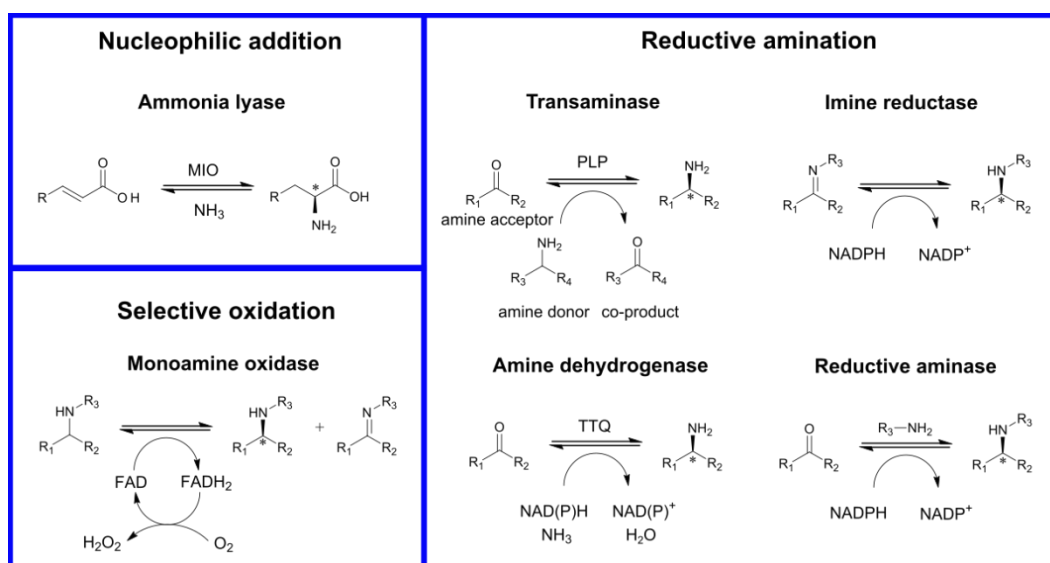


Figure 15: Different enzyme classes for stereoselective synthesis of chiral amines. Cofactor abbreviations: MIO - 3,5-dihydro-5-methyldiene-4H-imidazol-4-one; TTQ - Tryptophan tryptophylquinone; PLP - pyridoxal 5'-phosphate. Adapted from *Gomm et al.* 2017.<sup>112</sup>

Ammonia lyases are enzymes, that naturally catalyze the reversible elimination of amino groups from amino acids. Mechanistically similar aminomutases can also catalyze the translocation of amino groups through the formation of an unsaturated intermediate. Thus, the reversibility of this reaction can be used to perform nucleophilic addition of amines to  $\alpha,\beta$ -unsaturated carboxyl compounds, usually in the  $\alpha$ -position for ammonia lyases, as it is the natural position for proteinogenic amino acids. While synthetic examples of pharmaceutically relevant building blocks by ammonia lyases exist, they are nevertheless limited in their substrate scope due to the

need of adjacent carboxylic groups in their substrates. However, examples of ethanolamine ammonia lyases exist, where the reaction proceeds without the need for a carboxyl group, although no chiral molecule is formed.<sup>113</sup> Monoamine oxidases catalyze the stereoselective oxidation of amines to imines, being able to convert both primary and secondary/tertiary amines.<sup>114</sup> This trait can be effectively used in kinetic resolutions of racemic amine mixtures, but also in stereoselective chiral amine synthesis through reductive amination (as the means for the formation of an imine precursor).<sup>114,115</sup> The other mentioned enzyme classes catalyze reactions of reductive amination under consumption of reductive cofactors. All of those enzyme classes function under the formation of an imine/iminium intermediate in their active site, which is subsequently reduced through different mechanisms of electron transfer. IREDs catalyze the asymmetric reduction of imines under consumption of NADPH as their cofactor, relying on imine substrate feed or spontaneous imine formation under specific reaction conditions.<sup>116</sup> Reductive aminases, of which far fewer examples exist due to being a fairly recently employed enzyme class, can facilitate imine formation in their active site, prior to its reduction under the same mechanism, as IREDs. From a protein sequence-activity standpoint, IREDs and reductive aminases are very similar, to the point of not being distinguishable at a primary sequence level.<sup>117–119</sup> The drawback of IREDs and reductive aminases is their reliance on a fairly expensive cofactor (NADPH) and an already existent amine precursor, which is however compensated by their ability to synthesize secondary and tertiary amines. Amino acid dehydrogenases and, in particular, amine dehydrogenases solve one of those issues, utilizing the inexpensive ammonia as an amino source, but still relying on expensive cofactors of the NAD(P)H family to facilitate their imine transition state reduction. Amine dehydrogenases, sometimes through protein engineering, allow for the efficient synthesis of many primary amines from mostly inexpensive substrates.<sup>120,121</sup> Transaminases as an enzyme class catalyze the asymmetric transfer of an amino group between an amino donor and a carbonyl (ketone or aldehyde) compound. They utilize PLP as a cofactor, which serves as a shuttle for the amino group, binding and cleaving it from the amino donor and transferring it to the converted carbonyl compound. However, transaminases, like IREDs, rely on already existent amines or amino acids to serve as amino donors.<sup>112,122,123</sup> Further enzyme classes, less frequently employed for amine production, include Pictet-Spenglerases and berberine-bridge enzymes.<sup>124,125</sup>

### 1.8.1 Transaminases

Since transaminases are a crucial part of this work, they will be discussed in detail. As already mentioned, transaminases (or otherwise called aminotransferases) catalyze the transfer of amino groups between two molecules, an amino donor and an amino acceptor. There are several methods of classification for transaminases.<sup>126</sup> Transaminases are PLP-dependent enzymes, which are subdivided into seven classes based on their fold type and named after the first identified enzyme of this type. Among those seven fold types of PLP-dependent enzymes, transaminases are found in the fold



types I (named aspartate transaminase fold) and IV (named D-alanine transaminase fold). The type I fold is the most common transaminase fold type. The three-dimensional fold types can be subdivided into four further subgroups, based on the primary protein sequence relations: I - aspartate-, alanine-, tyrosine-, histidinol-phosphate- and phenylalanine transaminases; II - acetylornithine-, ornithine-,  $\omega$ -amino acid-, 4-aminobutyrate- and diaminopelargonate transaminases; III - D-amino acid- and branched-chain amino acid transaminases; IV - serine- and phosphoserine transaminases.<sup>126–131</sup>

Another classification method, more frequently referred to in literature, is the classification of transaminases based on their substrate specificities. This classification distinguishes between  $\alpha$ - and  $\omega$ -transaminases.  $\alpha$ -Transaminases can solely transfer an amino group bound in alpha-position to the carboxyl group (so-called  $\alpha$ -C-atom of amino acids) of the substrate.<sup>112,123,132</sup>  $\omega$ -Transaminases on the other hand facilitate amino group transfers further away from the carboxyl group of amino acids.<sup>112,123,132</sup> Here, some confusion can be found throughout different sources, because a further structurally based subdivision into  $\alpha$ -,  $\beta$ - and  $\gamma$ -transaminases exists, which also frequently correlates with their respective substrate preference (in terms of their respective substrate/structure Greek letter nomenclature).<sup>126,129</sup> Within the  $\omega$ -transaminases, the subgroup of amine transaminases (ATAs) exists. Transaminases of this subgroup are able to transfer amino groups between molecules without carboxylic moieties, thus also accepting simple ketones and aldehydes as substrates. ATAs are of particular interest for synthetic applications and found a broad applicability in stereospecific synthesis routes towards agrochemicals and pharmaceuticals.<sup>123</sup>

Mechanistically, transaminases rely on the cofactor PLP, complexed within their active site. Due to toxicity of ammonia to living cells, PLP acts as a temporary acceptor of the transferred amino group, effectively a shuttle for it, which is able to transfer electrons via forming a conjugated  $\pi$ -system. The mechanism follows a so-called Ping Pong Bi Bi pattern<sup>133</sup> and is shown in Figure 16.

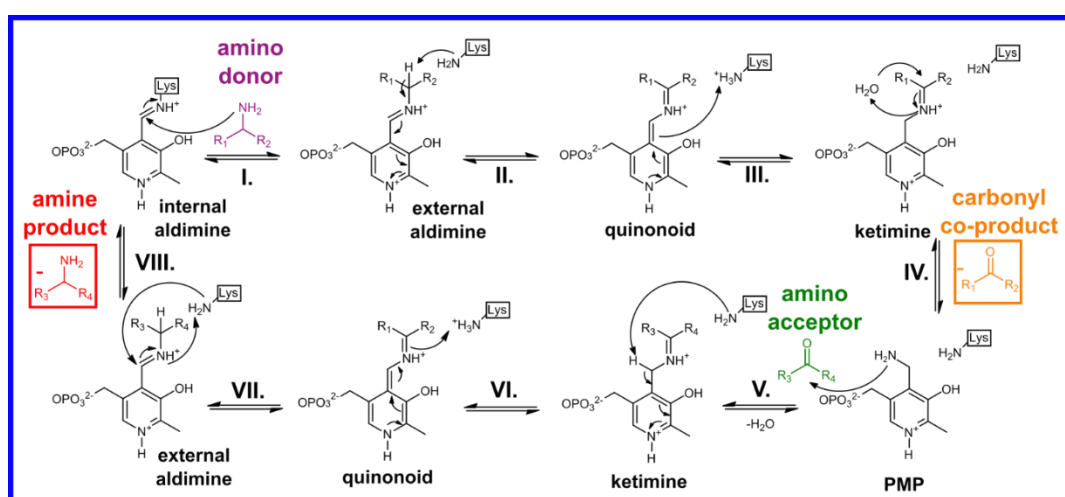


Figure 16: Mechanism of transaminase-catalyzed amino group transfer between an amino donor and amino acceptor molecule. The mechanism follows the Ping Pong Bi Bi pattern and relocates the electrons from the formed aldimine and ketimine states via a transition of PLP to a quinonoid with a conjugated  $\pi$ -system.<sup>133–135</sup>

Starting from PLP binding to the catalytic highly conserved catalytic lysine residue, a Schiff-base is formed (**I.**), allowing for a nucleophilic substitution of this internal aldimine by the amino donor, forming an external aldimine (**II.**). The freed lysine can in turn attack the  $\alpha$ -proton of the bound amino donor. The resulting negative charge is stabilized by the formation of a quinonoid system (**III.**). After the rearrangement of this system, the surplus proton is transferred from the lysine onto the imine-adjacent C-atom of PLP, forming a ketimine, which is subsequently hydrolyzed under consumption of water, freeing the carbonyl co-product of the reaction, formed from the amino donor (**IV.**). The amino group thereby remains bound to the PLP-residue, forming pyridoxamine 5'-phosphate (PMP). From this point, the mechanism mirrors its first half. The amino group of the PMP can bind to the amino acceptor carbonyl, forming a ketimine under the condensation of water (**V.**). This ketimine is then transformed to an internal aldimine through the attack of the catalytic lysine on the imine-adjacent PMP proton (**VI.**) and the resulting electron transfer and  $\pi$ -system rearrangement in the quinonoid system (**VII.**). In the final step (**VIII.**), the external aldimine is replaced by the internal aldimine with the catalytic lysine, freeing the amine product and regenerating PLP.<sup>133–135</sup>

Transaminase-catalyzed amine synthesis has its advantages and disadvantages described throughout literature. Among the main advantages of transaminases, their excellent stereoselectivity must be mentioned.<sup>122,136</sup> Due to their folding architecture, transaminases, and especially  $\omega$ -transaminases, usually possess two distinct binding pockets in the active site, a small one and a big one, in which other substrate functionalities can be accommodated.<sup>112,122,137–139</sup> Thus, a substrate can only be bound and coordinated into one specific position, facilitating only one enantiomer being produced in the reaction. The recycling of the cofactor PLP during the reaction without the need for an extra recycling system is also an advantage especially compared to other amine-producing enzymes.<sup>123</sup> Combined with the usual advantages of enzymes in general (e.g. mild reaction conditions, replacement of toxic metal catalysts/organic solvents), transaminases present a viable catalytic tool for stereospecific amine synthesis. Nevertheless, some drawbacks of transaminases have to be considered prior to their utilization. First of all, the very reason for the transaminase's stereoselectivity can be its drawback, since the binding pockets allow only for substrates with one bulky and one small (usually a proton or methyl group) substituent, while substrates with a bigger "small" substituent lead to a decrease in activity. This issue is usually resolved by protein engineering, widening the binding pockets through mutations in the protein.<sup>112,138–140</sup> Furthermore, transaminases may suffer from unfavorable reaction equilibria in terms of amine product formation, since their reaction mechanism is reversible. Their product yields are relatively low when the substrates are dosed stoichiometrically into the reaction.<sup>6,141,142</sup> This drawback can be alleviated by shifting the reaction equilibrium through reaction engineering. Often, the increase in the concentrations of the amino donor to a significant surplus is a chosen method, reaching 10-50-fold excesses of the amino donor molecule compared to the acceptor.<sup>141,142</sup> Amino donor concentrations of up to 1 M can be encountered in literature.<sup>143,144</sup> However, this can only be done to a certain degree, since transaminases can also show co-substrate inhibitions or co-product inhibitions.<sup>6</sup> Thus, co-product removal is also a

widely applied strategy. This can be realized through the evaporation of volatile co-products, like acetone (formed from isopropylamine amino donor), or the subsequent conversion of pyruvate (formed from alanine amino donor) in a reaction cascade, e.g. by combination with pyruvate decarboxylases, amino acid dehydrogenases or lactate dehydrogenases.<sup>112,141,142,145</sup> Also, transaminases face the challenges of product inhibition, which can only be circumvented by product removal from the reaction, which will be discussed in detail in a later section.

Due to their advantages, transaminases found their deserved place in scientific and industrial applications. This enzyme class can be employed in amine synthesis with two main synthetic approaches. The first application field would be kinetic resolution of racemic amine mixtures. Due to their high stereoselectivity, transaminases are a highly efficient resolving agent for kinetic resolutions, converting only one enantiomer back to its carbonyl form. Due to previously mentioned reaction equilibria characteristics, what is a challenge in amine formation turns into an advantage in this mode of operation, since, if the reaction equilibrium is on the side of the carbonyl compounds, the undesired enantiomer will be converted more efficiently. Nevertheless, the kinetic and, occasionally, dynamic kinetic resolutions using transaminases also work in the direction of amine synthesis from chiral racemic substrates.<sup>146–148</sup> The second application possibility would be asymmetric synthesis of amines from prochiral substrates (e.g. ketones). Having been shown to effectively catalyze the transamination of a variety of ketones and aldehydes<sup>122,123</sup>, transaminases are constantly being improved to broaden their substrate scope and modify their properties towards substrate acceptance, stability, etc.<sup>149–151</sup> Some transaminases have even been shown to be efficient catalysts in organic solvents, like MTBE.<sup>152</sup> In industrial processes, both synthetic pathways have found application.<sup>153,154</sup> Some examples of such industrial applications of transaminases are shown in Figure 17. In recent years, Merck & Co demonstrated a dynamic kinetic resolution in the kilogram-scale synthesis of the drug niraparib<sup>155</sup> (**I.**) and an asymmetric synthesis application in the synthesis of the experimental compound MK-7246<sup>156</sup> (**II.**), both utilizing a transaminase. Furthermore, Codexis and Merck & Co reported a highly efficient chemoenzymatic pathway for the synthesis of the drug sitagliptin (**III.**) under employ of an engineered transaminase, enabling a 53 % increase in process productivity and a 19 % reduction of waste due to the use of said transaminase.<sup>157</sup> In turn, Pfizer reported a transaminase-based DKR approach in the synthesis of a smoothened receptor inhibitor (SMO, **IV.**) for blood-related cancer therapy.<sup>158</sup>

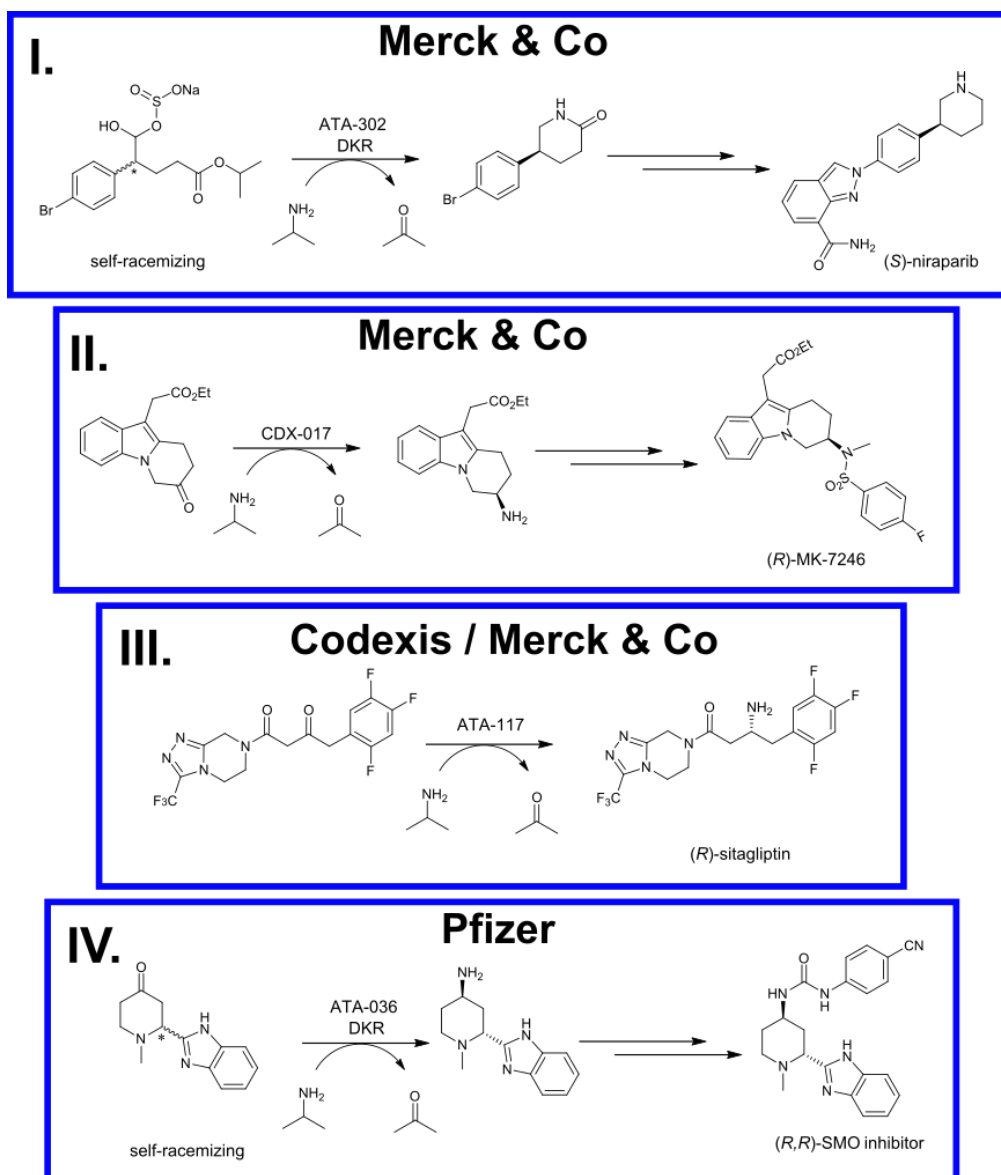


Figure 17: Examples of the industrial application of transaminases.<sup>155–158</sup>

## 1.8.2 Amine dehydrogenases

Amine dehydrogenases (AmDHs) as an enzyme class catalyze the stereospecific reversible reductive amination of ketones to amines under employ of a redox cofactor, utilizing ammonia as the amino donor. They are closely related to amino acid dehydrogenases (AADHs), which catalyze the oxidative deamination of amines to ketones (with ammonia as a co-product), but require the presence of a carboxylic group in the substrate (amino acid). However, this reaction is reversible and the reverse reductive amination is strongly preferred with equilibrium constants ( $K_{eq}$ ) for some AADHs reaching up to  $10^{14}$ - $10^{18}$ .<sup>159</sup> This fact combined with the usage of cheap ammonia and an overall better atom economy (compared to  $\omega$ -transaminases) makes

amine dehydrogenases a valuable option in the enzymatic toolbox for the asymmetric synthesis of primary amines.<sup>120,160</sup>

While amino acid dehydrogenases are a widely studied and utilized enzyme class<sup>159,161,162</sup>, not so many examples of pure amine dehydrogenases can be found in literature. That owes to the fact, that pure amine dehydrogenases are not so easy to come by. In general, amine dehydrogenases can be subdivided in natural amine dehydrogenases and non-natural amine dehydrogenases.<sup>120,163–165</sup> Of natural amine dehydrogenases discovered in diverse organisms, few examples possess the described activity towards ketones without a carboxylic group in proximity.<sup>120,165,166</sup> For some of those examples, however, no DNA or protein sequence could be identified, making those experiments not reproducible, while their selectivity and specific activity towards industrially applicable ketones were not satisfactory.<sup>163,164,166</sup> Further, more efficient native amine dehydrogenases were also discovered by genome mining, sometimes displaying catalytic promiscuity in the utilization of the redox cofactors NADH and NADPH, although previously known AmDHs were solely NADH-dependent.<sup>120,166–169</sup> The catalytic performance of those native AmDHs could then further be improved by protein engineering.<sup>167,170</sup> Altogether, a review from 2022 shows 25 experimentally validated native wild-type amine dehydrogenases and a review from 2024 shows over 30 native AmDHs, most of which were published in the last 10 years.<sup>120,160</sup> Thus, due to this shortage of wild-type amine dehydrogenases, a variety of non-natural amine dehydrogenases were developed in the last two decades. Such non-natural amine dehydrogenases have been obtained exclusively from L-AADHs, which is not surprising, given on one hand the similarity in the reaction mechanisms and, on the other hand, nature's dependence on proteinogenic L-amino acids.<sup>164</sup> Several protein engineering approaches have produced efficient amine dehydrogenase mutants, including ones derived from phenylalanine dehydrogenases<sup>171–174</sup> and leucine dehydrogenases.<sup>121,175–177</sup> Through domain shuffling of such AmDHs derived from both phenylalanine and leucine dehydrogenases, Bommarius *et al.* designed a chimeric AmDH of improved functionality and substrate scope, which was extended towards benzylic ketones.<sup>178</sup> Furthermore, although amine dehydrogenases natively utilize ammonia as their amino source, Tseliou *et al.* reported the generation of secondary amines with primary amine donors.<sup>165</sup> Furthermore, the same working group created a highly versatile amine dehydrogenase mutant LE-AmDH-v1, derived from an  $\epsilon$ -deaminating-L-lysine dehydrogenase. While having a broad substrate scope, including bulky substrates, it also possessed high thermostability ( $T_m = 69^\circ\text{C}$ ), aside from very high stereospecificity.<sup>164,179,180</sup> From all described literature, the present-day substrate scope of amine dehydrogenases includes linear and fatty acid ketones and aldehydes, benzyl ketones, aliphatic cyclic ketones and even polycyclic ketones and aldehydes.

Mechanistically, the reductive amination has few similarities to transaminase catalyzed reactions. The amino group is not shuttled by a cofactor, since it remains bound to the substrate throughout the imine formation process, while the substrate itself is not bound at all but coordinated in the active site (see Figure 18 A.). The ammonia nitrogen attacks the carbonyl group, forming an amino alcohol intermediate,

its charge being coordinated by adjacent amino acid residues (**I.**). This amino alcohol rearranges itself to an imine under the condensation of water (**II.**). The formed imine is then subsequently reduced under oxidation of the cofactor NADH to NAD<sup>+</sup> (**III.**), yielding the amine product (**IV.**).<sup>120,160,165</sup>

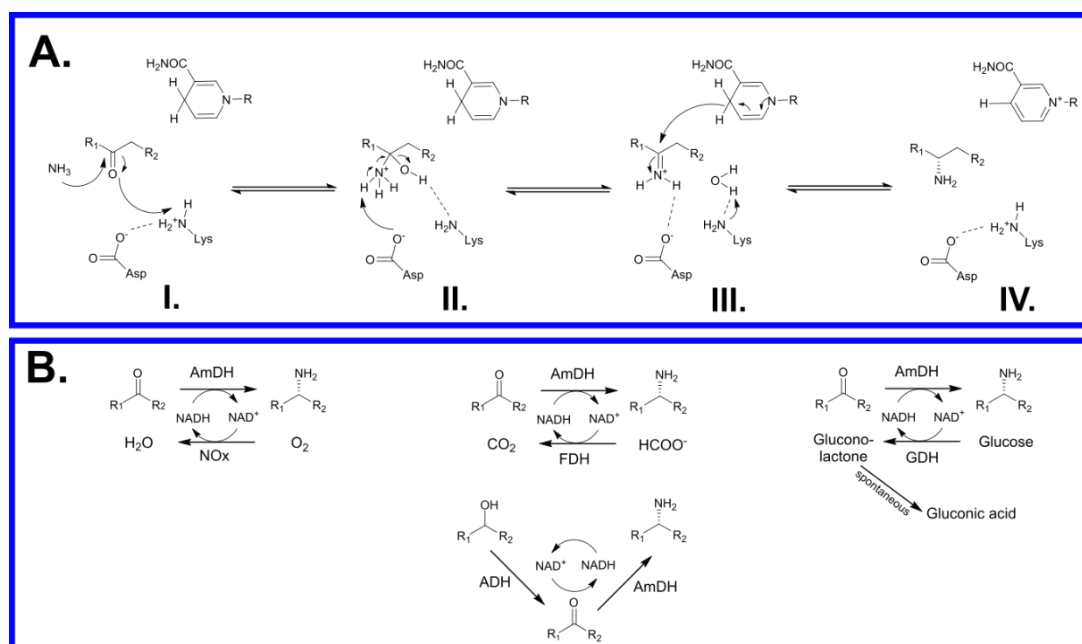


Figure 18: **A.** Mechanism of amine dehydrogenase catalysis for reductive amination. Adapted from *Liu et al.* 2022<sup>120</sup> and *Tseliou et al.* 2024<sup>160</sup>. **B.** Schematic possibilities of NADH cofactor regeneration through enzymatic cascades.<sup>120</sup>

As can be seen, the main drawback of amine dehydrogenase-catalyzed reactions is the consumption of the cofactor NADH during the reaction. As this cofactor is usually expensive and the reaction cannot proceed without it, regeneration of NADH is required to achieve higher substrate conversions in the reaction. In existing literature, this is realized through the utilization of enzymatic cascades, combining the AmDH reaction with enzymes requiring NAD<sup>+</sup> for their respective conversions. Examples of utilization of NADH-oxidases (NOx), formiate dehydrogenases (FDH), alcohol dehydrogenases (ADH) and glucose dehydrogenases (GDH) have been published in recent years and are shown schematically in Figure 18 **B.**<sup>120</sup>

## 1.9 Beta-chiral amines

A group of particular interest within chiral amines are  $\beta$ -chiral amines.  $\beta$ -chiral amines are defined by the positioning of their amino group. For  $\alpha$ -chiral amines, the amino group is situated directly at the chiral  $\alpha$ -C-atom. For  $\beta$ -chiral amines, the amino group is interspaced to the chiral center by another carbon moiety, bringing it into the  $\beta$ -position. Many of the  $\beta$ -chiral amine compounds possess physiological activity. Pharmaceuticals of this subgroup frequently are employed to medicate neurological issues, some of which are shown in Figure 19.

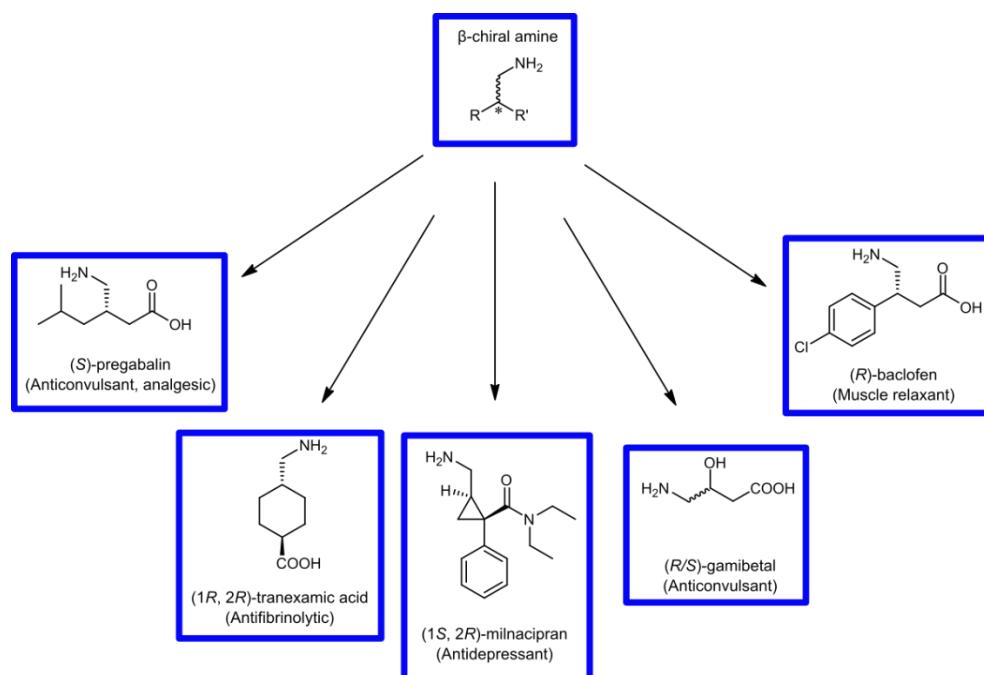


Figure 19: Examples for  $\beta$ -chiral amines as pharmaceuticals.

Chemical synthesis pathways for  $\beta$ -chiral amines generally mimic the ones for  $\alpha$ -chiral amines and can be subdivided into two groups (see Figure 20): asymmetric synthesis through either asymmetric alkylation or addition<sup>181–186</sup> or synthesis of chiral precursors<sup>187–191</sup>, which are then converted to amines through unspecific reactions and the reductive amination of chiral  $\alpha$ -branched aldehydes<sup>192</sup>, especially by the means of dynamic kinetic resolution.<sup>193</sup>

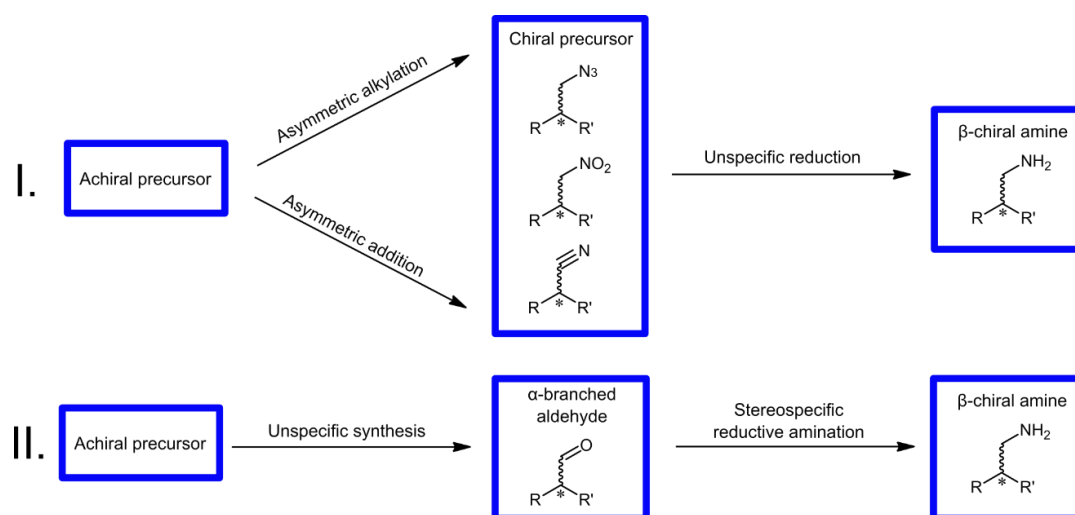


Figure 20: Synthesis pathways for obtainment of  $\beta$ -chiral amines. **I.** Shows possibilities asymmetric synthesis of precursors for a following reduction of amines. **II.** Demonstrates the reductive amination of chiral  $\alpha$ -branched aldehydes.

For the described approaches, some chemoenzymatic alternatives were developed over the years. In terms of the synthesis and conversion of chiral precursors to  $\beta$ -chiral amines, nitrilases have been employed in the hydrolysis of nitriles.<sup>194</sup> Biewenga *et al.* showed a one-pot three-step enzymatic cascade combining a michaelase and an

aldehyde dehydrogenase for the synthesis of GABA analogues.<sup>195</sup> The DKR-based reductive amination of racemic  $\alpha$ -branched aldehydes also demonstrates a variety of chemoenzymatic approaches to the synthesis of  $\beta$ -chiral amines. Most common are resolutions and cascades involving transaminases for a one-step conversion of the aldehyde moiety to an amine.<sup>72,148,196–199</sup> However, for the synthesis of secondary  $\beta$ -chiral amines, the enzyme class of imine reductases has also been employed in a similar manner.<sup>200,201</sup> Both approaches make use of the self-racemizing properties of  $\alpha$ -branched aldehydes through keto-enol tautomerization, allowing for excellent enantiomeric excesses of the obtained amines, although some of the employed transaminases have been shown to invert their stereospecificity depending on the bulkiness and functionalization of their respective substrate.<sup>196</sup>

## 1.10 Isomerases, racemases, mandelate racemase

As previously defined, isomerases are one of the main enzyme classes (EC-classification), catalyzing the conversion of one chemical isomer to another. According to EC-classification, they can be further subdivided into six subclasses, according to their respective catalytic functions: racemases and epimerases (EC 5.1.x.x), *cis-trans*-isomerases (EC 5.2.x.x), intramolecular oxidoreductases (EC 5.3.x.x), intramolecular transferases (EC 5.4.x.x), intramolecular lyases (EC 5.5.x.x) and isomerases altering macromolecular conformation (EC 5.6.x.x).<sup>202</sup> The number of classified isomerases is relatively small, compared to other EC classes, as they catalyze only 4 % of known biochemical reactions in their natural setting, mainly revolving around carbohydrate (sugar) metabolism.<sup>203</sup> Thus, most published works dealing with isomerases are also situated in sugar chemistry<sup>204</sup>, including the most widely known example of isomerase utilization in an industrial setting, the glucose isomerase (also known as xylose isomerase)<sup>205,206</sup>, utilized in the industrial production of high-fructose corn syrup (HFCS) since the 1970s. This enzyme converts glucose to its isomer, fructose, allowing for the enrichment of HFCS with fructose. Outside of sugar chemistry, several other isomerases have gained prominence in recent years. For instance, the styrene oxide isomerase has been shown to be a versatile enzyme, catalyzing the Meinwald rearrangement of epoxides to aldehydes or cyclic ketones. Thus, when combined in (chemo)enzymatic cascades, the enzyme allows for production of chiral alcohols,  $\alpha$ - and  $\beta$ -chiral amines and carboxylic acids.<sup>207</sup>

In the field of chiral chemistry, the subclass of racemases is important, especially in the field of dynamic kinetic resolutions of enantiomeric mixtures, since racemases catalyze the conversion of two enantiomers into each other, effectively racemizing enantioenriched mixtures, allowing for the conversion of the undesired enantiomer in DKR processes. Here, amino acid racemases are among the most studied racemase classes.<sup>73</sup> Amino acid racemases mainly follow two different mechanisms. There are PLP-dependent amino acid racemases, following a mechanism similar to transaminases, shuttling the amino group through imine bonds with the cofactor PLP (without dissociation of the substrate), and cofactor independent amino acid



racemases, facilitating racemization only through catalytic amino acids.<sup>208,209</sup> Due to a relative robustness of this enzyme class, examples of immobilization and the utilization of ISPR methods can be found for amino acid racemases throughout literature.<sup>73,210</sup> On the basis of amino acid racemases, an amine racemase has recently been developed, broadening the possibilities for a potential dynamic kinetic resolution of chiral amines.<sup>211</sup>

Another prominent racemase is the mandelate racemase from *Pseudomonas putida* ATCC 12633. It racemizes the mandelic acid molecule and thus can be used in the DKR of it. The enzyme itself is well studied, with its structure, substrate scope, immobilization techniques and mechanism having been published.<sup>209,212</sup> While the recombinant expression and purification of this enzyme in e.g. *E.coli* can encounter challenges through formation of inclusion bodies<sup>213</sup>, the enzyme shows remarkable robustness, since it retains activity even after incubation in organic solvents.<sup>214</sup> Unfortunately, due to the need of high water activity in the catalytic process, the enzyme itself is inactive in organic media.<sup>214,215</sup> The catalytic mechanism of the mandelate racemase is dependent on magnesium ions and facilitated by two catalytic residues: a lysine and a histidine (see Figure 21). The histidine attacks the free proton of the  $\alpha$ -C-atom, creating an aci-carboxylate intermediate. Through the rearrangement within the intermediate, the catalytic lysine is deprotonated, creating the other enantiomer of mandelic acid. This reaction is absolutely reversible and can run in the reverse direction, starting with the lysine attacking the free proton. The negative charges of the oxygens of the molecule are coordinated by a magnesium ion in the active site.<sup>216</sup>

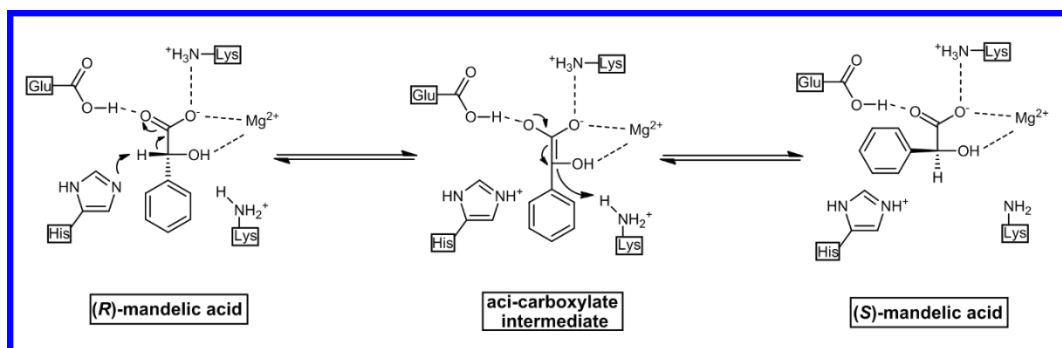


Figure 21: Mechanism of mandelate racemase from *Pseudomonas putida*. Adapted from Bearne *et al.* 2017<sup>216</sup>.

## 1.11 Circumvention of limitations in enzymatic catalysis

While the previously mentioned advantages of biocatalysis make it a viable option for utilization in chemical synthesis, its disadvantages (depending on the enzyme) can as well make its utilization counterproductive or not lucrative enough for a process. Drawbacks with enzyme thermo- and reaction stability, its substrate scope or unfavorable reaction equilibria coupled with possible substrate or product inhibitions may present a challenge for the successful employment of biocatalysts. It is not

unexpected, since enzymes are drawn out of their native environments and placed into unnatural settings. For instance, substrate loadings employed in industrial processes may exceed natural substrate concentrations by  $10^6$ - $10^9$  -fold (nM vs M).<sup>217</sup> Nevertheless, several paths revolving around both catalyst and reaction engineering lie open to even out such challenges.

### 1.11.1 Enzyme engineering

Since the structure-function relation for proteins applies to their catalytic function, it would be logical to assume, that the very same structure is responsible for other properties of an enzyme, like thermostability, solvent stability etc. Thus, by altering the enzyme's structure, its properties can also be altered. This assumption is the docking point for the discipline of enzyme (catalyst) engineering through directed evolution or rational design. Since the proteins tertiary structure is formed by amino acids, altering the primary amino acid sequence of a protein influences its folding and, in the end, structural properties. Proteins are usually produced by living organisms through expression from DNA, which carries the information about the proteins primary structure. So, the exchange of amino acids and subsequent altering the protein structure is performed at the DNA-level through the mutation of genes encoding the enzyme of interest. This can be done through random and rational methods.<sup>218-221</sup>

Random mutagenesis, as the name suggests, is based on mutating random amino acid positions within the enzyme through faulty DNA amplification. The obtained enzyme variants are then screened for the desired parameters and beneficial mutants are selected. Those can be subjected to further iterations of the same mutation approach, if necessary. Although it is one of the older approaches to mutagenesis, it is still successfully used up to this day to improve enzyme functions.<sup>222,223</sup>

For rational mutagenesis, many different approaches exist. The main goal of it would be the identification of key amino acid residues which can then be subjected to targeted mutation. Techniques here range from site-saturation mutagenesis, where single targeted amino acid positions are randomized throughout the 20 possible proteinogenic amino acids, to computationally driven approaches and newly emerging computational tools like AlphaFold.<sup>224,225</sup> Sometimes, such regions can be identified through homology screening, meaning, that different organisms may develop similar structural patterns for the same reaction catalysis, or even through the reconstruction of protein sequences from extinct species.<sup>224,226-228</sup>

In today's science, all existing methods can be combined and repeated in several iterative cycles, until the desired effects on the enzyme are reached. However, it is incorrect to assume, that all mutations introduced into the enzyme sequence and structure may be beneficial. Mutations can be destabilizing and lead to a decrease or loss of activity.<sup>229</sup> Thus, the field of protein design predominantly drifts towards rational computationally driven protein design, based on structural predictions for potential mutants, to avoid unbeneficial mutants and reduce the time needed for the

obtainment of a mutated enzyme with desired properties.<sup>225,230</sup> All in all, enzyme engineering through directed evolution is a powerful tool, having achieved the improvement in many properties for different enzymes, including solvent tolerance, thermostability, cofactor dependence, substrate scope, stereoselectivity and many others.<sup>231–235</sup>

### 1.11.2 Le Chatelier's principle

The other approach to circumvention of enzymatic drawbacks is reaction engineering. One of the main pillars of reaction engineering, including enzymatic reactions, is the equilibrium law after Le Chatelier. It states, that a reaction system is always trying to reach the equilibrium state. Thus, under this principle, as soon as one of the equilibrium determining factors like pressure, temperature or substrate/product concentration is altered, the system tries to compensate and readjust the equilibrium by counteracting the change. This in turn means, that if an exothermic reaction is cooled, it will produce more product. If products were to be removed from the reaction equilibrium, the reaction would intensify to readjust the product concentration.<sup>236</sup> This fact can be and is exploited in order to maximize reaction yields in industrial processes.

### 1.11.3 Enzymatic cascades

One of the paths for reaction engineering of enzymatic reactions is the cascading of enzymes. This method is essentially a simulation of naturally occurring processes within living cells, where reaction products are processed by subsequent (sometimes many) reaction steps and each of these steps is catalyzed by its own enzyme. Like this, the isolation and purification of the intermediates (and the loss of material) in a multi-step synthesis can be circumvented. This same principle also works for possible product inhibitions, since the resulting intermediates are processed by the next cascade step immediately.<sup>6,237</sup>

Enzymatic cascades are divided into five groups (see Figure 22): linear, parallel, orthogonal, convergent/divergent and cyclic. The application of such different cascade types may vary, depending on the chosen synthesis strategy. Linear cascades are a simple sequence of catalytic steps from multiple enzymes, leading to the final product.<sup>6,237</sup> It can however have its disadvantages, especially if each enzyme requires different cofactors or even pH optima. Sometimes those can be bypassed by a clever selection of catalysts, for example when the used reduced cofactor form of the first enzyme is reused by the second.<sup>238,239</sup>

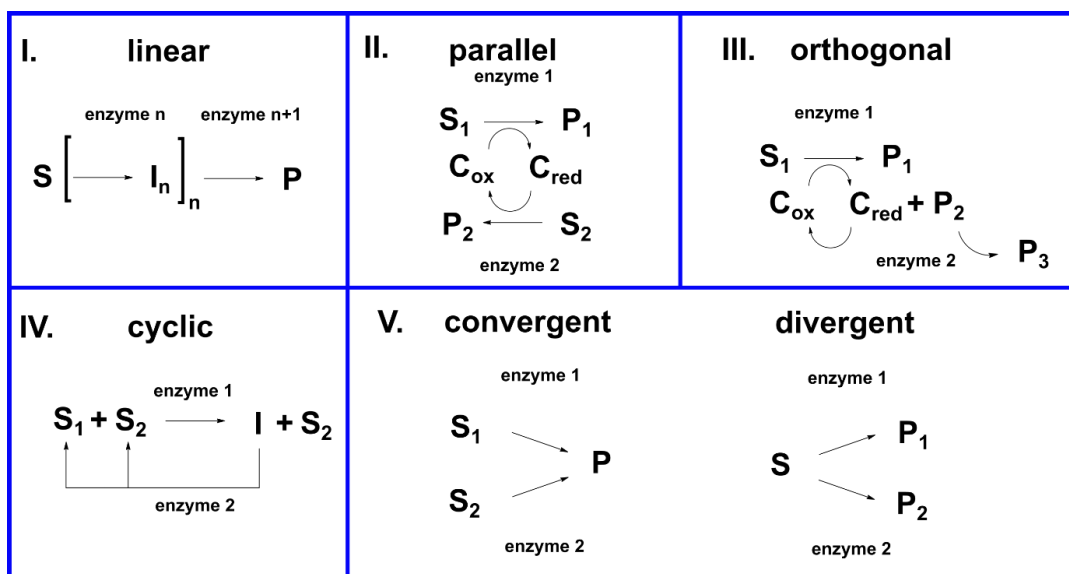


Figure 22: Types of enzymatic cascades. **I.** Linear cascades; **II.** Parallel cascades; **III.** Orthogonal cascades; **IV.** Cyclic cascades; **V.** Convergent and divergent cascades.

Parallel and orthogonal cascades are similar to each other. They are both used for shifts of reaction equilibria in redox reactions, which is especially important in terms of cofactor recycling. Here, the formation of a product is coupled with a formation of a by-product, e.g. a reduced cofactor form. This by-product can either be used (regeneration of cofactor to oxidized form) by a second enzymatic reaction happening in the reverse direction (oxidation or reduction) with a second substrate (parallel cascade) or serve as a substrate itself for a second enzyme converting it into another compound (orthogonal cascade), in both cases effectively removing it from the reaction equilibrium, thus achieving a pull to the product side. Enzymes like glucose dehydrogenases (GDHs) or formate dehydrogenases (FDHs) have found a broad application field for exactly those cascade types.<sup>240–243</sup> Convergent or divergent enzymatic cascades focus on a parallel conversion of one substrate towards two different products (divergent) or two substrates towards one product (convergent). In cyclic cascades, only one of two substrates is converted into an intermediate, which is in turn reconverted back into both initial substrates, which leads to the accumulation of one unconverted substrate in the mixture. Convergent and cyclic cascades are typical for deracemization of racemates, since the two used substrates can also be defined as two enantiomers.<sup>6</sup>

#### 1.11.4 Reaction engineering towards *in situ* product removal (ISPR) and *in situ* co-product removal (IScPR)

While enzymatic cascades mostly focus on the immediate further conversion of reaction products or by-products to shift reaction equilibria, it is always beneficial to evaluate, whether an enzymatic cascade is the simplest solution to product inhibition or equilibrium challenges. While cascades can be productive, they also complicate the reaction mixture by e.g. the need for several cofactors. Then again, stabilities and

inhibitions for multiple enzymes also have to be considered. Thus, other product and by-product removal strategies have also been developed. Those can be summarized under the terms *in situ* product removal (ISPR), sometimes also termed *in situ* product recovery, and IScPR (*in situ* co-product removal). ISPR is defined by the direct removal of reaction products from the reaction/catalyst amidst the progressing reaction via integrated simultaneous separation methods. Applying ISPR thus leads to fewer downstream processing steps for the biocatalytic processes, as well as reduced waste streams. This application field is fairly broad in terms of different separation methods in existence, which have to be selected according to the properties of the reaction product to be removed and the employed biocatalyst's properties.<sup>244–247</sup> Figure 23 shows a possible decision-making scheme on the selection of an appropriate separation method for combination with a biocatalytic reaction, based solely on possible product properties.<sup>248–251</sup>

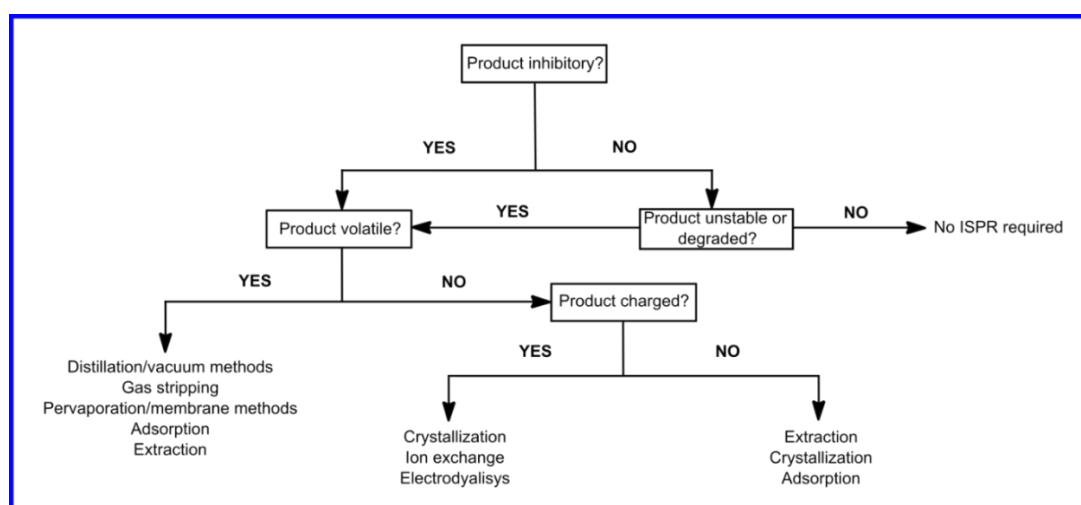


Figure 23: Flowchart for the selection of ISPR separation method based on the properties of the recovered product. Depending on the prevalent product properties and its stability one property may outweigh the other for the applied ISPR technique. Adapted from *van Hecke et al.* 2014, *Urbanus et al.* 2012 and *Stark et al.* 2003.<sup>248–250</sup>

If configured correctly, the advantages of ISPR have been described in literature. First of all, the main advantage of ISPR is the intensification of biocatalytic and fermentative processes in terms of productivity. Since product inhibition and product degradation can severely diminish productivity of processes, the transfer of the produced products directly out of the reaction equilibrium and, in some cases, the reaction itself altogether, increases productivity. Like this, product degradation can be prevented, while the removal from the equilibrium pushes the reaction towards the product side. Another advantage intertwined with productivity is product enrichment. Since some enzymes can naturally experience product inhibitions at very low product concentrations already, continuous product removal allows overall product concentrations in the reaction to reach higher levels, consequently making the separation process more effective in terms of isolated yields. This in turn also allows for higher substrate loadings for the processes, making them more lucrative for industrial applications.<sup>248</sup> ISPR applications can be fairly flexible in their configuration and operational mode (see Figure 24), since the integrated separation process can be

performed within the reactor (internal ISPR) or outside of the reactor (external ISPR), e.g. by cycling the reaction broth out of the reactor through a separation module and back into the reactor. Thus, also the direct and indirect modes of operation exist for ISPR modules. In the direct configurations, the biocatalyst is in direct contact with the product-separating phase, while in indirect configurations the contact is not present (e.g. blocked via a catalyst retention module).<sup>244–246</sup>

### ISPR configurations

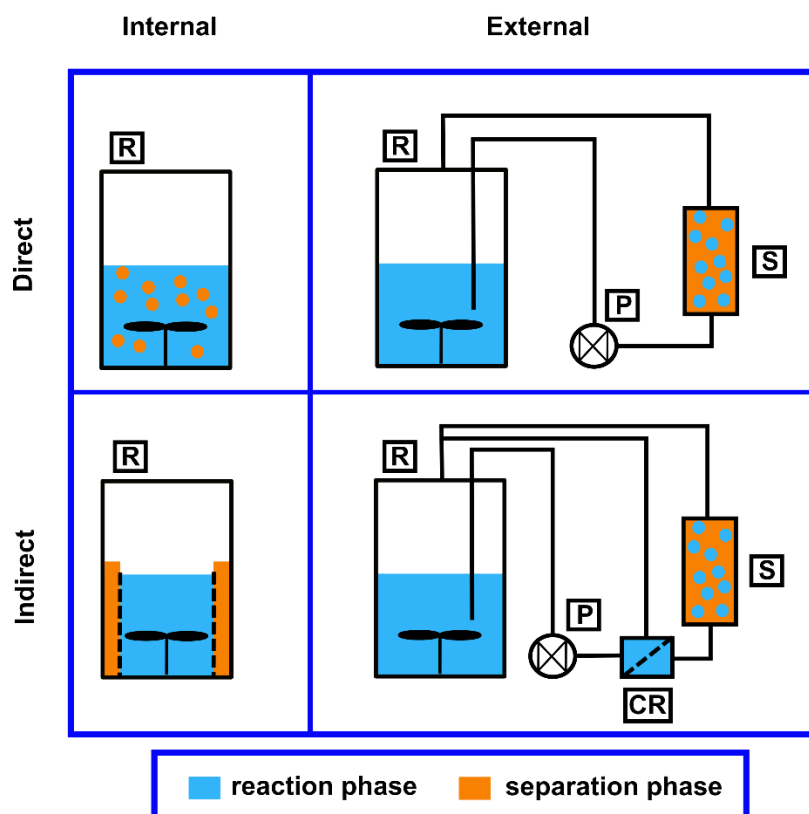


Figure 24: Schematic examples of different configurations and operation modes. R – reactor, S – separator, P – pump, CR – catalyst retention unit. Adapted from *Woodley et al.* 2008, *Buque-Taboada et al.* 2006 and *Freeman et al.* 1993.<sup>244–246</sup>

Several classes of ISPR-examples have been published over the past two decades. From a purely chemical standpoint, ISPR can be performed via the engineering of the substrates or co-substrates. This leads to examples like “smart” co-substrates. Essentially, the co-substrates (like amine donors in transamination reactions) are designed to undergo intrinsic rearrangements or reactions (like formation of ring structures) after the desired enzymatic reaction plays out, effectively denying their availability for the reverse reaction, thus removing those by-products from the reaction equilibrium. Those can be called self-eliminating.<sup>252–254</sup> Another possible approach would apply to volatile reaction products or by-products. Due to their volatility, it may be possible to remove them from aqueous media through simple pressure adjustments, using the principles of reduced pressure evaporation at mild temperatures. A constant reduced pressure or gas stream (so-called gas-stripping) would then carry away the product/by-product molecules from the forming gaseous phase, allowing the further

diffusion of by-product molecules into the gas phase, in turn allowing for further formation of those molecules in the aqueous phase (equilibrium shift).<sup>255–257</sup> However, considerations have to be made for the vapor pressures of the reaction components, so that the compound to be removed is not similar in vapor pressure to other substrates or products or the cosolvents. Ideally, the product would have the highest vapor pressure of them all. Since all reaction components would diffuse into the gas phase to some degree, this approach has the drawback of also extracting other reaction components, with possible losses in them and potential product impurities having to be considered.<sup>257</sup> Other options for ISPR are membrane-based approaches. For instance, volatile compounds can be recovered from the reaction by means of pervaporation (combination of permeability and evaporation), where a membrane permeable only/mostly for the desired product is applied between the (liquid phase) reaction and a gaseous extraction medium. The product permeates to the other side of the membrane, allowing it to evaporate (e.g. under reduced pressure/gas stream).<sup>258–260</sup> Like that, the disadvantages of normal evaporation or gas-stripping can be mitigated, allowing for the evaporation of only one desired compound. A similar principle is applied in the membrane distillation approach. A hydrophobic membrane is spun in contact with a heated reaction broth. This membrane does not allow for liquid water/polar compounds to permeate, however allows permeation for vaporized polar compounds. Thus, with the right heating mode, volatile organic compounds can be condensed outside the reaction under minimal loss of water in the reaction system.<sup>250,261,262</sup> Size-selective membranes can also be applied for simple diffusion-based methods, like dialysis. Here, pore-size is decisive, if small-size products are formed from big-size substrates, which then permeate the membrane due to osmosis into an extraction phase.<sup>263</sup> For charged compounds, this process can be accelerated by applying an electrical current for faster membrane permeation, resulting in the method of electrodialysis.<sup>264–266</sup> In electrodialysis, ion exchange membranes can be applied, allowing product permeation based on its charge (cation/anion exchange membranes). The same physical principles as for membrane-based ISPR approaches can also be applied to adsorption ISPR. In this ISPR field, specific surfaces or resins are mostly applied allowing for the adsorption of the product based on its properties (e.g. charge) or even affinity binding through surface modification, removing it from the solution and thus from the equilibrium.<sup>267–270</sup> Adsorption techniques can be applied for both charged and non-charged products.

A further ISPR field is simultaneous extraction of the reaction product, typically achieved in two-phase systems. Extraction processes for biocatalytic ISPR can be facilitated by e.g. hydrophobic, water-immiscible organic solvents. Such an approach requires the product to possess a better solubility in the extraction solvents than in water, allowing its efficient recovery with the extraction phase. While the utilization of classical organic solvents for this ISPR process, also called reactive extraction, is fairly common in literature<sup>271–273</sup>, examples of the utilization of hydrophobic polymers, like polyethylene glycol, or supercritical fluids also exist.<sup>274,275</sup> Nevertheless, this approach suffers from comparable drawbacks, as evaporation and gas-stripping. The extraction process can be fairly unselective, if the substrates or by-products also express a certain degree of hydrophobicity. Thus, reactive extraction

would also to some degree strip the reaction of substrates and contaminate the product isolate with undesired substances. Furthermore, the application of organic solvents may lead to the denaturation of the enzymes. However, this stability issue can be partially resolved through enzyme immobilization or the application of whole-cell biocatalysts. Improved reactive extraction strategies addressing those disadvantages have also been developed. In some cases, the extraction phase can be augmented by a complexing agent for the product, significantly improving the extraction selectivity.<sup>276</sup> Another possibility would be again the application of membranes in the process called perstraction (permeability and extraction). Here, a membrane is applied between the liquid reaction phase and a liquid extraction phase, facilitating the permeation of the desired product (again based on its properties, charged or non-charged) into the extraction phase.<sup>277,278</sup>

The previously described ISPR methods can be grouped based on liquid-to-liquid or liquid-to-gas product separation. Methods based on liquid-to-solid product separation also exist. Those are crystallization based ISPR methods, which will be discussed in detail in the next section. All in all, ISPR as a reaction engineering approach presents a powerful tool for the improvement of biocatalytic process productivity and lucrativeness in terms of shifting reaction equilibria and more efficient downstream processing of the obtained products.

## 1.12 Crystallization as a separation process

A solid state can be crystalline and amorphous, the defining property of a crystalline solid being the arrangement of particles in a highly organized coordinated three-dimensional pattern, a crystal lattice. Amorphous solids lack the degree of particle arrangement a crystalline state possesses, although some form of coordination may be present. Crystallization is thus defined as the formation process of a solid phase by the arrangement of particles in said lattice, forming a crystal.<sup>279</sup> Crystallization occurs spontaneously through fluctuations of the particle carrying phase (e.g. solution) in density and/or structure. This leads to a change in the free energy of the particles, which is compensated and lowered by the formation of an energetically minimized crystal state.<sup>280</sup> There are 32 possible crystal classes, a categorization based on all possible planes and axes of symmetry within observed crystal forms of cube (hexahedron), octahedron and cubo-octahedron (combination of both). Those are grouped into seven crystal systems, shown in Table 2.<sup>279</sup>



Table 2: Seven crystal systems and their defining properties.<sup>279</sup>

Crystal system	Further names	Nº of possible classes	Angles between 3D-axes	Length of 3D-axes	Examples of substances
<b>Regular</b>	Cubic Octahedral Isometric Tesseral	5	$\alpha = \beta = \gamma = 90^\circ$	$x = y = z$	NaCl
<b>Tetragonal</b>	Pyramidal Quadratic	7	$\alpha = \beta = \gamma = 90^\circ$	$x = y \neq z$	$\text{NiSO}_4 \cdot 7\text{H}_2\text{O}$
<b>Orthorhombic</b>	Rhombic Prismatic Isoclinic Trimetric	3	$\alpha = \beta = \gamma = 90^\circ$	$x \neq y \neq z$	$\text{AgNO}_3$
<b>Monoclinic</b>	Mono-symmetric Clinorhombic Oblique	3	$\alpha = \beta = 90^\circ \neq \gamma$	$x \neq y \neq z$	Oxalic acid
<b>Triclinic</b>	Anorthic Asymmetric	2	$\alpha \neq \beta \neq \gamma \neq 90^\circ$	$x \neq y \neq z$	$\text{CuSO}_4 \cdot 5\text{H}_2\text{O}$
<b>Trigonal</b>	Rhombohedral	5	$\alpha = \beta = \gamma \neq 90^\circ$	$x = y = z$	$\text{NaNO}_3$
<b>Hexagonal</b>	None	7	$\alpha = \beta = 90^\circ; \gamma = 120^\circ$	$x = y \neq z$	Water (ice)

Angles between the axes x and y have the designation  $\alpha$ , between y and z –  $\beta$  and between x and z –  $\gamma$ . The axes describe the positioning within a three-dimensional coordinate system.

In literature, several media exist, from which crystallization is achieved. Melts<sup>281</sup> and supercritical fluids ( $\text{CO}_2$ )<sup>282</sup> are among possible media for crystallization. Nevertheless, the most utilized phase, from which substances are (industrially) crystallized, is the liquid phase, a solution. Thus, if crystallization can be initiated within another phase (the carrying medium), it can be used as a separation technique by forming a new solid phase consisting of the desired particles, automatically removing them from the liquid phase. That is why crystallization is a very important separation and resolution technique for downstream processing in chemical and pharmaceutical industry, allowing for the crystallization of relatively pure substances from reaction or extraction media and their further recrystallization for purity increase. Hereby, solution crystallization (from liquid solvents) is the primary choice for pharmaceuticals and specialty organic compounds. Crystallization can be used for both simple product isolations from reactions and for chiral resolutions (crystallizing only one enantiomer of a racemate).<sup>283</sup>

Paramount for the estimation of crystallization conditions is the parameter of solubility. Each compound can be dissolved only to a certain concentration in a solvent of choice, this maximal concentration being called a solubility limit. A solution, in which the substance of choice concentration exceeds the solubility limit, is called supersaturated. Supersaturation can be maintained in a solution within a certain

(excess) concentration range for a certain period of time without the occurrence of crystallization. This range is called the metastable zone and the time until a solid phase is formed is titled the induction time. Within a supersaturated solution during the induction time, fluctuations of density and structure may occur. Those fluctuations lead to so-called nucleation. Nucleation is defined as the commencement of a new phase (solid for crystallization), nuclei being the seeds, around which crystallization may develop. In current literature, two nucleation models can be found (see Figure 25).<sup>279,283</sup>

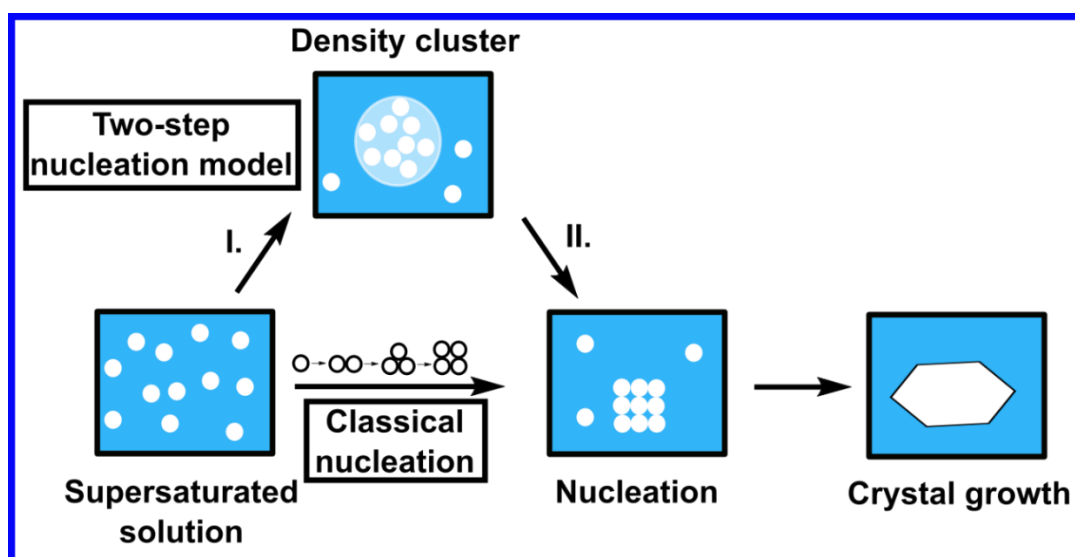


Figure 25: Schematic illustration of the nucleation models in literature. Adapted from *Chen et al.* 2011.<sup>280</sup>

The classical approach to nucleation describes the fluctuations in both density and structure to occur simultaneously, allowing the particles to stick together, gradually forming an organized nucleus. Initially, this nucleus formation increases the surface free energy change for small nuclei, partially prompting them to resolve again. Nevertheless, from a certain radius of the nucleus the free energy change reaches its maximum and begins to decrease, making the further growth of the crystal energetically beneficial. This change in free energy can be described through a term (2) composed of the change in bulk volume free energy difference between the first (liquid) and second (solid) phases ( $\Delta G_v$ ) and the change in surface free energy of the second phase per unit area ( $\Delta G_s$ ):

$$\Delta G = -\frac{4}{3}\pi r^3 \Delta G_v + 4\pi r^2 \Delta G_s \quad (2)$$

The two-step nucleation model, first introduced for protein crystallization<sup>284</sup>, states, that the fluctuations leading to nucleation rather are a transition from a structure fluctuation, forming a “superconcentrated” dense liquid droplet (density cluster), containing several particles of the compound (see Figure 25 I.), to a density fluctuation, reforming the droplet into a nucleus (Figure 25 II.).<sup>285</sup> Nucleation can further be distinguished into primary and secondary, where with the primary approach, the nuclei form as described above, while the secondary nucleation is artificially induced through seeding nuclei from a previously existent crystal into the

supersaturated solution.<sup>279</sup> Both supersaturation and nucleation are defining parameters for crystal growth and the resulting crystal size. By regulation of supersaturation and nucleation, the efficiency of crystallization can be regulated as well.<sup>279,283</sup> An example for such a regulation is the application of ultrasound during the crystallization process.<sup>286,287</sup> Ultrasound can facilitate an increase in nucleation (e.g. by breaking down forming crystals into secondary nuclei) but is not beneficial for crystal growth due to the same reason. A further influencing factor for supersaturation is the volume in which crystallization is to occur, as natural crystallization processes usually occur in confined volumes (e.g. pores of rocks).<sup>288</sup> For a solution to reach supersaturation, the solubility of a compound can be manipulated by temperature (increase for higher solubility and decrease for supersaturation) or by solvent change/mixing and its subsequent partial evaporation.<sup>283</sup>

To determine the conditions within a substance mixture (e.g. solution), in which the formation of a new phase (e.g. crystallization) by one of the substances of the solution may occur, a phase diagram of this mixture can be analyzed. A phase is the homogenous part of a system. The number of possible formed phases of a mixture is determined by the Gibbs phase rule (3):

$$F = C - P + 2 \quad (3)$$

where F is the number of degrees of freedom, C is the number of compounds and P is the number of formed phases.<sup>279</sup> As already described for crystallization, with a change in temperature, pressure, concentration (supersaturation) etc. a phase transition can occur. Phases are in equilibrium in an assortment of points along such varied conditions. The plotting of such equilibrium points against each other results in a phase diagram, from which the conditions for phase formations can be determined. A point, at which three phases can coexist, is called a triple point. In a two-component system (e.g. solvent and substance of interest), three factors determine phase formation: temperature, pressure and concentration (mole fractions).<sup>279</sup> In Figure 26, examples for binary phase diagrams of temperature plotted against the mole fractions of two components (A and B) are shown, highlighting three possible cases of crystallization behavior within such a system:

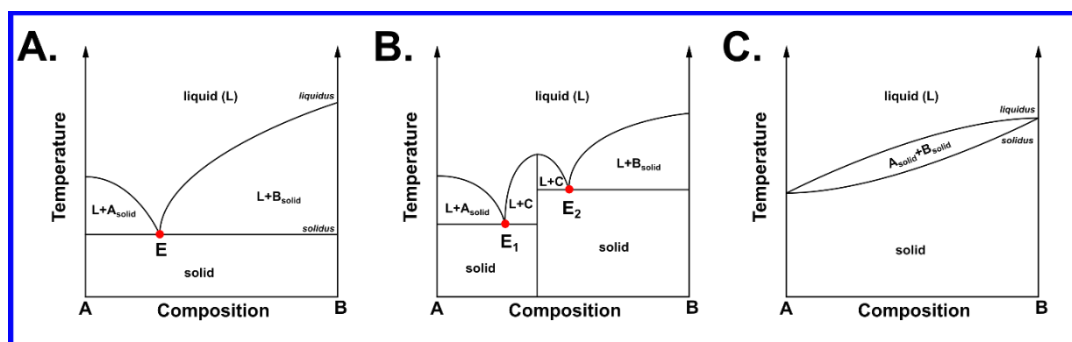


Figure 26: Binary phase diagrams for crystallization from a two-component system. **A.** Single eutectic system; **B.** Compound forming crystallization system; **C.** Mixed crystal system (solid solutions). A and B – substances forming the system, C – compound forming from both substances, E – eutectic point (marked in red). Adapted from Mullin 2004.<sup>279</sup>

The possibilities for the formed crystallization systems are dependent on the crystallization behavior of the substances in question. In the shown phase diagrams, the curves, called the liquidus, represent the condition transition line, beyond which both compounds exist in the liquid phase. The horizontal line or lines, called the solidus, represents the conditions transition, beyond which both compounds exist in their solid state. The point, where both liquidus curves and the solidus cross, is called the eutectic point. This is the transition point, at which the mixture's melting temperature is at a minimum. As can be seen, the position of the eutectic point can create two disproportionate triangular-shaped areas, at which a pure substance is crystallized. Thus, the bigger this disproportion (set by the positioning of the eutectic on the x-axis), the broader the set of conditions for the crystallization of only one substance from the mixture. For a single eutectic crystallization system, the phase diagram is fairly simple (see Figure 26 A.). Over the liquidus lines, only one liquid phase exists, containing both substances. In the triangular areas, formed by the liquidus, the solidus and the eutectic point, one of the substances crystallizes as a solid, while the other remains in the liquid phase. Beyond the solidus, both substances are solid.<sup>279</sup> The liquidus curves in a single eutectic system for a temperature-concentration diagram can be described by the Schröder-van Laar equation (4)<sup>289</sup>:

$$\ln(x) = \frac{\Delta H_m}{R} \left( \frac{1}{T_m} - \frac{1}{T} \right) \quad (4)$$

x is the mole fraction of the mixture,  $\Delta H_m$  – the melting enthalpy and T and  $T_m$  – the respective temperature and melting temperature.

For compound forming systems, the diagram is more complicated. Here, multiple different solids can be crystallized, formed by different proportions of the substances A and B (see Figure 26 B.). A typical example of such “compounds” consisting of both substances are hydrate salts, where water can be a part of the crystal lattice, but can be removed by e.g. drying. Due to the formation of a (or multiple) “compound”, the liquidus lines form several eutectic points with multiple different solidus lines, thus defining the regions of the “compound” crystallization beside the regions where the pure substances crystallize. Mixed crystal systems, also called solid solutions, are a special case for crystallization, since, as the name suggests, they form mixed crystals, in which both compounds are a necessary part of the crystal lattice. Thus, only one broad crystallization region exists (see Figure 26 C.) and the separation of the substances by crystallization becomes challenging.<sup>279</sup>

For three-component systems (e.g. solvent and two substances), ternary phase diagrams can be prepared (see Figure 27), plotting the molar fractions of the compounds in question against each other. As can be seen, all three crystallization systems display a similar behavior to the two-component systems binary phase diagrams, presenting similar patterns for a single eutectic (Figure 27 A.) and mixed crystal systems (Figure 27 C.). For a compound forming system (Figure 27 B.) the pattern of the crystallization areas is a little different than for the binary phase diagram, however the same areas of “compound” and pure substance crystallization are still present.<sup>279</sup>

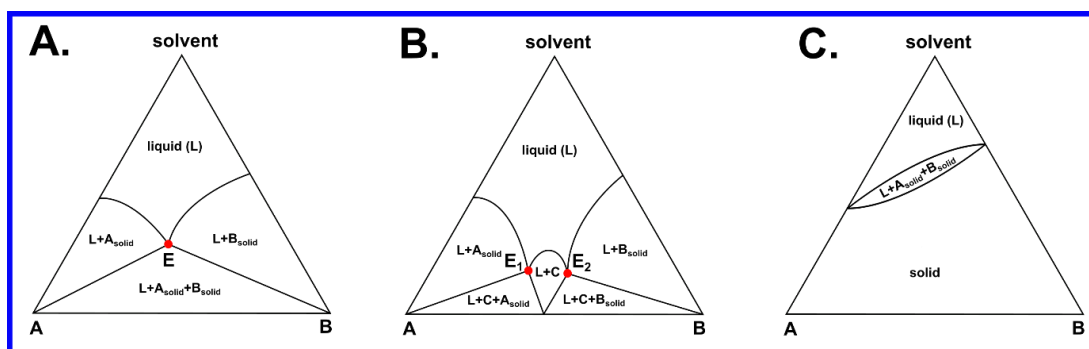


Figure 27: Exemplary ternary phase diagrams for a three-component system at a fixed temperature. **A.** Single eutectic system; **B.** Compound forming crystallization system; **C.** Mixed crystal system (solid solutions). A and B – substances forming the system, C – compound forming from both substances, E – eutectic point (marked in red). Adapted from Mullin 2004.<sup>279</sup>

A special case for phase diagrams is represented by racemic mixtures of two enantiomers, which can be viewed as the two substances in solution. Racemates can be divided into conglomerates and true racemates. Conglomerates are defined as an equimolar mixture of single enantiomer crystals, while true racemates crystallize as mixed crystals from both enantiomers.<sup>290</sup> Conglomerates are estimated to constitute 5-20 % of racemic mixtures, with the majority being true racemates.<sup>290,291</sup> Figure 28 shows the ternary phase diagrams for both cases.

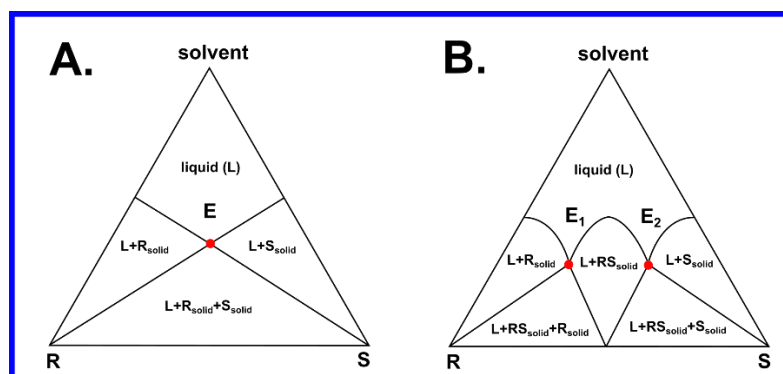


Figure 28: Ternary phase diagrams for racemic mixtures. **A.** Conglomerate; **B.** Racemate. R and S – enantiomers forming the system, RS – crystallizing racemate, E – eutectic point (marked in red). Adapted from Wang *et al.* 2008.<sup>290</sup>

Enantiomers possess the same chemical constitution, thus, their physical and chemical properties are also the same. This fact is reflected in the presented phase diagrams of racemic mixtures, since they display an absolute symmetry between the areas of crystallization. For conglomerates, resolution through crystallization is simplified, since only mono-substance crystals can be formed. Thus, the field of one enantiomer crystallizing without the other is fairly broad. For true racemates, however, the formation of racemic crystals has to be considered in the selection of crystallization conditions, narrowing the set of conditions for pure enantiomer crystallization.<sup>290</sup>

### 1.12.1 *In situ* product crystallization (ISPC)

While the value and popularity of crystallization for downstream processing cannot be undervalued, another application possibility for crystallization exists within the ISPR-approach to chemical and biocatalytic reactions. Within the biocatalytic community, this approach is titled “*in situ* product crystallization” (ISPC), while in the chemical and engineering communities the term “reactive crystallization” prevails.<sup>291</sup> The ISPC concept, as any ISPR concept, focuses on the removal of reaction products from the reaction phase to another phase, the solid phase, through crystallization. This offers several advantages. Some of those advantages are, of course, shared with other ISPR approaches, such as the increase in process productivity and selectivity, circumvention of (co-)product inhibitions and the protection of unstable/reactive products through removal. However, another advantage compared to liquid-liquid and liquid-gaseous ISPR can be found in the simplification of downstream processing, since the solid product can be filtered from the reaction broth (and recrystallized, if needed), reducing the number of downstream processing steps.<sup>291,292</sup>

Modes of operation for ISPC in terms of technical setup mimic the configurations in which ISPR also can be performed (see Figure 24). Crystallization can be facilitated internally and externally in the reactor-separator setup, while the direct or indirect contact of the (bio)catalyst with the crystallization phase determines the direct or indirect mode.<sup>292</sup> In terms of chemical properties of the crystallized compounds, three modes of operation can be distinguished: direct product crystallization, salt product crystallization and compound product crystallization. Direct product crystallization is based on the low solubility of the product compound in the solvent of choice, prompting it to precipitate. Thus, when this precipitation of the product is ignored, the employed catalyst’s productivity is wrongfully characterized as very high, although a simple equilibrium shift occurs through product crystallization.<sup>292</sup> Direct crystallization can occur spontaneously or can be induced by artificially lowering the product solubility by acidification, temperature control or other means.<sup>291</sup> Salt crystallization, on the other hand, must be induced. If the reaction product has the potential to form ions (e.g. through the presence of potentially ionic functional groups), a counterion can be added to form a product salt, which has much lower solubility in the solvent of choice, prompting it to crystallize out. Here, the counterion can be already present in the reaction (e.g. from previous steps) or can be added during the reaction process. Compound product crystallization can be defined as co-crystallization. It can occur spontaneously, co-crystallizing another compound from the reaction with the product (e.g. solvent for the formation of a solvate), or induced by the addition of a co-crystallizing compound. Direct product crystallization is probably the most preferred for industrial processes, since the crystallization of a single desired product compound reduces production costs (not needing other crystallizing agents) and downstream processing steps, eventually needing only final purification steps. However, direct crystallization is not so frequently achieved, since it relies only on the solubility properties of the product and cannot always be sufficiently induced. Nevertheless, examples can be found throughout literature. An

example of direct product crystallization was presented by Merck & Co for the synthesis of the anti-viral drug islatravir in a multi-step enzymatic cascade (shown in Figure 29 A.) At the end of the process, the pure islatravir crystallized due to low solubility with a purity of 95 % and an overall process yield of 51 % (determined on the basis of all four steps).<sup>293</sup> For salt ISPC, significantly more examples exist in literature. Those range from simple precipitation of metal salts from fermentation processes<sup>294,295</sup>, to the formation of more complex salts, as shown by Ren *et al.* (see Figure 29 B.) on the example of bulky quaternary ammonium salts of different dihydroxybenzoic acids as means to push the reaction equilibrium of a decarboxylase.<sup>296</sup> ISPC can also be used for the removal of undesired or inhibiting co-products of the reaction, which was recently shown by Merck & Co for an alternative chemoenzymatic route towards islatravir, removing the inhibiting hydrogenphosphate co-product ions as a simple calcium salt.<sup>297</sup> For compound crystallization ISPC, examples for the crystallization of solvates are frequently found. In particular, several  $\beta$ -lactam antibiotics have been described to crystallize as mono- or trihydrates from reactions catalyzed by penicillin G acylase, allowing for the development of several efficient ISPC-based processes for their production (see Figure 29 C.), also helping to protect the antibiotic product from secondary hydrolysis.<sup>298–300</sup> However, processes actively utilizing co-crystallization of products with other organic compounds can also be found throughout literature.<sup>301</sup>

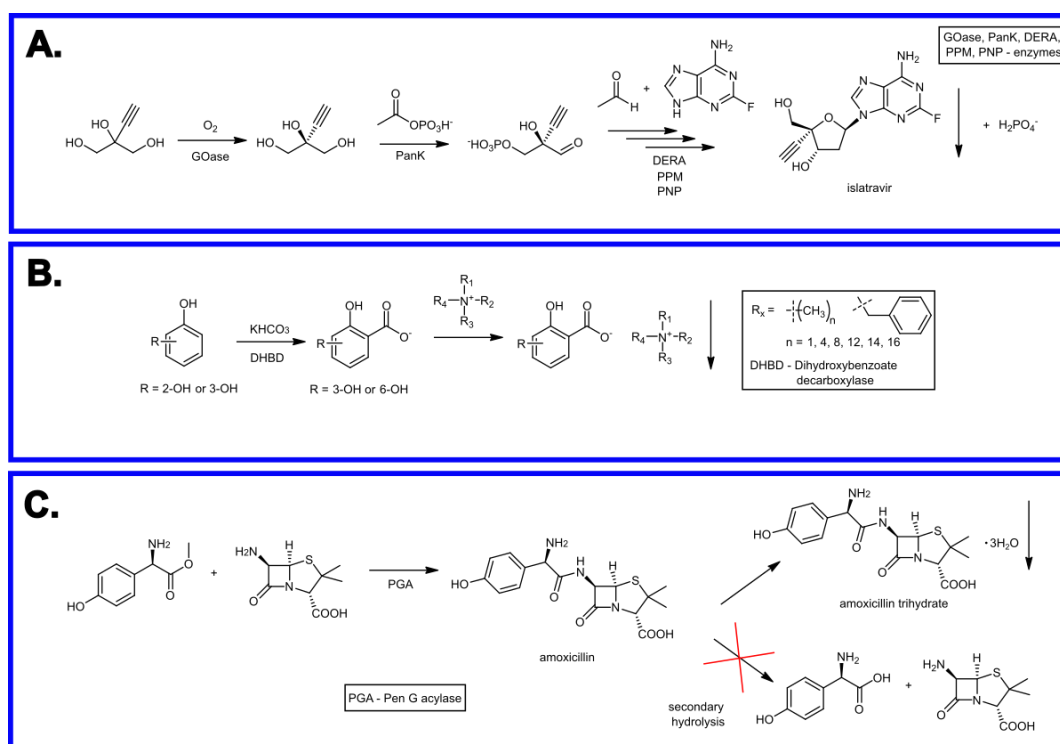


Figure 29: Examples for direct, salt and compound ISPC from literature. **A.** Direct ISPC of islatravir from a multi-step enzymatic cascade.<sup>293</sup> **B.** Salt ISPC of dihydroxybenzoic acid from a carboxylase-catalyzed reaction as quaternary ammonium salts.<sup>296</sup> **C.** Compound ISPC of an amoxicillin solvate from a penicillin G acylase-catalyzed reaction. Crystallization prevents secondary hydrolysis of the reaction product.<sup>298</sup>

While crystallization is often used in classical chiral resolutions, it can also be utilized for dynamic kinetic resolutions to push the reaction equilibria towards the product side within an ISPC approach. Amphoteric compounds, like amino acids, display the lowest solubilities at neutral pH values (if only one amino and one carboxyl group are present). Thus, this can be exploited for direct product crystallization, especially if the amino acid possesses a hydrophobic side chain. This was shown by Encarnación-Gómez *et al.* in a case study on the chemoenzymatic stereoinversion and dynamic kinetic resolution of DL-phenylalanine and DL-methionine towards the respective L-amino acids. The crystallization itself was induced by cooling and achieved good process productivities.<sup>302</sup> A similar approach, combining enzymatic racemization with preferential crystallization has been shown by Würges *et al.* for the dynamic kinetic resolution of DL-asparagine.<sup>303</sup> The former approach make use of the direct product crystallization mode of ISPC, the latter approach crystallizes a monohydrate compound.

### 1.12.2 ISPC of amines

For amines, ISPC is often applied in the mode of salt crystallization, since the amine compounds tend to form ammonium cations. Thus, ISPC approaches can be encountered throughout literature, showing the application possibilities of reactive crystallization of amines. Hereby, ISPC concepts can be found both for enzymatic reactions, and as an improvement mechanism for existing classical (organic) chemistry synthesis approaches. In particular, Diab *et al.* show an optimization study for the synthesis of the anti-HIV drug nevirapine, where organic synthesis is coupled with continuous crystallization of nevirapine, purifying it in the process.<sup>304</sup> Quon *et al.* show a potent system for the efficient crystallization of the drug aliskiren as a hemifumarate salt. Continuous reactive crystallization of aliskiren is performed from a balanced mixture of ethanol and ethyl acetate and reaches high yields (> 92 %) and very high purities (> 99 %).<sup>305</sup> Reactive crystallization has also been applied for the chiral resolution of a variety of chiral amines from organic solvents by Kwan *et al.* Here, the amines were racemized using an iridium-based catalyst in continuous flow and crystallized as diastereomeric salts with either (*S*)-mandelic acid or (*S*)-ditoluoyltartaric acid, with diastereomeric excesses of the product salts reaching 96 % and yields of the enantioenriched phase reaching 80 %.<sup>306</sup> Another interesting approach for the reactive crystallization of amines can be found in the covalent formation of insoluble amides, their crystallization and recovery of the amine by bond breakage. Such an approach can be found for the synthesis of pharmaceuticals<sup>307,308</sup> and explosives precursors<sup>309</sup> as well as in the dynamic kinetic resolution of mandelic acid.<sup>310</sup>

For enzymatic amine synthesis, the application of ISPC has been particularly well studied for the enzyme class of transaminases. Hülsewede *et al.* proposed a concept of reactive crystallization of chiral amines (e.g. 1-phenylethylamine) from transaminase-catalyzed reactions. Here, a small organic amine, isopropylamine (IPA), was used as



the amine donor in the asymmetric synthesis of 1-phenylethylamine from a prochiral ketone (see Figure 30). This reaction, however, suffers from an unfavorable reaction equilibrium and (co-)product inhibition. Thus, crystallization was applied to shift this reaction equilibrium. The amine donor was dozed in as a salt of a bulky carboxylic acid, possessing limited solubility in water. Only a portion of the amine donor would dissolve and then be consumed by the reaction. This would free up the counterion (carboxylate) to form a salt with the amine product. This carboxylate anion was selected to have a much lower solubility as a product salt than the amino donor salt, ensuring efficient product crystallization, as shown by the high substrate conversion of > 99 %. In parallel, the co-product of the reaction, acetone, was continuously removed by evaporation under reduced pressure, shifting the reaction equilibrium even more.<sup>311,312</sup> This concept was further tested for a variety of chiral amines in transaminase-based reactions<sup>313,314</sup> and adapted into a semi-continuous ISPC approach for a highly efficient synthesis of (*S*)-(3-methoxyphenyl)ethylamine by Neuburger *et al.*, reaching cumulated yields of > 1 M of product amine salt on a preparative scale.<sup>315</sup>

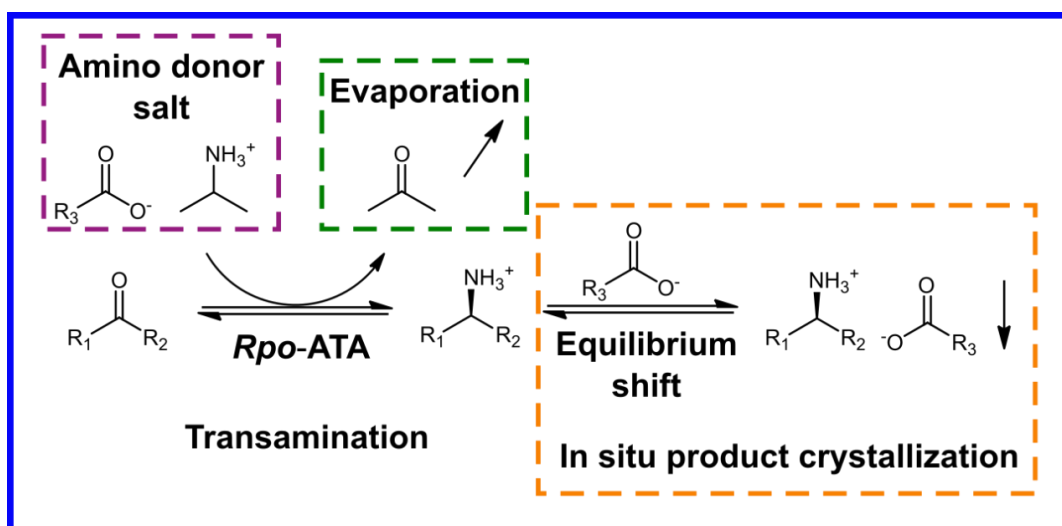


Figure 30: Concept of amine salt ISPC for the asymmetric synthesis of chiral amines proposed by Hülsewede *et al.* The amino donor is applied to the reaction as a salt and is consumed, allowing the counterion to crystallize with the product as a product salt.<sup>311,312</sup>

### 1.12.3 Crystallization and ISPR approaches for the production of enantiopure mandelic acid

Mandelic acid is an important building block and chiral agent for resolutions of racemic mixtures.<sup>316,317</sup> Several drugs, such as cyclandelate, clopidogrel and homatropine carry the base structure of mandelic acid or are its esters.<sup>316,318</sup> Thus, many approaches have been used to obtain mandelic acid as an enantiopure compound.

Usually, enantiopure mandelic acid is gained through classical resolution approaches, mostly employing diastereomeric crystallization.<sup>319–322</sup> With this approach, a chiral resolving agent is added to a racemic mixture to form two diastereomeric salts, which

would be equal in constitution but different in their physicochemical properties, including solubility in the solvent of choice, allowing to selectively crystallize only one diastereomeric salt (see Figure 31). However, as already mentioned, the efficacy of such a resolution is capped at the 50 % yield mark due to the availability of both enantiomers.

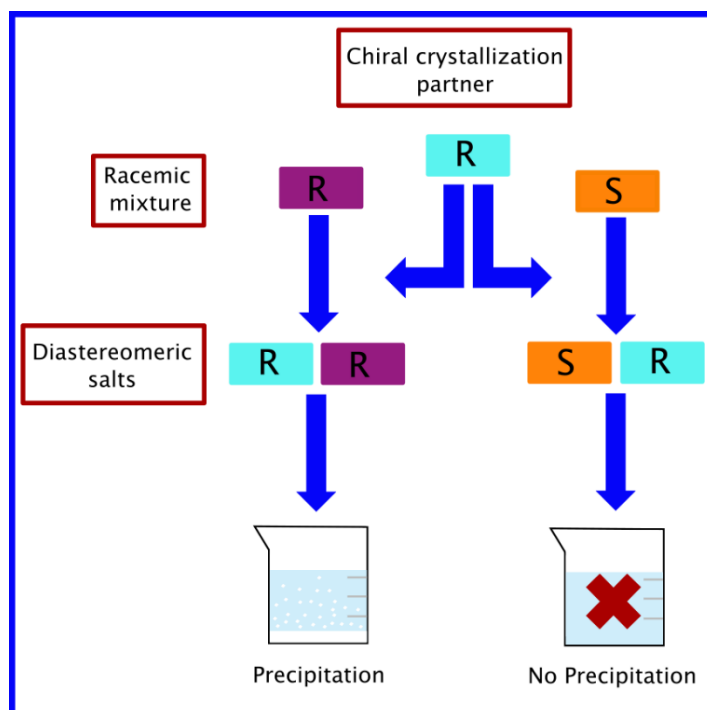


Figure 31: Concept of diastereomeric salt crystallization as means of kinetic resolution of racemic mixtures

Further, chemocatalytic stereospecific synthesis is also utilized.<sup>323,324</sup> While showing excellent yields and enantiomeric excesses of the produced mandelic acid derivatives, those synthesis strategies also employ a number of harsh reaction conditions, posing the question for the sustainability of such synthesis. Another approach frequently utilized for the obtainment of enantiopure mandelic acid would be KR and DKR, also already described in its principle. For the DKR of mandelic acid, the approaches differ in the selection of a racemizing agent and the resolving agent. With both aspects, enzymes are gaining ground, due to natural stereospecificity (resolving agent) or naturally occurring racemizing properties (racemizing agent). While enzyme classes like lipases may qualify as the resolving agent for mandelic acid and its derivatives<sup>318,325</sup>, few come into question as a racemizing agent. One prominent possibility for this purpose are mandelate racemases.<sup>215,326,327</sup>

In literature, there are also some examples of the application of *in situ* product removal in the synthesis of mandelic acid, mostly utilized to shift reaction equilibria of mandelate nitrilases in the DKR of mandelonitrile to mandelic acid, but those are scarce.<sup>328,329</sup> Nevertheless, a work combining the mandelate racemase enzyme coupled to ISPR was published by Wrzosek *et al.*, where chiral liquid chromatography was utilized as the resolving agent of the DKR of mandelic acid on a continuous basis, showing high yields and enantiomeric excesses of the enantiopure product.<sup>330</sup>

## 2. Objectives of this work

This work's main goal was to test different salt crystallization approaches and to integrate those into the biocatalytic synthesis of different chiral compounds, which serve as building blocks in the production of pharmaceuticals and fine chemicals. The general applicability of those crystallization techniques and their influence on the reaction system had to be evaluated for the efficiency in improving the synthesis yields and product separation. On the basis of this evaluation, a general toolbox of crystallization applications for biocatalytic reactions and the advantages of integrated product crystallization had to be showcased with the help of case studies on several structurally different model substrates.

Several routes of integrated product crystallization were considered. The existing concept for amine product salt crystallization, previously proposed by Hülsewede *et al.*<sup>312</sup>, was to be tested in another role. Although it was previously utilized for reactive crystallization of chiral amines in a continuous reaction setting, preliminary solubility data of the screenings showed, that the system also possessed potential as a straightforward approach for post-reaction product separation as a product salt, especially if reactive salt crystallization was not possible due to e.g. inhibition of the enzyme. This crystallization approach was to be tested for its selectivity towards the reaction product (amine) in the presence of large surpluses of low molecular weight amino donors (e.g. IPA) as those are usually present in biocatalytic amine synthesis. Furthermore, since other biocatalysts for amine synthesis also make use of large surpluses of their respective amino donors (e.g. amine dehydrogenases and ammonia), the post-reaction product isolation approach could also be tried for a possible transfer potential to those new reaction systems, since it was originally developed for transaminases only. For this purpose, a comparable model substrate had to be chosen, known to be reliably produced by both enzyme classes.

However, the scope of the reactive crystallization also had to be tested. Since the concept was previously tried exclusively for  $\alpha$ -chiral primary amines produced in a transaminase-catalyzed reaction, the substrate scope had to be tested for the  $\beta$ -chiral amine class, which is also a pharmaceutically relevant compound class, like the  $\alpha$ -chiral amines. Thus, since transaminases have been shown in literature to produce  $\beta$ -chiral primary amines, the reactive salt crystallization concept was to be tested in the synthesis of  $\beta$ -chiral amines, especially since possible substrates for this synthesis can possess self-racemizing properties allowing to perform a dynamic kinetic resolution through transamination.

Beside asymmetric synthesis, enantiopure compounds can be produced through the resolution of their respective racemates. Those are usually resolved via diastereomeric crystallization from organic solvent systems. So, if this concept would have to be integrated into biocatalytic synthesis, it would need to be adapted for aqueous media. With this adaptation, a chiral model compound, mandelic acid, had to be resolved to achieve high enantiomeric purity of the isolated enantiomer. This concept would

further need to be combined with biocatalytic reactions. This approach would need to be tested by integrating enzymatic racemization of mandelic acid with simultaneous diastereomeric salt crystallization, creating a concept for dynamic kinetic resolution of racemates of pharmaceutically relevant compounds through reactive diastereomeric salt crystallization.

For all three crystallization approaches, the respective reaction and crystallization conditions would need to be tested to achieve optimal yield improvements and enantiomeric purities of the target compounds. Moreover, the introduced integrated crystallization concepts would need to be tested on preparative scale to obtain a proof of concept of applicability in large-scale synthetic approaches, with the target being the introduction of integrated and reactive crystallization into biocatalytic industrial applications.

### 3. Case study I: Crystallization for selective post-reaction downstream processing of amines from enzymatic reactions

The previously described reactive crystallization concept developed by Hülsewede *et al.*<sup>312</sup> has proven a successful tool in the improvement of transaminase-catalyzed amine synthesis due to its ability to shift the reaction equilibrium to the product side by crystallizing the product amine as a carboxylate salt. The concept itself worked with dozing the carboxylate counterion into the reaction as a salt of the amino donor, which would be consumed during the reaction, allowing the free carboxylate to crystallize with the product (see Figure 30). While the concept was successfully applied in the synthesis of different chiral amines on a large scale<sup>315</sup>, it still had a significant challenge. As described by Hülsewede *et al.*, most of the tested “bulky” carboxylate counterions acted as inhibitors to several different tested transaminases even at lesser concentrations of 12.5-50 mM.<sup>312</sup> In fact, the discussed salt crystallization approach obtained a proof of concept with only one transaminase *Rpo*-ATA (*Sp*ATA in Hülsewede *et al.*) from the organism *Ruegeria pomeroyi* (old name: *Silicibacter pomeroyi*) due to it being the less inhibited one of the tested transaminase palette. Connected to this, a final choice of the carboxylate (3,3-diphenyl propionic acid – 3DPPA) was partially based on the fact, that its inhibitory effect was less constituted in solution due to low solubility. In the end, this fact allowed for a continuous process in a suspension-to-suspension setting, with only a small portion of the carboxylate being fully dissolved in the solution at any given point in time, yielding its inhibitory effect negligible. However, although the *Rpo*-ATA is a fairly versatile enzyme with a broad substrate spectrum, as proven by Hülsewede *et al.* and Tiedemann *et al.*<sup>311,313,314</sup>, it is mostly (*S*)-selective. Thus, the reactive crystallization concept would be limited to finding another “fitting” transaminase, which would survive the inhibition by a “bulky” counterion, if the (*R*)-enantiomer of a product would be required.

Nevertheless, this concept could be reworked to circumvent that limitation. If it was used solely for the purpose of post-reaction amino product isolation, there would be no inhibitory effects of the counterion on the enzyme. Here, the selective crystallization of only one of the two amines present in solution (amino donor vs amino product) would be paramount to gain versatility in application possibilities throughout any transaminase-catalyzed reaction system. If the counterion would be selected correctly, then the amino product could be crystallized into the solid phase as a carboxylate salt, while the amino donor would remain in solution. This can be achieved, if the solubility of the amino donor salt would be significantly higher than the solubility of the product salt (with the same counterion). Furthermore, as a simple means of downstream processing and product isolation, this system could in turn be tested with other enzymatic systems, such as amine dehydrogenases. Those typically

also use low molecular weight amino donors (ammonia, comparable to isopropylamine for transaminases), which are present in solution as ammonium cations. Thus, the separation of the amino product from the amino donor directly out of the reaction broth would in theory also be achievable via product salt crystallization. The study presented below obtained a proof of concept for both those points by achieving selective post-reaction product salt crystallization for both transaminase- and amine-dehydrogenase catalyzed reaction systems and establishing it as a viable downstream processing option by showing high yields and very high purities of the amino product salts.

For the study, 1-phenylethylamine was chosen as a model amino product to be isolated, since this chiral amine and important building block was previously shown in literature to be produced by both enzymatic classes of transaminases and amine dehydrogenases. As the model enzymes, the *Rpo*-ATA was chosen for the transaminase class and the genetically engineered LE-AmDH-v1 by Tseliou *et al.* was chosen for the amine dehydrogenases.<sup>164,312</sup> For both enzymatic systems, the usage of significant surpluses of their respective low molecular weight amino donor (IPA or ammonia, up to 2 M concentrations known in literature) is well established. Thus, for both systems, a carboxylate counterion would be needed to be found to have a much higher solubility as this donor salt, than as the product salt, to overcome the possible surplus interference and crystallize the product without significant impurities of the amino donor. Therefore, a solubility screening was performed for 10 counterions, which were selected based on preliminary works by Andrea Mildner and the screening performed by Hülsewede *et al.*<sup>312</sup> for the reactive crystallization concept. This solubility screening (Table 3) was performed on both (IPA and ammonia) amino donor salts of the selected enzymatic systems, as well as the common model product, (*S*)-1-phenylethylamine, which was chosen to be enantiomerically pure due to the high stereoselectivity of both enzymes. It has to be noted, that the carboxylates in the screening were achiral, thus, the solubilities measured for the (*S*)-1-phenylethylamine salts would also be true and applicable for the (*R*)-enantiomer salts, since enantiomers do not differ in their physical and chemical properties and no further stereocenters were introduced.

Table 3: Solubility screening of different ammonium salts of the carboxylates for post-reaction (*S*)-1-phenylethylamine salt crystallization.

Counterion	( <i>S</i> )-1-phenylethylamine salt solubility (mM)	IPA salt solubility (mM)	Ammonium salt solubility (mM)
3DPPA	5.4 ± 0.1	51.7 ± 0.3	216.5 ± 87.5
2DPPA	4.0 ± 0.1	78.6 ± 0.2	219.4 ± 23.2
<b>DPAA</b>	<b>10.8 ± 0.1</b>	<b>168.2 ± 1.3</b>	<b>223.5 ± 47.8</b>
4BPA	13.3 ± 0.5	83.6 ± 16.6	236.6 ± 56.0
<b>34CA</b>	<b>24.0 ± 0.7</b>	<b>203.1 ± 1.0</b>	<b>165.3 ± 49.0</b>
PCPA	18.9 ± 0.1	89.8 ± 0.5	192.8 ± 37.3
<b>43CNA</b>	<b>20.1 ± 0.4</b>	<b>1066.1 ± 20.0</b>	<b>2195.1 ± 121.7</b>
25CNA	62.5 ± 0.5	1529.2 ± 384.6	1714.8 ± 135.5
2BPA	62.5 ± 1.0	649.8 ± 24.3	1092.8 ± 74.2
PFA	69.1 ± 0.5	328.8 ± 35.4	470.1 ± 250.5

Based on the results of the screening 3 counterions were selected, shown in Figure 32: DPAA (diphenylacetic acid), 34CA (3,4-dichlorobenzoic acid) and 43CNA (4-chloro-3-nitrobenzoic acid). Those three possessed a very low product salt solubility (< 25 mM), while showing high amino donor salt solubilities. Although some other screening candidates had higher amino donor salt solubilities (e.g. 25CNA), their product salts also had a fairly high solubility. Thus, they were excluded from further investigation to maximize the obtained yields.

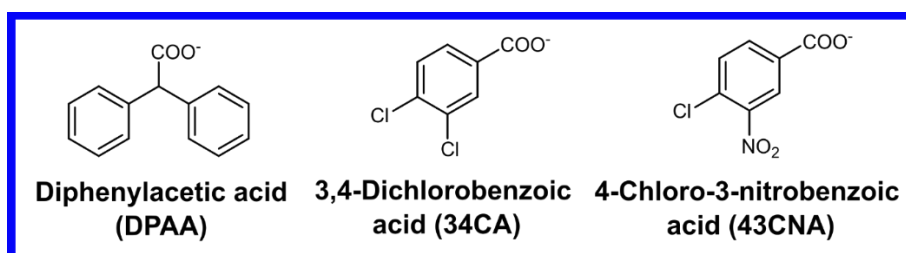


Figure 32: Carboxylate counterions for post-reaction (*S*)-1-phenylethylamine salt crystallization, selected based on the screening results.

The three selected carboxylates were subjected to a parameter screening to test the selectivity and effectiveness of the product salt crystallization. Here, in modelled reaction solutions containing 50 mM of the reaction product ((*S*)-1-phenylethylamine) and varied concentrations of the amino donor (50-1000 mM IPA or 250-2000 mM ammonia), the crystallization process was initiated by the addition of varying amounts

of the carboxylate anion (50-250 mM). Furthermore, the influence of temperature on the crystallization efficiency was also screened. Here, the performance of the carboxylates varied. DPAA performed very well in terms of crystallizing very high product yields with both a transaminase- (IPA as amino donor) and an amine dehydrogenase-catalyzed (ammonia as amino donor) systems, with yields reaching the 99 % mark. But in terms of selectivity, DPAA also crystallized a significant (over 10 %) amount of IPA impurities, especially with high IPA-amino donor concentrations present, making it unfit as a selective crystallizing agent for transaminase-based reactions. Nevertheless, when ammonia was the amino donor, DPAA showed the overall best performance in yields and purity of the product salts, making it ideally qualified as a selective crystallization tool for amine dehydrogenase-based systems. 34CA showed a mediocre performance in for both reaction systems in terms of yields and selectivity of product salt crystallization. In both systems, the yields with 34CA revolved around 60-80 %. 34CA also could withstand a significant surplus (1000 mM) of IPA, with the purity dropping only to 90 %. But 34CA was not able to withstand high ammonia concentrations, with product salt purity falling below the 70 % mark at 2000 mM  $\text{NH}_4^+$ . 43CNA performed better than 34CA as the counterion for product crystallization in both reaction systems. It showed product salt yields of 80-90 % and withstood high surpluses of both IPA and ammonia, with the product salt purities never falling below the 90 % mark, usually revolving at  $> 95$  %. Thus, 43CNA had the most versatility, being an effective counterion for both the transaminase- and amine dehydrogenase-catalyzed systems. For amine dehydrogenases, it was only slightly beaten by DPAA in terms of obtained product salt yield, but was further utilized for transaminase-based reactions.

For the further investigation of the selectivity of the product crystallization, ternary phase diagrams of the possible salt pairs were prepared. For transaminase reaction systems, the IPA-(*S*)-1PEA-43CNA salt pair was investigated (see Figure 33), for amine dehydrogenase reaction systems - the  $\text{NH}_4^+$ -(*S*)-1PEA-DPAA salt pair. Both phase diagrams showed a single eutectic system for the crystallization behavior of the salt pair mixtures. Both phase diagrams also displayed extreme asymmetry with the positioning of the eutectic point, allowing for a very broad set of crystallization conditions for the crystallization of the (*S*)-1PEA product salts, proving the robustness of the selective salt crystallization systems and its broad applicability, withstanding high surpluses of interfering amino donors in different reaction conditions with the chosen counterions.



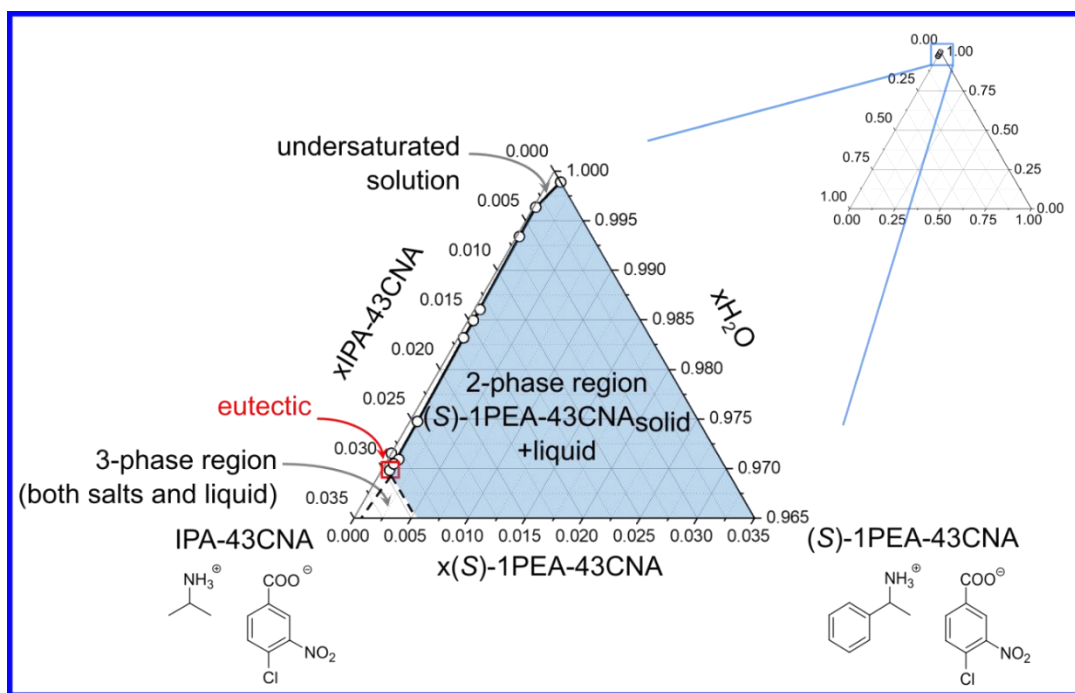


Figure 33: Exemplary phase diagram of the IPA-(S)-1PEA-43CNA salt pair. The positioning of the eutectic point on the extreme left allows for a broad spectrum of variability for the salt pair molar ratios to crystallize the pure product salt.

The final setup of the post-reaction product crystallization was tested on some real enzymatic reactions catalyzed by *Rpo*-ATA and LE-AmDH-v1. Both reactions produced approximately 50-70 mM of 1-phenylethylamine and were subjected to post-reaction product crystallization with 43CNA (transaminase) and DPAA (amine dehydrogenase). The obtained crystallized yields and product salt purities were fairly high (see Table 4) and can be seen as a proof of concept for both enzyme reaction systems. The post-reaction product crystallization concept showed very high selectivity and broad applicability as a downstream processing method for amine products from transaminase and amine dehydrogenase reaction broth. The presence of further ions, like cofactors, was shown to not affect the crystallization process, underlined by the high product salt purities.

Table 4: Crystallization yields and product salt purities of the preparative-scale enzymatic synthesis of 1-phenylethylamine.

Enzyme	1-phenylethylamine final concentration	Amino donor concentration in reaction	Crystallization yield	Product salt purity*
<i>Rpo</i> -ATA	72 mM	1500 mM	84 %	96 %
LE-AmDH-v1	55 mM	2000 mM	98 %	97 %

\*Determined by NMR

**Manuscript Title: “Crystallization-based downstream processing of  $\omega$ -transaminase- and amine dehydrogenase-catalyzed reactions”**

**Feodor Belov as the first author contributed the following to this manuscript: developed the concept of the study, performed most of the experiments and data curation, as well as the formal analysis of the data, its investigation and validation, developed the methodology and wrote the original draft of the manuscript, including all the visualization.** Andrea Mildner as the second author helped in the development of the concept and methodology by performing some preliminary tests, while also helping in the editing and review of the manuscript. Tanja Knaus and Francesco G. Mutti provided the genetic material and methodology needed for the use of the LE-AmDH-v1 amine dehydrogenase and helped in the editing and review of the manuscript. Jan von Langermann also helped in the theoretical conceptualization of the manuscript and provided the funding and resources needed for the practical work, as well as helping in the editing and review of the manuscript.

## 4. Case study II: Broadening the product scope of pharmaceutically relevant amine classes for reactive crystallization

Transaminases are mechanistically trimmed to produce primary amines as their transamination products. However, most of the works published for the transaminase enzyme class focuses on  $\alpha$ -chiral primary amines, meaning that the amino group is situated directly at the stereocenter. Considering the accepted theory about how the active site of transaminases is formed (one small and one big substrate binding pockets, coordinating the substrate positioning),  $\alpha$ -chiral amines can be considered as the more common, “native” form of the transamination product. However, literature shows, that transaminases can also produce other classes of primary chiral amines, like  $\beta$ -chiral amines.<sup>72,148,196</sup> Those are important chemicals, especially relevant as pharmaceuticals. But, due to the described mechanistic/steric hindrances, the synthesis of such compounds can become challenging for transaminases, leading to a decrease in yields. Nevertheless, there is potential in the utilization of transaminases due to their high stereospecificity. Furthermore, since such primary  $\beta$ -chiral amines would be synthesized by transamination from  $\alpha$ -branched aldehyde substrates, their intrinsic tautomerism would allow for the aldehyde’s racemization, in turn allowing to perform a dynamic kinetic resolution (see Figure 34) and maximizing the yield of the desired  $\beta$ -chiral amine enantiomer.

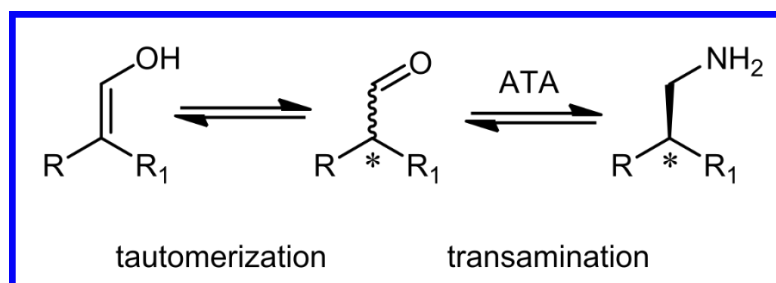


Figure 34: Transaminase-catalyzed DKR synthesis approach for  $\beta$ -chiral amines starting from auto-racemizing (via tautomerism)  $\alpha$ -branched aldehydes.

As can be seen, the only hindrance in realizing such a synthesis would be the unfavorable reaction equilibria of transaminases multiplied by possible steric hindrances of the substrate positioning in the active site. Here, the reactive crystallization concept by Hülsewede *et al.*<sup>312</sup> could be applied to resolve this issue. Since it was never before tested for the synthesis of  $\beta$ -chiral amines, we decided to apply it to further broaden its application scope in the synthesis of primary chiral amines. For that purpose, we chose a model compound, which was previously successfully synthesized by Fuchs *et al.* via transamination,  $\beta$ -methylphenethylamine (sometimes also abbreviated  $\beta$ -MPEA).<sup>72</sup> As the corresponding model transaminase, the well-established *Rpo*-ATA, which was also previously used by Hülsewede *et al.*, was chosen. In initial tests, *Rpo*-ATA showed conversion of the  $\alpha$ -branched racemic

aldehyde 2-phenylpropanal to  $\beta$ -methylphenethylamine. However, the presence of another by-product could be determined in those reactions. The by-product could be identified as acetophenone. Due to significant levels of this by-product (meaning significant substrate loss for the reaction), the source of its formation was further analyzed. Tests for pH-levels, light and the removal of air from the reaction solution revealed, that the formation of acetophenone was significantly hindered, when air oxygen was removed from the reaction (see Figure 35). This inhibition of by-product formation in turn facilitated better synthesis yields of the transamination reaction as a whole.

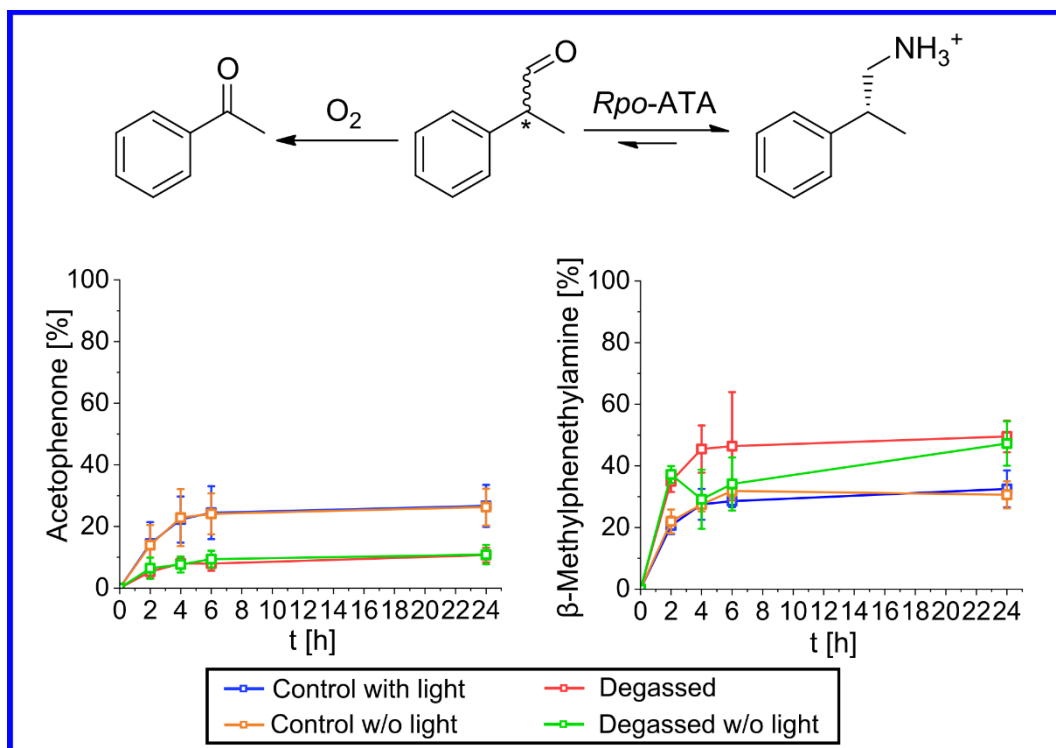


Figure 35: The influence of air oxygen and light on the formation of the acetophenone by-product and reaction yields, tested by degassing the reaction solutions and protecting them from light.

To integrate the reactive crystallization concept with this reaction, a suitable crystallization counterion for the  $\beta$ -methylphenethylamine product salt needed to be found. Thus, a screening was performed using the ECS Acid Screening Kit (produced by Enzymicals), showing five promising candidates for the carboxylate counterions. Those were subjected to a further solubility screening to determine their solubility gap between the IPA salt solubilities (amino donor salt) and their respective product salts.  $\beta$ -Methylphenethylamine ((*S*)-enantiomer used in the screening) was kept enantiomerically pure to simulate the high stereospecificity of the transaminase, however the determined solubilities are also true for the other (*R*)-enantiomer, since all carboxylates of the product salts are achiral. The solubilities are shown in Table 5:

Table 5: Amino donor (IPA) and product salt solubilities for the chosen counterion carboxylates.

Counterion	( <i>S</i> )- $\beta$ -methylphenethylamine salt solubility (mM)	IPA salt solubility (mM)
3DPPA	14.4 $\pm$ 8.5	51.7 $\pm$ 0.3
2DPPA	18.6 $\pm$ 3.6	78.6 $\pm$ 0.2
DPAA	25.5 $\pm$ 5.8	168.2 $\pm$ 1.3
BPA	18.4 $\pm$ 3.8	40.7 $\pm$ 1.0
4BPA	15.4 $\pm$ 5.7	83.6 $\pm$ 16.6

Based on those results, DPAA was excluded from further investigation to maximize future product yields due to its product salt having a solubility > 25 mM. All other counterions were subjected to a screening to determine their ISPC potential and to successfully integrate reactive crystallization into the workflow. It was started at 50 mM counterion concentrations to check for possible inhibitions of the enzymatic reaction, the counterions being utilized as amino donor (IPA) salts. Based on this screening, 3DPPA was excluded from further investigation due to showing inhibitory effects on this reaction at this minor concentration already (see Figure 36). The concentrations of the remaining three counterions in the enzymatic reaction setup were gradually increased to determine the concentrations facilitating the most yield increase benefits for the reaction through reactive product salt crystallization. Here, concentrations between 100 and 150 mM proved to be most beneficial, with 2DPPA outperforming the other two counterions in terms of yield (see Figure 36).

Having determined 2DPPA as the counterion of choice, a proof of concept for the successful integration of ISPC into the enzymatic *Rpo*-ATA-catalyzed synthesis of  $\beta$ -methylphenethylamine was obtained on a preparative scale. Experiments were performed with substrate concentrations of 100 and 200 mM and reached high yields, which were compared to control reactions without the integrated reactive crystallization (see Table 6). On the highest scale of 50 ml the reaction yielded 240 mM (63.2 % yield) of the product amine, amounting to a process productivity of approximately 16 g/l·d. *Rpo*-ATA, although being an (*S*)-selective enzyme with primary  $\alpha$ -chiral amines, changed its stereoselectivity for the  $\beta$ -chiral amine product, producing (*R*)- $\beta$ -methylphenethylamine with an enantiomeric excess of up to 99 %.

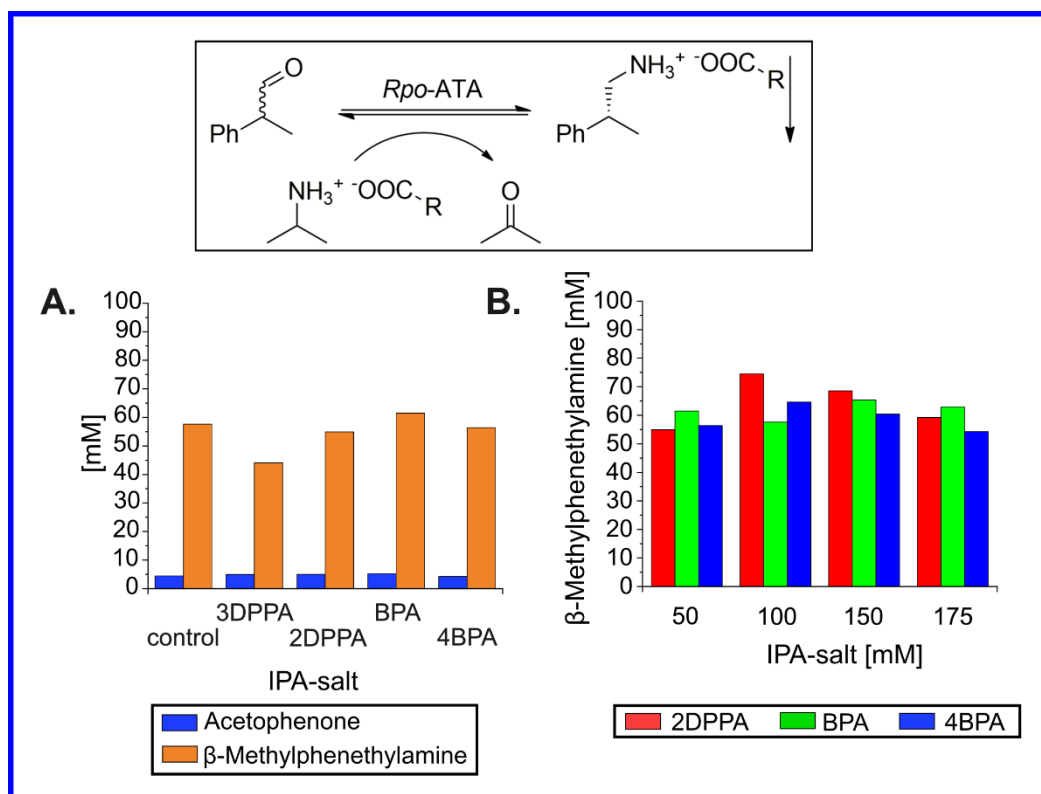


Figure 36: Results of screening for counterion inhibitions and their gradual concentration increase, determining 2DPPA as the best suited counterion for reactive crystallization of β-methylphenethylamine. **A.** Inhibition screening with 50 mM of counterion. **B.** Determination of ideal counterion concentrations. All reactions were performed with 100 mM of initial 2-phenylpropanal (substrate) concentrations.

Table 6: Yields and enantiomeric excesses of the preparative-scale β-methylphenethylamine synthesis.

Reaction volume (ml)	Substrate concentration (mM)	2DPPA counterion concentration (mM)	Yield (%)	Enantiomeric excess (%)
5	100	150	64.4	n.d.
5	100	0	28.7	n.d.
5	200	300	79.0	99.0 ( <i>R</i> )
5	200	0	43.0	94,6 ( <i>R</i> )
50	200	300	63.2	98.6 ( <i>R</i> )
50	200	0	43.3	96.8 ( <i>R</i> )

**Manuscript Title: “Crystallization Assisted Dynamic Kinetic Resolution for the Synthesis of (*R*)- $\beta$ -Methylphenethylamine”**

**Feodor Belov as the first author contributed the following to this manuscript: developed the concept of the study, performed most of the experiments and data curation, as well as the formal analysis of the data, its investigation and validation, developed the methodology and wrote the original draft of the manuscript, including all the visualization.** Alina Gazizova as the second author helped in the measurement of the enantiomeric excess of the reactions by performing the LC-MS analysis, while also helping in the editing and review of the manuscript. Hannah Bork performed the synthesis of halogenated 2-phenylpropanals, which were tested for their activity with the Rpo-ATA enzyme, while also helping in the editing and review of the manuscript. Harald Gröger conceptualized the proposed mechanism of radical chain reaction degradation of 2-phenylpropanal, while also helping in the editing and review of the manuscript. Jan von Langermann also helped in the theoretical conceptualization of the manuscript and provided the funding and resources needed for the practical work, as well as helping in the editing and review of the manuscript.





## 5. Case study III: Combining diastereomeric salt crystallization with enzymatic racemization for the resolution of chiral carboxylic acids

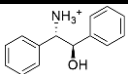
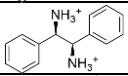
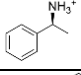
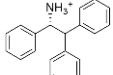
When enantiopure compounds are produced from their respective racemates, classical chiral or kinetic resolutions are mostly employed. In terms of product crystallization, approaches of diastereomeric crystallization are mostly chosen. For that purpose, organic solvents quite often find employ in such processes.<sup>320–322</sup> Standard-issue chiral resolutions of course always possess their main drawback of yield, since they can convert only a maximal theoretical cap of 50 % of the utilized racemate, leaving the undesired enantiomer unprocessed. Opposed to that, in biocatalysis, as demonstrated on the basis of the previous two case studies, crystallization with the help of achiral compounds is widely employed (e.g. achiral counterion for an amine product leading to product salt crystallization).<sup>311–315</sup> But even without the employ of a crystallization partner, in spontaneous or compound forming ISPC, the enantiopurity of the product is still defined only by the reaction itself. This means, that the utilized enzyme (catalyst) defines the enantiomeric excess of the product. While this fact can be beneficial if the utilized enzyme is highly stereospecific, producing 99 % enantiomeric excesses without the need to complicate the reaction system, an enzyme for such an application cannot always be found, especially when dealing with unnatural substrates. Thus, either catalyst engineering or another method for enantiopure product obtainment would be required. Here, a combination of diastereomeric crystallization with enzymatic synthesis can be applied. Diastereomeric crystallization is based on crystallizing only one diastereomer (based on only one of the product enantiomers) from the solvent of choice due to a difference in physical and chemical properties between diastereomers. Thus, in the case of insufficient enantiospecificity of the chosen enzyme, a chiral crystallization partner can be applied to the mixture of product enantiomers to preferentially crystallize only one product enantiomer as a diastereomer, significantly enriching the resulting enantiomeric excess. However, such an approach is very underrepresented in literature up to date.<sup>306</sup>

In the presented work, it was decided to develop and test such a concept on the basis of mandelic acid. Mandelic acid is an important chiral building block and a base structure for several pharmaceuticals, including cyclandelate, homatropine and clopidogrel.<sup>331,332</sup> While several approaches for chiral resolution through diastereomeric salt- or co-crystallization exist<sup>310,320–322</sup>, no approaches utilize diastereomeric crystallization for any kind of dynamic kinetic resolution of mandelic acid to circumvent the 50 % theoretical yield mark. This approach would require a simultaneous racemization of the remaining undesired enantiomer of mandelic acid to realize the DKR-approach, which up to date has been realized only via an enzymatic cascade between a mandelate racemase and a lipase<sup>327</sup> or via the coupling of the

mandelate racemase enzyme to stereospecific chromatography.<sup>330</sup> That is why we decided to use diastereomeric salt crystallization as the resolving agent in the DKR of mandelic acid, since the enzymatic racemization of mandelic acid via mandelate racemases has been fairly well studied, including its mechanism and the expression and preparation of the biocatalyst.<sup>213,216</sup> We also decided to increase the sustainability of the process by performing the crystallization in water, avoiding the need for organic solvents typically used for this purpose.

The first challenge, that needed to be overcome in this endeavor, was the finding of a suitable crystallization counterion. Mandelic acid possesses a very high solubility in water on its own, amounting to approximately 1 mol/l (over 150 g/kg of water for racemic mandelic acid, approximately half this amount for enantiopure mandelic acid).<sup>333</sup> Due to this fact, a variety of bulky chiral amine counterions were chosen, based on the work of the Hirose group<sup>321,334,335</sup>, which introduced the resolution of mandelic acid as a diastereomeric salt of (1*R*,2*S*)-2-amino-1,2-diphenylethanol ((1*R*,2*S*)-ADPE). We tried out several structurally similar counterions, including (*S*)-1-phenylethylamine ((*S*)-1PEA), (1*R*,2*R*)-1,2-diphenylethanediamine ((1*R*,2*R*)-DPEN) and (*R*)-1,2,2-triphenylethylamine ((*R*)-122TPEA), creating diastereomeric salt pairs of both enantiomers of mandelic acid and measuring their solubility in water. The results of the measurements can be seen in Table 7:

Table 7: Solubility screening of the diastereomeric mandelate salt pairs with selected amine counterions in water.

Amine counterion	Structure of amine counterion	Solubility of ( <i>R</i> )-MA salt, mM	Solubility of ( <i>S</i> )-MA salt, mM
(1 <i>R</i> ,2 <i>S</i> )-ADPE		67.1 ± 6.8	56.3 ± 2.7
(1 <i>R</i> ,2 <i>R</i> )-DPEN		33.6 ± 4.8	88.5 ± 3.1
( <i>S</i> )-1PEA		6138.9 ± 370.9	204.1 ± 12.1
( <i>R</i> )-122TPEA		4.9 ± 1.1	9.3 ± 0.9

(1*R*,2*R*)-DPEN salts were measured as monoamine salts.

Two counterions showed a sufficient gap in the solubilities of their respective mandelate salts: (1*R*,2*R*)-DPEN and (*S*)-1PEA. This gap would allow to crystallize only one enantiomer of mandelic acid as a product salt, while the other one would mostly remain in solution. Thus, their performance in resolution experiments for racemic mandelic acid was tested (with varied amounts of counterion and racemic mandelic acid) and evaluated based on the achieved enantiomeric excess of enantiomerically enriched product salts (see Table 8):

Table 8: Results of the diastereomeric crystallization screening of (1*R*,2*R*)-DPEN and (*S*)-1PEA as potential resolving agents for racemic mandelic acid.

Racemic mandelate, mM	Amine Counterion	Counterion, mM	<i>ee</i> of product salt
1000	( <i>S</i> )-1PEA	500	66.7 ± 7.0% ( <i>S</i> )
500	( <i>S</i> )-1PEA	500	67.6 ± 1.6% ( <i>S</i> )
1000	( <i>S</i> )-1PEA	400	63.9 ± 1.8% ( <i>S</i> )
1000	( <i>S</i> )-1PEA	300	74.9 ± 9.4% ( <i>S</i> )
1000	( <i>S</i> )-1PEA	250	77.5 ± 11.1% ( <i>S</i> )
1000	( <i>S</i> )-1PEA	200	77.2 ± 0.7% ( <i>S</i> )
200	(1 <i>R</i> ,2 <i>R</i> )-DPEN	150	79.9 ± 2.6% ( <i>R</i> )
200	(1 <i>R</i> ,2 <i>R</i> )-DPEN	100	84.3 ± 2.8% ( <i>R</i> )
200	(1 <i>R</i> ,2 <i>R</i> )-DPEN	75	86.8 ± 4.3 % ( <i>R</i> )

As can be seen, (*S*)-1PEA had to be excluded from further investigation due to its inability to reach an enantiomeric excess of at least 80 % for the crystallized product salt. (1*R*,2*R*)-DPEN, on the other hand, showed promising data in terms of reached enantiomeric excess, although its solubility limits bound it to lower concentrations of mandelic acid for the resolutions. Nevertheless, when combined with racemization through a mandelate racemase, process continuity could be achieved and a higher yield accumulated over time.

A reaction setup with the addition of the mandelate racemase enzyme (as the racemizing agent) was planned and executed with different varying concentrations of the (1*R*,2*R*)-DPEN counterion. The introduction of racemization of the uncrystallized mandelate enantiomer to the crystallization resolution process thus turned it into a DKR. As can be seen from Figure 37, while (1*R*,2*R*)-DPEN was kept at low concentrations, the yields of both the DKR-based setup and the control without racemization were comparable, the enantiomeric excess of the product salt staying fairly high at 90 %. However, the doubling of the counterion concentration allowed for a much higher yield in the DKR-based approach, while only insignificantly increasing the yield of the control, also leading to a slight decrease of enantiomeric excess for the control experiments.

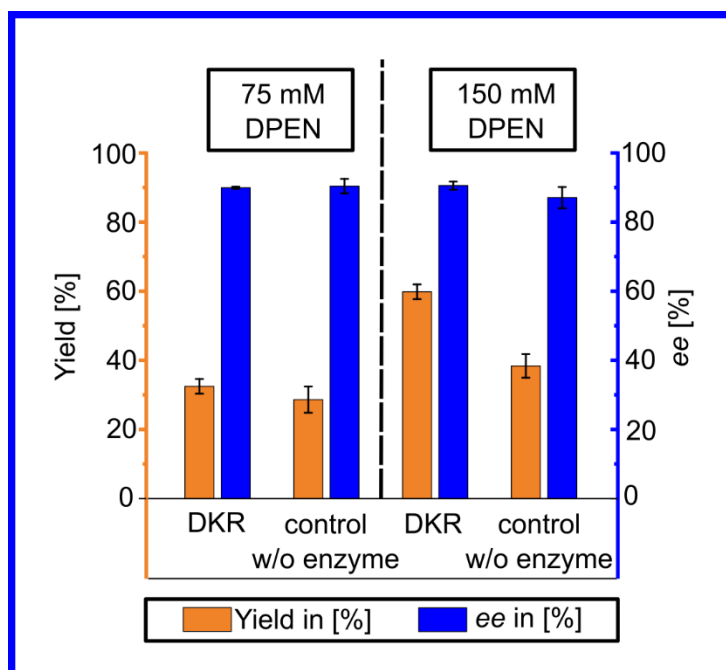


Figure 37: Yield and enantiomeric excess of the DKR-based mandelate crystallization experiments and controls (without mandelate racemase) with varying concentrations of (1R,2R)-DPEN.

Reaching yields of up to 60 % on a small scale, the applicability of this concept was further tested on preparative scale of 50 ml, reaching a yield of 60.3 % and an enantiomeric excess of 95 %. From the harvested product salt, mandelic acid was isolated with an isolated yield of 56 % and a purity of 94 %, proving the success of the introduced concept of dynamic kinetic resolution of mandelic acid by combination of diastereomeric salt crystallization with enzymatic racemization.

**Manuscript Title: “Crystallization-integrated mandelate racemase-catalyzed dynamic kinetic resolution of racemic mandelic acid”**

**Feodor Belov as the first author contributed the following to this manuscript: developed the concept of the study, performed the experiments and data curation, as well as the formal analysis of the data, its investigation and validation, developed the methodology and wrote the original draft of the manuscript, including all the visualization.** Alexandra Lieb as the second author mainly helped in the gathering and analysis of XRPD data, as well as helping in the editing and review of the manuscript. Jan von Langermann helped in the theoretical conceptualization of the manuscript and provided the funding and resources needed for the practical work, as well as helping in the editing and review of the manuscript.

## 6. Conclusion and Outlook

This work focused on the integration of crystallization methods to optimize biocatalytic provision of chiral pharmaceutically relevant compounds. The main goal was to achieve the optimization of classical biocatalytic synthesis in terms of yield output and the easing of further downstream processing steps. On the basis of three case studies, different forms of crystallization were tested out for different goals and reaction setups. In all three cases, a significant improvement of yields and downstream processing of the obtained products was achieved.

The first case study focused on selective crystallization of amine products from transaminase- or amine dehydrogenase-catalyzed reactions, which are prone to high surpluses of low molecular weight amino donors. The study managed to establish a post-reaction product salt crystallization approach from the reaction broths, with which the amino product could be selectively crystallized from the reaction mixture with very high purity (only trace amounts of the amino donors). Two counterions for the amino products (43CNA and DPAA) were found for each type of reaction (transaminase or amine dehydrogenase respectively) to be successfully applied in preparative scale proof-of-concept experiments. Here, 43CNA achieved a crystallization yield of 84 % from a transaminase-catalyzed reaction for 72 mM of the product amine (60.5 mM crystallized) with a purity of the product salt of 96 %. An even greater efficiency was shown by DPAA in the amine dehydrogenase-catalyzed setup, where 98 % of 55 mM product amine were successfully crystallized with a purity of 97 %. The selective crystallization approach proved its robustness and reproducibility, since the crystallizations were performed at very high interfering amino donor concentrations 1.5-2 M (20-35-fold higher concentrations compared to the product amine). Thus, this study showcased the potential for application of selective crystallization as a downstream processing technique in the enzymatic synthesis of chiral amines. In general, since this work showcased the robustness of the proposed crystallization approach towards high amino donor concentrations, this concept could be applicable to any enzymatic amine synthesis route using low molecular weight amino donors. Thus, it is reasonable to assume, that this system can be applicable for at least the ammonia lyase enzyme class (utilizing ammonia as an amino donor, similar to amine dehydrogenases). Further classes in question would be reductive aminases and imine reductases, which can produce secondary amines from primary amino donors. However, the crystallization behavior of secondary amines in terms of salt formation could also be more complex, thus a further investigation would be required. Furthermore, the extent of possible pure product crystallization has not yet been tested to the fullest. According to the acquired ternary phase diagrams, the reaction systems show a very broad set of reaction conditions, from which the amine products could be crystallized with a high purity. Thus, crystallizations of higher product concentrations can be possible, however, the dosage of the counterions (43CNA or DPAA) also has to be analyzed accordingly to not exceed the solubility limits of the amino donor salts, thus decreasing the purity of the crystallized products. Such boundaries can be the

subject of a further study into the application range of the proposed selective product salt crystallization system, showcasing the extent of its efficiency. The promising results of this study advocate for a broader use of selective crystallization in the downstream processing of amine products in opposition to standard extraction- and chromatography-based methods, showing the potential for shortening of the downstream processing pipeline and, thus, the isolation costs of amine products from biocatalytic synthesis.

For the second presented case study, the concept of integrated *in situ* product salt crystallization was chosen. In literature, this concept has been applied to  $\alpha$ -chiral amines from transaminase-catalyzed reactions<sup>311–315</sup>, but never to the class of  $\beta$ -chiral amines. This work successfully proved the applicability of the introduced *in situ* product crystallization system for the transaminase-catalyzed production of  $\beta$ -chiral amines, proving the versatility of the concept, developed by Hülsewede *et al.* for almost any kind of transaminase-catalyzed reaction. Native yields of the *Rpo*-ATA enzyme in the synthesis of  $\beta$ -methylphenethylamine, reaching approximately 40 %, were improved by integrated product crystallization to 60–80 %, with process productivity on highest scale of 16 g/l·d. Furthermore, this study also diminished a significant source of substrate “bleeding” through oxidation to acetophenone as a by-product by the simple measure of degassing the experiments, also proposing the possible mechanism of substrate degradation through oxygen. The success of this study opens up new possibilities for the integration of the *in situ* product salt crystallization concept into the synthesis of  $\beta$ -chiral amines, especially in pharmaceutical industry. Previous studies on transaminase-catalyzed synthesis of the drug pregabalin and precursors for the drug brivaracetam<sup>196</sup> showed imperfect yields with many enzyme variants, usually amounting to 30–70 % conversions on a 50 mM substrate scale. Through *in situ* product salt crystallization, those yields can be improved significantly by shifting the equilibrium of the enzymatic transamination by ISPR. However, despite almost perfect enantiomeric excesses (95–99 %) achieved in this study by the *Rpo*-ATA enzyme, the literary research showcased, that yield is not always the main challenge in the production of  $\beta$ -chiral amines for most transaminases, but rather the enantiomeric excess. Examples throughout literature were encountered, where usually very stereospecific transaminases produced almost racemic mixtures (e.g. *ee* of 4 %) <sup>196</sup> of the  $\beta$ -chiral product, while in most cases the enantiomeric excess was around 50–60 %. <sup>72,148,196</sup> This is explainable by the geometry of  $\beta$ -chiral amines, since the additional CH<sub>2</sub>-moiety separating the amino group from the chiral center can sterically interfere with substrate positioning in the highly conserved small and big substrate binding pocket of the transaminases, leading to possible inversions in stereopreference or decreases in stereoselectivity due to randomized substrate positioning (or, in the case of  $\alpha$ -chiral aldehydes, increased acceptance of the undesired enantiomer). Thus, especially for such cases, another *in situ* product crystallization concept would need to be developed, which would not only improve the yield by crystallizing the product out of the reaction, but would also improve the enantiopurity of the crystallized product phase leaving the undesired product enantiomer in solution, allowing it to be reconverted back to the substrate (reverse reaction of transaminases) and to be converted into the new proportions to the desired enantiomer. The iteration

effect of this back-and-forth conversion-crystallization-reconversion process would lead to the accumulation of (ideally) an enantiopure crystallized product phase over time.

Thus, in the third presented case study, an attempt was made to develop exactly such a concept through the introduction of integrated diastereomeric crystallization of mandelic acid from an enzymatic reaction in an aqueous phase with the help of a chiral amine counterion. Since mandelic acid also is a relevant precursor for the production of several pharmaceuticals, the introduced approach would not only be applicable for better crystallization of chiral amines, but would also present a viable option for the resolution and enantiospecific crystallization of pharmaceutically relevant carboxylic acids. The presented work managed to successfully couple enzymatic racemization of mandelic acid with diastereomeric salt crystallization, a technique frequently used in standard-issue chiral resolutions of racemates, in a DKR-based process. Yields of up to 60 % (calculated from the amount of utilized racemate, not a single enantiomer) were achieved with a very good enantiomeric excess of 95 % on preparative scale. Thus, a concept for enantioselective product salt crystallization from aqueous enzymatic reactions could be established, with a potential to get even better yields. For such an improvement, an investigation into the ternary phase diagram of the solubilities of the diastereomeric mandelate salts would be necessary, showcasing the limits of applicability (especially the maximum mandelic acid and counterion concentrations). However, the third case study just developed a preliminary concept, which has several possible routes of application development. First of all, it would be possible to utilize it for the DKR of other pharmaceutically relevant carboxylic acids, like ibuprofen, ketoprofen or naproxen<sup>336</sup>, if the right racemizing agent for them could be found. Then again, this concept could be inverted to utilize enantiopure mandelic acid to realize the proposed improvement of enantiomeric excesses in transaminase-catalyzed production of chiral amines. For  $\beta$ -chiral amines this concept would be simpler, since the  $\alpha$ -chiral aldehyde substrates already possess self-racemizing properties through keto-enol tautomerization. Nevertheless, this concept would also be applicable for  $\alpha$ -chiral amines, although slower reaction rates can be expected with the more stable achiral ketone substrates (however, the reverse reaction of the undesired enantiomer would in turn be faster, as it would be energetically preferred). Then, this concept could also be developed into the form of an enzymatic cascade, where the costlier enantiopure mandelic acid could be replaced by a racemate with the addition of a mandelate racemase to the mixture. Like that, the diastereomeric mandelate salt of the overproduced product enantiomer would crystallize first, while the unused mandelate enantiomer would be racemized, ensuring a constant supply of the needed mandelate enantiomer to the process. Replacing the enantiopure mandelate with a cheap racemate would thus save some costs to the establishment of the process while retaining its benefits.

To conclude, the presented work aimed to showcase the versatility of integrated crystallization methods for different types of applications in enzymatically catalyzed reactions, especially in the production of chiral amines. The findings of this work strongly encourage the utilization of integrated crystallization methods in biocatalytic

reactions, since they can not only mitigate some of the disadvantages of imperfect enzymatic catalysts with non-native substrates by increasing process productivities, but also shorten the downstream processing and purification pipelines, saving time and costs in the production of enantiopure compounds.



# Bibliography

- 1 D. G. Truhlar, Interpretation of the activation energy, *J. Chem. Educ.*, 1978, **55**, 309.
- 2 M. Menzinger and R. Wolfgang, The Meaning and Use of the Arrhenius Activation Energy, *Angew. Chem. Int. Ed. Engl.*, 1969, **8**, 438–444.
- 3 K. J. Laidler, The development of the Arrhenius equation, *J. Chem. Educ.*, 1984, **61**, 494.
- 4 Z. A. Piskulich, O. O. Mesele and W. H. Thompson, Activation Energies and Beyond, *J. Phys. Chem. A*, 2019, **123**, 7185–7194.
- 5 E. Roduner, Understanding catalysis, *Chem. Soc. Rev.*, 2014, **43**, 8226–8239.
- 6 K. Faber, *Biotransformations in Organic Chemistry*, Springer International Publishing, Cham, 2018, pp. 1-30, 31-314, 315-406.
- 7 A. Schmid, J. S. Dordick, B. Hauer, A. Kiener, M. Wubbolts and B. Witholt, Industrial biocatalysis today and tomorrow, *Nature*, 2001, **409**, 258–268.
- 8 D. Alonso and A. Mondragón, Mechanisms of catalytic RNA molecules, *Biochem. Soc. Trans.*, 2021, **49**, 1529–1535.
- 9 S. K. Silverman, Catalytic DNA: Scope, Applications, and Biochemistry of Deoxyribozymes, *Trends Biochem. Sci.*, 2016, **41**, 595–609.
- 10 A. S. Bommarius and B. R. Riebel, eds., *Biocatalysis*, Wiley, Weinheim, 2004, pp. 1-18, 19-42, 91-134.
- 11 <https://enzyme.expasy.org/>, (accessed 6 November 2024).
- 12 <https://www.uniprot.org/uniprotkb?query=enzyme>, (accessed 6 November 2024).
- 13 [https://nc.iucnredlist.org/redlist/content/attachment\\_files/2024-2\\_RL\\_Table\\_1a.pdf](https://nc.iucnredlist.org/redlist/content/attachment_files/2024-2_RL_Table_1a.pdf), (accessed 6 November 2024).
- 14 D. Whitford, *Proteins. Structure and function*, Wiley, Chichester, 2005, pp. 39-83.
- 15 C. M. Dobson, Protein folding and misfolding, *Nature*, 2003, **426**, 884–890.
- 16 J. D. Bryngelson, J. N. Onuchic, N. D. Socci and P. G. Wolynes, Funnels, pathways, and the energy landscape of protein folding: a synthesis, *Proteins*, 1995, **21**, 167–195.
- 17 P. E. Leopold, M. Montal and J. N. Onuchic, Protein folding funnels: a kinetic approach to the sequence-structure relationship, *PNAS*, 1992, **89**, 8721–8725.
- 18 D. Balchin, M. Hayer-Hartl and F. U. Hartl, Recent advances in understanding catalysis of protein folding by molecular chaperones, *FEBS Lett.*, 2020, **594**, 2770–2781.
- 19 B. Kalinowska, M. Banach, Z. Wiśniowski, L. Konieczny and I. Roterman, Is the hydrophobic core a universal structural element in proteins?, *J. Mol. Model.*, 2017, **23**, 205.
- 20 L. A. de Graaf, Denaturation of proteins from a non-food perspective, *J. Biotechnol.*, 2000, **79**, 299–306.
- 21 K. Griebenow and A. M. Klibanov, On Protein Denaturation in Aqueous–Organic Mixtures but Not in Pure Organic Solvents, *J. Am. Chem. Soc.*, 1996, **118**, 11695–11700.
- 22 D. E. Koshland, The Key–Lock Theory and the Induced Fit Theory, *Angew. Chem. Int. Ed. Engl.*, 1995, **33**, 2375–2378.
- 23 D. Herschlag, The role of induced fit and conformational changes of enzymes in specificity and catalysis, *Bioorg. Chem.*, 1988, **16**, 62–96.
- 24 D. M. Blow, J. J. Birktoft and B. S. Hartley, Role of a buried acid group in the mechanism of action of chymotrypsin, *Nature*, 1969, **221**, 337–340.
- 25 G. Dodson and A. Wlodawer, Catalytic triads and their relatives, *Trends Biochem. Sci.*, 1998, **23**, 347–352.
- 26 R. Wieczorek, K. Adamala, T. Gasperi, F. Polticelli and P. Stano, Small and Random Peptides: An Unexplored Reservoir of Potentially Functional Primitive Organocatalysts. The Case of Seryl-Histidine, *Life*, 2017, **7**. DOI: 10.3390/life7020019.
- 27 A. Rauwerdink and R. J. Kazlauskas, How the Same Core Catalytic Machinery Catalyzes 17 Different Reactions: the Serine-Histidine-Aspartate Catalytic Triad of  $\alpha/\beta$ -Hydrolase Fold Enzymes, *ACS Catal.*, 2015, **5**, 6153–6176.

- 28 R. Friedman and A. Caflisch, On the orientation of the catalytic dyad in aspartic proteases, *Proteins*, 2010, **78**, 1575–1582.
- 29 P. Brozic, S. Turk, T. Lanisnik Rizner and S. Gobec, Discovery of new inhibitors of aldo-keto reductase 1C1 by structure-based virtual screening, *Mol. Cell. Endocrinol.*, 2009, **301**, 245–250.
- 30 M. Richter, Functional diversity of organic molecule enzyme cofactors, *Nat. Prod. Rep.*, 2013, **30**, 1324–1345.
- 31 C. Andreini, I. Bertini, G. Cavallaro, G. L. Holliday and J. M. Thornton, Metal ions in biological catalysis: from enzyme databases to general principles, *J. Biol. Inorg. Chem.*, 2008, **13**, 1205–1218.
- 32 P.-L. Hagedoorn, M. Pabst and U. Hanefeld, The metal cofactor: stationary or mobile?, *Appl. Microbiol. Biotechnol.*, 2024, **108**, 391.
- 33 J. D. Fischer, G. L. Holliday, S. A. Rahman and J. M. Thornton, The structures and physicochemical properties of organic cofactors in biocatalysis, *J. Mol. Biol.*, 2010, **403**, 803–824.
- 34 K. Hult and P. Berglund, Enzyme promiscuity: mechanism and applications, *Trends Biotechnol.*, 2007, **25**, 231–238.
- 35 O. Khersonsky and D. S. Tawfik, Enzyme promiscuity: a mechanistic and evolutionary perspective, *Annu. Rev. Biochem.*, 2010, **79**, 471–505.
- 36 M. Martinelle and K. Hult, Kinetics of acyl transfer reactions in organic media catalysed by *Candida antarctica* lipase B, *Biochim. Biophys. Acta*, 1995, **1251**, 191–197.
- 37 F. Secundo, G. Carrea, C. Soregaroli, D. Varinelli and R. Morrone, Activity of different *Candida antarctica* lipase B formulations in organic solvents, *Biotechnol. Bioeng.*, 2001, **73**, 157–163.
- 38 A. A. Saboury, Enzyme inhibition and activation: A general theory, *J. Iran. Chem. Soc.*, 2009, **6**, 219–229.
- 39 A. Tuley and W. Fast, The Taxonomy of Covalent Inhibitors, *Biochemistry*, 2018, **57**, 3326–3337.
- 40 W. Müller-Esterl, *Biochemie*, Springer Berlin Heidelberg, Berlin, Heidelberg, 2018, pp. 156–170.
- 41 V. Leskovac, *Comprehensive Enzyme Kinetics*, Kluwer Academic Publishers, Boston, 2004, pp. 73–94.
- 42 S. Li, in *Chemical Reaction Engineering*, Elsevier, 2017, pp. 491–539.
- 43 K. Miyanaga and H. Unno, in *Comprehensive Biotechnology*, Elsevier, 2014, pp. 47–60.
- 44 J. Pleiss, Thermodynamic Activity-Based Interpretation of Enzyme Kinetics, *Trends Biotechnol.*, 2017, **35**, 379–382.
- 45 A. Ouertani, M. Neifar, R. Ouertani, A. S. Masmoudi and A. Cherif, Effectiveness of enzyme inhibitors in biomedicine and pharmacotherapy, *ATROA*, 2019, **5**. DOI: 10.15406/atroa.2019.05.00104.
- 46 R. A. Copeland, M. R. Harpel and P. J. Tummino, Targeting enzyme inhibitors in drug discovery, *Expert Opin. Ther. Targets*, 2007, **11**, 967–978.
- 47 D. W. Cushman and M. A. Ondetti, Design of angiotensin converting enzyme inhibitors, *Nat. Med.*, 1999, **5**, 1110–1113.
- 48 C. Flexner, HIV-protease inhibitors, *N. Engl. J. Med.*, 1998, **338**, 1281–1292.
- 49 R. S. Cahn, C. Ingold and V. Prelog, Specification of Molecular Chirality, *Angew. Chem. Int. Ed. Engl.*, 1966, **5**, 385–415.
- 50 H. P. Latscha, U. Kazmaier and H. Klein, *Organische Chemie*, Springer Berlin Heidelberg, Berlin, Heidelberg, 2016, pp. 77–92, 183–195, 379–398.
- 51 J. Brecher, Graphical representation of stereochemical configuration (IUPAC Recommendations 2006), *Pure Appl. Chem.*, 2006, **78**, 1897–1970.
- 52 R. E. Gawley, Do the Terms “% ee” and “% de” Make Sense as Expressions of Stereoisomer Composition or Stereoselectivity?, *J. Org. Chem.*, 2006, **71**, 2411–2416.
- 53 S. H. Wilen, *Stereochemistry of organic compounds*, Wiley, New York, 1994, pp. 153–295.
- 54 C.-H. Gu and D. J. Grant, in *Chiral Analysis*, Elsevier, 2006, pp. 47–77.
- 55 M. E. Tiritan, C. Fernandes, A. S. Maia, M. Pinto and Q. B. Cass, Enantiomeric ratios: Why so many notations?, *J. Chromatogr. A*, 2018, **1569**, 1–7.
- 56 A. A. Spasov, I. N. Iezhitsa, P. M. Vassiliev, A. A. Ozerov and R. Agarwal, in *Pharmacology of Drug Stereoisomers*, Springer Nature Singapore, Singapore, 2022, pp. 35–73.
- 57 R. U. McVicker and N. M. O'Boyle, Chirality of New Drug Approvals (2013–2022): Trends and Perspectives, *J. Med. Chem.*, 2024, **67**, 2305–2320.

- 58 J. Sui, N. Wang, J. Wang, X. Huang, T. Wang, L. Zhou and H. Hao, Strategies for chiral separation: from racemate to enantiomer, *Chem. Sci.*, 2023, **14**, 11955–12003.
- 59 T. Toyooka, Resolution of chiral drugs by liquid chromatography based upon diastereomer formation with chiral derivatization reagents, *J. Biochem. Biophys. Meth.*, 2002, **54**, 25–56.
- 60 K. Mislow, Stereochemical terminology and its discontents, *Chirality*, 2002, **14**, 126–134.
- 61 M. Reist, B. Testa, P.-A. Carrupt, M. Jung and V. Schurig, Racemization, enantiomerization, diastereomerization, and epimerization: Their meaning and pharmacological significance, *Chirality*, 1995, **7**, 396–400.
- 62 S. H. Wilen, A. Collet and J. Jacques, Strategies in optical resolutions, *Tetrahedron*, 1977, **33**, 2725–2736.
- 63 F. Faigl, E. Fogassy, M. Nógrádi, E. Pálovics and J. Schindler, Strategies in optical resolution: a practical guide, *Tetrahedron: Asymmetry*, 2008, **19**, 519–536.
- 64 J. M. Keith, J. F. Larrow and E. N. Jacobsen, Practical Considerations in Kinetic Resolution Reactions, *Adv. Synth. Catal.*, 2001, **343**, 5–26.
- 65 Y. Simeo', W. Kroutil and K. Faber, in *Biocatalysis in the pharmaceutical and biotechnology industries*, CRC Press/Taylor & Francis, Boca Raton, 2007, pp. 27–52.
- 66 F. Kühn, S. Katsuragi, Y. Oki, C. Scholz, S. Akai and H. Gröger, Dynamic kinetic resolution of a tertiary alcohol, *Chem. Commun.*, 2020, **56**, 2885–2888.
- 67 H. Pellissier, Recent developments in organocatalytic dynamic kinetic resolution, *Tetrahedron*, 2016, **72**, 3133–3150.
- 68 E. Fogassy, M. Nógrádi, D. Kozma, G. Egri, E. Pálovics and V. Kiss, Optical resolution methods, *Org. Biomol. Chem.*, 2006, **4**, 3011–3030.
- 69 F. F. Huerta, A. B. E. Minidis and J.-E. Bäckvall, Racemisation in asymmetric synthesis. Dynamic kinetic resolution and related processes in enzyme and metal catalysis, *Chem. Soc. Rev.*, 2001, **30**, 321–331.
- 70 X. Zhang, F. Chang, F. Zhu, T. Xu and Y. Zhang, Optimization of the medium composition and product extraction for R -mandelic acid using recombinant Escherichia coli expressing Alcaligenes sp. nitrilase, *J. Chem. Res.*, 2022, **46**. DOI: 10.1177/17475198221109155.
- 71 C. Tortora, C. Mai, F. Cascella, M. Mauksch, A. Seidel-Morgenstern, H. Lorenz and S. B. Tsogoeva, Speeding up Viedma Deracemization through Water-catalyzed and Reactant Self-catalyzed Racemization, *ChemPhysChem*, 2020, **21**, 1775–1787.
- 72 C. S. Fuchs, M. Hollauf, M. Meissner, R. C. Simon, T. Besset, J. N. H. Reek, W. Riethorst, F. Zepeck and W. Kroutil, Dynamic Kinetic Resolution of 2-Phenylpropanal Derivatives to Yield  $\beta$ -Chiral Primary Amines via Bioamination, *Adv. Synth. Catal.*, 2014, **356**, 2257–2265.
- 73 C. Femmer, M. Bechtold, T. M. Roberts and S. Panke, Exploiting racemases, *Appl. Microbiol. Biotechnol.*, 2016, **100**, 7423–7436.
- 74 G. L. Thejashree, E. Doris, E. Gravel and I. N. N. Namboothiri, Kinetic and Dynamic Kinetic Resolution by Dual Catalysis, *Eur. J. Org. Chem.*, 2022, **2022**. DOI: 10.1002/ejoc.202201035.
- 75 Y. Kim, J. Park and M.-J. Kim, Dynamic Kinetic Resolution of Amines and Amino Acids by Enzyme–Metal Cocatalysis, *ChemCatChem*, 2011, **3**, 271–277.
- 76 J. H. Lee, K. Han, M.-J. Kim and J. Park, Chemoenzymatic Dynamic Kinetic Resolution of Alcohols and Amines, *Eur. J. Org. Chem.*, 2010, **2010**, 999–1015.
- 77 P. Odman, L. A. Wessjohann and U. T. Bornscheuer, Chemoenzymatic dynamic kinetic resolution of acyloins, *J. Org. Chem.*, 2005, **70**, 9551–9555.
- 78 M. M. Musa, Enzymatic racemization of alcohols and amines: An approach for bi-enzymatic dynamic kinetic resolution, *Chirality*, 2020, **32**, 147–157.
- 79 M. Hönig, P. Sondermann, N. J. Turner and E. M. Carreira, Enantioselective Chemo- and Biocatalysis: Partners in Retrosynthesis, *Angew. Chem. Int. Ed. Engl.*, 2017, **56**, 8942–8973.
- 80 T. C. Nugent and M. El-Shazly, Chiral Amine Synthesis – Recent Developments and Trends for Enamide Reduction, Reductive Amination, and Imine Reduction, *Adv. Synth. Catal.*, 2010, **352**, 753–819.
- 81 M. Breuer, K. Ditrach, T. Habicher, B. Hauer, M. Kessler, R. Stürmer and T. Zelinski, Industrial methods for the production of optically active intermediates, *Angew. Chem. Int. Ed. Engl.*, 2004, **43**, 788–824.

- 82 M. Otmar, J. Gaálová, J. Žitka, L. Brožová, P. Cuřínová, M. Kohout, Š. Hovorka, J. E. Bara, B. van der Bruggen, J. Jirsák and P. Izák, Preparation of PSEBS membranes bearing (S)-(-)-methylbenzylamine as chiral selector, *Eur. Polym. J.*, 2020, **122**, 109381.
- 83 C. Zu, B. N. Brewer, B. Wang and M. E. Koscho, Tertiary amine appended derivatives of N-(3,5-dinitrobenzoyl)leucine as chiral selectors for enantiomer assays by electrospray ionization mass spectrometry, *Anal. Chem.*, 2005, **77**, 5019–5027.
- 84 U. B. Nair and D. W. Armstrong, Evaluation of Two Amine-Functionalized Cyclodextrins as Chiral Selectors in Capillary Electrophoresis: Comparisons to Vancomycin, *Microchem. J.*, 1997, **57**, 199–217.
- 85 A. Kišić, M. Stephan and B. Mohar, ansa -Ruthenium(II) Complexes of DPEN-SO<sub>2</sub>N(Me)(CH<sub>2</sub>)<sub>6</sub>(η<sup>6</sup>-aryl) Conjugate Ligands for Asymmetric Transfer Hydrogenation of Aryl Ketones, *Adv. Synth. Catal.*, 2014, **356**, 3193–3198.
- 86 H. Cheng, J. Hao, H. Wang, C. Xi, X. Meng, S. Cai and F. Zhao, (R,R)-DPEN-modified Ru/γ-Al<sub>2</sub>O<sub>3</sub>—An efficient heterogeneous catalyst for enantioselective hydrogenation of acetophenone, *J. Mol. Catal. A Chem.*, 2007, **278**, 6–11.
- 87 S. France, D. J. Guerin, S. J. Miller and T. Lectka, Nucleophilic chiral amines as catalysts in asymmetric synthesis, *Chem. Rev.*, 2003, **103**, 2985–3012.
- 88 D. Ghislieri and N. J. Turner, Biocatalytic Approaches to the Synthesis of Enantiomerically Pure Chiral Amines, *Top. Catal.*, 2014, **57**, 284–300.
- 89 S. H. Jeon, M. Kim, H.-K. Han and W. Lee, Direct enantiomer separation of thyroxine in pharmaceuticals using crown ether type chiral stationary phase, *Arch. Pharmacol. Res.*, 2010, **33**, 1419–1423.
- 90 J. P. Bantle, J. H. Oppenheimer, H. L. Schwartz, D. B. Hunninghake, J. L. Probstfield and R. F. Hanson, TSH response to TRH in euthyroid, hypercholesterolemic patients treated with graded doses of dextrothyroxine, *Metab. Clin. Exp.*, 1981, **30**, 63–66.
- 91 Y. Wei, S. Xia, C. He, W. Xiong and H. Xu, Highly enantioselective production of a chiral intermediate of sitagliptin by a novel isolate of *Pseudomonas pseudoalcaligenes*, *Biotechnol. Lett.*, 2016, **38**, 841–846.
- 92 N. Vargesson, Thalidomide-induced teratogenesis: history and mechanisms, *Birth Defects Res. C Embryo Today*, 2015, **105**, 140–156.
- 93 Y. Gao, R. Chen and Y. Ma, Synthesis of Asymmetrical 2,6-Diarylpyridines from Linear α,β,γ,δ-Unsaturated Ketones by Addition of Ammonium Formate Followed by Annulation, *Synthesis*, 2019, **51**, 3875–3882.
- 94 M. S. Gibson and R. W. Bradshaw, The Gabriel Synthesis of Primary Amines, *Angew. Chem. Int. Ed. Engl.*, 1968, **7**, 919–930.
- 95 C. B. Pollard and D. C. Young, The mechanism of the Leuckart reaction, *J. Org. Chem.*, 1951, **16**, 661–672.
- 96 E. R. Alexander and R. B. Wildman, Studies on the mechanism of the Leuckart reaction, *J. Am. Chem. Soc.*, 1948, **70**, 1187–1189.
- 97 S. H. Pine and B. L. Sanchez, Formic acid-formaldehyde methylation of amines, *J. Org. Chem.*, 1971, **36**, 829–832.
- 98 E. D. Cox and J. M. Cook, The Pictet-Spengler condensation: a new direction for an old reaction, *Chem. Rev.*, 1995, **95**, 1797–1842.
- 99 O. I. Afanasyev, E. Kuchuk, D. L. Usanov and D. Chusov, Reductive Amination in the Synthesis of Pharmaceuticals, *Chem. Rev.*, 2019, **119**, 11857–11911.
- 100 A. Cabré, X. Verdager and A. Riera, Recent Advances in the Enantioselective Synthesis of Chiral Amines via Transition Metal-Catalyzed Asymmetric Hydrogenation, *Chem. Rev.*, 2022, **122**, 269–339.
- 101 T. C. Nugent, *Chiral Amine Synthesis. Methods, Developments and Applications*, John Wiley & Sons Incorporated, Weinheim, 1st edn., 2009.
- 102 Z. Wu, W. Wang, H. Guo, G. Gao, H. Huang and M. Chang, Iridium-catalyzed direct asymmetric reductive amination utilizing primary alkyl amines as the N-sources, *Nat. Commun.*, 2022, **13**, 3344.
- 103 Z. Wu, S. Du, G. Gao, W. Yang, X. Yang, H. Huang and M. Chang, Secondary amines as coupling partners in direct catalytic asymmetric reductive amination, *Chem. Sci.*, 2019, **10**, 4509–4514.

- 104 C. Wang and J. Xiao, in *Stereoselective Formation of Amines*, ed. W. Li and X. Zhang, Springer Berlin Heidelberg, Berlin, Heidelberg, 2014, pp. 261–282.
- 105 T. E. Müller, K. C. Hultsch, M. Yus, F. Foubelo and M. Tada, Hydroamination: direct addition of amines to alkenes and alkynes, *Chem. Rev.*, 2008, **108**, 3795–3892.
- 106 K. Yamada and K. Tomioka, Copper-catalyzed asymmetric alkylation of imines with dialkylzinc and related reactions, *Chem. Rev.*, 2008, **108**, 2874–2886.
- 107 R. Kadyrov and T. H. Riermeier, Highly Enantioselective Hydrogen-Transfer Reductive Amination: Catalytic Asymmetric Synthesis of Primary Amines, *Angew. Chem.*, 2003, **115**, 5630–5632.
- 108 T. Irrgang and R. Kempe, Transition-Metal-Catalyzed Reductive Amination Employing Hydrogen, *Chem. Rev.*, 2020, **120**, 9583–9674.
- 109 C. Li, B. Villa-Marcos and J. Xiao, Metal-Brønsted acid cooperative catalysis for asymmetric reductive amination, *J. Am. Chem. Soc.*, 2009, **131**, 6967–6969.
- 110 D. Steinhuebel, Y. Sun, K. Matsumura, N. Sayo and T. Saito, Direct asymmetric reductive amination, *J. Am. Chem. Soc.*, 2009, **131**, 11316–11317.
- 111 J.-H. Xie, S.-F. Zhu and Q.-L. Zhou, Transition metal-catalyzed enantioselective hydrogenation of enamines and imines, *Chem. Rev.*, 2011, **111**, 1713–1760.
- 112 A. Gomm and E. O'Reilly, Transaminases for chiral amine synthesis, *Curr. Opin. Chem. Biol.*, 2018, **43**, 106–112.
- 113 F. Parmeggiani, N. J. Weise, S. T. Ahmed and N. J. Turner, Synthetic and Therapeutic Applications of Ammonia-lyases and Aminomutases, *Chem. Rev.*, 2018, **118**, 73–118.
- 114 D. Ghislieri, A. P. Green, M. Pontini, S. C. Willies, I. Rowles, A. Frank, G. Grogan and N. J. Turner, Engineering an enantioselective amine oxidase for the synthesis of pharmaceutical building blocks and alkaloid natural products, *J. Am. Chem. Soc.*, 2013, **135**, 10863–10869.
- 115 V. F. Batista, J. L. Galman, D. C. G. A. Pinto, A. M. S. Silva and N. J. Turner, Monoamine Oxidase: Tunable Activity for Amine Resolution and Functionalization, *ACS Catal.*, 2018, **8**, 11889–11907.
- 116 J. Mangas-Sanchez, S. P. France, S. L. Montgomery, G. A. Aleku, H. Man, M. Sharma, J. I. Ramsden, G. Grogan and N. J. Turner, Imine reductases (IREDs), *Curr. Opin. Chem. Biol.*, 2017, **37**, 19–25.
- 117 G. A. Aleku, Imine Reductases and Reductive Aminases in Organic Synthesis, *ACS Catal.*, 2024, **14**, 14308–14329.
- 118 A. K. Gilio, T. W. Thorpe, A. Heyam, M. R. Petchey, B. Pogrányi, S. P. France, R. M. Howard, M. J. Karmilowicz, R. Lewis, N. Turner and G. Grogan, A Reductive Aminase Switches to Imine Reductase Mode for a Bulky Amine Substrate, *ACS Catal.*, 2023, **13**, 1669–1677.
- 119 B.-B. Li, J. Zhang, F.-F. Chen, Q. Chen, J.-H. Xu and G.-W. Zheng, Direct reductive amination of ketones with amines by reductive aminases, *Green Synth. Catal.*, 2021, **2**, 345–349.
- 120 J. Liu, W. Kong, J. Bai, Y. Li, L. Dong, L. Zhou, Y. Liu, J. Gao, R. T. Bradshaw Allen, N. J. Turner and Y. Jiang, Amine dehydrogenases: Current status and potential value for chiral amine synthesis, *Chem Catal.*, 2022, **2**, 1288–1314.
- 121 F.-F. Chen, G.-W. Zheng, L. Liu, H. Li, Q. Chen, F.-L. Li, C.-X. Li and J.-H. Xu, Reshaping the Active Pocket of Amine Dehydrogenases for Asymmetric Synthesis of Bulky Aliphatic Amines, *ACS Catal.*, 2018, **8**, 2622–2628.
- 122 F. Guo and P. Berglund, Transaminase biocatalysis: optimization and application, *Green Chem.*, 2017, **19**, 333–360.
- 123 I. Slabu, J. L. Galman, R. C. Lloyd and N. J. Turner, Discovery, Engineering, and Synthetic Application of Transaminase Biocatalysts, *ACS Catal.*, 2017, **7**, 8263–8284.
- 124 B. R. Lichman, J. Zhao, H. C. Hailes and J. M. Ward, Enzyme catalysed Pictet-Spengler formation of chiral 1,1'-disubstituted- and spiro-tetrahydroisoquinolines, *Nat. Commun.*, 2017, **8**, 14883.
- 125 J. H. Schrittwieser, B. Groenendaal, V. Resch, D. Ghislieri, S. Wallner, E.-M. Fischereder, E. Fuchs, B. Grischek, J. H. Sattler, P. Macheroux, N. J. Turner and W. Kroutil, Deracemization by simultaneous bio-oxidative kinetic resolution and stereoinversion, *Angew. Chem. Int. Ed. Engl.*, 2014, **53**, 3731–3734.
- 126 P. Berglund, M. S. Humble and C. Branneby, in *Comprehensive Chirality*, Elsevier, 2012, pp. 390–401.

- 127 A. I. Denesyuk, K. A. Denessiouk, T. Korpela and M. S. Johnson, Functional attributes of the phosphate group binding cup of pyridoxal phosphate-dependent enzymes, *J. Mol. Biol.*, 2002, **316**, 155–172.
- 128 J. N. Janssonius, Structure, evolution and action of vitamin B6-dependent enzymes, *Curr. Opin. Struct. Biol.*, 1998, **8**, 759–769.
- 129 P. K. Mehta, T. I. Hale and P. Christen, Aminotransferases: demonstration of homology and division into evolutionary subgroups, *Eur. J. Biochem.*, 1993, **214**, 549–561.
- 130 R. Percudani and A. Peracchi, The B6 database: a tool for the description and classification of vitamin B6-dependent enzymatic activities and of the corresponding protein families, *BMC Bioinform.*, 2009, **10**, 273.
- 131 E. Sandmeier, T. I. Hale and P. Christen, Multiple evolutionary origin of pyridoxal-5'-phosphate-dependent amino acid decarboxylases, *Eur. J. Biochem.*, 1994, **221**, 997–1002.
- 132 M. S. Malik, E.-S. Park and J.-S. Shin, Features and technical applications of  $\omega$ -transaminases, *Appl. Microbiol. Biotechnol.*, 2012, **94**, 1163–1171.
- 133 C. P. Henson and W. W. Cleland, Kinetic studies of glutamic oxaloacetic transaminase isozymes, *Biochemistry*, 1964, **3**, 338–345.
- 134 A. Łyskowski, C. Gruber, G. Steinkellner, M. Schürmann, H. Schwab, K. Gruber and K. Steiner, Crystal structure of an (R)-selective  $\omega$ -transaminase from *Aspergillus terreus*, *PLoS one*, 2014, **9**, e87350.
- 135 C. Ramírez-Palacios, H. J. Wijma, S. Thallmair, S. J. Marrink and D. B. Janssen, Computational Prediction of  $\omega$ -Transaminase Specificity by a Combination of Docking and Molecular Dynamics Simulations, *J. Chem. Inf. Model.*, 2021, **61**, 5569–5580.
- 136 D. Koszelewski, K. Tauber, K. Faber and W. Kroutil, omega-Transaminases for the synthesis of non-racemic alpha-chiral primary amines, *Trends Biotechnol.*, 2010, **28**, 324–332.
- 137 F. Steffen-Munsberg, C. Vickers, A. Thontowi, S. Schätzle, T. Meinhardt, M. Svedendahl Humble, H. Land, P. Berglund, U. T. Bornscheuer and M. Höhne, Revealing the Structural Basis of Promiscuous Amine Transaminase Activity, *ChemCatChem*, 2013, **5**, 154–157.
- 138 J.-S. Shin and B.-G. Kim, Exploring the active site of amine:pyruvate aminotransferase on the basis of the substrate structure-reactivity relationship: how the enzyme controls substrate specificity and stereoselectivity, *J. Org. Chem.*, 2002, **67**, 2848–2853.
- 139 A. Nobili, F. Steffen-Munsberg, H. Kohls, I. Trentin, C. Schulzke, M. Höhne and U. T. Bornscheuer, Engineering the Active Site of the Amine Transaminase from *Vibrio fluvialis* for the Asymmetric Synthesis of Aryl-Alkyl Amines and Amino Alcohols, *ChemCatChem*, 2015, **7**, 757–760.
- 140 I. V. Pavlidis, M. S. Weiß, M. Genz, P. Spurr, S. P. Hanlon, B. Wirz, H. Iding and U. T. Bornscheuer, Identification of (S)-selective transaminases for the asymmetric synthesis of bulky chiral amines, *Nat. Chem.*, 2016, **8**, 1076–1082.
- 141 M. D. Patil, G. Grogan, A. Bommaris and H. Yun, Recent Advances in  $\omega$ -Transaminase-Mediated Biocatalysis for the Enantioselective Synthesis of Chiral Amines, *Catalysts*, 2018, **8**, 254.
- 142 H. Kohls, F. Steffen-Munsberg and M. Höhne, Recent achievements in developing the biocatalytic toolbox for chiral amine synthesis, *Curr. Opin. Chem. Biol.*, 2014, **19**, 180–192.
- 143 Y. Xie, J. Wang, L. Yang, W. Wang, Q. Liu, H. Wang and D. Wei, The identification and application of a robust  $\omega$ -transaminase with high tolerance towards substrates and isopropylamine from a directed soil metagenome, *Catal. Sci. Technol.*, 2022, **12**, 2162–2175.
- 144 A. W. H. Dawood, M. S. Weiß, C. Schulz, I. V. Pavlidis, H. Iding, R. O. M. A. de Souza and U. T. Bornscheuer, Isopropylamine as Amine Donor in Transaminase-Catalyzed Reactions: Better Acceptance through Reaction and Enzyme Engineering, *ChemCatChem*, 2018, **10**, 3943–3949.
- 145 S. Mathew, D. Renn and M. Rueping, Advances in One-Pot Chiral Amine Synthesis Enabled by Amine Transaminase Cascades: Pushing the Boundaries of Complexity, *ACS Catal.*, 2023, **13**, 5584–5598.
- 146 T. Heinks, J. Paulus, S. Koopmeiners, T. Beuel, N. Sewald, M. Höhne, U. T. Bornscheuer and G. Fischer von Mollard, Recombinant l-Amino Acid Oxidase with Broad Substrate Spectrum for Co-substrate Recycling in (S)-Selective Transaminase-Catalyzed Kinetic Resolutions, *ChemBioChem*, 2022, **23**, e202200329.

- 147 M. D. Truppo, N. J. Turner and J. D. Rozzell, Efficient kinetic resolution of racemic amines using a transaminase in combination with an amino acid oxidase, *Chem. Commun.*, 2009, 2127–2129.
- 148 D. Koszelewski, D. Clay, K. Faber and W. Kroutil, Synthesis of 4-phenylpyrrolidin-2-one via dynamic kinetic resolution catalyzed by  $\omega$ -transaminases, *J. Mol. Catal. B Enzym.*, 2009, **60**, 191–194.
- 149 H.-L. Liu, P.-H. Yi, J.-M. Wu, F. Cheng, Z.-Q. Liu, L.-Q. Jin, Y.-P. Xue and Y.-G. Zheng, Identification of a novel thermostable transaminase and its application in L-phosphinothricin biosynthesis, *Appl. Microbiol. Biotechnol.*, 2024, **108**, 184.
- 150 M. J. Menke, Y.-F. Ao and U. T. Bornscheuer, Practical Machine Learning-Assisted Design Protocol for Protein Engineering: Transaminase Engineering for the Conversion of Bulky Substrates, *ACS Catal.*, 2024, **14**, 6462–6469.
- 151 S. Qiu, C.-L. Ju, T. Wang, J. Chen, Y.-T. Cui, L.-Q. Wang, F.-F. Fan and J. Huang, Evolving  $\omega$ -amine transaminase AtATA guided by substrate-enzyme binding free energy for enhancing activity and stability against non-natural substrates, *Appl. Environ. Microbiol.*, 2024, **90**, e0054324.
- 152 F. G. Mutti and W. Kroutil, Asymmetric Bio-amination of Ketones in Organic Solvents, *Adv. Synth. Catal.*, 2012, **354**, 3409–3413.
- 153 Y. Cui, Y. Gao and L. Yang, Transaminase catalyzed asymmetric synthesis of active pharmaceutical ingredients, *Green Synth. Catal.*, 2024. DOI: 10.1016/j.gresc.2024.03.003.
- 154 S. A. Kelly, S. Pohle, S. Wharry, S. Mix, C. C. R. Allen, T. S. Moody and B. F. Gilmore, Application of  $\omega$ -Transaminases in the Pharmaceutical Industry, *Chem. Rev.*, 2018, **118**, 349–367.
- 155 C. K. Chung, P. G. Bulger, B. Kosjek, K. M. Belyk, N. Rivera, M. E. Scott, G. R. Humphrey, J. Limanto, D. C. Bachert and K. M. Emerson, Process Development of C–N Cross-Coupling and Enantioselective Biocatalytic Reactions for the Asymmetric Synthesis of Niraparib, *Org. Process Res. Dev.*, 2014, **18**, 215–227.
- 156 C. Molinaro, P. G. Bulger, E. E. Lee, B. Kosjek, S. Lau, D. Gauvreau, M. E. Howard, D. J. Wallace and P. D. O'Shea, CRTH2 antagonist MK-7246: a synthetic evolution from discovery through development, *J. Org. Chem.*, 2012, **77**, 2299–2309.
- 157 C. K. Savile, J. M. Janey, E. C. Mundorff, J. C. Moore, S. Tam, W. R. Jarvis, J. C. Colbeck, A. Krebber, F. J. Fleitz, J. Brands, P. N. Devine, G. W. Huisman and G. J. Hughes, Biocatalytic asymmetric synthesis of chiral amines from ketones applied to sitagliptin manufacture, *Science*, 2010, **329**, 305–309.
- 158 Z. Peng, J. W. Wong, E. C. Hansen, A. L. A. Puchlopek-Dermenci and H. J. Clarke, Development of a concise, asymmetric synthesis of a smoothened receptor (SMO) inhibitor: enzymatic transamination of a 4-piperidinone with dynamic kinetic resolution, *Org. Lett.*, 2014, **16**, 860–863.
- 159 F. Zhou, Y. Xu, Y. Nie and X. Mu, Substrate-Specific Engineering of Amino Acid Dehydrogenase Superfamily for Synthesis of a Variety of Chiral Amines and Amino Acids, *Catalysts*, 2022, **12**, 380.
- 160 V. Tseliou, M. F. Masman, T. Knaus and F. G. Mutti, Current Status of Amine Dehydrogenases: From Active Site Architecture to Diverse Applications Across a Broad Substrate Spectrum, *ChemCatChem*, 2024, **16**. DOI: 10.1002/cctc.202400469.
- 161 N. M. Brunhuber and J. S. Blanchard, The biochemistry and enzymology of amino acid dehydrogenases, *Crit. Rev. Biochem. Mol. Biol.*, 1994, **29**, 415–467.
- 162 T. Ohshima and K. Soda, Biochemistry and biotechnology of amino acid dehydrogenases, *Adv. Biochem. Eng./Biotechnol.*, 1990, **42**, 187–209.
- 163 T. Knaus, W. Böhmer and F. G. Mutti, Amine dehydrogenases: efficient biocatalysts for the reductive amination of carbonyl compounds, *Green Chem.*, 2017, **19**, 453–463.
- 164 V. Tseliou, T. Knaus, M. F. Masman, M. L. Corrado and F. G. Mutti, Generation of amine dehydrogenases with increased catalytic performance and substrate scope from  $\epsilon$ -deaminating L-Lysine dehydrogenase, *Nat. Commun.*, 2019, **10**, 3717.
- 165 V. Tseliou, M. F. Masman, W. Böhmer, T. Knaus and F. G. Mutti, Mechanistic Insight into the Catalytic Promiscuity of Amine Dehydrogenases: Asymmetric Synthesis of Secondary and Primary Amines, *ChemBioChem*, 2019, **20**, 800–812.
- 166 O. Mayol, S. David, E. Darii, A. Debard, A. Mariage, V. Pellouin, J.-L. Petit, M. Salanoubat, V. de Berardinis, A. Zapparucha and C. Vergne-Vaxelaire, Asymmetric reductive amination by a wild-

- type amine dehydrogenase from the thermophilic bacteria *Picrotoga mobilis*, *Catal. Sci. Technol.*, 2016, **6**, 7421–7428.
- 167 O. Mayol, K. Bastard, L. Beloti, A. Frese, J. P. Turkenburg, J.-L. Petit, A. Mariage, A. Debard, V. Pellouin, A. Perret, V. de Berardinis, A. Zaparucha, G. Grogan and C. Vergne-Vaxelaire, A family of native amine dehydrogenases for the asymmetric reductive amination of ketones, *Nat. Catal.*, 2019, **2**, 324–333.
  - 168 S. Lee, H. Jeon, P. Giri, U.-J. Lee, H. Jung, S. Lim, S. Sarak, T. P. Khobragade, B.-G. Kim and H. Yun, The Reductive Amination of Carbonyl Compounds Using Native Amine Dehydrogenase from *Laribacter hongkongensis*, *Biotechnol. Bioprocess Eng.*, 2021, **26**, 384–391.
  - 169 A. A. Caparco, E. Pelletier, J. L. Petit, A. Jouenne, B. R. Bommarius, V. de Berardinis, A. Zaparucha, J. A. Champion, A. S. Bommarius and C. Vergne-Vaxelaire, Metagenomic Mining for Amine Dehydrogenase Discovery, *Adv. Synth. Catal.*, 2020, **362**, 2427–2436.
  - 170 R.-F. Cai, L. Liu, F.-F. Chen, A. Li, J.-H. Xu and G.-W. Zheng, Reductive Amination of Biobased Levulinic Acid to Unnatural Chiral  $\gamma$ -Amino Acid Using an Engineered Amine Dehydrogenase, *ACS Sustain. Chem. Eng.*, 2020, **8**, 17054–17061.
  - 171 M. J. Abrahamson, J. W. Wong and A. S. Bommarius, The Evolution of an Amine Dehydrogenase Biocatalyst for the Asymmetric Production of Chiral Amines, *Adv. Synth. Catal.*, 2013, **355**, 1780–1786.
  - 172 L. J. Ye, H. H. Toh, Y. Yang, J. P. Adams, R. Snajdrova and Z. Li, Engineering of Amine Dehydrogenase for Asymmetric Reductive Amination of Ketone by Evolving *Rhodococcus* Phenylalanine Dehydrogenase, *ACS Catal.*, 2015, **5**, 1119–1122.
  - 173 L. Liu, D.-H. Wang, F.-F. Chen, Z.-J. Zhang, Q. Chen, J.-H. Xu, Z.-L. Wang and G.-W. Zheng, Development of an engineered thermostable amine dehydrogenase for the synthesis of structurally diverse chiral amines, *Catal. Sci. Technol.*, 2020, **10**, 2353–2358.
  - 174 A. Pushpanath, E. Siirola, A. Bornadel, D. Woodlock and U. Schell, Understanding and Overcoming the Limitations of *Bacillus badius* and *Caldalkalibacillus thermarum* Amine Dehydrogenases for Biocatalytic Reductive Amination, *ACS Catal.*, 2017, **7**, 3204–3209.
  - 175 M. J. Abrahamson, E. Vázquez-Figueroa, N. B. Woodall, J. C. Moore and A. S. Bommarius, Development of an amine dehydrogenase for synthesis of chiral amines, *Angew. Chem. Int. Ed. Engl.*, 2012, **51**, 3969–3972.
  - 176 J. Löwe, A. A. Ingram and H. Gröger, Enantioselective synthesis of amines via reductive amination with a dehydrogenase mutant from *Exigobacterium sibiricum*: Substrate scope, co-solvent tolerance and biocatalyst immobilization, *Bioorg. Med. Chem.*, 2018, **26**, 1387–1392.
  - 177 R. D. Franklin, C. J. Mount, B. R. Bommarius and A. S. Bommarius, Separate Sets of Mutations Enhance Activity and Substrate Scope of Amine Dehydrogenase, *ChemCatChem*, 2020, **12**, 2436–2439.
  - 178 B. R. Bommarius, M. Schürmann and A. S. Bommarius, A novel chimeric amine dehydrogenase shows altered substrate specificity compared to its parent enzymes, *Chem. Commun.*, 2014, **50**, 14953–14955.
  - 179 V. Tseliou, T. Knaus, J. Vilím, M. F. Masman and F. G. Mutti, Kinetic Resolution of Racemic Primary Amines Using *Geobacillus stearothermophilus* Amine Dehydrogenase Variant, *ChemCatChem*, 2020, **12**, 2184–2188.
  - 180 F. Croci, J. Vilím, T. Adamopoulou, V. Tseliou, P. J. Schoenmakers, T. Knaus and F. G. Mutti, Continuous Flow Biocatalytic Reductive Amination by Co-Entrapping Dehydrogenases with Agarose Gel in a 3D-Printed Mould Reactor, *ChemBioChem*, 2022, **23**, e202200549.
  - 181 F. Colpaert, S. Manginckx and N. de Kimpe, Asymmetric synthesis of chiral N-sulfinyl 3-alkyl- and 3-arylpiperidines by  $\alpha$ -alkylation of N-sulfinyl imidates with 1-chloro-3-iodopropane, *J. Org. Chem.*, 2011, **76**, 234–244.
  - 182 D. Enders and H. Schubert, Enantioselective Synthesis of  $\beta$ -Substituted Primary Amines;  $\alpha$ -Alkylation/Reductive Amination of Aldehydes via SAMP-Hydrazones, *Angew. Chem. Int. Ed. Engl.*, 1984, **23**, 365–366.
  - 183 J. He, Y. Xue, B. Han, C. Zhang, Y. Wang and S. Zhu, Nickel-Catalyzed Asymmetric Reductive 1,2-Carboamination of Unactivated Alkenes, *Angew. Chem. Int. Ed. Engl.*, 2020, **59**, 2328–2332.
  - 184 V. Jullian, Enantioselective Synthesis of  $\beta$ -Substituted Primary and Secondary Amines by Alkylation of (R)-Phenylglycinol Amide Enolates, *Synthesis*, 1997, **1997**, 1091–1097.



- 185 M. N. Kliemann, S. Teeuwen, C. Weike, G. Franciò and W. Leitner, Rhodium-Catalyzed Asymmetric Hydrohydrazonemethylation of Styrenes: Access to Chiral Hydrazones, Hydrazides, Hydrazines and Amines, *Adv. Synth. Catal.*, 2022, **364**, 4006–4012.
- 186 K. Ren, R. Yuan, Y.-Y. Gui, X.-W. Chen, S.-Y. Min, B.-Q. Wang and D.-G. Yu, Cu-catalyzed reductive aminomethylation of 1,3-dienes with N O -acetals: facile construction of  $\beta$ -chiral amines with quaternary stereocenters, *Org. Chem. Front.*, 2023, **10**, 467–472.
- 187 C. Czekelius and E. M. Carreira, Catalytic Enantioselective Conjugate Reduction of  $\beta,\beta$ -Disubstituted Nitroalkenes, *Angew. Chem.*, 2003, **115**, 4941–4943.
- 188 H. Huang and E. N. Jacobsen, Highly enantioselective direct conjugate addition of ketones to nitroalkenes promoted by a chiral primary amine-thiourea catalyst, *J. Am. Chem. Soc.*, 2006, **128**, 7170–7171.
- 189 N. J. A. Martin, L. Ozores and B. List, Organocatalytic asymmetric transfer hydrogenation of nitroolefins, *J. Am. Chem. Soc.*, 2007, **129**, 8976–8977.
- 190 D. Wang, N. Zhu, P. Chen, Z. Lin and G. Liu, Enantioselective Decarboxylative Cyanation Employing Cooperative Photoredox Catalysis and Copper Catalysis, *J. Am. Chem. Soc.*, 2017, **139**, 15632–15635.
- 191 Z.-K. Xue, N.-K. Fu and S.-Z. Luo, Asymmetric hydroazidation of  $\alpha$  -substituted vinyl ketones catalyzed by chiral primary amine, *Chin. Chem. Lett.*, 2017, **28**, 1083–1086.
- 192 A. Carella, G. Ramos Ferronato, E. Marotta, A. Mazzanti, P. Righi and C. Paolucci, Betti's base for crystallization-induced deracemization of substituted aldehydes: synthesis of enantiopure amorolfine and fenpropimorph, *Org. Biomol. Chem.*, 2017, **15**, 2968–2978.
- 193 S. Hoffmann, M. Nicoletti and B. List, Catalytic asymmetric reductive amination of aldehydes via dynamic kinetic resolution, *J. Am. Chem. Soc.*, 2006, **128**, 13074–13075.
- 194 Y. Duan, P. Yao, J. Ren, C. Han, Q. Li, J. Yuan, J. Feng, Q. Wu and D. Zhu, Biocatalytic desymmetrization of 3-substituted glutaronitriles by nitrilases. A convenient chemoenzymatic access to optically active (S)-Pregabalin and (R)-Baclofen, *Sci. China Chem.*, 2014, **57**, 1164–1171.
- 195 L. Biewenga, T. Saravanan, A. Kunzendorf, J.-Y. van der Meer, T. Pijning, P. G. Tepper, R. van Merkerk, S. J. Charnock, A.-M. W. H. Thunnissen and G. J. Poelarends, Enantioselective Synthesis of Pharmaceutically Active  $\gamma$ -Aminobutyric Acids Using a Tailor-Made Artificial Michaelase in One-Pot Cascade Reactions, *ACS Catal.*, 2019, **9**, 1503–1513.
- 196 C. S. Fuchs, J. E. Farnberger, G. Steinkellner, J. H. Sattler, M. Pickl, R. C. Simon, F. Zepeck, K. Gruber and W. Kroutil, Asymmetric Amination of  $\alpha$ -Chiral Aliphatic Aldehydes via Dynamic Kinetic Resolution to Access Stereocomplementary Brivaracetam and Pregabalin Precursors, *Adv. Synth. Catal.*, 2018, **360**, 768–778.
- 197 N. Richter, J. E. Farnberger, D. Pressnitz, H. Lechner, F. Zepeck and W. Kroutil, A system for  $\omega$ -transaminase mediated (R)-amination using l -alanine as an amine donor, *Green Chem.*, 2015, **17**, 2952–2958.
- 198 W. W. L. See, X. Li and Z. Li, Biocatalytic Cascade Conversion of Racemic Epoxides to ( S )-2-Arylpropionic Acids, ( R )- and ( S )-2-Arylpropyl Amines, *Adv. Synth. Catal.*, 2023, **365**, 68–77.
- 199 R. Xin, W. W. L. See, H. Yun, X. Li and Z. Li, Enzyme-Catalyzed Meinwald Rearrangement with an Unusual Regioselective and Stereospecific 1,2-Methyl Shift, *Angew. Chem. Int. Ed. Engl.*, 2022, **61**, e202204889.
- 200 P. Matzel, S. Wenske, S. Merdivan, S. Günther and M. Höhne, Synthesis of  $\beta$ -Chiral Amines by Dynamic Kinetic Resolution of  $\alpha$ -Branched Aldehydes Applying Imine Reductases, *ChemCatChem*, 2019, **11**, 4281–4285.
- 201 R. Jin, Z. Xu, J. Feng, M. Wang, P. Yao, Q. Wu and D. Zhu, Stereocomplementary Synthesis of  $\beta$ -Aryl Propanamines by Enzymatic Dynamic Kinetic Resolution-Reductive Amination, *Eur. J. Org. Chem.*, 2023, **26**. DOI: 10.1002/ejoc.202300476.
- 202 <https://enzyme.expasy.org/enzyme-byclass.html>, (accessed 6 November 2024).
- 203 S. Martinez Cuesta, N. Furnham, S. A. Rahman, I. Sillitoe and J. M. Thornton, The evolution of enzyme function in the isomerases, *Curr. Opin. Struct. Biol.*, 2014, **26**, 121–130.
- 204 L. Jin, Q. Wan, S. Ouyang, L. Zheng, X. Cai, X. Zhang, J. Shen, D. Jia, Z. Liu and Y. Zheng, Isomerase and epimerase: overview and practical application in production of functional sugars, *Crit. Rev. Food Sci. Nutr.*, 2024, **64**, 13133–13148.
- 205 B. L. Bengston and W. R. Lamm, Process for Isomerizing Glucose to Fructose, US3654800, 1972.

- 206 K. H. Nam, Glucose Isomerase: Functions, Structures, and Applications, *Appl. Sci.*, 2022, **12**, 428.
- 207 J. P. S. Choo and Z. Li, Styrene Oxide Isomerase Catalyzed Meinwald Rearrangement Reaction: Discovery and Application in Single-Step and One-Pot Cascade Reactions, *Org. Process Res. Dev.*, 2022, **26**, 1960–1970.
- 208 T. Yoshimura and N. Esak, Amino acid racemases: functions and mechanisms, *J. Biosci. Bioeng.*, 2003, **96**, 103–109.
- 209 M. D. Lloyd, M. Yevglevskis, A. Nathubhai, T. D. James, M. D. Threadgill and T. J. Woodman, Racemases and epimerases operating through a 1,1-proton transfer mechanism: reactivity, mechanism and inhibition, *Chem. Soc. Rev.*, 2021, **50**, 5952–5984.
- 210 I. Harriehausen, J. Bollmann, T. Carneiro, K. Bettenbrock and A. Seidel-Morgenstern, Characterization of an Immobilized Amino Acid Racemase for Potential Application in Enantioselective Chromatographic Resolution Processes, *Catalysts*, 2021, **11**, 726.
- 211 S.-W. Han, Y. Jang, J. Kook, J. Jang and J.-S. Shin, Reprogramming biocatalytic futile cycles through computational engineering of stereochemical promiscuity to create an amine racemase, *Nat. Commun.*, 2024, **15**, 49.
- 212 U. Felfer, M. Goriup, M. F. Koegl, U. Wagner, B. Larissegger-Schnell, K. Faber and W. Kroutil, The Substrate Spectrum of Mandelate Racemase: Minimum Structural Requirements for Substrates and Substrate Model, *Adv. Synth. Catal.*, 2005, **347**, 951–961.
- 213 A. Narmandakh and S. L. Bearne, Purification of recombinant mandelate racemase: improved catalytic activity, *Protein Expr. Purif.*, 2010, **69**, 39–46.
- 214 M. Pogorevc, H. Stecher and K. Faber, A caveat for the use of log P values for the assessment of the biocompatibility of organic solvents, *Biotechnol. Lett.*, 2002, **24**, 857–860.
- 215 N. Kaftzik, Mandelate racemase activity in ionic liquids: scopes and limitations, *J. Mol. Catal. A Chem.*, 2004, **214**, 107–112.
- 216 S. L. Bearne and M. St Maurice, A Paradigm for CH Bond Cleavage: Structural and Functional Aspects of Transition State Stabilization by Mandelate Racemase, *Adv. Protein Chem. Struct. Biol.*, 2017, **109**, 113–160.
- 217 G. J. Lye and J. M. Woodley, Application of in situ product-removal techniques to biocatalytic processes, *Trends Biotechnol.*, 1999, **17**, 395–402.
- 218 M. Ali, H. M. Ishqi and Q. Husain, Enzyme engineering: Reshaping the biocatalytic functions, *Biotechnol. Bioeng.*, 2020, **117**, 1877–1894.
- 219 I. Da Victorino Silva Amatto, N. Da Gonsales Rosa-Garzon, F. Antônio de Oliveira Simões, F. Santiago, N. Da Pereira Silva Leite, J. Raspante Martins and H. Cabral, Enzyme engineering and its industrial applications, *Biotechnol. Appl. Biochem.*, 2022, **69**, 389–409.
- 220 S. Sen, V. Venkata Dasu and B. Mandal, Developments in directed evolution for improving enzyme functions, *Appl. Biochem. Biotechnol.*, 2007, **143**, 212–223.
- 221 J.-Y. van der Meer, L. Biewenga and G. J. Poelarends, The Generation and Exploitation of Protein Mutability Landscapes for Enzyme Engineering, *ChemBioChem*, 2016, **17**, 1792–1799.
- 222 Y. Xu, Y. Wu, X. Lv, G. Sun, H. Zhang, T. Chen, G. Du, J. Li and L. Liu, Design and construction of novel biocatalyst for bioprocessing: Recent advances and future outlook, *Bioresour. Technol.*, 2021, **332**, 125071.
- 223 N. E. Labrou, Random mutagenesis methods for in vitro directed enzyme evolution, *Curr. Protein Pept. Sci.*, 2010, **11**, 91–100.
- 224 R. Chowdhury and C. D. Maranas, From directed evolution to computational enzyme engineering—A review, *AIChE J.*, 2020, **66**. DOI: 10.1002/aic.16847.
- 225 J. Jumper, R. Evans, A. Pritzel, T. Green, M. Figurnov, O. Ronneberger, K. Tunyasuvunakool, R. Bates, A. Židek, A. Potapenko, A. Bridgland, C. Meyer, S. A. A. Kohl, A. J. Ballard, A. Cowie, B. Romera-Paredes, S. Nikolov, R. Jain, J. Adler, T. Back, S. Petersen, D. Reiman, E. Clancy, M. Zielinski, M. Steinegger, M. Pacholska, T. Berghammer, S. Bodenstein, D. Silver, O. Vinyals, A. W. Senior, K. Kavukcuoglu, P. Kohli and D. Hassabis, Highly accurate protein structure prediction with AlphaFold, *Nature*, 2021, **596**, 583–589.
- 226 J. A. Gerlt and P. C. Babbitt, Divergent evolution of enzymatic function: mechanistically diverse superfamilies and functionally distinct suprafamilies, *Annu. Rev. Biochem.*, 2001, **70**, 209–246.
- 227 M. Wiltgen, in *Encyclopedia of Bioinformatics and Computational Biology*, Elsevier, 2019, pp. 38–61.

- 228 R. Merkl and R. Sterner, Reconstruction of ancestral enzymes, *Perspect. Sci.*, 2016, **9**, 17–23.
- 229 R. Chen, Enzyme engineering: rational redesign versus directed evolution, *Trends Biotechnol.*, 2001, **19**, 13–14.
- 230 L. Zhou, C. Tao, X. Shen, X. Sun, J. Wang and Q. Yuan, Unlocking the potential of enzyme engineering via rational computational design strategies, *Biotechnol. Adv.*, 2024, **73**, 108376.
- 231 Y. Qi, M. Chen, T. Jin, W. Chong, Z. Zhang, B. Nian and Y. Hu, Computer-aided engineering of lipases solvent tolerance enhanced their applications in sugar esters synthesis: State of the art, *Trends Food Sci. Technol.*, 2024, **144**, 104323.
- 232 N. G. Nezhad, R. N. Z. R. A. Rahman, Y. M. Normi, S. N. Oslan, F. M. Shariff and T. C. Leow, Thermostability engineering of industrial enzymes through structure modification, *Appl. Microbiol. Biotechnol.*, 2022, **106**, 4845–4866.
- 233 Z.-N. You, Q. Chen, S.-C. Shi, M.-M. Zheng, J. Pan, X.-L. Qian, C.-X. Li and J.-H. Xu, Switching Cofactor Dependence of 7 $\beta$ -Hydroxysteroid Dehydrogenase for Cost-Effective Production of Ursodeoxycholic Acid, *ACS Catal.*, 2019, **9**, 466–473.
- 234 X. Jiang, Y. Chen, S. Zhou, B. Pan, J. Tian, X. Xu, X. Cheng, Y.-Z. Chen and J. Yang, Engineering of Methionine Sulfoxide Reductase A with Expanded Substrate Scope for Deracemization of Sulfinyl Esters, *ACS Sustain. Chem. Eng.*, 2024, **12**, 11987–11996.
- 235 L. G. Otten, F. Hollmann and I. W. C. E. Arends, Enzyme engineering for enantioselectivity: from trial-and-error to rational design?, *Trends Biotechnol.*, 2010, **28**, 46–54.
- 236 M. Kheilová and M. Štrunc, Is the Le Chatelier-Braun Principle Valid in General in Linear Nonequilibrium Thermodynamics?, *J. Non-Equilib. Thermodyn.*, 1995, **20**. DOI: 10.1515/jnet.1995.20.1.19.
- 237 J. H. Schrittwieser, S. Velikogne, M. Hall and W. Kroutil, Artificial Biocatalytic Linear Cascades for Preparation of Organic Molecules, *Chem. Rev.*, 2018, **118**, 270–348.
- 238 C. C. Gruber, B. M. Nestl, J. Gross, P. Hildebrandt, U. T. Bornscheuer, K. Faber and W. Kroutil, Emulation of racemase activity by employing a pair of stereocomplementary biocatalysts, *Chemistry*, 2007, **13**, 8271–8276.
- 239 F. G. Mutti, T. Knaus, N. S. Scrutton, M. Breuer and N. J. Turner, Conversion of alcohols to enantiopure amines through dual-enzyme hydrogen-borrowing cascades, *Science*, 2015, **349**, 1525–1529.
- 240 A. I. Benítez-Mateos, D. Roura Padrosa and F. Paradisi, Multistep enzyme cascades as a route towards green and sustainable pharmaceutical syntheses, *Nat. Chem.*, 2022, **14**, 489–499.
- 241 F. Hollmann, I. W. C. E. Arends and D. Holtmann, Enzymatic reductions for the chemist, *Green Chem.*, 2011, **13**, 2285.
- 242 W. Liu and P. Wang, Cofactor regeneration for sustainable enzymatic biosynthesis, *Biotechnol. Adv.*, 2007, **25**, 369–384.
- 243 X. Wang, T. Saba, H. H. Yiu, R. F. Howe, J. A. Anderson and J. Shi, Cofactor NAD(P)H Regeneration Inspired by Heterogeneous Pathways, *Chem*, 2017, **2**, 621–654.
- 244 E. M. Buque-Taboada, A. J. J. Straathof, J. J. Heijnen and L. A. M. van der Wielen, In situ product recovery (ISPR) by crystallization: basic principles, design, and potential applications in whole-cell biocatalysis, *Appl. Microbiol. Biotechnol.*, 2006, **71**, 1–12.
- 245 A. Freeman, J. M. Woodley and M. D. Lilly, In situ product removal as a tool for bioprocessing, *Nat. Biotechnol.*, 1993, **11**, 1007–1012.
- 246 U. A. Salas-Villalobos and O. Aguilar, In situ product removal, *Phys. Sci. Rev.*, 2024, **9**, 3223–3239.
- 247 J. M. Woodley, M. Bisschops, A. J. J. Straathof and M. Ottens, Future directions for in-situ product removal (ISPR), *J. Chem. Technol. Biotechnol.*, 2008, **83**, 121–123.
- 248 W. van Hecke, G. Kaur and H. de Wever, Advances in in-situ product recovery (ISPR) in whole cell biotechnology during the last decade, *Biotechnol. Adv.*, 2014, **32**, 1245–1255.
- 249 J. Urbanus, C. Roelands, D. Verdoes and J. H. ter Horst, Intensified crystallization in complex media: Heuristics for crystallization of platform chemicals, *Chem. Eng. Sci.*, 2012, **77**, 18–25.
- 250 D. Stark and U. von Stockar, In situ product removal (ISPR) in whole cell biotechnology during the last twenty years, *Adv. Biochem. Eng./Biotechnol.*, 2003, **80**, 149–175.

- 251 A. G. Santos, T. L. de Albuquerque, B. D. Ribeiro and M. A. Z. Coelho, In situ product recovery techniques aiming to obtain biotechnological products: A glance to current knowledge, *Biotechnol. Appl. Biochem.*, 2021, **68**, 1044–1057.
- 252 A. Gomm, W. Lewis, A. P. Green and E. O'Reilly, A New Generation of Smart Amine Donors for Transaminase-Mediated Biotransformations, *Chemistry*, 2016, **22**, 12692–12695.
- 253 A. P. Green, N. J. Turner and E. O'Reilly, Chiral amine synthesis using  $\omega$ -transaminases: an amine donor that displaces equilibria and enables high-throughput screening, *Angew. Chem. Int. Ed. Engl.*, 2014, **53**, 10714–10717.
- 254 B. Wang, H. Land and P. Berglund, An efficient single-enzymatic cascade for asymmetric synthesis of chiral amines catalyzed by  $\omega$ -transaminase, *Chem. Commun.*, 2013, **49**, 161–163.
- 255 Di Cai, S. Hu, Q. Miao, C. Chen, H. Chen, C. Zhang, P. Li, P. Qin and T. Tan, Two-stage pervaporation process for effective in situ removal acetone-butanol-ethanol from fermentation broth, *Bioresour. Technol.*, 2017, **224**, 380–388.
- 256 P. Tufvesson, C. Bach and J. M. Woodley, A model to assess the feasibility of shifting reaction equilibrium by acetone removal in the transamination of ketones using 2-propylamine, *Biotechnol. Bioeng.*, 2014, **111**, 309–319.
- 257 S. J. Calvin, D. Mangan, I. Miskelly, T. S. Moody and P. J. Stevenson, Overcoming Equilibrium Issues with Carbonyl Reductase Enzymes, *Org. Process Res. Dev.*, 2012, **16**, 82–86.
- 258 M. Topf, T. Ingram, T. Mehling, T. Brinkmann and I. Smirnova, Product recovery in surfactant-based separation processes: Pervaporation of toluene from concentrated surfactant solutions, *J. Membr. Sci.*, 2013, **444**, 32–40.
- 259 M. M. W. Etschmann, D. Sell and J. Schrader, Production of 2-phenylethanol and 2-phenylethylacetate from L-phenylalanine by coupling whole-cell biocatalysis with organophilic pervaporation, *Biotechnol. Bioeng.*, 2005, **92**, 624–634.
- 260 X. Kong, A. He, J. Zhao, H. Wu, J. Ma, C. Wei, W. Jin and M. Jiang, Efficient acetone–butanol–ethanol (ABE) production by a butanol-tolerant mutant of *Clostridium beijerinckii* in a fermentation–pervaporation coupled process, *Biochem. Eng. J.*, 2016, **105**, 90–96.
- 261 A. Alkhudhiri, N. Darwish and N. Hilal, Membrane distillation: A comprehensive review, *Desalination*, 2012, **287**, 2–18.
- 262 M. Baranciewicz and M. Gryta, Ethanol production in a bioreactor with an integrated membrane distillation module, *Chem. Pap.*, 2012, **66**. DOI: 10.2478/s11696-011-0088-0.
- 263 C. Ayafor, A. C. Chang, A. Patel, U. Abid, D. Xie, M. J. Sobkowicz and H.-W. Wong, In-Situ Product Removal for the Enzymatic Depolymerization of Poly(ethylene terephthalate) via a Membrane Reactor, *ChemSusChem*, 2025, **18**, e202400698.
- 264 L. van der Hauwaert, A. Regueira, L. Selder, A.-P. Zeng and M. Mauricio-Iglesias, Optimising bioreactor processes with in-situ product removal using mathematical programming: A case study for propionate production, *Comput. Chem. Eng.*, 2022, **168**, 108059.
- 265 L. Selder, W. Sabra, N. Jürgensen, A. Lakshmanan and A.-P. Zeng, Co-cultures with integrated in situ product removal for lactate-based propionic acid production, *Bioprocess Biosyst. Eng.*, 2020, **43**, 1027–1035.
- 266 Z. Lazarova, V. Beschkov and S. Velizarov, Electro-membrane separations in biotechnology, *Phys. Sci. Rev.*, 2020, **5**. DOI: 10.1515/psr-2018-0063.
- 267 L.-E. Meyer, H. Brundiek and J. von Langermann, Integration of ion exchange resin materials for a downstream-processing approach of an imine reductase-catalyzed reaction, *Biotechnol. Prog.*, 2020, **36**, e3024.
- 268 L.-E. Meyer, K. Plasch, U. Kragl and J. von Langermann, Adsorbent-Based Downstream-Processing of the Decarboxylase-Based Synthesis of 2,6-Dihydroxy-4-methylbenzoic Acid, *Org. Process Res. Dev.*, 2018, **22**, 963–970.
- 269 P. Wang, Y. Wang and Z. Su, Microbial production of propionic acid with *Propionibacterium freudenreichii* using an anion exchanger-based in situ product recovery (ISPR) process with direct and indirect contact of cells, *Appl. Biochem. Biotechnol.*, 2012, **166**, 974–986.
- 270 S.-W. Han and J.-S. Shin, In situ removal of inhibitory products with ion exchange resins for enhanced synthesis of chiral amines using  $\omega$ -transaminase, *Biochem. Eng. J.*, 2020, **162**, 107718.
- 271 H. Schewe, M. A. Mirata and J. Schrader, Bioprocess engineering for microbial synthesis and conversion of isoprenoids, *Adv. Biochem. Eng./Biotechnol.*, 2015, **148**, 251–286.

- 272 N. Büscher, C. Spille, J. K. Kracht, G. V. Sayoga, A. W. H. Dawood, M. I. Maiwald, D. Herzog, M. Schlüter and A. Liese, Countercurrently Operated Reactive Extractor with an Additively Manufactured Enzyme Carrier Structure, *Org. Process Res. Dev.*, 2020, **24**, 1621–1628.
- 273 S. Tönjes, E. Uitterhaegen, K. de Winter and W. Soetaert, Reactive extraction technologies for organic acids in industrial fermentation processes – A review, *Sep. Purif. Technol.*, 2025, **356**, 129881.
- 274 A. Virklund, A. T. Nielsen and J. M. Woodley, Biocatalysis with In-Situ Product Removal Improves p-Coumaric Acid Production, *ChemBioChem*, 2024, **25**, e202400178.
- 275 J. T. Boock, A. J. E. Freedman, G. A. Tompsett, S. K. Muse, A. J. Allen, L. A. Jackson, B. Castro-Dominguez, M. T. Timko, K. L. J. Prather and J. R. Thompson, Engineered microbial biofuel production and recovery under supercritical carbon dioxide, *Nat. Commun.*, 2019, **10**, 587.
- 276 M. Doeker, L. Grabowski, D. Rother and A. Jupke, In situ reactive extraction with oleic acid for process intensification in amine transaminase catalyzed reactions, *Green Chem.*, 2022, **24**, 295–304.
- 277 I. Červeňanský, M. Mihaľ and J. Markoš, Potential application of perfusion and pertraction for in situ product removal in biocatalytic 2-phenylethanol production, *Sep. Purif. Technol.*, 2017, **183**, 11–20.
- 278 L. Heerema, N. Wierckx, M. Roelands, J. H. Hanemaaijer, E. Goetheer, D. Verdoes and J. Keurentjes, In situ phenol removal from fed-batch fermentations of solvent tolerant *Pseudomonas putida* S12 by pertraction, *Biochem. Eng. J.*, 2011, **53**, 245–252.
- 279 J. W. Mullin, *Crystallization*, Elsevier Science & Technology, Oxford, 4th edn., 2001, pp. 1-31, 86-134, 135-180, 181-215, 216-288.
- 280 J. Chen, B. Sarma, J. M. B. Evans and A. S. Myerson, Pharmaceutical Crystallization, *Cryst. Growth Des.*, 2011, **11**, 887–895.
- 281 J. Ulrich and H. C. Bülau, in *Handbook of Industrial Crystallization*, Elsevier, 2002, pp. 161–179.
- 282 B. Harjo, K. M. Ng and C. Wibowo, Synthesis of Supercritical Crystallization Processes, *Ind. Eng. Chem. Res.*, 2005, **44**, 8248–8259.
- 283 H.-H. Tung, E. L. Paul, M. Midler and J. A. McCauley, *Crystallization of Organic Compounds. An industrial perspective*, Wiley, Hoboken, N.J., 2009, pp. 1-12, 13-48, 101-116, 137-166, 167-178.
- 284 O. Galkin, K. Chen, R. L. Nagel, R. E. Hirsch and P. G. Vekilov, Liquid-liquid separation in solutions of normal and sickle cell hemoglobin, *PNAS*, 2002, **99**, 8479–8483.
- 285 P. G. Vekilov, The two-step mechanism of nucleation of crystals in solution, *Nanoscale*, 2010, **2**, 2346–2357.
- 286 Z. K. Nagy and R. D. Braatz, Advances and new directions in crystallization control, *Annu. Rev. Chem. Biomol. Eng.*, 2012, **3**, 55–75.
- 287 F. Yu, Y. Mao, H. Zhao, X. Zhang, T. Wang, M. Yuan, S. Ding, N. Wang, X. Huang and H. Hao, Enhancement of Continuous Crystallization of Lysozyme through Ultrasound, *Org. Process Res. Dev.*, 2021, **25**, 2508–2515.
- 288 F. C. Meldrum and C. O'Shaughnessy, Crystallization in Confinement, *Adv. Mater.*, 2020, **32**, e2001068.
- 289 R. I. Nessim, Applicability of the Schroeder-van Laar relation to multi-mixtures of liquid crystals of the phenyl benzoate type, *Thermochim. Acta*, 2000, **343**, 1–6.
- 290 Y. Wang and A. M. Chen, Enantioenrichment by Crystallization, *Org. Process Res. Dev.*, 2008, **12**, 282–290.
- 291 M. A. McDonald, H. Salami, P. R. Harris, C. E. Lagerman, X. Yang, A. S. Bommarius, M. A. Grover and R. W. Rousseau, Reactive crystallization: a review, *React. Chem. Eng.*, 2021, **6**, 364–400.
- 292 D. Hülsewede, L.-E. Meyer and J. von Langermann, Application of In Situ Product Crystallization and Related Techniques in Biocatalytic Processes, *Chemistry*, 2019, **25**, 4871–4884.
- 293 M. A. Huffman, A. Fryszkowska, O. Alvizo, M. Borra-Garske, K. R. Campos, K. A. Canada, P. N. Devine, Da Duan, J. H. Forstater, S. T. Grosser, H. M. Halsey, G. J. Hughes, J. Jo, L. A. Joyce, J. N. Kolev, J. Liang, K. M. Maloney, B. F. Mann, N. M. Marshall, M. McLaughlin, J. C. Moore, G. S. Murphy, C. C. Nawrat, J. Nazor, S. Novick, N. R. Patel, A. Rodriguez-Granillo, S. A. Robaire, E. C. Sherer, M. D. Truppo, A. M. Whittaker, D. Verma, L. Xiao, Y. Xu and H. Yang, Design of an in vitro biocatalytic cascade for the manufacture of islatravir, *Science*, 2019, **366**, 1255–1259.

- 294 Y. Wang, Di Cai, C. Chen, Z. Wang, P. Qin and T. Tan, Efficient magnesium lactate production with in situ product removal by crystallization, *Bioresour. Technol.*, 2015, **198**, 658–663.
- 295 K.-K. Cheng, X.-B. Zhao, J. Zeng, R.-C. Wu, Y.-Z. Xu, D.-H. Liu and J.-A. Zhang, Downstream processing of biotechnological produced succinic acid, *Appl. Microbiol. Biotechnol.*, 2012, **95**, 841–850.
- 296 J. Ren, P. Yao, S. Yu, W. Dong, Q. Chen, J. Feng, Q. Wu and D. Zhu, An Unprecedented Effective Enzymatic Carboxylation of Phenols, *ACS Catal.*, 2016, **6**, 564–567.
- 297 C. C. Nawrat, A. M. Whittaker, M. A. Huffman, M. McLaughlin, R. D. Cohen, T. Andreani, B. Ding, H. Li, M. Weisel and D. M. Tschaen, Nine-Step Stereoselective Synthesis of Islatravir from Deoxyribose, *Org. Lett.*, 2020, **22**, 2167–2172.
- 298 H. Salami, P. R. Harris, D. C. Yu, A. S. Bommarius, R. W. Rousseau and M. A. Grover, Periodic wet milling as a solution to size-based separation of crystal products from biocatalyst for continuous reactive crystallization, *Chem. Eng. Res. Des.*, 2022, **177**, 473–483.
- 299 L. G. Encarnación-Gómez, A. S. Bommarius and R. W. Rousseau, Reactive crystallization of  $\beta$ -lactam antibiotics: strategies to enhance productivity and purity of ampicillin, *React. Chem. Eng.*, 2016, **1**, 321–329.
- 300 M. A. McDonald, G. D. Marshall, A. S. Bommarius, M. A. Grover and R. W. Rousseau, Crystallization Kinetics of Cephalexin Monohydrate in the Presence of Cephalexin Precursors, *Cryst. Growth Des.*, 2019, **19**, 5065–5074.
- 301 J. Urbanus, C. P. M. Roelands, D. Verdoes, P. J. Jansens and J. H. ter Horst, Co-Crystallization as a Separation Technology: Controlling Product Concentrations by Co-Crystals, *Cryst. Growth Des.*, 2010, **10**, 1171–1179.
- 302 L. G. Encarnación-Gómez, A. S. Bommarius and R. W. Rousseau, Reactive crystallization of selected enantiomers: Chemo-enzymatic stereoinversion of amino acids at supersaturated conditions, *Chem. Eng. Sci.*, 2015, **122**, 416–425.
- 303 K. Würges, K. Petrusevska-Seebach, M. P. Elsner and S. Lütz, Enzyme-assisted physicochemical enantioseparation processes-Part III: Overcoming yield limitations by dynamic kinetic resolution of asparagine via preferential crystallization and enzymatic racemization, *Biotechnol. Bioeng.*, 2009, **104**, 1235–1239.
- 304 S. Diab, D. T. McQuade, B. F. Gupton and D. I. Gerogiorgis, Process Design and Optimization for the Continuous Manufacturing of Nevirapine, an Active Pharmaceutical Ingredient for HIV Treatment, *Org. Process Res. Dev.*, 2019, **23**, 320–333.
- 305 J. L. Quon, H. Zhang, A. Alvarez, J. Evans, A. S. Myerson and B. L. Trout, Continuous Crystallization of Aliskiren Hemifumarate, *Cryst. Growth Des.*, 2012, **12**, 3036–3044.
- 306 M. H. T. Kwan, J. Breen, M. Bowden, L. Conway, B. Crossley, M. F. Jones, R. Munday, N. P. B. Pokar, T. Screen and A. J. Blacker, Continuous Flow Chiral Amine Racemization Applied to Continuously Recirculating Dynamic Diastereomeric Crystallizations, *J. Org. Chem.*, 2021, **86**, 2458–2473.
- 307 C. S. Polster, K. P. Cole, C. L. Burcham, B. M. Campbell, A. L. Frederick, M. M. Hansen, M. Harding, M. R. Heller, M. T. Miller, J. L. Phillips, P. M. Pollock and N. Zaborenko, Pilot-Scale Continuous Production of LY2886721: Amide Formation and Reactive Crystallization, *Org. Process Res. Dev.*, 2014, **18**, 1295–1309.
- 308 J. R. Dunetz, J. Magano and G. A. Weisenburger, Large-Scale Applications of Amide Coupling Reagents for the Synthesis of Pharmaceuticals, *Org. Process Res. Dev.*, 2016, **20**, 140–177.
- 309 R. Liu, M. Huang, X. Yao, S. Chen, S. Wang and Z. Suo, Gas-liquid reactive crystallization kinetics of 2,4,6-triamino-1,3,5-trinitrobenzene in the semi-batch procedure, *J. Cryst. Growth*, 2018, **491**, 6–15.
- 310 T. Lerdwiriyanupap, R. Cedeno, P. Nalaoh, S. Bureekaew, V. Promarak and A. E. Flood, Enantiopurification of Mandelic Acid by Crystallization-Induced Diastereomer Transformation: An Experimental and Computational Study, *Cryst. Growth Des.*, 2023, **23**, 2001–2010.
- 311 D. Hülsewede, J.-N. Dohm and J. von Langermann, Donor Amine Salt-Based Continuous in situ-Product Crystallization in Amine Transaminase-Catalyzed Reactions, *Adv. Synth. Catal.*, 2019, **361**, 2727–2733.

- 312 D. Hülsewede, M. Tänzler, P. Süss, A. Mildner, U. Menyes and J. von Langermann, Development of an in situ-Product Crystallization (ISPC)-Concept to Shift the Reaction Equilibria of Selected Amine Transaminase-Catalyzed Reactions, *Eur. J. Org. Chem.*, 2018, **2018**, 2130–2133.
- 313 S. Tiedemann, J. E. Neuburger, A. Gazizova and J. von Langermann, Continuous Preparative Application of Amine Transaminase-Catalyzed Reactions with Integrated Crystallization, *Eur. J. Org. Chem.*, 2024, **27**. DOI: 10.1002/ejoc.202400068.
- 314 D. Hülsewede, E. Temmel, P. Kumm and J. von Langermann, Concept Study for an Integrated Reactor-Crystallizer Process for the Continuous Biocatalytic Synthesis of (S)-1-(3-Methoxyphenyl)ethylamine, *Crystals*, 2020, **10**, 345.
- 315 J. Neuburger, F. Helmholz, S. Tiedemann, P. Lehmann, P. Süss, U. Menyes and J. von Langermann, Implementation and scale-up of a semi-continuous transaminase-catalyzed reactive crystallization for the preparation of (S)-(3-methoxyphenyl)ethylamine, *Chem. Eng. Process.: Process Intensif.*, 2021, **168**, 108578.
- 316 K. Ni, H. Wang, L. Zhao, M. Zhang, S. Zhang, Y. Ren and D. Wei, Efficient production of (R)-(-)-mandelic acid in biphasic system by immobilized recombinant E. coli, *J. Biotechnol.*, 2013, **167**, 433–440.
- 317 K. Kinbara, K. Sakai, Y. Hashimoto, H. Nohira and K. Saigo, Design of resolving reagents: p-substituted mandelic acids as resolving reagents for 1-arylalkylamines, *Tetrahedron: Asymmetry*, 1996, **7**, 1539–1542.
- 318 S. Wang, T. Shi, Z. Fang, C. Liu, W. He, N. Zhu, Y. Hu, X. Li and K. Guo, Enzymatic kinetic resolution in flow for chiral mandelic acids, *J. Flow Chem.*, 2022, **12**, 227–235.
- 319 G. Kesslin and K. W. Kelly, Resolution of racemic mandelic acid, US4322548A, 1982.
- 320 Z. Szeleczky, P. Bagi, E. Pálovics and E. Fogassy, The effect of SDE on the separation of diastereomeric salts: a case study for the resolution of mandelic acid derivatives with Pregabalin, *Tetrahedron: Asymmetry*, 2014, **25**, 1095–1099.
- 321 K. Kodama, K. Kawasaki, M. Yi, K. Tsukamoto, H. Shitara and T. Hirose, Solvent-Induced Chirality Switching in the Enantioseparation of Halogen-Substituted Mandelic Acids: Structural Effects on Molecular Packing, *Cryst. Growth Des.*, 2019, **19**, 7153–7159.
- 322 X.-H. Pham, J.-M. Kim, S.-M. Chang, I. Kim and W.-S. Kim, Enantioseparation of D/L-mandelic acid with L-phenylalanine in diastereomeric crystallization, *J. Mol. Catal. B Enzym.*, 2009, **60**, 87–92.
- 323 T. Yutthalekha, C. Wattanakit, V. Lapeyre, S. Nokbin, C. Warakulwit, J. Limtrakul and A. Kuhn, Asymmetric synthesis using chiral-encoded metal, *Nat. Commun.*, 2016, **7**, 12678.
- 324 P.-C. Yan, J.-H. Xie, X.-D. Zhang, K. Chen, Y.-Q. Li, Q.-L. Zhou and D.-Q. Che, Direct asymmetric hydrogenation of  $\alpha$ -keto acids by using the highly efficient chiral spiro iridium catalysts, *Chem. Commun.*, 2014, **50**, 15987–15990.
- 325 S. Chen, F. Liu, K. Zhang, H. Huang, H. Wang, J. Zhou, J. Zhang, Y. Gong, D. Zhang, Y. Chen, C. Lin and B. Wang, An efficient enzymatic aminolysis for kinetic resolution of aromatic  $\alpha$ -hydroxyl acid in non-aqueous media, *Tetrahedron Lett.*, 2016, **57**, 5312–5314.
- 326 M. Goriup, U. T. Strauss, U. Felfer, W. Krouitl and K. Faber, Substrate spectrum of mandelate racemase, *J. Mol. Catal. B Enzym.*, 2001, **15**, 207–211.
- 327 U. T. Strauss and K. Faber, Deracemization of ( $\pm$ )-mandelic acid using a lipase–mandelate racemase two-enzyme system, *Tetrahedron: Asymmetry*, 1999, **10**, 4079–4081.
- 328 Y.-P. Xue, Z.-Q. Liu, M. Xu, Y.-J. Wang, Y.-G. Zheng and Y.-C. Shen, Enhanced biotransformation of (R,S)-mandelonitrile to (R)-(-)-mandelic acid with in situ production removal by addition of resin, *Biochem. Eng. J.*, 2010, **53**, 143–149.
- 329 Y.-P. Xue, M. Xu, H.-S. Chen, Z.-Q. Liu, Y.-J. Wang and Y.-G. Zheng, A Novel Integrated Bioprocess for Efficient Production of (R)-(-)-Mandelic Acid with Immobilized *Alcaligenes faecalis* ZJUTB10, *Org. Process Res. Dev.*, 2013, **17**, 213–220.
- 330 K. Wrzosek, I. Harriehausen and A. Seidel-Morgenstern, Combination of Enantioselective Preparative Chromatography and Racemization: Experimental Demonstration and Model-Based Process Optimization, *Org. Process Res. Dev.*, 2018, **22**, 1761–1771.
- 331 B. Jakob, I. Slimani, A. Diehl, N. Hamdi and G. Manolikakes, Palladium-Catalyzed Decarboxylative 1,2-Addition of Carboxylic Acids to Glyoxylic Acid Esters, *Eur. J. Org. Chem.*, 2021, **2021**, 6340–6346.

- 332 A. Saeed, D. Shahzad, M. Faisal, F. A. Larik, H. R. El-Seedi and P. A. Channar, Developments in the synthesis of the antiplatelet and antithrombotic drug (S)-clopidogrel, *Chirality*, 2017, **29**, 684–707.
- 333 V. M. Profir, E. Furusjö, L.-G. Danielsson and Å. C. Rasmuson, Study of the Crystallization of Mandelic Acid in Water Using in Situ ATR–IR Spectroscopy, *Cryst. Growth Des.*, 2002, **2**, 273–279.
- 334 H. Shitara, T. Shintani, K. Kodama and T. Hirose, Solvent-induced reversed stereoselectivity in reciprocal resolutions of mandelic acid and erythro-2-amino-1,2-diphenylethanol, *J. Org. Chem.*, 2013, **78**, 9309–9316.
- 335 K. Kodama, H. Shitara and T. Hirose, Chirality Switching in Optical Resolution of Mandelic Acid in C1–C4 Alcohols: Elucidation of Solvent Effects Based on X-ray Crystal Structures of Diastereomeric Salts, *Cryst. Growth Des.*, 2014, **14**, 3549–3556.
- 336 A. Akdeniz, L. Mosca, T. Minami and P. Anzenbacher, Sensing of enantiomeric excess in chiral carboxylic acids, *Chem. Commun.*, 2015, **51**, 5770–5773.



# List of publications

## As first author

- 02/2025†** Belov F., Lieb A., von Langermann J.  
 “Crystallization-integrated mandelate racemase-catalyzed dynamic kinetic resolution of racemic mandelic acid”, *Reaction Chemistry & Engineering*, 2025, accepted, doi: 10.1039/d4re00576g
- 04/2024†** Belov F., Gazizova A., Bork H., Gröger H., von Langermann J.  
 “Crystallization assisted dynamic kinetic resolution for the synthesis of (*R*)- $\beta$ -methylphenethylamine”, *ChemBioChem*, 2024, **25**(16), e202400203, doi: 10.1002/cbic.202400203.
- 03/2023†** Belov F., Mildner A., Knaus T., Mutti F., von Langermann J.  
 “Crystallization-based downstream processing of  $\omega$ -transaminase- and amine dehydrogenase-catalyzed reactions”, *Reaction Chemistry & Engineering*, 2023, **8**, 1427-1439, doi: 10.1039/d2re00496h.
- 01/2022** Belov F., Villinger A., von Langermann J.  
 “(*R*)-Baclofen [(*R*)-4-amino-3-(4-chloro-phen-yl)butanoic acid].”, *Acta Crystallographica E*, 2022, **78**(1), 33-35, doi: 10.1107/S2056989021012809.

## Shared first authorship

- 2025** Belov F.\*, Bork H.\*, Höhne M., Gröger H., von Langermann J.  
 “Retrosynthetic route toward a de novo enantioselective total synthesis of (*S*)-baclofen based on metal-catalyzed hydroformylation and enzymatic transamination”, submitted to *ChemBioChem*, 2025.  
 doi: 10.1002/cbic.202500108 ; \* equal contribution to work

## As co-author

- 11/2024** Spang J., Bork H., Belov F., von Langermann J., Vorholt A., Gröger H.  
 “One-pot hydroaminomethylation of alkenes under formation of primary amines by combining hydroformylation at 20 bar of syngas and biocatalytic transamination in water”, *Org. Biomol. Chem.*, 2025, **23**, 688-692, doi: 10.1039/d4ob01513d.

Die mit „†” markierten Publikationen gehören zum Hauptteil dieser kumulativen Dissertation.

# Appendix

This part contains the original publications addressed in the chapters 3 to 5 and the formalities of the thesis.

# Publication 1: Crystallization-based downstream processing of $\omega$ -transaminase- and amine dehydrogenase-catalyzed reactions

F. Belov, A. Mildner, T. Knaus, F. G. Mutti and J. von Langermann

*Reaction Chemistry & Engineering*, 2023,8(6), 1427-1439.

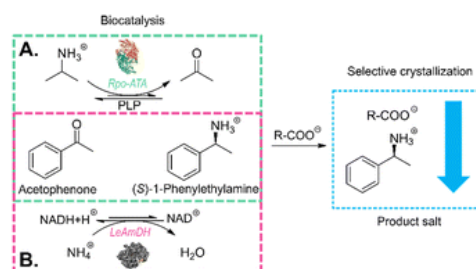
Received: 14<sup>th</sup> November 2022

Accepted: 21<sup>th</sup> March 2023

DOI: 10.1039/d2re00496h

## Abstract:

Biocatalytic synthesis is a powerful and frequently chosen method for the production of chiral amines. Unfortunately, these biocatalytic reactions often result in complex mixtures, bearing many components aside from the main product amine such as residual co-substrates, co-products, cofactors and buffer salts. This issue typically requires an additional effort during downstream processing towards the isolation of the desired chiral amine. For instance, transaminase- and amine dehydrogenase-catalyzed reactions, which often use high surpluses of amine or ammonia co-substrates, face complications in removing the residual amine donor or unreacted substrate and salts from the isolated amine products, thus complicating and increasing the costs of the process of product isolation and purification. This study explores the selective removal of chiral amines from model amine transaminase and amine dehydrogenase-catalyzed reactions *via* a salt-based specific crystallization step. The product amine is precipitated directly in one step from the reaction mixture as a product ammonium salt, which can easily be filtered from the reaction mixture, while the other reactants remain unchanged in solution for potential re-use.





Cite this: *React. Chem. Eng.*, 2023, 8, 1427

## Crystallization-based downstream processing of $\omega$ -transaminase- and amine dehydrogenase-catalyzed reactions†

Feodor Belov,<sup>a</sup> Andrea Mildner,<sup>b</sup> Tanja Knaus,<sup>c</sup> Francesco G. Mutti<sup>c</sup> and Jan von Langermann<sup>d,\*</sup>

Biocatalytic synthesis is a powerful and frequently chosen method for the production of chiral amines. Unfortunately, these biocatalytic reactions often result in complex mixtures, bearing many components aside from the main product amine such as residual co-substrates, co-products, cofactors and buffer salts. This issue typically requires an additional effort during downstream processing towards the isolation of the desired chiral amine. For instance, transaminase- and amine dehydrogenase-catalyzed reactions, which often use high surpluses of amine or ammonia co-substrates, face complications in removing the residual amine donor or unreacted substrate and salts from the isolated amine products, thus complicating and increasing the costs of the process of product isolation and purification. This study explores the selective removal of chiral amines from model amine transaminase and amine dehydrogenase-catalyzed reactions via a salt-based specific crystallization step. The product amine is precipitated directly in one step from the reaction mixture as a product ammonium salt, which can easily be filtered from the reaction mixture, while the other reactants remain unchanged in solution for potential re-use.

Received 14th November 2022,  
Accepted 21st March 2023

DOI: 10.1039/d2re00496h

rsc.li/reaction-engineering

### Introduction

Enzyme catalysis is a frequently used approach in the synthesis of complex chiral compounds. The benefits of enzymatic synthesis approaches compared to conventional organic synthesis typically include high enantioselectivity towards the synthesis of relevant products. This often also includes mild and environmentally friendly reaction conditions, such as moderate temperatures, an aqueous (main) solvent system and typically non-toxic reagents and starting materials.<sup>1–3</sup> Since the early 2000s biocatalysis found its way into many industrial applications and developed itself from an industrial niche of kinetic resolution of just a few substances, mainly catalyzed by hydrolases, to a global tool for pharmaceutical and chemical synthesis.<sup>1–7</sup> With the global enzyme market reaching up to an estimated 11.47 billion \$US

in 2021, it is projected to reach 20.31 billion \$US by 2030, while the market of enzyme derived products is even larger.<sup>8</sup> However, even though the benefits of enzymatic synthesis often outweigh its limitations, there are some major challenges that the enzymatic processes face: biocatalyst stability, occasional dependency on expensive cofactors, unfavorable reaction equilibria and often rather complex downstream processing issues.<sup>1–3,6,9</sup>

One significant class of chemical compounds increasingly produced through enzymatic reactions are chiral amines.<sup>1,10–15</sup> Finding usage as building blocks especially in pharmaceutical synthesis, up to an estimated 40% of currently commercialized APIs contain an optically active amine group.<sup>16,17</sup> Over the years, many enzymatic classes have been adopted for this purpose, among such transaminases (TAs), amine dehydrogenases (AmDHs), imine reductases (IREDs), P450 monooxygenases (P450s) and others.<sup>18–23</sup>

This work will focus on the reaction systems of TAs and AmDHs. TAs are known to occasionally face challenges, e.g. unfavorable equilibria and inhibitions, thus, the establishment of reaction systems for TAs can require additional effort.<sup>18,24–26</sup> While the enzymes can be improved via enzyme engineering, process limitations still constrain their full potential.<sup>26,27</sup> Examples of approaches to circumvent limitations of transaminase-catalyzed reaction systems involve raising the amine donor concentrations to very high

<sup>a</sup> Biocatalytic Synthesis Group, Institute of Chemistry, University of Rostock, Albert-Einstein-Str. 3A, 18059 Rostock, Germany

<sup>b</sup> Institute for Chemical and Thermal Process Engineering, Center of Pharmaceutical Engineering, Technische Universität Braunschweig, D-38106 Braunschweig, Germany

<sup>c</sup> HIMS-Biocat Group, Van't Hoff Institute for Molecular Sciences, University of Amsterdam, Science Park 904, 1098 XH Amsterdam, Netherlands

<sup>d</sup> Biocatalysis, Institute of Chemistry, Otto-von-Guericke-University Magdeburg, Universitätsplatz 2, 39106 Magdeburg, Germany. E-mail: jan.langermann@ovgu.de  
† Electronic supplementary information (ESI) available. See DOI: <https://doi.org/10.1039/d2re00496h>



excesses or shifting reaction equilibria through enzymatic cascades or more technical approaches.<sup>28–36</sup>

This statement is also true for AmDHs, which require an excess of ammonia as an amine donor to shift the equilibrium. In addition, these high concentrations are also needed due to the high  $K_M$  (Michaelis–Menten constant) for ammonia. High  $K_M$  values for ammonia are a distinguishing feature for most wild-type amino acid dehydrogenases and engineered AmDHs thereof, as well as wild-type AmDHs.<sup>37–43</sup>

Reagent excesses may in turn impede downstream processing since high concentrations of the substrates, such as amine donors, may complicate product recovery based on conventional means of product extraction and chromatography.<sup>44,45</sup> In this context, crystallization of the desired product from the reaction broth may offer an alternative downstream processing route, as it focuses on a specific low solubility of a single target compound. Consequently, crystallization is often applied as a processing step for the production of chiral compounds. A major application example thereof is the diastereomeric salt resolution through selective crystallization,<sup>46–49</sup> when a counterion of defined chirality is added to an enantiomer mixture, yielding diastereomeric salts with differing solubilities.

Noteworthy, a direct combination of asymmetric biocatalytic synthesis and crystallization is present within the concept of *in situ* product crystallization (ISPC), otherwise known as reactive crystallization, and has proven to be effective in transaminase-catalyzed reactions.<sup>27,50–54</sup>

However, ISPC may encounter challenges, such as enzyme inhibition by the applied counterion or mechanical challenges (e.g. stirring).<sup>53,55</sup> Thus, as an alternative, post-reaction product crystallization can be used for downstream processing, which still retains the high selectivity of the product crystallization. It allows for the use of any compound to facilitate crystallization, hence a counter-ion for the product can be selected based on the factors deemed as necessary. This study aims to highlight the benefits of the post-reaction crystallization downstream processing approach. We focus on the development of a straight-forward crystallization strategy, which is applicable for product recovery from TA- and AmDH-derived reaction media. The study was performed around the well-established model reaction that converts acetophenone into (*S*)-1-phenylethylamine ((*S*)-1PEA), known in literature to be optimized for both enzyme classes. The amine products were removed as the ammonium salt of a carboxylic acid anion, while the amine donors, broadly applied in a significant surplus, as well as other reactants remained in solution. For that purpose, a screening of solubility margins between the amine donor and amine product salts was performed for a variety of possible carboxylic acid anions (see Fig. 1). With a selection of anions from the screening, the influence of several factors, such as temperature, amine donor concentrations and acid anion concentrations, on product isolation yields and purities was investigated. The results of

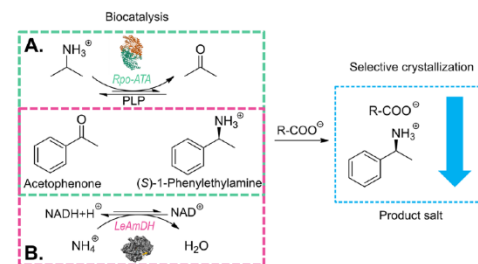


**Fig. 1** Reaction scheme of enzymatic approaches for the production of (*S*)-1-phenylethylamine used in this paper: A. scheme for the reaction catalyzed by the wild-type transaminase from *Ruegeria pomeroyi* with isopropylamine (IPA) as the amine donor (green box); B. scheme for the reaction catalyzed by the amine dehydrogenase (LE-AmDH-v1) engineered from the *L*-lysine- $\epsilon$ -deaminating dehydrogenase from *Geobacillus stearothermophilus* with ammonium ions as the amine donor (pink box).

this investigation were validated on real enzymatic reaction media.

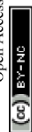
## Results and discussion

### Determination of the crystallizing agent

The determination of possible crystallizing agents is a crucial step for the subsequent crystallization. Taking into account that in the model systems there will always be at least two amine counterions available for crystallization, namely (*S*)-1PEA as the product and IPA/ammonium as the amine donor, one main consideration had to be made in the selection of the corresponding carboxylic acid anions as crystallizing agents. The solubility of the resulting (*S*)-1PEA salt had to be held as low as possible, while the solubility of the amine donor salt had to be held as high as possible. This principle of the crystallizing agent selection would allow for relatively high yields of product recovery from the reaction broth (minimal product salt solubility) whilst ensuring high purities of the crystallized product due to exclusion of isopropylamine (TA) or ammonia (AmDH) (via maximum amine donor salt solubility).

Ten potential carboxylate anions (see Fig. 2) were selected based on a previous screening by Hülsewede *et al.* (ESI† Hülsewede *et al.*; pp. 14–16)<sup>53</sup> and ranked according to solubility differences of the resulting salt pairs. The results of the solubility measurements are shown in Table 1.

The anions were sorted according to their respective quotient (see Table 1) of the amine donor (IPA and ammonium) salt solubility to the product salt solubility ((*S*)-1PEA). In addition, acid anions resulting in high product salt solubilities (e.g. 25CNA) >25 mM and low amine donor salt solubilities (e.g. 3DPPA) <150 mM were excluded to maximize product crystallization yields and amine donor impurities in the product salt. Moreover, the



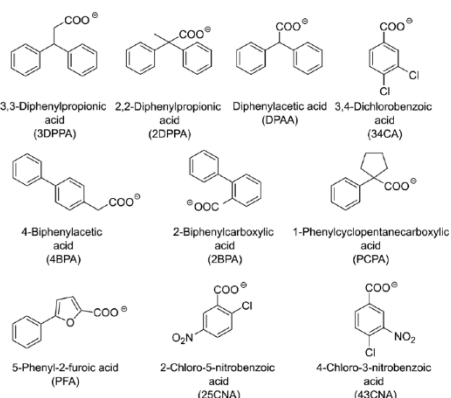


Fig. 2 Carboxylate anions utilized in the solubility screening.

majority of the carboxylic acids screened in this work do not possess any noteworthy toxicities. Only 4BPA is known to be toxic to humans and was thus excluded from further experiments.

On this basis, three carboxylic acid anions matched those criteria and thus were selected for the subsequent crystallization conditions screening: DPAA, 34CA and 43CNA. It has to be mentioned, that the desired salt qualities for *in situ* product crystallization differ from its use as a downstream processing strategy. Please note that this screening was performed as a mean for qualitative evaluation of pure substance amine salts to narrow down a potential list of candidates for effective product crystallization. Thus, any effects of the solubility product and the influence of side components on the final solubility in the reaction media are not considered.

### Crystallization condition screening for transaminase-catalyzed reactions

After the determination of the respective salt pair solubilities and the selection of three possible carboxylic acid anions, a reaction model solution was created to allow for the investigation of the main factors for crystallization processes, mainly towards crystallized (S)-1PEA yields and obtained purities. As model conditions, the following parameters were chosen: the pH was kept at 7.5 with 50 mM phosphate buffer, (S)-1PEA concentration was kept at 50 mM to represent a somewhat high product concentration for the chosen reaction systems, starting from  $\geq 100$  mM substrate. With this constellation, the range of IPA, carboxylic anion concentrations, as well as the temperature were varied and tested as possible influencing parameters. The determined trends for those parameters are shown in Fig. 3. One must keep in mind that the reported results represent the initial precipitation of material without any additional washing steps that will lead to higher purities (see below for transaminase- and amine dehydrogenase-catalyzed reactions). As shown in Fig. 3, all three tested carboxylic anions chosen for this analysis basically follow the same trends, when the respective concentration is varied at a fixed amount of 500 mM isopropylamine ( $T = 22$  °C). With increasing concentrations of the carboxylic anions in solution, product amine crystallization yield increases (1A through 3A). As expected, this leads to an increase of crystallization of the undesired isopropylamine salt, hence causing a decrease in the crystallized product purity. The effect is significant while using DPAA (1A), but only minor changes are found with 34CA and 43CNA (2A and 3A). The best combination was found to be 43CNA with almost 90% yield and 95% purity (without additional washing steps). The parallel effect of a variation of applied isopropylamine shows a similar trend (1B through 3B). An addition of considerable amounts of

Table 1 Results of the solubility screening of IPA-, ammonium and (S)-1PEA salts of potential carboxylic anion candidates at 30 °C

Acid anion	IPA-salt/(S)-1PEA salt quotient				Ammonium salt/(S)-1PEA salt quotient
		IPA-salt solubility (mM)	(S)-1PEA salt solubility (mM)	Ammonium salt solubility (mM)	
3DPPA	9.6	51.7 ± 0.3	5.4 ± 0.1	216.5 ± 87.5	40.1
2DPPA	19.7	78.6 ± 0.2	4.0 ± 0.1	219.4 ± 23.2	54.9
DPAA	15.6	168.2 ± 1.3	10.8 ± 0.1	223.5 ± 47.8	20.7
4BPA	6.3	83.6 ± 16.6	13.3 ± 0.5	236.6 ± 56.0	17.8
34CA	8.5	203.1 ± 1.0	24.0 ± 0.7	165.3 ± 49.0	6.9
PCPA	4.8	89.8 ± 0.5	18.9 ± 0.1	192.8 ± 37.3	10.2
43CNA	53.0	1066.1 ± 20.0	20.1 ± 0.4	2195.1 ± 121.7	109.2
25CNA	24.5	1529.2 ± 384.6	62.5 ± 0.5	1714.8 ± 135.5	27.4
2BPA	10.4	649.8 ± 24.3	62.5 ± 1.0	1092.8 ± 74.2	17.5
PFA	4.8	328.8 ± 35.4	69.1 ± 0.5	470.1 ± 250.5	6.8



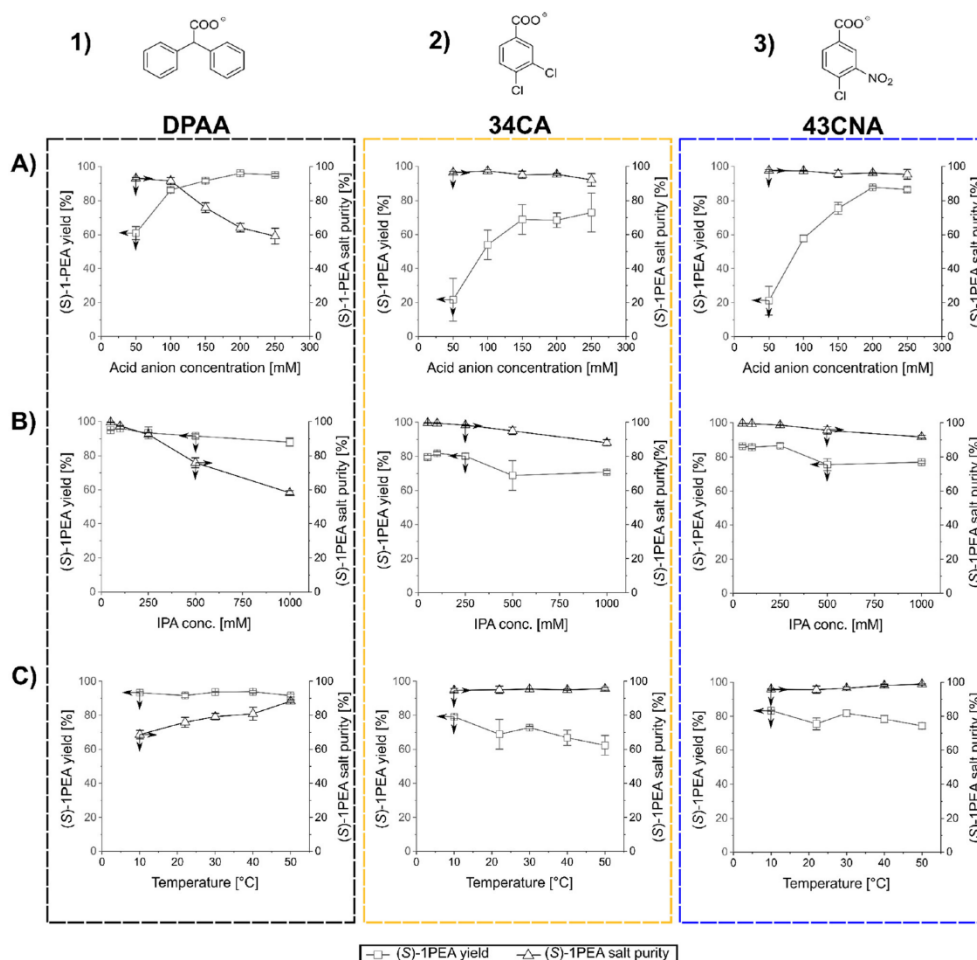


Fig. 3 Results of the parameter screening for the IPA-(S)-1PEA salt pair (transaminase reaction system). The columns show all three screened parameters for a particular carboxylic anion (marked above), while the rows show a certain parameter: A) varied acid anion concentration with 50 mM (S)-1PEA, 500 mM IPA, pH 7.5,  $T = 22^\circ\text{C}$ ; B) varied IPA concentration with 50 mM (S)-1PEA, 150 mM carboxylic anion, pH 7.5,  $T = 22^\circ\text{C}$ ; C) varied crystallization temperature with 50 mM (S)-1PEA, 500 mM IPA, 150 mM carboxylic anion, pH 7.5. The shown arrows indicate the corresponding axes.

isopropylamine into solution clearly leads to a decrease in yield and purity for all three anions, although, for 34CA and 43CNA the crystallized purity could still be kept relatively high at  $\geq 90\%$  (2B and 3B). Those decreases can easily be explained with the increasing ratio of donor isopropylamine (IPA) to product amine ((S)-1PEA) of 10:1 (500 mM IPA) and 20:1 (1000 mM IPA). An unexpected behavior was found with the shown effect of temperature on the investigated crystallization (1C through 3C). DPAA shows a remarkable increase of purity at higher temperatures, while the yield

seems to not be affected at all (both at ca. 90%, 1C). This can partially be explained through the increase in solubility of the obtained IPA-DPAA salt, seeming to be heavily affected by temperature. The disproportion in the solubilities of the salt pairs causes the increase in crystallization purity, since the solubility increase affects the IPA-salts more significantly than the (S)-1PEA-salts. The other carboxylic ions remain relatively stable with a slight decrease of the observed yield over the same temperature range (2C and 3C). However, with these other two carboxylic ions a considerably higher purity

was obtained with up to >99%, while still retaining a 70% yield (3C).

In summary, 43CNA has proven to be the most suited for crystallization of product amines from transaminase reactions under chosen conditions, having its product crystallization behavior least affected by the parameter variation in terms of crystallized product purities, while also retaining high product yields. One must note that those observations are relevant for reaction setups with roughly 50 mM product amine, whereas the yields and purity will

increase at higher and decrease at lower product concentrations. Hence, higher product concentrations are preferred.

#### Crystallization condition screening for amine dehydrogenase-catalyzed reactions

The screening of crystallization conditions for amine dehydrogenase-catalyzed reactions was handled in a similar manner as shown above. The most relevant change is the

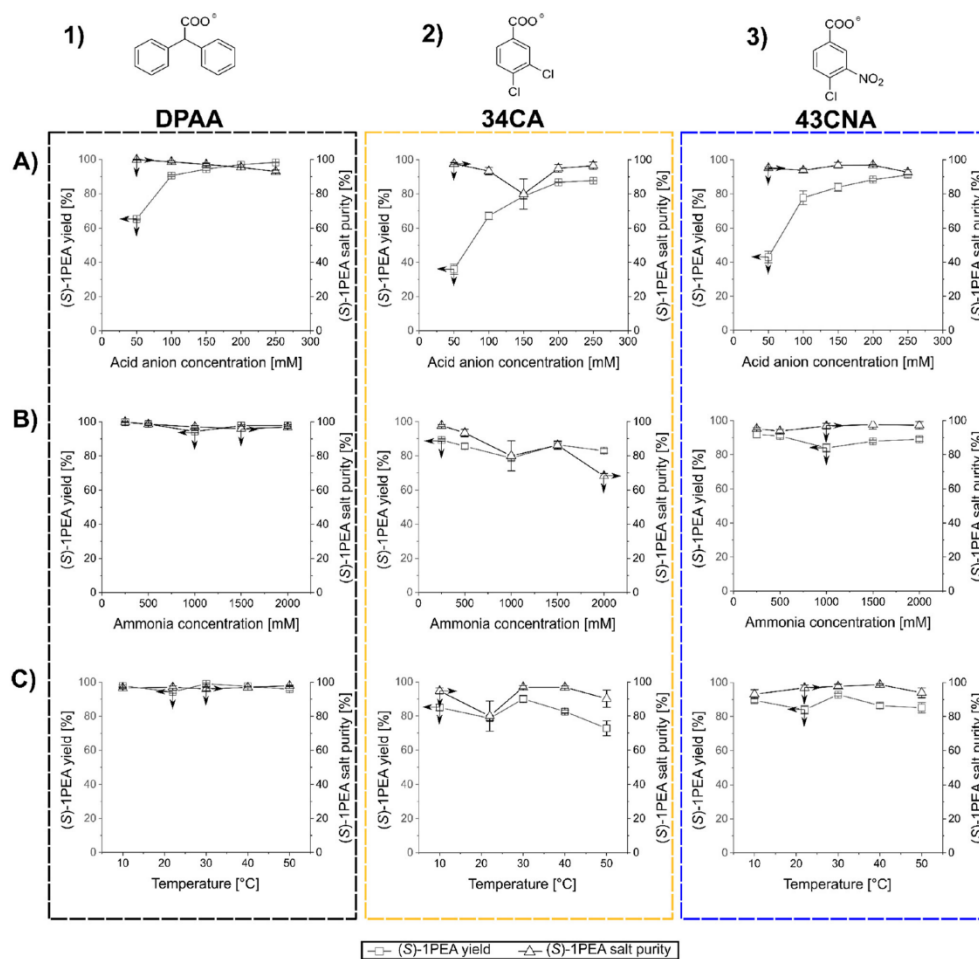


**Fig. 4** Results of the parameter screening for the ammonium - (S)-1PEA salt pair. The columns show all three screened parameters for a particular carboxylic anion (marked above), while the rows show a certain parameter: A) varied acid anion concentration with 50 mM (S)-1PEA, 1000 mM  $\text{NH}_4^+$ , pH 7.5,  $T = 22^\circ\text{C}$ ; B) varied ammonium concentration with 50 mM (S)-1PEA, 150 mM carboxylic anion, pH 7.5,  $T = 22^\circ\text{C}$ ; C) varied crystallization temperature with 50 mM (S)-1PEA, 1000 mM  $\text{NH}_4^+$ , 150 mM carboxylic anion, pH 7.5,  $T = 22^\circ\text{C}$ . The shown arrows indicate the corresponding axes.





replacement of isopropylamine with significantly higher amounts of ammonia, which is required for amine dehydrogenase-catalyzed reaction. Model reactions were conceptualized in a similar manner with the same parameters as shown above (pH 7.5,  $c((S)\text{-IPEA}) = 50 \text{ mM}$ , 50 mM phosphate buffer). Those parameters were chosen for comparability with the transaminase conditions, since usually other buffers and pH values are set for AmDH reactions. Since this study focuses on the downstream processing of the resulting reaction product, such relatively mild conditions could be easily adjusted for product crystallization after an AmDH reaction would reach its equilibrium. Temperature, carboxylic anion and ammonia concentrations were screened as variable parameters influencing crystallization. The determined trends for those parameters are shown in Fig. 4.

The results with the chosen three carboxylic anions follow roughly the same trend in comparison to the IPA-( $S$ )-IPEA salt pair discussed above, but in general higher yields and purities were obtained. The difference between isopropylamine and ammonia *versus* ( $S$ )-IPEA in precipitation is mainly caused by the higher solubilities of ammonium salts in comparison to isopropylammonium salts (also see Table 1).

An increased concentration of acid anion (at  $T = 22 \text{ }^{\circ}\text{C}$ ) within the crystallization solution again produces a significant yield increase, as expected, with a decrease of purity (1A–3A). The use of DPAA shows the highest yields with only a slight decrease of purity at higher concentrations (1A). For 34CA and 43CNA the yields are lower, however it is similarly coupled to a moderate purity decrease (2A and 3A) with a noticeable, but currently unclear dip at 150 mM 34CA. Regardless, high yields and purities of  $\geq 90\%$  were eventually obtained with all three chosen counterions.

As for the variation of ammonium concentration (1B through 3B), DPAA showed a remarkable efficiency at even the highest ammonia concentrations with consistently high purities and yields (1B). These results allow to withstand enormously high ammonia concentrations and keep a high product salt purity with mounting ammonium concentrations. Lower, but still relatively good yields and purities were observed with the use of 43CNA, consistently at above 80 and 90% respectively (3B). The purities and yields with the use of 34CA experienced a relatively high decrease with an increase of ammonium in solution (2B). Here, only this anion follows the trends outlined for mounting donor amine concentration, as shown for isopropylamine in Fig. 3 with having both yield and purity decreased significantly. The point, that DPAA and 43CNA product salts could keep relatively high yields and product salt purities even at ammonium concentrations of 2 M can as well be associated with the solubility differences as shown in Table 1.

Finally, temperatures affect the results again along the trends as outlined for the first salt pairs for transaminases (1C through 3C). An increase of temperatures provoked only insignificant crystallization yield decreases for DPAA and

43CNA, while their product salt purities remained constant on a very high level. DPAA was found again to be the most versatile counterion for high yields and purities at  $\geq 95\%$  (1C). As for 34CA, here the crystallization yield dropped significantly with an increase in crystallization temperature, what would follow the same explanation, as for the IPA salt pairs (2C). This is explained through the highest ( $S$ )-IPEA-salt and lowest ammonium salt solubility among the three salt pairs (also see Table 1), meaning, that at the most extreme temperature of  $50 \text{ }^{\circ}\text{C}$  the disproportion between the solubilities within the 34CA salt pair was not sufficient to keep the high purity of the crystallized product salt in check (2C).

In summary, considering the generated data, DPAA was proven to be the best suited for the amine dehydrogenase reaction system among the three tested anions, being able to generate the highest product salt purities throughout all tested condition extremes, while also generating the highest crystallization yields.

### Preparative application of amine crystallization

After the determination of suitable crystallization conditions for all three selected carboxylic anions, two exemplary reactions were performed to show the efficacy of the proposed crystallization systems for downstream processing of biocatalyzed reactions.

### Transaminase-catalyzed reaction example

The enzyme chosen for the practical application example for biocatalytic transamination was the transaminase from *Ruegeria pomeroyi* (PDB-code: 3HMU; herein abbreviated as *Rpo*-TA), as *E. coli* whole cells. It has consistently shown to efficiently convert acetophenone into ( $S$ )-1-phenylethylamine with high stereoselectivity in the presence of isopropylamine as amine donor.<sup>53,55</sup> The reaction (300 mM acetophenone, 1500 mM IPA, pH 7.5) was performed under a constant vacuum to enable a slight reaction equilibrium shift towards the product side by removing acetone as the by-product. The reaction was monitored *via* gas chromatography. After 96 h, the reaction mixture was cleared of the residual cells by centrifugation and a product concentration of approximately 72 mM was determined.

The following crystallization as described in the experimental section initially produced an overall product crystallization yield of 89% with a product purity of 80%. The product salt was then washed with water, which increased the salt purity to 96%, corresponding to a yield of 84% after the washing step. To provide an explanation for the efficiency of the selective crystallization step we decided to determine the underlying ternary phase diagram. The phase diagram for the IPA/( $S$ )-IPEA-43CNA salt pair is provided in Fig. 5. The phase diagram shows an extreme asymmetry between the solubilities of the IPA salt and the ( $S$ )-IPEA salt. Noteworthy, the position of the eutectic is found to be extremely to the left hand side, creating an enormous



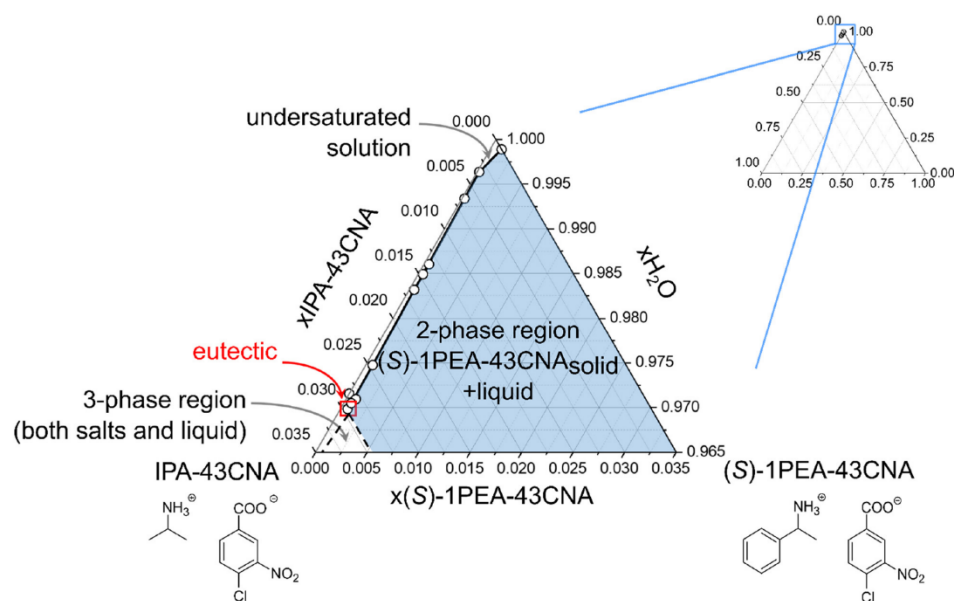


Fig. 5 Ternary phase diagram of the IPA/(S)-1PEA-43CNA salt pair in 10 mM phosphate buffer, pH 7.5.

asymmetry in the phase behavior. Through such a disproportion coupled with very low (S)-1PEA salt saturation concentration (Fig. 5), a very broad zone for possible pure (S)-1PEA salt crystallization is created, with the eutectic point signifying the borderline crystallization proportions within the salt pair. Such a broad selection for the crystallization possibilities of pure (S)-1PEA salt crystallization again shows a broad applicability of the tested system on different reaction setups for efficient and specific amine product crystallization from the reaction broths.

#### Amine dehydrogenase-catalyzed reactions

A similar proof of concept for the selective product crystallization was obtained for the amine dehydrogenase-catalyzed reaction. An engineered amine dehydrogenase (LE-AmDH-v1) originated from the  $\epsilon$ -lysine- $\epsilon$ -deaminating dehydrogenase from *Geobacillus stearothermophilus*, as reported by Tseliou *et al.*, was selected and used as a cell-free extract obtained from *E. coli*.<sup>37,56,57</sup> LE-AmDH-v1 was previously shown to convert acetophenone to (S)-1-phenylethylamine with high stereoselectivity and activity. The catalyst was used as cell-free extract to achieve uniformity with the cofactor regenerating formate dehydrogenase (FDH) from *Candida boidinii*, used in the reaction system as a pure protein suspension. The reaction (100 mM acetophenone, 2 M ammonium, pH 8.5) was performed according to the experimental section and monitored *via* gas chromatography.

After 72 h, the reaction mixture was cleared of the residual protein by centrifugation and the product concentration was determined at 55 mM. In the following crystallization step, an almost total yield could be obtained (99.9%) with an already very high purity of 94%, which approximately correlates with the screening study (see Fig. 4B). The crystallized product was again subjected to a washing step, yielding 97% purity with a remaining insignificant drop of yield to 98%.

Similar to the 43CNA salt pair (see Fig. 5), a ternary phase diagram was prepared for the DPAA salt pair to prove the broad applicability of this crystallization system as a potential downstream processing strategy. The phase diagram for the ammonium/(S)-1PEA-DPAA salt pair is shown in Fig. 6. The disproportion and asymmetry of the phase diagram in Fig. 6 is even greater, than for the 43CNA salt pair in Fig. 5. The eutectic is barely measurable at  $x > 0.99$  and thus the zone for selective (S)-1PEA salt crystallization is expanded, incl. an even higher potential concentration of ammonia in the reaction mixture.

## Experimental section

### Salt preparation

5 mmol of the corresponding carboxylic acid were dissolved in 20 ml methyl *tert*-butyl ether (MTBE) at room temperature. Mild heating up to 60 °C was applied, if necessary, to speed up the dissolution process. After dissolution of the carboxylic

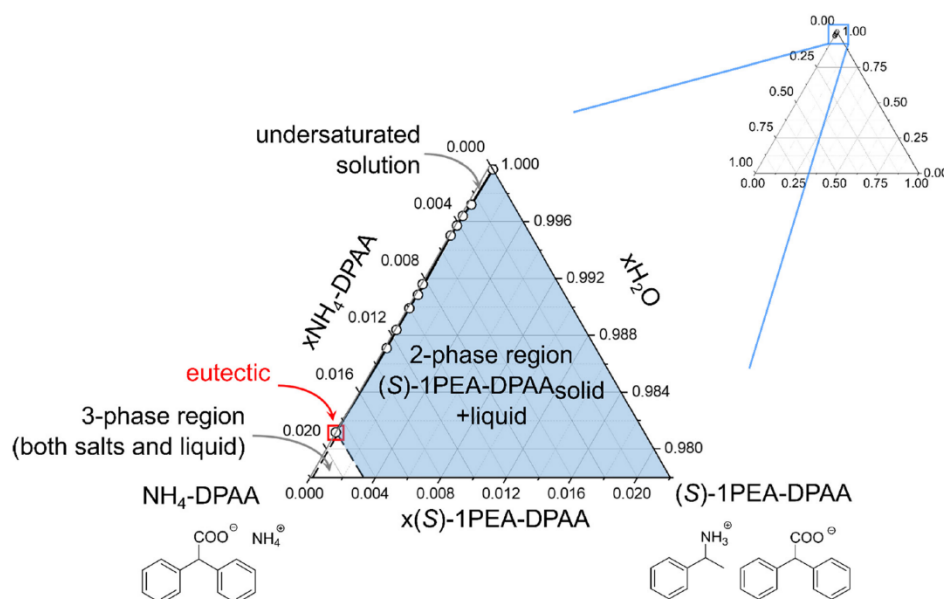


Fig. 6 Ternary phase diagram of the ammonium/(S)-1PEA-DPAA salt pair in 10 mM phosphate buffer, pH 7.5.

acid, 5 mmol of the corresponding amine were slowly added to the solution under constant stirring/shaking to avoid partial oversaturation. While isopropylamine and (S)-1-phenylethylamine were added as a pure liquid, ammonia was utilized/applied as a 25% (v/v) aqueous solution. The resulting mixture/suspension was thoroughly stirred/shaken and left for one hour at room temperature. Afterwards, the mixture/suspension was filtered to isolate the desired amine salt. The isolated salts were dried at room temperature overnight and verified *via*  $^1\text{H}$ - and  $^{13}\text{C}$ -NMR.

#### Solubility measurements

An appropriate amount of the corresponding amine salt was dissolved in 2 ml of high-purity water. Salt was added, until solution saturation was achieved. The saturated solution was shaken at 30 °C and 1000 rpm for 72 hours to achieve the dissolution equilibrium. The pH value was kept at 7. In the following step, the solutions were centrifuged for 5 min at 14 000 rpm and the resulting aqueous phase was filtered through 0.25  $\mu\text{m}$  syringe filters to remove traces of crystalline salt. The aqueous phase was filtered into previously weighed vials. After that, the vials were weighted again to determine the exact amount of water in the sample. The water was evaporated at 40 °C under a constant argon stream in a Thermo Scientific Pierce ReactiTherm I & ReactiVap I heating and evaporation unit. The evaporated samples were weighed in the vials and the solubility of the amine salt was

calculated. The experiments were performed in triplicates for each salt.

#### Precipitation from model solutions

To survey the crystallization parameters, the following experimental model was used. Two separate 10 ml aqueous solutions were prepared in 50 mM phosphate buffer, adjusted to a pH of 7.5 after preparation. One solution, referred to as the "amine solution", contained 100 mM (S)-1PEA and variable amounts of IPA or ammonia. The other solution, referred to as the "acid solution", contained the carboxylic acid used for precipitation in the form of a  $\text{Na}^+$ -salt. Such sodium salts were prepared by dissolving 1.5 g of the pure carboxylic acid in 50 ml of MTBE and adding 2 ml of a saturated NaOH-solution. The resulting sodium salt was filtered and dried overnight at RT.

To initiate (S)-1PEA precipitation, the acid solution was added to the amine solution in a dropwise manner under constant stirring at 700 rpm. Beforehand, GC-samples were drawn from the amine solutions as the initial amine concentration marker. The resulting precipitating mixture of 20 ml was left stirring for 30 minutes, evening out the crystallization equilibrium. Thus, the experimental model worked with an end concentration of (S)-1PEA of 50 mM, thus halving the amine concentration of the amine solution and the carboxylic anion concentration of the acid solution.



The equilibrated precipitated mixtures were analyzed for yield and purity of the resulting (S)-1PEA salt.

For crystallization yield analysis, GC-samples were taken according to the protocol below and compared to the initial concentration samples from prior to the crystallization procedure. Crystallization yield was calculated as:

$$\text{cr. yield} = 100\% - (n(\text{product in solution})/n(\text{product initial})) \times 100\%$$

It has to be noted that the initial product amount would be calculated from a concentration measurement from the 10 ml amine solution, while the dissolved product amount after crystallization would be calculated from a concentration measurement from the 20 ml mixed solution after removing the crystallized salt.

In order to analyze the purity of the obtained (S)-1PEA salts, those were filtered from the precipitation mixtures and dried prior to being analyzed via  $^1\text{H-NMR}$  (in  $\text{DMSO-}d_6$ ). The purity was derived from the ratio of amine salt specific peaks (IPA/ammonium-salt to (S)-1PEA) to each other (see ESI† for further information).

**Gas chromatography.** For the preparation of the gas chromatography measurements, 100  $\mu\text{l}$  samples were drawn from amine containing solutions. 20  $\mu\text{l}$  of saturated sodium hydroxide solution were added to facilitate amine deprotonation. The samples were vortexed. 140  $\mu\text{l}$  of cyclopentyl methyl ether (CPME) were added per sample. With this, an extraction was performed by vortexing the samples for 1 minute at max. speed. After phase separation, 50  $\mu\text{l}$  of the CPME-phase were drawn for GC-analysis. This sample aliquot was added to 50  $\mu\text{l}$  of pure CPME and 20  $\mu\text{l}$  of 25 mM *n*-decane solution in CPME as an internal standard, thus yielding a 120  $\mu\text{l}$  sample for GC-measurements.

The measurements were performed on a Thermo Fisher Trace 1310 gas chromatograph equipped with a flame ionization detector (FID). A J&W column (0.25 mm  $\times$  30 m  $\times$  0.25  $\mu\text{m}$ , HP-5 phase) by Agilent Technologies (series number 19091J-433), shortened for 1 mm on each end was used. Helium and synth air were used as the carrier. The following temperature program was used: starting temperature: 90  $^\circ\text{C}$ ; 1. 90–100  $^\circ\text{C}$ : rate of 2  $^\circ\text{C min}^{-1}$ ; 2. 100–130  $^\circ\text{C}$ : rate of 20  $^\circ\text{C min}^{-1}$ ; 3. 130–180  $^\circ\text{C}$ : rate of 10  $^\circ\text{C min}^{-1}$ ; Split factor 35.0. The chromatograms were refined and analyzed via the Thermo Xcalibur Qual Browser software by Thermo Fisher. For amine quantification, the obtained amine peak areas were normalized with the internal standard, scaled for the internal standard value of 100 000 sqU and then the amine concentration was calculated according to the calibration parameters (see ESI† for amine calibration curve).

### Biocatalyst preparation

Biocatalysts were prepared through overexpression in *E. coli* BL21 cells.

**Heat-shock transformation into BL21 cells.** For the transformation, chemocompetent *E. coli* BL21 cells (50  $\mu\text{l}$  aliquots) were thawed on ice for 10 min. After that, 1  $\mu\text{l}$  of the available plasmid preparation was added to the cell suspension. The cells were then incubated for 30 min on ice. In the following step, the cell aliquot was placed into a prewarmed heating block for 30 s at 42  $^\circ\text{C}$  and placed back onto the ice immediately after, chilling on ice for 5 min. 950  $\mu\text{l}$  of LB medium were added to the cells. This suspension was incubated at 37  $^\circ\text{C}$  and 900 rpm for 1 hour. Variable volumes were plated onto selective LB-agar plates (ampicillin selection for *Rpo*-TA, kanamycin selection for LE-AmDH-v1). The plates were incubated overnight at 37  $^\circ\text{C}$ .

**Overnight cultivation.** All overnight cultures were inoculated as 5 ml of LB medium and supplemented with antibiotics to a final concentration of either 0.05  $\text{mg ml}^{-1}$  of kanamycin or 0.1  $\text{mg ml}^{-1}$  ampicillin. Cultures were grown overnight (18 h) at 37  $^\circ\text{C}$  and 900 rpm.

**Preparation of cryostocks.** To preserve the transformed strains made over the course of this work, cryostocks of those were made. For this purpose, 800  $\mu\text{l}$  of overnight cultures were mixed with 200  $\mu\text{l}$  of sterile glycerol (resulting in 20% v/v glycerol stocks) and frozen at  $-80^\circ\text{C}$ .

**Expression.** The expression cultures were grown in auto-induction medium for T7-promoter based expression systems (AIM, formulated after Studier 2005<sup>58</sup>) in 1 l flasks. 500 ml of AIM were taken per flask. 500  $\mu\text{l}$  of ampicillin/kanamycin (1:1000) were added. The cultures were inoculated to an OD600 of approximately 0.05 from overnight cultures. The cultures were first incubated at 37  $^\circ\text{C}$  for 5–6 hours and afterwards at 30  $^\circ\text{C}$  for 18 hours under constant shaking at 150 rpm. After a 24 hour cultivation the cells were harvested via centrifugation at  $4000 \times g$  for 10 min at 4  $^\circ\text{C}$ . The pellets were resuspended in 5 ml of utilized buffer (10 mM phosphate buffer for lyophilization) and centrifuged again at  $4000 \times g$  for 10 min at 4  $^\circ\text{C}$ . After resuspension in 5 ml of the utilized buffer, the pellet suspensions were unified and lyophilized or frozen at  $-20^\circ\text{C}$  (only prior to lysis).

AIM – auto-induction medium preparation: the following components were mixed together: 950 ml  $\text{ddH}_2\text{O}$ , 10 g tryptone, 5 g yeast extract, 2.68 g  $\text{NH}_4\text{Cl}$ , 0.71 g  $\text{Na}_2\text{SO}_4$ , 5 g glycerol 85%, 0.5 g glucose, 2 g lactose and the resulting solution sterilized by autoclave. After the cooling to RT, the following solutions were added: 1 ml 2 M  $\text{MgSO}_4$  (0.22  $\mu\text{m}$  filter sterilized), 40 ml 1 M  $\text{K}_2\text{HPO}_4$  (autoclaved), 10 ml 1 M  $\text{KH}_2\text{PO}_4$  (autoclaved) and the appropriate antibiotic(s) were added before usage.

**Cell lysis.** For cell lysis, the frozen cell suspension was thawed in a water bath at 37  $^\circ\text{C}$ . 2  $\mu\text{l ml}^{-1}$  DNase I solution were added to the suspension. Cells were lysed through sonication by a Hielscher UP200S ultrasonic processor at an amplitude of 55% for 10 min (5 cycles of 1 min sonication and 1 min rest) while being chilled on ice. After lysis, the lysate suspension was centrifuged at  $10\,000 \times g$  for 30 min at 4  $^\circ\text{C}$ . The cleared lysate supernatant was collected and lyophilized.



## Enzyme activity assays

**Transaminase.** Enzyme activity was measured with a Specord 200 spectrophotometer from Analytik Jena (Jena, Germany) at a wavelength of 245 nm using the acetophenone extinction coefficient of  $11.852 \text{ mM}^{-1} \text{ cm}^{-1}$ . A 50 mM potassium phosphate buffer solution with 0.25% (v/v) DMSO was adjusted to pH 8 with saturated NaOH solution and conc. HCl to be used for all further solutions. 250  $\mu\text{L}$  of the buffer solution, 250  $\mu\text{L}$  of a 10 mM (S)-1-phenylethylamine solution in buffer and 250  $\mu\text{L}$  of a 10 mM sodium pyruvate solution in buffer were premixed in the measurement cuvettes. The enzyme samples were prepared by dissolving 1 mg of dry weight whole cells in 1800  $\mu\text{L}$  of buffer and adding 200  $\mu\text{L}$  of a 10 mM pyridoxal phosphate solution in buffer. 250  $\mu\text{L}$  of this enzyme mix were then added to the pre-pipetted samples, briefly stirred and measured immediately. All experiments were measured against a reference solution by replacing the enzyme mix with 50  $\mu\text{L}$  of the 10 mM pyridoxal phosphate and 200  $\mu\text{L}$  of buffer. Specific enzyme activity was calculated through the slope of acetophenone extinction over the course of 60 s.

**Amine dehydrogenase.** AmDH activity was measured via NADH absorption decrease. A 500 mM acetophenone stock solution in DMSO was diluted to 350 mM with 2 M  $\text{HCOO}^- \text{NH}_4^+/\text{NH}_3$  buffer (pH 8.5). A 50 mM NADH stock solution in 50 mM phosphate buffer (pH 8) was prepared, then further diluted to 10 mM with 2 M  $\text{HCOO}^- \text{NH}_4^+/\text{NH}_3$  buffer. 1 mg of the prepared freeze-dried cell-free extract was dissolved in 2 ml of 2 M  $\text{HCOO}^- \text{NH}_4^+/\text{NH}_3$  buffer as the enzyme stock solution.

For the measurement, 639  $\mu\text{L}$  of the 2 M  $\text{HCOO}^- \text{NH}_4^+/\text{NH}_3$  buffer (pH 8.5) were mixed with 86  $\mu\text{L}$  of the 350 mM acetophenone solution and 250  $\mu\text{L}$  of the enzyme solution. The mixture was prewarmed at 60  $^\circ\text{C}$  for 2 min. To start the measurement, 25  $\mu\text{L}$  of the 10 mM NADH solution were added to the sample. NADH absorption decrease at 360 nm was measured for 1 min, its linear slope being used to calculate enzymatic activity according to the Lambert–Beer law (NADH extinction at 360 nm  $\epsilon = 4250 \text{ M}^{-1} \text{ cm}^{-1}$ ). A mixture of 914  $\mu\text{L}$  of 2 M  $\text{HCOO}^- \text{NH}_4^+/\text{NH}_3$  buffer with 86  $\mu\text{L}$  of the acetophenone solution were used as the reference. All measurements were performed in a triplicate.

Reaction procedure with (S)-selective transaminase from *Ruegeria pomeroyi* (Rpo-TA)

To obtain a practical demonstration for the described product crystallization, enzymatic batch reactions with an (S)-selective transaminase from *Ruegeria pomeroyi* were made. For this purpose, 1283  $\mu\text{L}$  of pure IPA were dissolved in 10 ml 50 mM sodium phosphate buffer to a final concentration of 1500 mM IPA with the addition of 6.18 mg PLP (final concentration 2.5 mM) at pH 7.5. The pH was adjusted to 7.5 with conc. HCl and NaOH. 16.75 U  $\text{mL}^{-1}$  (670 mg) of cultivated dry weight *E. coli* cells bearing the overexpressed Rpo-TA (previously measured enzyme activity 250 mU  $\text{mg}^{-1}$ ,

see ENZYME ACTIVITY ASSAYS) were added to the reaction mixture. The pH was again adjusted to 7.5. To start the reaction, 350  $\mu\text{L}$  acetophenone were added (equals to 300 mM). The reaction was incubated at 30  $^\circ\text{C}$  under constant stirring and a vacuum of 300 mbar for 96 h. For reaction monitoring, 100  $\mu\text{L}$  samples were drawn every 24 h (see GC-method). The reactions were prepared in a triplicate to ensure sufficient volumes for product crystallization.

After determining the reaction yields, cell material was removed from the reaction solutions via two centrifugation steps. The first centrifugation was performed at  $4000 \times g$  and 4  $^\circ\text{C}$  for 10 min, whereafter the cleared supernatant was transferred into new tubes and centrifuged at  $10\,000 \times g$  and 4  $^\circ\text{C}$  for 10 min. 10 ml of the cleared unified supernatant were then subjected to product crystallization. For this purpose, pure  $43\text{CNA}^- \text{Na}^+$  salt was added to the supernatant to a final concentration of 150 mM. After the sodium salt dissolution, the pH was briefly adjusted to 7.5. The solution was left shaking at room temperature (22  $^\circ\text{C}$ ) over night. Afterwards it was filtered to separate the product salt. The salt was dried and analyzed via NMR to determine its purity. The filtrate was analyzed via GC to determine the total yield. To ensure sufficient purity, the filtered salt was washed three times with 2 ml of pure  $\text{H}_2\text{O}$ . After each washing step, samples were drawn for purity (NMR) and product loss (filtrate) analysis.

Reaction procedure with engineered amine dehydrogenase from L-lysine-( $\epsilon$ -deaminating) dehydrogenase from *Geobacillus stearothermophilus* (LE-AmDH-v1)

To obtain a practical demonstration for product crystallization from amine dehydrogenase reactions, an enzymatic batch reaction with the LE-AmDH-v1 was initiated. For this purpose, 132.7 mg  $\text{NAD}^+$  (final concentration 10 mM) were dissolved in 20 ml of a 2 M  $\text{NH}_4^+ \text{HCOO}^-$  buffer at a pH of 8.5. 30 U  $\text{mL}^{-1}$  (2 g) of freeze-dried cell-free extract from *E. coli* bearing the overexpressed LE-AmDH-v1 (previously measured enzyme activity 300 mU  $\text{mg}^{-1}$ , see ENZYME ACTIVITY ASSAY) were added to the reaction mixture. 213  $\mu\text{L}$  (16 U) FDH solution by Megazyme were added from a 75 U  $\text{mL}^{-1}$  stock solution. The pH was adjusted to 8.5 with conc. HCl and NaOH. To start the reaction, 234  $\mu\text{L}$  pure acetophenone were added (equals to 100 mM). The reaction was incubated at 30  $^\circ\text{C}$  under constant shaking for 72 h. For reaction monitoring, 100  $\mu\text{L}$  samples were drawn every 24 h (see GC-method).

After determining the reaction yields, protein was removed from the reaction solutions via centrifugation at  $10\,000 \times g$  and 4  $^\circ\text{C}$  for 10 min. 10 ml of the cleared supernatant were then subjected to product crystallization. For this purpose, pure  $\text{DPAA}^- \text{Na}^+$  salt was added to the supernatant to a final concentration of 150 mM. After the sodium salt dissolution, the pH was briefly adjusted to 7.5. The solution was left shaking at room temperature (22  $^\circ\text{C}$ ) overnight. Afterwards it was filtered to separate the product salt. The salt was dried



and analyzed *via* NMR to determine its purity. The filtrate was analyzed *via* GC to determine the total yield. To ensure sufficient purity, the filtered salt was washed three times with 2 ml of pure H<sub>2</sub>O. After each washing step, samples were drawn for purity (NMR) and product loss (filtrate) analysis.

#### Generation of chosen phase diagrams for utilized salt pairs

For further examination of the crystallization mechanisms, phase diagrams of the NH<sub>4</sub><sup>+</sup>/(S)-1PEA-DPAA and IPA/(S)-1PEA-43CNA were prepared. For this purpose, the two salts of each salt pair were mixed in 9 different proportions (with additionally each pure salt as a control) and dissolved in 0.01 M phosphate buffer (pH 7.5) until a saturated solution was formed. To compensate for the dissolved parts, the same salt proportion mixture was added to each sample individually. The salts were left to dissolve at 25 °C and 150 rpm for 6 days (or until no further pH changes occurred) to reach solution saturation. Additional salt mixture was added on the second day, the pH was readjusted every 2 days.

The salt solutions were centrifuged at 10 000 × g for 5 min and the supernatant was filtered through 0.2 µm filters to remove all residual salt crystals. Afterwards, solution samples of approx. 1 ml were evaporated in a Thermo Scientific Pierce ReactiTherm I & ReactiVap I heating and evaporation unit under a constant argon stream. As was the case with other solubility measurements, the sample vials were weighed three times: empty, when filled with the samples (to determine the exact water amount) and after evaporation. The final ratios of the salt mixtures were determined *via* NMR.

This data was summarized and the mole fractions of the used salts and water could be calculated. Those mole fractions were then mapped against each other as a ternary diagram with the Origin 2021 software, resulting into a ternary phase diagram of the salt pair.

## Conclusion

The claimed systems for post-reaction crystallization downstream processing were successfully tested for both the transaminase- and amine dehydrogenase-catalyzed reaction setups. Through a broad parameter variation, the ideal salt pairs within the tested scope could be determined. A proof of concept was obtained within realistic enzymatic reactions performed incl. high amine donor concentrations (1.5–2 M) for maximal interference simulation with the downstream processing. Nevertheless, very high purities of the amine product coupled with high yields in product recovery could be achieved. The following investigation into the salt pairs crystallization behavior by means of the ternary phase diagrams revealed a very broad spectrum of possible reaction setups, within which the amine products could be specifically crystallized despite extreme amine donor concentrations.

The product itself can easily be recovered from the obtained product salt as described by Neuburger *et al.*<sup>54</sup> While demonstrating a high efficiency, this method also allows for almost full recycling of the

applied carboxylic acid through simple acidification, including its non-precipitated excesses for subsequent crystallizations.

Our proposed method for amine downstream processing from enzymatic reactions proved to be fairly versatile while also being relatively facile to accomplish. The broader selection of the tested salt pairs and their acquired solubility data offers an even broader palette to suit individual needs for post-reaction amine crystallization from enzymatic reactions.

## Author contributions

Feodor Belov: conceptualization, data curation, formal analysis, methodology, investigation, validation, visualization, writing – original draft; Andrea Mildner: conceptualization, methodology, investigation, writing – review & editing; Tanja Knaus: methodology, writing – review & editing; Francesco G. Mutti: resources, supervision, writing – review & editing; Jan von Langermann: conceptualization, funding acquisition, project administration, resources, supervision, writing – review & editing.

## Conflicts of interest

There are no conflicts to declare.

## Acknowledgements

Funding for F. B. and J. v. L. by Central SME Innovation Programme (ZIM, projects 16KN073233 and ZF4402103CR9) and the Heisenberg Programme of the Deutsche Forschungsgemeinschaft (project number 450014604) is gratefully acknowledged. The authors thank the research group of Prof. Mirko Basen (Institute of Biological Science, University of Rostock) especially with Dr. Maria Lehmann and Dr. Ralf-Jörg Fischer and the research group of Prof. Kragl (Institute of Chemistry, University of Rostock) especially with Sandra Diederich for their ongoing support and fruitful discussions.

## Notes and references

- 1 S. Wu, R. Snajdrova, J. C. Moore, K. Baldenius and U. T. Bornscheuer, *Angew. Chem., Int. Ed.*, 2021, **60**(1), 88.
- 2 E. L. Bell, W. Finnigan, S. P. France, A. P. Green, M. A. Hayes, L. J. Hepworth, S. L. Lovelock, H. Niikura, S. Osuna, E. Romero, K. S. Ryan, N. J. Turner and S. L. Flitsch, *Nat. Rev. Methods Primers*, 2021, **1**, 46.
- 3 D. Yi, T. Bayer, C. P. S. Badenhurst, S. Wu, M. Doerr, M. Höhne and U. T. Bornscheuer, *Chem. Soc. Rev.*, 2021, **50**(14), 8003.
- 4 R. A. Sheldon and D. Brady, *ChemSusChem*, 2019, **12**(13), 2859.
- 5 R. A. Sheldon and J. M. Woodley, *Chem. Rev.*, 2018, **118**(2), 801.
- 6 B. Hauer, *ACS Catal.*, 2020, **10**(15), 8418.





- 7 P. N. Devine, R. M. Howard, R. Kumar, M. P. Thompson, M. D. Truppo and N. J. Turner, *Nat. Rev. Chem.*, 2018, **2**(12), 409.
- 8 <https://www.grandviewresearch.com/industry-analysis/enzymes-industry>, access 20.10.2022 15:15.
- 9 D. J. Timson, *Fermentation*, 2019, **5**(2), 39.
- 10 E. E. Ferrandi and D. Monti, *World J. Microbiol. Biotechnol.*, 2017, **34**(1), 13.
- 11 M. Höhne and U. T. Bornscheuer, *ChemCatChem*, 2009, **1**(1), 42.
- 12 E. Cigan, B. Eggbauer, J. H. Schrittwieser and W. Kroutil, *RSC Adv.*, 2021, **11**(45), 28223.
- 13 H. Gröger, *Appl. Microbiol. Biotechnol.*, 2019, **103**(1), 83.
- 14 H. Kohls, F. Steffen-Munsberg and M. Höhne, *Curr. Opin. Chem. Biol.*, 2014, **19**, 180.
- 15 F. G. Mutti and T. Knaus, *Enzymes Applied to the Synthesis of Amines*, in *Biocatalysis for Practitioners*, ed. G. de Gonzalo and I. Lavandera, Wiley, 2021, pp. 143–180.
- 16 D. Ghislieri and N. J. Turner, *Top. Catal.*, 2014, **57**(5), 284.
- 17 M. Breuer, K. Ditrach, T. Habicher, B. Hauer, M. Kessler, R. Stürmer and T. Zelinski, *Angew. Chem., Int. Ed.*, 2004, **43**(7), 788.
- 18 M. D. Patil, G. Grogan, A. Bommaris and H. Yun, *Catalysts*, 2018, **8**(7), 254.
- 19 M. D. Patil, G. Grogan, A. Bommaris and H. Yun, *ACS Catal.*, 2018, **8**(12), 10985.
- 20 A. Gomm and E. O'Reilly, *Curr. Opin. Chem. Biol.*, 2018, **43**, 106.
- 21 S. C. Cosgrove, J. I. Ramsden, J. Mangas-Sanchez and N. J. Turner, *Biocatalytic Synthesis of Chiral Amines Using Oxidoreductases*, in *Methodologies in Amine Synthesis*, ed. A. Ricci and L. Bernardi, Wiley, 2021, pp. 243–283.
- 22 J. Mangas-Sanchez, S. P. France, S. L. Montgomery, G. A. Aleku, H. Man, M. Sharma, J. I. Ramsden, G. Grogan and N. J. Turner, *Curr. Opin. Chem. Biol.*, 2017, **37**, 19.
- 23 L. Ducrot, M. Bennett, G. Grogan and C. Vergne-Vaxelaire, *Adv. Synth. Catal.*, 2021, **363**(2), 328.
- 24 D. Koszelewski, K. Tauber, K. Faber and W. Kroutil, *Trends Biotechnol.*, 2010, **28**(6), 324.
- 25 M. Voges, R. Abu, M. T. Gundersen, C. Held, J. M. Woodley and G. Sadowski, *Org. Process Res. Dev.*, 2017, **21**(7), 976.
- 26 F. Guo and P. Berglund, *Green Chem.*, 2017, **19**(2), 333.
- 27 D. Hülsewede, L.-E. Meyer and J. von Langermann, *Chemistry*, 2019, **25**(19), 4871.
- 28 A. Gomm, W. Lewis, A. P. Green and E. O'Reilly, *Chemistry*, 2016, **22**(36), 12692.
- 29 J. L. Galman, I. Slabu, N. J. Weise, C. Iglesias, F. Parmeggiani, R. C. Lloyd and N. J. Turner, *Green Chem.*, 2017, **19**(2), 361.
- 30 A. P. Green, N. J. Turner and E. O'Reilly, *Angew. Chem., Int. Ed.*, 2014, **53**(40), 10714.
- 31 E. O'Reilly, C. Iglesias, D. Ghislieri, J. Hopwood, J. L. Galman, R. C. Lloyd and N. J. Turner, *Angew. Chem.*, 2014, **126**(9), 2479.
- 32 D. Koszelewski, I. Lavandera, D. Clay, G. M. Guebitz, D. Rozzell and W. Kroutil, *Angew. Chem., Int. Ed.*, 2008, **47**(48), 9337.
- 33 L. Martínez-Montero, V. Gotor, V. Gotor-Fernández and I. Lavandera, *Adv. Synth. Catal.*, 2016, **358**(10), 1618.
- 34 S. E. Payer, J. H. Schrittwieser and W. Kroutil, *Eur. J. Org. Chem.*, 2017, **2017**(17), 2553.
- 35 T. Börner, G. Rehn, C. Grey and P. Adlercreutz, *Org. Process Res. Dev.*, 2015, **19**(7), 793.
- 36 M. Doeker, L. Grabowski, D. Rother and A. Jupke, *Green Chem.*, 2022, **24**(1), 295.
- 37 V. Tseliou, T. Knaus, M. F. Masman, M. L. Corrado and F. G. Mutti, *Nat. Commun.*, 2019, **10**(1), 3717.
- 38 L. Liu, D.-H. Wang, F.-F. Chen, Z.-J. Zhang, Q. Chen, J.-H. Xu, Z.-L. Wang and G.-W. Zheng, *Catal. Sci. Technol.*, 2020, **10**(8), 2353.
- 39 A. Pushpanath, E. Siirola, A. Bornadel, D. Woodlock and U. Schell, *ACS Catal.*, 2017, **7**(5), 3204.
- 40 B. R. Bommaris, M. Schürmann and A. S. Bommaris, *Chem. Commun.*, 2014, **50**(95), 14953.
- 41 O. Mayol, K. Bastard, L. Beloti, A. Frese, J. P. Turkenburg, J.-L. Petit, A. Mariage, A. Debar, V. Pellouin, A. Perret, V. de Berardinis, A. Zaparucha, G. Grogan and C. Vergne-Vaxelaire, *Nat. Catal.*, 2019, **2**(4), 324.
- 42 M. J. Abrahamson, E. Vázquez-Figueroa, N. B. Woodall, J. C. Moore and A. S. Bommaris, *Angew. Chem., Int. Ed.*, 2012, **51**(16), 3969.
- 43 A. A. Caparco, E. Pelletier, J. L. Petit, A. Jouenne, B. R. Bommaris, V. Berardinis, A. Zaparucha, J. A. Champion, A. S. Bommaris and C. Vergne-Vaxelaire, *Adv. Synth. Catal.*, 2020, **362**(12), 2427.
- 44 C. Matassa, D. Ormerod, U. T. Bornscheuer, M. Höhne and Y. Satyawali, *Process Biochem.*, 2019, **80**, 17.
- 45 I. Slabu, J. L. Galman, C. Iglesias, N. J. Weise, R. C. Lloyd and N. J. Turner, *Catal. Today*, 2018, **306**, 96.
- 46 J. W. Westley, R. H. Evans and J. F. Blount, *J. Am. Chem. Soc.*, 1977, **99**(18), 6057.
- 47 M. H. T. Kwan, J. Breen, M. Bowden, L. Conway, B. Crossley, M. F. Jones, R. Munday, N. P. B. Pokar, T. Screen and A. J. Blacker, *J. Org. Chem.*, 2021, **86**(3), 2458.
- 48 F. C. Ferreira, N. F. Ghazali, U. Cocchini and A. G. Livingston, *Tetrahedron: Asymmetry*, 2006, **17**(9), 1337.
- 49 F.-X. Gendron, J. Mahieux, M. Sanselme and G. Coquerel, *Cryst. Growth Des.*, 2019, **19**(8), 4793.
- 50 J. Urbanus, C. Roelands, D. Verdoes and J. H. ter Horst, *Chem. Eng. Sci.*, 2012, **77**, 18.
- 51 J. Ren, P. Yao, S. Yu, W. Dong, Q. Chen, J. Feng, Q. Wu and D. Zhu, *ACS Catal.*, 2016, **6**(2), 564.
- 52 J. Bao, K. Koumatsu, K. Furumoto, M. Yoshimoto, K. Fukunaga and K. Nakao, *Chem. Eng. Sci.*, 2001, **56**(21–22), 6165.
- 53 D. Hülsewede, M. Tänzler, P. Süß, A. Mildner, U. Menyes and J. von Langermann, *Eur. J. Org. Chem.*, 2018, **2018**(18), 2130.
- 54 J. Neuburger, F. Helmholz, S. Tiedemann, P. Lehmann, P. Süß, U. Menyes and J. von Langermann, *Chem. Eng. Process.*, 2021, **168**, 108578.



- 55 D. Hülsewede, J.-N. Dohm and J. von Langermann, *Adv. Synth. Catal.*, 2019, **361**(11), 2727.
- 56 V. Tseliou, T. Knaus, J. Vilim, M. F. Masman and F. G. Mutti, *ChemCatChem*, 2020, **12**(8), 2184.
- 57 V. Tseliou, D. Schilder, M. F. Masman, T. Knaus and F. G. Mutti, *Chemistry*, 2021, **27**(10), 3315.
- 58 F. W. Studier, *Protein Expression Purif.*, 2005, **41**(1), 207.





## Publication 2: Crystallization Assisted Dynamic Kinetic Resolution for the Synthesis of (*R*)- $\beta$ -Methylphenethylamine

F. Belov, A. Gazizova, H. Bork, H. Gröger and J. von Langermann

*ChemBioChem*, 2024, 25(16), e202400203.

Received: 05<sup>th</sup> March 2024

Accepted: 11<sup>th</sup> April 2024

DOI: 10.1002/cbic.202400203

### Abstract:

This study explores a combination of the concept of enantioselective enzymatic synthesis of  $\beta$ -chiral amines through transamination with *in situ* product crystallization (ISPC) to overcome product inhibition. Using 2-phenylpropanal as a readily available and easily racemizing substrate of choice, (*R*)- $\beta$ -methylphenethylamine ((*R*)-2-phenylpropan-1-amine) concentrations of up to 250 mM and enantiomeric excesses of up to 99 % are achieved when using a commercially available transaminase from *Ruegeria pomeroyi* in a fed-batch based dynamic kinetic resolution reaction on preparative scale. The source of substrate decomposition during the reaction is also investigated and the resulting unwanted byproduct formation is successfully reduced to insignificant levels.



# Crystallization Assisted Dynamic Kinetic Resolution for the Synthesis of (R)- $\beta$ -Methylphenethylamine

Feodor Belov,<sup>[a]</sup> Alina Gazizova,<sup>[b]</sup> Hannah Bork,<sup>[c]</sup> Harald Gröger,<sup>[c]</sup> and Jan von Langermann<sup>\*[a]</sup>

This study explores a combination of the concept of enantioselective enzymatic synthesis of  $\beta$ -chiral amines through transamination with *in situ* product crystallization (ISPC) to overcome product inhibition. Using 2-phenylpropanal as a readily available and easily racemizing substrate of choice, (R)- $\beta$ -methylphenethylamine ((R)-2-phenylpropan-1-amine) concentrations of up to 250 mM and enantiomeric excesses of up to 99% are

achieved when using a commercially available transaminase from *Ruegeria pomeroyi* in a fed-batch based dynamic kinetic resolution reaction on preparative scale. The source of substrate decomposition during the reaction is also investigated and the resulting unwanted byproduct formation is successfully reduced to insignificant levels.

## Introduction

Chiral amines are a very important compound class, utilized predominantly as building blocks in pharmaceutical and agrochemical synthesis.<sup>[1,2,3,4,5]</sup> An estimated 40% of active pharmaceutical ingredients (APIs) contain amine moieties.<sup>[6–9]</sup> Hence, efficient synthetic pathways for the production of such chiral building blocks are highly desired. Purely chemical approaches, such as reductive amination via metal catalysts, nucleophilic addition or diastereomeric crystallization of enantiomerically pure amine salts,<sup>[6]</sup> may face challenges due to harsh reaction conditions or a generally high amount of waste produced in the reaction caused by the use of protective groups or discarding of the undesired enantiomer.<sup>[1,2,4,5,10]</sup>

Here, enzymatic synthesis approaches present a well-applicable alternative to conventional chemical synthesis, allowing to circumvent some of the mentioned challenges. Typically operating at mild reaction conditions, enzymes possess a high initial enantioselectivity as catalysts, which can

be engineered to even higher levels.<sup>[11]</sup> Although facing several limitations, such as stability, disadvantageous reaction equilibria and cofactor dependency, themselves, the benefits of one-step enantioselective synthesis usually outweigh the need for extra effort for enzymatic catalysis.

A spectrum of enzyme classes, depending on the desired reaction conditions, can be employed for amine production: amine and amino acid dehydrogenases, P450 monooxygenases and amine oxidases, imine reductases, lipases, Pictet-Spenglerases, berberine bridge enzymes and transaminases.<sup>[6–9]</sup> The latter are a well-established enzyme class of pyridoxal-5'-phosphate-dependent (PLP-dependent) transferases, which transfer amino groups between an amine donor and an amine acceptor. This work will focus on amine transaminases (ATAs), a subgroup of  $\omega$ -transaminases, which found a broad applicability in enantioselective amine synthesis, converting carbonyl moieties into amino groups without requiring the presence of a carboxylic group in the substrate.<sup>[12]</sup>

$\omega$ -Transaminases (and ATAs in particular) have mainly been utilized in the synthesis of primary  $\alpha$ -chiral amines.<sup>[1,8,13,14]</sup> However, only comparably few examples have been published in terms of  $\beta$ -chiral amine chemoenzymatic synthetic approaches, while chemical methods still prevail in such for  $\beta$ -chiral amines.<sup>[15]</sup> Fuchs *et al.* has shown a practical application of transaminases for a one-step synthesis of  $\beta$ -chiral amines from  $\alpha$ -chiral aldehydes in 2014. The paper reported high yields of desired  $\beta$ -chiral amine products accompanied by high enantiomeric excesses of the products, all based on the self-racemizing properties of 2-phenylpropanal and its derivatives as chosen substrates in this dynamic kinetic resolution (DKR) and the stereoselectivity of the utilized enzymes.<sup>[13]</sup> This line of work was continued by Fuchs *et al.*, resulting in a paper about a practical application for the synthesis of  $\beta$ -chiral amine API precursors for pregabalin and brivaracetam.<sup>[16]</sup> Other approaches for DKR-based synthesis of  $\beta$ -chiral amines include the works of Koszelewski *et al.*,<sup>[17]</sup> and Chung *et al.*<sup>[18]</sup> In 2022, another such conversion was shown for  $\alpha$ -branched aldehydes as part of an enzymatic cascade starting with epoxides as the

[a] M. Sc. F. Belov, Prof. Dr. J. von Langermann  
Institute of Chemistry, Biocatalytic Synthesis Group  
Otto von Guericke University of Magdeburg  
Building 28, Universitätsplatz 2, 39106 Magdeburg (Germany)  
E-mail: jan.langermann@ovgu.de

[b] M. Sc. A. Gazizova  
Institute of Chemistry, Department of Technical Chemistry  
University of Rostock  
Albert-Einstein-Str. 3A, 18059 Rostock (Germany)

[c] M. Sc. H. Bork, Prof. Dr. H. Gröger  
Faculty of Chemistry  
Bielefeld University  
Universitätsstrasse 25, 33615 Bielefeld (Germany)

Supporting information for this article is available on the WWW under <https://doi.org/10.1002/cbic.202400203>

© 2024 The Authors. ChemBioChem published by Wiley-VCH GmbH. This is an open access article under the terms of the Creative Commons Attribution Non-Commercial NoDerivs License, which permits use and distribution in any medium, provided the original work is properly cited, the use is non-commercial and no modifications or adaptations are made.

substrate.<sup>[19]</sup> The enzymatic toolbox for this application was also broadened by adapting the IRED enzyme class to synthesize a number of secondary  $\beta$ -chiral amines from  $\alpha$ -branched aldehydes.<sup>[20]</sup> However, all those publications, except for Chung *et al.*, worked with relatively low substrate loadings, the highest being the preparative scale experiments of Fuchs *et al.* 2014 with a 50 mM substrate concentration.

With transaminases facing product inhibitions and unfavorable reaction equilibria, it may become difficult to realize a scalable and technically attractive enzymatic synthesis unless specifically tailored enzymes can be designed. To circumvent such unfavorable reaction equilibria, methods like self-eliminating amine donors, enzymatic cascades, raising the amine donor concentrations to extremely high disproportionate excesses, *in situ* product extraction or other chemical engineering approaches are employed.<sup>[21,22]</sup> However, commonly utilized high reagent excesses may not only complicate downstream processing and conventional product isolation (e.g. chromatography), but also present an additional economic burden due to increased reagent costs and high waste amounts unless the recycling of those reagents can be realized. In order to overcome such limitations, product crystallization offers an alternative route to pure product isolation from reaction media. Product crystallization can be applied as a simple means for post-reaction downstream processing,<sup>[23]</sup> or on a continuous process basis, shifting the reaction equilibrium to the product side via removing the reaction product to the solid phase. This concept is called reactive crystallization or *in situ* product crystallization (ISPC). While encountering its own limitations, such as potential enzyme inhibitions through the utilized counterions or stirring complications due to the forming of a suspension, it allows for a continuous reaction equilibrium shift to the product side, hence facilitating the circumvention of any possible product inhibition by crystallizing it out of said equilibrium. When the right counterion is found, very high product yields can be achieved on a continuous or a semi-continuous basis.<sup>[22,24–27]</sup>

With this work, we aim to combine previous successful concepts for the enzymatic synthesis of  $\beta$ -chiral amines with ISPC to achieve an improvement of existing preparative conversions of the  $\alpha$ -branched aldehyde 2-phenylpropanal towards the  $\beta$ -chiral amine (*R*)-2-phenylpropan-1-amine ((*R*)- $\beta$ -methylphenethylamine). By combining the ISPC concept with the transaminase from *Ruegeria pomeroyi* (*Rpo*-ATA, see Figure 1), we succeeded in running the process with high product concentrations and enantiomeric excesses in preparative scale fed-batch reactions. Furthermore, we identified the source of an unwanted byproduct formation during the reaction and successfully diminished its negative effects and substrate decomposition.

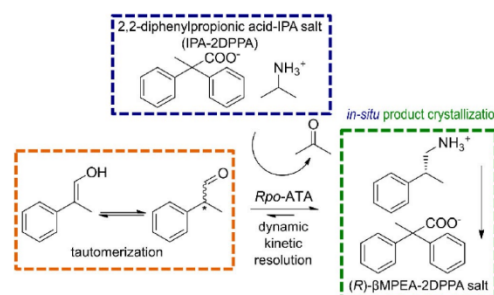


**Figure 1.** Concept of the ISPC-driven DKR of 2-phenylpropanal to (*R*)- $\beta$ -methylphenethylamine.

## Results and Discussion

### Initial Reactions

For our work, the commercially available and well-studied transaminase from *Ruegeria pomeroyi* (formerly *Silicibacter pomeroyi*) was chosen. The enzyme has shown a broad spectrum of accepted substrates, converting a variety of bulky ketones and its derivatives, and excellent stereoselectivity, mostly towards the (*S*)-enantiomer of  $\alpha$ -chiral amines.<sup>[24–27,28]</sup> Initial reactions performed with the enzyme and 2-phenylpropanal as its substrate, although producing promising product yields, showed significant formation of a by-product, which proved to be acetophenone (data not shown). Hence, it was decided to analyze this by-product formation further, since it was reported in previous publications as well.<sup>[13,29]</sup> Furthermore, two halogenated substrates, 2-(4-chlorophenyl)propanal and 2-(4-fluorophenyl)propanal, synthesized via hydroformylation (see SI), were also tested, however both only facilitated yields of under 2%.

### Limiting Formation of the Acetophenone Side Product

Three potential reasons for acetophenone formation from 2-phenylpropanal were investigated (see Figure 2). At first, the influence of pH on acetophenone formation was analyzed. For this purpose, the normally used transaminase reaction mixture was adjusted to different pH values and 50 mM of 2-phenylpropanal were added to those solutions. The reaction mixtures were shaken at 25 °C and samples were taken at certain time points. Hence, a graph of acetophenone formation over time at different pH values could be prepared (see Figure 2 A). As can be seen, increasing basic pH-values led to an increase in acetophenone formation, culminating into almost 35% of the initial substrate degrading to acetophenone at pH 9 after 24 hours, while slightly acidic pH values kept the acetophenone formation at a much lower level. However, although at acidic pH values acetophenone formation remained relatively low at 5–10% from the initial substrate concentrations, keeping the

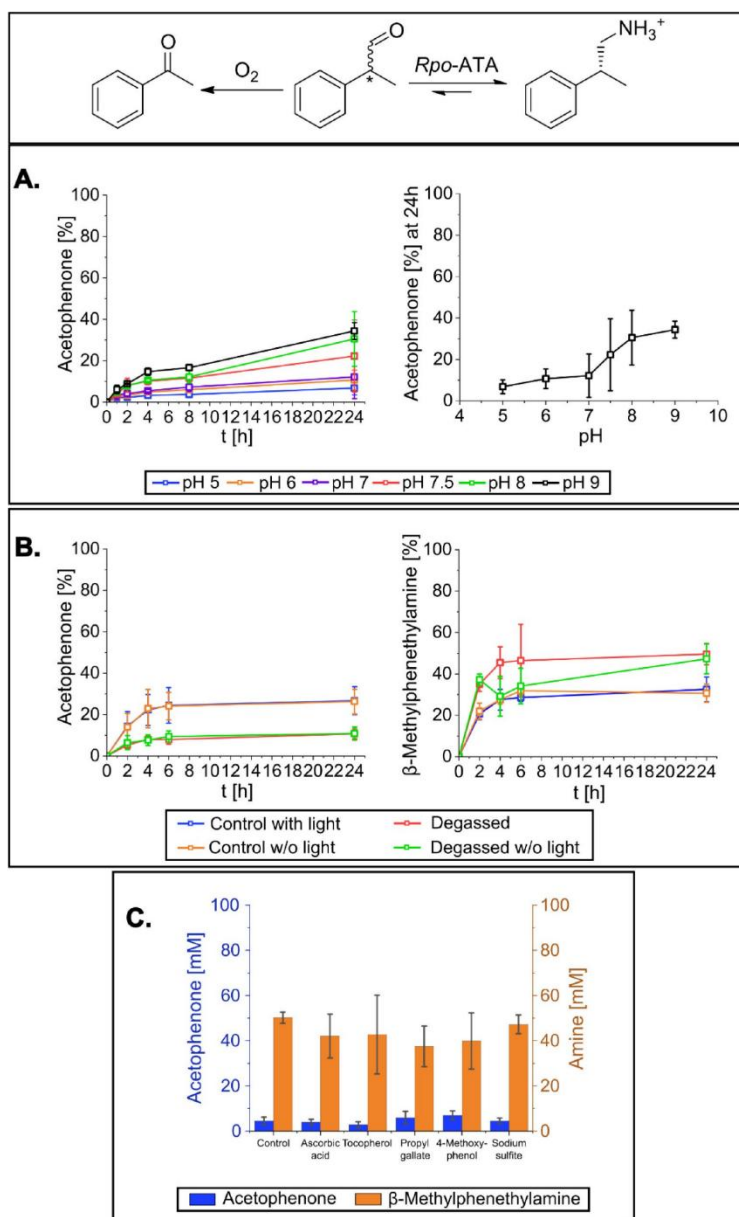


**Figure 2.** Results of the parameter screening for acetophenone formation. A.: Influence of pH on acetophenone formation; 50 mM triethanolamine (TEA) buffer, 2.5 mM PLP, 250 mM IPA, 50 mM 2-phenylpropanal, 25 °C, 150 rpm, 2 ml, 24 h. B.: Influence of air and light on acetophenone formation; 50 mM TEA buffer, 2.5 mM PLP, 250 mM IPA, 100 mM 2-phenylpropanal, 7.5 U/ml dry weight whole cells, pH 7.5, RT (22–23 °C), 150 rpm, 2 ml, 24 h. C.: Influence of antioxidants on acetophenone formation, 50 mM TEA buffer, 2.5 mM PLP, 250 mM IPA, 100 mM 2-phenylpropanal, 10 mM antioxidant, 7.5 U/ml dry weight whole cells, pH 7.5, RT (22–23 °C), 150 rpm, 2 ml, degassed, 24 h.



reactions at low pH values does not represent a favored solution due to transaminase pH optima lying in rather basic environments.

Thus, as next parameters the potential influence of air oxygen (for possible oxidation of the substrate) and light were tested. For this purpose, reactions with 100 mM 2-phenylpropanal and 7.5 U/ml enzyme were carried out in both a degassed and a non-degassed reaction broth (see Figure 2B). For light protection, clear vials were replaced by amber-colored vials and additionally covered with aluminum foil. As shown in the graph in Figure 2B, a simple degassing significantly decreased the amount of formed acetophenone, although the reactions were performed at a slightly basic pH of 7.5. The overall acetophenone formation decreased 2.5-fold from 26 mM (25% of the initial substrate concentration) in non-degassed solutions to approximately 10 mM (10% of the initial substrate concentration) in degassed solutions. It has to be noted, that due to taking multiple samples, the acetophenone formation might have been increased in the degassed reactions, which was later strengthened by lesser acetophenone formation values in degassed reactions, where only 24-hour samples were taken. Light, however, did not have a significant effect on acetophenone formation. Hence, we could identify oxygen as the main reason for the formation of the acetophenone by-product through aldehyde oxidation.

A proposed mechanism for the acetophenone formation, which is based on the presence of radical intermediates, is shown in Figure 3. Accordingly, a tertiary radical of type I stabilized by the phenyl substituent would be formed in an initial step, followed by an addition of  $O_2$  under formation of a peroxy radical (II). Subsequent homolytic cleavage of the C–H bond of the aldehyde moiety within a 5-membered transition state then furnishes a carbonyl radical (III), which then undergoes a decarbonylation and the thermodynamically favored cleavage of the O–O bond under formation of acetophenone. This cleavage of the thermodynamically labile O–O bond in III

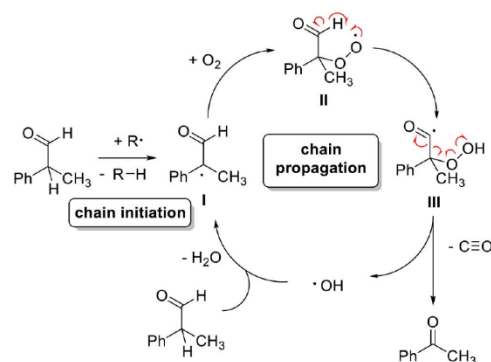


**Figure 3.** Proposed mechanism of acetophenone formation from 2-phenylpropanal under influence of oxygen from air. The degradation of 2-phenylpropanal proceeds in the form of a radical chain reaction and contains a decarbonylation step.

also represents a major driving force in this process and furnishes a hydroxy radical. The latter one is then suitable to initiate the next reaction cycle (chain propagation) by hydrogen abstraction, thus being converted to water.

Taking into account the key role of  $O_2$ , a simple degassing would suppress this side-reaction towards insignificant levels. A decrease in acetophenone formation, in turn, led to an increase in the formation of the desired  $\beta$ -methylphenethylamine during the enzymatic transamination reaction from 30 mM to 50 mM final concentrations (thus corresponding to a 65% increase). In an attempt to completely eliminate the side-reaction, we added anti-oxidants at a 10 mM concentration to the reaction mixture (see Figure 2C). However, no significant improvement was observed with any tried anti-oxidant. Only  $\alpha$ -tocopherol and sodium thiosulphate showed a slight decrease in the amount of formed acetophenone, a fact later applied in the preparative experiments, while other anti-oxidants rather demonstrated inhibitory effects on the enzymatic reaction, yielding no significant benefit.

### Screening for Suitable Crystallization Partners and Solubility Measurements

After resolving the issue of substrate decomposition, a preliminary study for  $\beta$ -methylphenethylamine crystallization was performed. The goal was to establish an *in situ* product crystallization driven reaction, which would allow for a continuous process of  $\beta$ -methylphenethylamine production. Hence, two criteria had to be met. First of all, as shown in Figure 1, the ISPC concept would be applied onto the amines of the reaction, resulting in the possible formation of the salt pair of IPA-carboxylates and  $\beta$ -methylphenethylamine-carboxylates. In order to achieve an attractive basis for post-reaction downstream-processing, the solubility of the IPA salt (amine donor) would be needed to be kept as high as possible, while the solubility of the  $\beta$ -methylphenethylamine-salt (product salt) would be needed to be kept as low as possible. The other prerequisite for an efficient process would be to keep the solubility of the product salt as low as possible to realize a better effect of the equilibrium shifting. The removal of the maximum amount of product from the reaction broth would be beneficial in order to prevent product inhibition of the biocatalyst and achieve a maximal pull of the reaction towards the product side.

To determine possible crystallization partners for the amine reaction product, a screening of carboxylic anions was carried out using the ECS Acid Screening Kit (by Enzymicals). This screening produced nine possible hits for enantiomerically pure (S)- $\beta$ -methylphenethylamine, four of which were considered as weak hits due to the lack of crystal formation. The strong hits are listed in Table 1 (all hits and the screening plate are found in SI Figure 1 and SI Table 1).

A further investigation on the product salts of the most promising hits was performed. After creating such product salts from enantiomerically pure (R)- or (S)- $\beta$ -methylphenethylamine and the corresponding carboxylates, they were subjected to a solubility screening to determine the possibility of their usage

**Table 1.** Listing of  $\beta$ -methylphenethylamine screening results including their structures.

Hit	Carboxylate anion	Structure
1	3,3-Diphenylpropionic acid (3DPPA)	
2	2,2-Diphenylpropionic acid (2DPPA)	
3	Diphenylacetic acid (DPAA)	
4	Biphenyl-4-carboxylic acid (BPA)	
5	4-Biphenylacetic acid (4BPA)	

for a continuous ISPC-process. For this application, the product salt solubility would need to be kept as low as possible, while the salt solubility of the amine donor (IPA) would require to be held as high as possible, or at least significantly higher, than the product salt solubility. Since the IPA salt solubilities of the carboxylates in question were mostly known from our previous works,<sup>[23]</sup> we measured the solubilities of chosen product salts (see Table 2). However, for the sake of sufficient product isolation from the reaction broth, a cut-off for the product salt solubilities was set at 25 mM. Hence, all product salts with higher solubilities were excluded from further investigation. This narrowed the range of the salt anions to only 4 possible candidates: 3DPPA, 2DPPA, BPA and 4BPA. These carboxylate anions were further tested in the enzymatic reaction to determine, whether they might have an inhibitory effect on the enzyme and thus be not suitable for a continuous process.

#### Determining ISPC Potential of Screening Results

Inhibitory effects of the chosen four salts were tested in small scale experiments by adding varying concentrations of the

**Table 2.** Solubility of enantiomerically pure  $\beta$ -methylphenethylamine and IPA salts for strong screening hits.

Salt anion	IPA-salt solubility [mM]	Product salt solubility [mM]
3DPPA	51.7 $\pm$ 0.3 <sup>[23]</sup>	14.4 $\pm$ 8.5
2DPPA	78.6 $\pm$ 0.2 <sup>[23]</sup>	18.6 $\pm$ 3.6
DPAA	168.2 $\pm$ 1.3 <sup>[23]</sup>	25.5 $\pm$ 5.8
BPA	40.7 $\pm$ 1.0	18.4 $\pm$ 3.8
4BPA	83.6 $\pm$ 16.6 <sup>[23]</sup>	15.4 $\pm$ 5.7

corresponding IPA salts to the reaction as an ISPC starter and comparing the overall yields of such augmented reactions to a salt-free control. Since salt-free experiments previously yielded approximately 50 mM product concentrations (see Figure 2B) when starting from 100 mM 2-phenylpropanal, the first inhibitory test was performed with a 50 mM IPA salt concentration to match the estimated product formation and 200 mM free IPA (250 mM overall IPA concentration). The results are shown in Figure 4.

Herein, while no significant improvement in reaction yields could be achieved, the 3DPPA anion was shown to moderately inhibit the reaction at a 50 mM concentration, manifesting in a 12% yield drop. Hence it was excluded from further experiments (see Figure 4A). Further tests with the remaining three IPA-carboxylate salts were performed at salt concentrations of 100 mM, 150 mM and 175 mM (see Figure 4B). While at all three salt concentrations an increase in product formation was found compared to the salt-free control, it has to be noted, that with mounting concentrations of the carboxylate, product formation first reached 20–30% improved values, but started to decrease again. The difference in product formation between 100 mM and 150 mM salt anion concentrations was rather negligible and at 175 mM product formation almost returned to the salt-free control levels. This coincided with noted difficulties in the proper mixing of the reaction solutions. Based on this observed correlation and its highest overall product yields (see Figure 4), the 2DPPA salt anion was chosen for further ISPC-based experiments.

Although all the initial data showed good potential for ISPC with the chosen salt anion, we decided to survey the full scale of the crystallization potential of the chosen

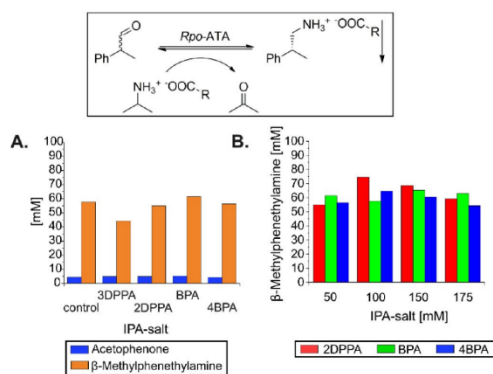


**Figure 4.** Results of the determination of ISPC potential for chosen carboxylates. A.: Inhibitory test with 50 mM IPA-salt; 50 mM triethanolamine (TEA) buffer, 2.5 mM PLP, 200 mM IPA, 50 mM IPA salt, 100 mM 2-phenylpropanal, 7.5 U/ml dryweight whole cells, RT (22–23 °C), 150 rpm, 2 ml, degassed, 24 h. B.: Determination of ideal carboxylate anion concentration for possible ISPC; 50 mM TEA buffer, 2.5 mM PLP, 250 mM overall IPA, varying IPA salt (see graph) and free IPA concentrations, 100 mM 2-phenylpropanal, 7.5 U/ml dryweight whole cells, pH 7.5, RT (22–23 °C), 150 rpm, 2 ml, degassed, 24 h.

IPA- $\beta$ MPEA-2DPPA salt pair. For this purpose, a phase diagram of this salt pair in aqueous media was prepared (see Figure 5).

While the solubility difference between the amine donor salt (IPA-2DPPA) and the product salt ((*R*)- $\beta$ MPEA-2DPPA) was only approximately 50 mM, the resulting phase diagram showed a very wide asymmetry between possible crystallization conditions of the corresponding salt. This asymmetry, due to the significant shift of the eutectic towards the left-hand side, benefited the crystallization of the product salt within a very broad set of crystallization conditions. Thus, the diagram confirmed a real benefit for the improvement of the reaction yield via ISPC through the utilization of 2DPPA. Hence, as a next step experiments on a preparative scale were conducted utilizing 2DPPA as a salt anion.

#### Transfer to Preparative Reaction Conditions

For the preparative reactions, the format of a fed-batch was chosen. Here, the amounts of 2-phenylpropanal and IPA were refilled to the initial concentrations every 24 h after measurement, using only IPA-2DPPA salt to refill the consumed IPA for ISPC-driven reactions, while creating a suitable comparison to unsupplemented controls over time.

At first, the volume was scaled up from 2 ml to 5 ml (Table 3, entries 1 and 2). This was done to probe possible challenges of elevating the reaction volumes. As can be seen, while the ISPC-driven reaction kept the approximately same product levels (70% yield), as in 2 ml small-scale reactions, the yield of the salt-free control dropped by more than 50% after 24 h, not managing to surmount the 50 mM product concentration mark even after 48 h. Hence, since the general ISPC-driven concept did not face any challenges yet, it was decided to continue with an increase of the utilized substrate concentrations.

The substrate concentrations were all doubled and kept at the same proportions of 2-phenylpropanal to overall IPA concentration and free IPA to IPA-2DPPA salt concentrations (Table 3, entries 3 and 4). Here the salt-free control again did not reach the usual small-scale yields of 50% after 24 hours of reaction time (entry 4). After 48 hours, the yields dropped significantly, obviously reaching a product inhibition limit. In contrast, for ISPC driven reactions, the overall yields stayed quite high, reaching the usual small-scale 60–70% yields after 24 h, while after 48 hours still producing a significant amount of product. With this result, it was decided to further scale up the reaction volume. As shown throughout the entries 5 to 8 in Table 3, the described tendencies were also present during the volume increase up to 50 ml. Here, the reaction produced a record of 80% yield after 24 h, although the yield dropped to 40% in the next 24 hours (entry 7). This derives from the fact, that the reaction mixture is rather heterogeneous with at least an undissolved 2-phenylpropanal phase and whole cells biocatalyst, aqueous reaction mixture and, in case of ISPC, with two additional partially soluble solids (IPA-2DPPA as the donor salt and  $\beta$ MPEA-2DPPA as the product salt). This eventually leads to mixing discrepancies between different reaction volumes and thus a variation in reaction velocities, which lead to differences in product concentrations after 24 hours. However, the final equilibrium-based product concentration after 48 hours remains comparable throughout the entries 3, 5 and 7, as well as 4, 6 and 8. Nevertheless, all reactively crystallized reactions managed to surpass an overall product concentration of 200 mM after 48 hours. Further, the ISPC-driven concept provided an overall yield increase of 80–90% compared to the salt-free controls throughout a 10-fold volume increase and the doubling of substrate concentrations. Hence the ISPC concept proved successful in the facilitated yield increase and the ensuring of a constant process continuity. The measured enantiomeric excesses of the reactions also proved to be quite high, even displaying a slight increase in ISPC-driven reactions.

#### Conclusions

The chosen ISPC concept proved to be successful for the synthesis of the  $\beta$ -chiral amine  $\beta$ MPEA. A yield improvement of up to 90% compared to the controls was achieved, while the overall product concentration reached 240–260 mM in a preparative scale reaction. The oxygen-driven decomposition of the 2-phenylpropanal substrate was investigated and the subsequent formation of acetophenone was lowered to a mere 5% of the utilized substrate. A viable concept for the production of  $\beta$ -chiral amines with the potential for further scale-up was established. The utilization of a semi-continuous approach, as described by Neuburger *et al.*,<sup>[24]</sup> may offer a concept for even higher overall yields, since the continuous approach of a fed-batch is bound to face stirring challenges over longer reaction periods due to the amount of formed product salt. However, the offered approach allows for a facile reaction process with a straightforward post-reaction down-

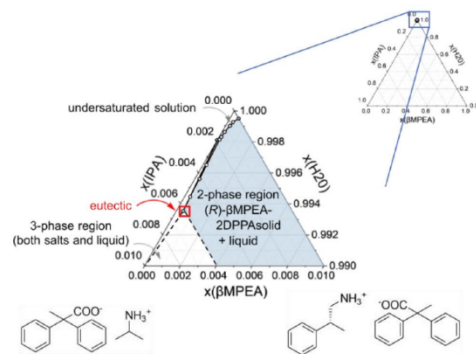


**Figure 5.** Ternary phase diagram of the IPA- $\beta$ MPEA-2DPPA salt pair. The sector of possible  $\beta$ MPEA-2DPPA salt crystallization conditions (at RT) is colored light blue.

**Table 3.** Results of the ISPC-driven reactions on preparative scale.

Entry	Volume [ml]	2-phenylpropanal concentration [mM]	IPA concentration [mM]	2DPPA concentration [mM]	Acetophenone concentration [mM] after 24 h	$\beta$ MPA concentration [mM] after 24 h	Acetophenone concentration [mM] after 48 h	$\beta$ MPA concentration [mM] after 48 h	Overall yield after 48 h	ee after 48 h
1	5	100	250	150	18.9	68.0	42.9	120.5	64.4 %	n.d.
2	5	100	250	0	2.6	28.6	13.1	37.6	28.7 %	n.d.
3	5	200	500	300	14.7	100.6	58.8	249.0	79.0 %	99.0 % (R)
4	5	200	500	0	11.7	86.7	30.4	128.4	43.0 %	94.6 % (R)
5	10	200	500	300	7.7	118.4	14.6	268.7	82.3 %	98.9 % (R)
6	10	200	500	0	6.5	129.8	18.3	149.3	44.4 %	92.8 % (R)
7	50	200	500	300	13.2	161.7	14.1	237.0	63.2 %	98.6 % (R)
8	50	200	500	0	8.9	93.3	17.9	131.1	43.3 %	96.8 % (R)

stream processing approach of salt filtration/centrifugation coupled with the amine recovery by alkaline extraction.

## Experimental Section

### Enzyme Activity Assay

Enzyme activity was measured with a Specord 200 spectrophotometer from Analytik Jena (Jena, Germany) at a wavelength of 245 nm using the acetophenone extinction coefficient of  $11.852 \text{ (mM} \cdot \text{cm)}^{-1}$ . A 50 mM sodium phosphate buffer solution with 0.25 % (v/v) DMSO was adjusted to pH 8 with saturated NaOH solution and conc. HCl to be used for all further solutions. 250  $\mu\text{l}$  of the buffer solution, 250  $\mu\text{l}$  of a 10 mM (S)-1-phenylethylamine solution in buffer and 250  $\mu\text{l}$  of a 10 mM sodium pyruvate solution in buffer were premixed in the measurement cuvettes. The enzyme samples were prepared by dissolving 1 mg of dry weight whole cells in 1800  $\mu\text{l}$  of buffer and adding 200  $\mu\text{l}$  of a 10 mM pyridoxal phosphate solution in buffer. 250  $\mu\text{l}$  of this enzyme mix were then added to the pre-pipetted samples, briefly shaken and measured immediately. All experiments were measured against a reference solution by replacing the enzyme mix with 50  $\mu\text{l}$  of the 10 mM pyridoxal phosphate and 200  $\mu\text{l}$  of buffer. Specific enzyme activity was calculated through the slope of acetophenone extinction over the course of 60 s (see SI section 4.4).

### IPA- and $\beta$ MPA-Salt Preparation

A desired amount of the chosen carboxylic acid (e.g. 2DPPA) was dissolved in 10–100 ml of cyclopentyl methyl ether (CPME) at room temperature. Mild heating up to 60 °C was applied, if necessary, to speed up the dissolution process. An equimolar amount of amine (IPA or  $\beta$ MPA) was added to the solution under constant stirring. The resulting suspension was left for one hour at room temperature under stirring. Afterwards, the residual CPME was evaporated to obtain the maximal yield of the desired salt.

### Phase Diagram Preparation

The salts of the salt pair in question were mixed in 9 different molar ratios (with additionally each pure salt as a control) and dissolved in high-purity water. The pH was adjusted to 7.5 with weak HCl and NaOH solutions. The vials were shaken at room temperature and 150 rpm for at least five days or until no pH change occurred. The dissolved salts were compensated with the same salt ratio mixtures. The salt solutions were centrifuged at 10 000xg for 5 min and the supernatant was filtered through 0.25  $\mu\text{m}$  filters to remove all residual salt crystals. Filtrate samples of approximately 1 ml were evaporated in a Thermo Scientific Pierce ReactiTherm I & ReactiVap I heating and evaporation unit under a constant argon stream. The sample vials were weighed three times: empty, filled with the filtrate and evaporated. Ratios of the dissolved salts were determined via NMR. Mole fractions of the salts and water were calculated from this data and plotted in the ternary diagram format with the Origin 2023 software.

### Analysis via Gas Chromatography

All reactions were monitored via gas chromatography on a Thermo Fisher Trace 1310 gas chromatograph equipped with a flame ionization detector (FID). A J&W column (0.25 mmx30 m x 0.25  $\mu\text{m}$ , HP-5 phase) by Agilent Technologies (series number 19091J-433), shortened for 1 mm on each end was used. Helium and synthetic



air were used as the carrier. The chromatograms were refined and analyzed via the Thermo Xcalibur Qual Browser software by Thermo Fisher. For amine quantification, the obtained amine peak areas were normalized with the internal standard, scaled for the internal standard value of 100000 sqU and then the amine concentration was calculated according to the calibration parameters.

### Fed-Batch Concept

Reactions in the preparative format were conducted by utilizing a 50 mM triethanolamine (TEA) buffer (pH 7.5). Pyridoxal phosphate was added to the selected buffer to a final concentration of 2.5 mM. Pure IPA was added to the buffer solution to a desired final concentration (500 mM in reactions without ISPC, 200 mM in reactions with ISPC). The pH was adjusted to 7.5 with conc. HCl and NaOH solutions. The obtained buffer solution was degassed for 2–4 hours by passing an argon stream through it.

To start the reactions, 7.5 U/ml of dry weight *E. coli* cells bearing the overexpressed *Rpo-ATA* enzyme were added to the buffer solution (specific activity was defined through a standard acetophenone assay, see SI section 4.4). For ISPC-experiments, IPA-2DPPA salt was added to a final concentration of 300 mM. To the 50 ml reactions, 10 mM of sodium sulfite was added. The mixture was mixed thoroughly, the pH was adjusted to 7.5. The reactions were started by adding substrate to the reaction mixture to a final concentration of 200 mM. The reactions were stirred at 900 rpm and room temperature (22 °C) and samples were drawn each 24 hours. After 24 hours, the samples were measured via GC to quantify the residual IPA and substrate levels in the reaction. IPA and substrate were then refilled to reach their respective initial concentrations. Please note that this addition of substrates will result in a slight increase of reaction volume (<5%).

### Sample Derivatization and Chirality Measurement

Enantiomeric excess was determined via LC–MS analysis on a Dionex UltiMate™ 3000 (LC), LTQ XL™ (MS) with a Phenomenex® Kinetex® C18 column (150×2.1 mm, 2.6 μm) at constant oven temperature of 35 °C with an eluent composition of 50:50 (v/v-1) MeOH:H<sub>2</sub>O (+0.1% formic acid) (isocratic) and a flow rate: 0.2 ml min<sup>-1</sup>. The detection was done via MS for the specific mass of the derivatized amine and in parallel via UV/VIS at 254 nm. Samples were derivatized with 1.5 mM 2,3,4,6-Tetra-O-acetyl-β-D-glucopyranosyl-isothiocyanate and 1.5 mM NEt<sub>3</sub> in acetonitrile.

### Supporting Information

Supporting information is provided. The authors have cited additional references within the Supporting Information.<sup>[23,30]</sup>

### Acknowledgements

Funding for F.B. and J.v.L. by Central SME Innovation Programme (ZIM, projects 16KN073233 and ZF4402103CR9) and the Heisenberg Programme of the Deutsche Forschungsgemeinschaft (project number 450014604) is gratefully acknowledged. The authors thank the research group of Prof. Mirko Basen (Institute of Biological Science, University of Rostock) especially with Dr. Maria Lehmann, Christoph Prohaska and Dr. Ralf-Jörg Fischer and the research group of Prof. Kragl (Institute

of Chemistry, University of Rostock) especially with Sandra Diederich for their ongoing support and fruitful discussions. The used LTQ XL LC/MS system was co-financed by the European Union from the European Regional Development Fund GHS-17-0034 under the Operational Program Mecklenburg-Vorpommern 2014–2020 – Investments in growth and employment. Open Access funding enabled and organized by Projekt DEAL.

### Conflict of Interests

The Authors declare no conflict of interest.

### Data Availability Statement

The data that support the findings of this study are available in the supplementary material of this article.

**Keywords:** amine · crystallization · DKR · enzyme · ISPR

- [1] E. E. Ferrandi, D. Monti, *World J. Microbiol. Biotechnol.* **2017**, *34*, 13.
- [2] a) D. Ghislieri, N. J. Turner, *Top. Catal.* **2014**, *57*, 284–300; b) C. K. Savile, J. M. Janey, E. C. Mundorff, J. C. Moore, S. Tam, W. R. Jarvis, J. C. Colbeck, A. Krebber, F. J. Fleitz, J. Brands, P. N. Devine, G. W. Huisman, G. J. Hughes, *Science* **2010**, *329*, 305–309.
- [3] a) N. J. Turner, *Nat. Chem. Biol.* **2009**, *5*, 567–573; b) E. Cigan, B. Eggbauer, J. H. Schrittwieser, W. Kroutil, *RSC Adv.* **2021**, *11*, 28223–28270.
- [4] a) H. Gröger, *Appl. Microbiol. Biotechnol.* **2019**, *103*, 83–95; b) H. Kohls, F. Steffen-Munsberg, M. Höhne, *Curr. Op. Chem. Biol.* **2014**, *19*, 180–192.
- [5] a) O. I. Afanasyev, E. Kuchuk, D. L. Usanov, D. Chusov, *Chem. Rev.* **2019**, *119*, 11857–11911; b) T. C. Nugent in *Chiral Amine Synthesis. Methods, Developments and Applications* (Eds.: T. C. Nugent), Wiley-VCH, **2010**, 225–245.
- [6] W. Zawodny, S. L. Montgomery, *Catalysts* **2022**, *12*, 595.
- [7] a) M. D. Patil, G. Grogan, A. Bommaris, H. Yun, *ACS Catal.* **2018**, *8*, 10985–11015; b) E. Abdelraheem, M. Damian, F. G. Mutti in *Reference Module in Chemistry, Molecular Sciences and Chemical Engineering*, Elsevier, **2022**.
- [8] A. Gomm, E. O'Reilly, *Curr. Op. Chem. Biol.* **2018**, *43*, 106–112.
- [9] S. C. Cosgrove, J. I. Ramsden, J. Mangas-Sanchez, N. J. Turner in *Methodologies in Amine Synthesis* (Eds.: A. Ricci, L. Bernardi), Wiley, **2021**, 243–283.
- [10] a) F.-F. Chen, X.-F. He, X.-X. Zhu, Z. Zhang, X.-Y. Shen, Q. Chen, J.-H. Xu, N. J. Turner, G.-W. Zheng, *J. Am. Chem. Soc.* **2023**, *145*(7), 4015–4025; b) S. D. Roughley, A. M. Jordan, *J. Med. Chem.* **2011**, *54*, 3451–3479.
- [11] a) S. Wu, R. Snajdrova, J. C. Moore, K. Baldeus, U. T. Bornscheuer, *Angew. Chem. Int. Ed.* **2021**, *60*, 88–119; b) E. L. Bell, W. Finnigan, S. P. France, A. P. Green, M. A. Hayes, L. J. Hepworth, S. L. Lovelock, H. Niikura, S. Osuna, E. Romero, *Nat. Rev. Methods Primers* **2021**, *1*, 46; c) D. Yi, T. Bayer, C. P. S. Badenhorst, S. Wu, M. Doerr, M. Höhne, U. T. Bornscheuer, *Chem. Soc. Rev.* **2021**, *50*, 8003–8049; d) L. G. Otten, F. Hollmann, I. W. C. E. Arends, *Trends Biotechnol.* **2010**, *28*, 46–54.
- [12] I. Slabu, J. L. Galman, R. C. Lloyd, N. J. Turner, *ACS Catal.* **2017**, *7*, 8263–8284.
- [13] C. S. Fuchs, M. Hollauf, M. Meissner, R. C. Simon, T. Besset, J. N. H. Reek, W. Riethorst, F. Zepeck, W. Kroutil, *Adv. Synth. Catal.* **2014**, *356*, 2257–2265.
- [14] S. A. Kelly, S. Pohle, S. Wharry, S. Mix, C. C. R. Allen, T. S. Moody, B. F. Gilmore, *Chem. Rev.* **2018**, *118*, 349–367.
- [15] a) K. Ren, R. Yuan, Y.-Y. Gui, X.-W. Chen, S.-Y. Min, B.-Q. Wang, D.-G. Yu, *Org. Chem. Front.* **2023**, *10*, 467–472; b) M. N. Kliemann, S. Teeuwen, C. Weihe, G. Franciò, W. Leitner, *Adv. Synth. Catal.* **2022**, *364*, 4006–4012; c) J. He, Y. Xue, B. Han, C. Zhang, Y. Wang, S. Zhu, *Angew. Chem. Int. Ed.* **2020**, *59*, 2328–2332; d) S. Zhu, S. L. Buchwald, *J. Am. Chem. Soc.* **2014**, *136*, 15913–15916.

- [16] C. S. Fuchs, J. E. Farnberger, G. Steinkellner, J. H. Sattler, M. Pickl, R. C. Simon, F. Zepeck, K. Gruber, W. Kroutil, *Adv. Synth. Catal.* **2018**, *360*, 768–778.
- [17] D. Koszelewski, D. Clay, K. Faber, W. Kroutil, *J. Mol. Cat. B: Enzymatic* **2009**, *60*, 191–194.
- [18] C. K. Chung, P. G. Bulger, B. Kosjek, K. M. Belyk, N. Rivera, M. E. Scott, G. R. Humphrey, J. Limanto, D. C. Bachert, K. M. Emerson, *Org. Process Res. Dev.* **2014**, *18*, 215–227.
- [19] a) R. Xin, W. W. L. See, H. Yun, X. Li, Z. Li, *Angew. Chem. Int. Ed.* **2022**, *61*, e202204889; b) W. W. L. See, X. Li, Z. Li, *Adv. Synth. Catal.* **2023**, *365*, 68–77.
- [20] a) P. Matzel, S. Wenske, S. Merdivan, S. Günther, M. Höhne, *ChemCatChem* **2019**, *11*, 4281–4285; b) R. Jin, Z. Xu, J. Feng, M. Wang, P. Yao, Q. Wu, D. Zhu, *Eur. J. Org. Chem.* **2023**, *26*, e202300476.
- [21] a) A. Gomm, W. Lewis, A. P. Green, E. O'Reilly, *Chem. Eur. J.* **2016**, *22*, 12692–12695; b) J. L. Galman, I. Slabu, N. J. Weise, C. Iglesias, F. Parmeggiani, R. C. Lloyd, N. J. Turner, *Green Chem.* **2017**, *19*, 361–366; c) A. P. Green, N. J. Turner, E. O'Reilly, *Angew. Chem. Int. Ed.* **2014**, *53*, 10714–10717; d) E. O'Reilly, C. Iglesias, D. Ghislieri, J. Hopwood, J. L. Galman, R. C. Lloyd, N. J. Turner, *Angew. Chem.* **2014**, *126*, 2479–2482; e) D. Koszelewski, I. Lavandera, D. Clay, G. M. Guebitz, D. Rozzell, W. Kroutil, *Angew. Chem. Int. Ed.* **2008**, *47*, 9337–9340; f) H. Zhou, L. Meng, X. Yin, Y. Liu, J. Wu, G. Xu, M. Wu, L. Yang, *Appl. Cat. A: General* **2020**, *589*, 117239; g) L. Martínez-Montero, V. Gotor, V. Gotor-Fernández, I. Lavandera, *Adv. Synth. Catal.* **2016**, *358*, 1618–1624; h) S. E. Payer, J. H. Schrittwieser, W. Kroutil, *Eur. J. Org. Chem.* **2017**, *17*, 2553–2559; i) C. K. Winkler, J. H. Schrittwieser, W. Kroutil, *ACS Cent. Sci.* **2021**, *7*, 55–71; j) T. Börner, G. Rehn, C. Grey, P. Adlercreutz, *Org. Process Res. Dev.* **2015**, *19*, 793–799; k) M. Doecker, L. Grabowski, D. Rother, A. Jupke, *Green Chem.* **2022**, *24*, 295–304; l) J. Yang, A. Buekenhoudt, M. van Dael, P. Luis, Y. Satyawali, R. Malina, S. Lizin, *Org. Process Res. Dev.* **2022**, *26*, 2052–2066; m) C. Matassa, D. Ormerod, U. T. Bornscheuer, M. Höhne, Y. Satyawali, *ChemCatChem* **2020**, *12*, 1288–1291; n) F. Guo, P. Berglund, *Green Chem.* **2017**, *19*, 333–360.
- [22] D. Hülsewede, L.-E. Meyer, J. von Langermann, *Chem. Eur. J.* **2019**, *25*, 4871–4884.
- [23] F. Belov, A. Mildner, T. Knaus, F. G. Mutti, J. von Langermann, *React. Chem. Eng.* **2023**, *8*, 1427–1439.
- [24] J. Neuburger, F. Helmholz, S. Tiedemann, P. Lehmann, P. Süss, U. Menyes, J. von Langermann, *Chem. Eng. Process.* **2021**, *168*, 108578.
- [25] D. Hülsewede, J.-N. Dohm, J. von Langermann, *Adv. Synth. Catal.* **2019**, *361*, 2727–2733.
- [26] D. Hülsewede, M. Tänzler, P. Süss, A. Mildner, U. Menyes, J. von Langermann, *Eur. J. Org. Chem.* **2018**, *18*, 2130–2133.
- [27] D. Hülsewede, E. Temmel, P. Kumm, J. von Langermann, *Crystals* **2020**, *10*, 345.
- [28] a) M. Kollipara, P. Matzel, U. Bornscheuer, M. Höhne, *Chem. Ing. Techn.* **2022**, *94*, 1836–1844; b) S. Calvelage, M. Dörr, M. Höhne, U. T. Bornscheuer, *Adv. Synth. Catal.* **2017**, *359*, 4235–4243; c) F. Steffen-Munsberg, C. Vickers, A. Thontowi, S. Schätzle, T. Meinhardt, M. Svedendahl Humble, H. Land, P. Berglund, U. T. Bornscheuer, M. Höhne, *ChemCatChem* **2013**, *5*, 154–157.
- [29] C. Rapp, S. Pival-Marko, E. Tassano, B. Nidetzky, R. Kratzer, *BMC Biotechnol.* **2021**, *21*, 58.
- [30] F. W. Studier, *Protein Expression Purif.* **2005**, *41*, 207–234.

Manuscript received: March 5, 2024

Revised manuscript received: April 5, 2024

Accepted manuscript online: April 11, 2024

Version of record online: May 15, 2024

# Publication 3: Crystallization-integrated mandelate racemase-catalyzed dynamic kinetic resolution of racemic mandelic acid

F. Belov, A. Lieb and J. von Langermann

*Reaction Chemistry & Engineering*, 2025, 10(5), 1145-1153.

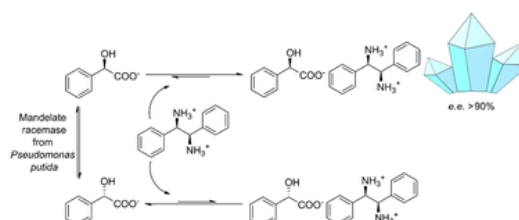
Received: 25<sup>th</sup> November 2024

Accepted: 12<sup>th</sup> February 2025

DOI: 10.1039/d4re00576g

## Abstract:

Classical approaches for the preparation of enantiopure mandelic acid conventionally employ chiral resolution methods like diastereomeric crystallization or kinetic resolution. Those are, however, limited by their theoretical yield of 50% of the utilized racemate. Dynamic kinetic resolution solves this challenge by the addition of a racemization step for the unprocessed enantiomer, maximizing yields. For mandelic acid, a special enzyme class of mandelate racemases can perform this racemization step. In this study, we combine enzymatic racemization of mandelic acid with diastereomeric salt crystallization of (*R*)-mandelic acid to achieve a chemoenzymatic dynamic kinetic resolution of mandelic acid at mild conditions in water.





Cite this: *React. Chem. Eng.*, 2025, 10, 1145

Received 25th November 2024,  
Accepted 12th February 2025

DOI: 10.1039/d4re00576g

rsc.li/reaction-engineering

## Crystallization-integrated mandelate racemase-catalyzed dynamic kinetic resolution of racemic mandelic acid†

Feodor Belov,<sup>a</sup> Alexandra Lieb<sup>b</sup> and Jan von Langermann <sup>\*,a</sup>

Classical approaches for the preparation of enantiopure mandelic acid conventionally employ chiral resolution methods like diastereomeric crystallization or kinetic resolution. Those are, however, limited by their theoretical yield of 50% of the utilized racemate. Dynamic kinetic resolution solves this challenge by the addition of a racemization step for the unprocessed enantiomer, maximizing yields. For mandelic acid, a special enzyme class of mandelate racemases can perform this racemization step. In this study, we combine enzymatic racemization of mandelic acid with diastereomeric salt crystallization of (*R*)-mandelic acid to achieve a chemoenzymatic dynamic kinetic resolution of mandelic acid at mild conditions in water.

### Introduction

The synthesis of chiral chemical substances is one of the most important areas of research and the basis for their application in e.g. pharmaceutical and agrochemical products.<sup>1–9</sup> Normally, the preparation of enantiomerically pure compounds is divided into two general routes. Firstly, asymmetric synthesis, which typically converts an achiral compound into one of the desired enantiomers using an enantioselective catalyst. Due to the high demands to the enantiomeric purity of many chemical compounds, the use of a highly enantioselective catalyst is necessary. Secondly, the separation of usually inexpensive racemic mixtures, whereby separation methods such as chromatography and crystallization can be used in addition to catalytic methods. This concept is usually referred to as chiral resolution (CR), while the utilization of catalysts in the separation process is called kinetic resolution (KR). In KR approaches, different reaction kinetics of the two enantiomers with a selective (bio)catalyst enable the separation of the racemic compound, ideally with a strong difference in reaction rates (conversion for one enantiomer much faster than for the other enantiomer).<sup>1–3,7–10</sup>

Enzymes usually possess a high substrate specificity and enantioselectivity, making them an already tailored catalyst for the desired reaction and broadly applied in KRs. Additionally,

enzymes can perform reactions at very mild conditions, thus allowing for aqueous reaction media and environmentally friendly processes as a bonus.<sup>10–15</sup> Nevertheless, the main limitation of “standard-issue” chemical and kinetic resolutions is its highest achievable theoretical yield: only 50% of the utilized racemate are theoretically able to be converted to the desired enantiomeric product, while leaving 50% of the “undesired” enantiomer unprocessed. Here, a dynamic kinetic resolution (DKR) approach can improve yield beyond 50% in favour of the desired enantiomer in which the kinetic resolution step is combined with the continuous racemization of the remaining, typically undesired enantiomer, allowing for theoretical yields of up to 100%.<sup>1,3,7,9,16,17</sup> However, the additional racemization step needs to be accommodated by the process requirements within the DKR to function in parallel to the enantioselective synthesis reaction. To be more specific, ideally the racemization needs to be faster than the conversion of the undesired enantiomer into the product, effectively preventing the accumulation of the undesired enantiomer.<sup>1,3,9</sup> Racemization itself can be achieved spontaneously, e.g. by labile stereocenters incl. keto-enol tautomerism, but typically needs to be induced by specific chemicals or (bio)catalytic reaction systems.<sup>1,3,18–20</sup> Even though less utilized, enzymatic (biocatalytic) racemization through racemases (E.C. 5.1.X.X) is of particular interest. Although, opposed to most other enzymes, their stereoselectivity is essentially non-existent, their sole purpose is to be able to bind both enantiomers of its substrate in order to convert it into the other.<sup>21</sup> Thus, racemases also found their place in DKR-based processes as a the racemizing agent.<sup>21,22</sup>

An example, where resolution methods are often utilized, is the obtainment of enantiopure mandelic acid. Classical chemical methods usually produce a racemate of mandelic

<sup>a</sup> Institute of Chemistry, Biocatalytic Synthesis Group, Otto-von-Guericke University Magdeburg, Universitätsplatz 2, 39106 Magdeburg, Germany.

E-mail: jan.langermann@ovgu.de

<sup>b</sup> Institute of Chemistry, Industrial Chemistry, Otto-von-Guericke University Magdeburg, Universitätsplatz 2, 39106 Magdeburg, Germany

† Electronic supplementary information (ESI) available. See DOI: <https://doi.org/10.1039/d4re00576g>



acid, which then has to be separated.<sup>23,24</sup> For this purpose some KR- and DKR-based chemoenzymatic approaches are found in literature.<sup>24–36</sup>

Other alternatives for enantiopure mandelic acid production include aforementioned asymmetric synthetic approaches (both enzymatic and chemical)<sup>37–39</sup> and diastereomeric salt crystallization as means of chiral resolution. The latter approach utilizes different chemical properties of the corresponding diastereomeric salts, thus (co-)crystallizing the different mandelate enantiomers with a chiral resolving agent.<sup>40–50</sup>

This study focuses on the enzymatic racemization of mandelic acid and its integration into a diastereoselective crystallization step. This is achieved by mandelate racemases that are mostly utilized as a racemizing agent in DKR-based approaches towards enantiopure mandelic acid (derivatives) and require a secondary (bio)catalytic reaction system to derivatize mandelic acid in a biocatalytic cascade<sup>51–53</sup> or a separation method, as shown for a chromatography approach in the works of Wrzosek *et al.*<sup>54–56</sup> The presented combined biocatalysis-crystallization DKR is designed to efficiently convert racemic mandelic acid to (*R*)-mandelic acid without the need to form the above mentioned mandelic acid derivative that eventually needs to be converted back to mandelic acid with extra process steps. It enables high yields and eases the downstream processing by synchronous *in situ* product crystallization (ISPC) of the desired mandelate enantiomer as its diastereomeric salt (see Fig. 1). The concept includes a simple fed-batch approach with high substrate concentrations and the removal of enantioenriched (*R*)-mandelic acid salt after the reaction process.

## Results and discussion

Due to the need for high water activity for the selected mandelate racemase from *Pseudomonas putida* (E.C. 5.1.2.2), the racemization needs to be performed in aqueous media,<sup>53</sup> since its utilization in organic solvents has shown a complete loss of catalytic activity, although the enzyme itself retains activity when extracted back into aqueous media.<sup>57</sup> Unfortunately, most of the available literature about diastereomeric crystallization of mandelic acid (MA) makes use of organic solvents, while mandelic acid itself already possesses a very high solubility in water (approx. 1 M). Thus,

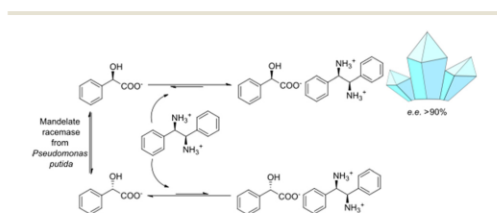


Fig. 1 Concept scheme for the proposed crystallization-based DKR of mandelic acid.

the search for an enantiospecific crystallization partner for diastereomeric salt resolution would need to have a “bulky”, preferentially hydrophobic structural base (thus lowering the solubility of the diastereomeric product salt) and ideally be commercially available for a broader applicability. Based on those ground rules, (1*R*,2*S*)-2-amino-1,2-diphenylethanol ((1*R*,2*S*)-ADPE) from prior works by Hirose *et al.*<sup>45–47</sup> was chosen as a bulky chiral amine to crystallize with mandelic acid. To further possible options for crystallization partners, several structurally similar and commercially available bulky amines were selected: (*S*)-1-phenylethylamine ((*S*)-1PEA), (1*R*,2*R*)-1,2-diphenylethanediamine ((1*R*,2*R*)-DPEN) and (*R*)-1,2,2-triphenylethylamine ((*R*)-122TPEA).

### Solubility screening

The main criterium towards the choice of the amine-based resolving agent was decided to be the solubility since it directly relates to the maximal yield. The solubilities of the above selected amines as diastereomeric salts with (*R*)- and (*S*)-mandelic acid were investigated in the aqueous reaction medium and then compared according to the overall solubility difference between the corresponding diastereomeric salts and to the other salt pairs (Table 1).

Two potential crystallization partners were eliminated right away. (*R*)-122TPEA had very low overall solubilities of both diastereomeric mandelate salts, while (1*R*,2*S*)-ADPE did not have a sufficient solubility gap between its diastereomeric mandelate salts. The remaining two of the selected diastereomeric salt pairs exhibited a high discrepancy between the different enantiomer salts of mandelic acid with (1*R*,2*R*)-DPEN at low concentrations and (*S*)-1PEA at relatively high concentrations. Interestingly, those two salt pairs showed a preference towards crystallizing different enantiomers of mandelic acid. The most promising option appears to be (1*R*,2*R*)-DPEN with diastereomeric salt solubilities of 33.6 and 88.5 mM, respectively, which facilitates a sufficiently low concentration towards the targeted (*R*)-enantiomer of mandelic acid. With (*S*)-1PEA, the less soluble salt of (*S*)-mandelic acid possessed a relatively high solubility of ca. 200 mM, however due to its counterpart being very soluble at >6 M and the selected mandelate racemase being able to work at high substrate concentrations, it still presented a viable option.

### Optimizing diastereomeric salt crystallization conditions

Having identified two potential resolving amine counterions, it was decided to attempt to form a first impression for the efficacy of the resolution of mandelic acid with those counterions. Therefore, simple crystallization experiments on a small scale of 1 ml were executed with varying racemic mandelate and amine counterion concentrations. It has to be noted, that both mandelate and the amine counterions were utilized as sodium (mandelate) or hydrochloride/di-hydrochloride salts ((*S*)-1PEA and (1*R*,2*R*)-DPEN respectively). Since the ability to selectively crystallize only one enantiomer of mandelic acid was deemed the most important parameter





**Table 1** Solubility screening for the diastereomeric salt pairs with selected amine counterions in water

Amine counterion	Structure of amine counterion	Solubility of ( <i>R</i> )-MA salt, mM	Solubility of ( <i>S</i> )-MA salt, mM
(1 <i>R</i> ,2 <i>S</i> )-ADPE		67.1 ± 6.8	56.3 ± 2.7
(1 <i>R</i> ,2 <i>R</i> )-DPEN		33.6 ± 4.8	88.5 ± 3.1
( <i>S</i> )-1PEA		6138.9 ± 370.9	204.1 ± 12.1
( <i>R</i> )-122TPEA		4.9 ± 1.1	9.3 ± 0.9

The solubility screening was performed at 30 °C in pure ddH<sub>2</sub>O at pH 7, the pH was adjusted with weak NaOH and HCl solutions, when needed. (1*R*,2*R*)-DPEN salts were measured as monoamine salts.

of the experiments, the yield was not measured, focusing solely on the enantiopurity of the crystallization phase. The resulting enantiomeric excesses of the formed product salts are shown in Table 2.

Although the (*S*)-1PEA mandelate salts showed an exorbitant solubility difference between its respective (*S*)- and (*R*)-MA salts, it failed to reach enantiomeric excesses over 80% for its precipitated product, nearing this limit only for relatively low counterion concentrations, which would mean low yields of the enantiomerically enriched product phase. On the contrary, (1*R*,2*R*)-DPEN demonstrated fairly good enantiomeric excesses of up to 87% although its diastereomeric salts solubility limits were not that much apart. An increase in counterion concentrations led to a slight decrease of enantiomeric excess of the crystallized mandelate salts from 87% at 75 mM of (1*R*,2*R*)-DPEN to 80% at 150 mM of (1*R*,2*R*)-DPEN. But since those were only preliminary experiments with a short time for crystallization of 3 hours, those values were acceptable and open to adjustment *via* longer crystallization times. Hence, it was chosen to continue with (1*R*,2*R*)-DPEN as the crystallization partner for mandelic acid resolution.

### Small-scale DKR experiments and enantiomeric excess optimization

As the highest enantiomeric excess was obtained using 200 mM of racemic mandelic acid and 75 mM of (1*R*,2*R*)-DPEN as the chiral resolving agent, those concentrations were chosen for the initial DKR-based experiments. A corresponding control experiment was also performed and compared in triplicates of DKR- and chiral resolution based (controls without enzyme) reactions. The resulting yields and enantiomeric excesses are shown in Fig. 2 (left). This data shows, that both the CR and DKR-based approaches show similar results. The DKR-based yield might have been slightly better with 32.4% *versus* 28.5% for CR-based control, while the CR-based *ee* of 90.3% slightly surpassed the DKR-based *ee* of 89.9%.

Based on the presented observations, it was decided to retry the DKR- to CR-comparison with a higher concentration of 150 mM (1*R*,2*R*)-DPEN according to the procedure utilized with 75 mM (1*R*,2*R*)-DPEN on a fed-batch basis, the results shown in Fig. 2 (right). As can be seen, while the enantiomeric excess stays on the same fairly high level of 90%, the yield is improved

**Table 2** Results of crystallization screening of (1*R*,2*R*)-DPEN and (*S*)-1PEA as potential resolving agents for racemic mandelic acid

Racemic mandelate, mM	Amine counterion	Counterion, mM	<i>ee</i> of product salt
1000	( <i>S</i> )-1PEA	500	66.7 ± 7.0% ( <i>S</i> )
500	( <i>S</i> )-1PEA	500	67.6 ± 1.6% ( <i>S</i> )
250	( <i>S</i> )-1PEA	500	n.d.
100	( <i>S</i> )-1PEA	500	n.d.
1000	( <i>S</i> )-1PEA	400	63.9 ± 1.8% ( <i>S</i> )
1000	( <i>S</i> )-1PEA	300	74.9 ± 9.4% ( <i>S</i> )
1000	( <i>S</i> )-1PEA	250	77.5 ± 11.1% ( <i>S</i> )
1000	( <i>S</i> )-1PEA	200	77.2 ± 0.7% ( <i>S</i> )
1000	( <i>S</i> )-1PEA	100	n.d.
200	(1 <i>R</i> ,2 <i>R</i> )-DPEN	150	79.9 ± 2.6% ( <i>R</i> )
200	(1 <i>R</i> ,2 <i>R</i> )-DPEN	100	84.3 ± 2.8% ( <i>R</i> )
200	(1 <i>R</i> ,2 <i>R</i> )-DPEN	75	86.8 ± 4.3% ( <i>R</i> )
200	(1 <i>R</i> ,2 <i>R</i> )-DPEN	50	n.d.

Enantiomeric excess was determined by HPLC analysis of dried precipitated salts, which were harvested after 3 h at RT and 750 rpm. Where no product salt precipitate was obtained, the experiments are marked with "n.d."



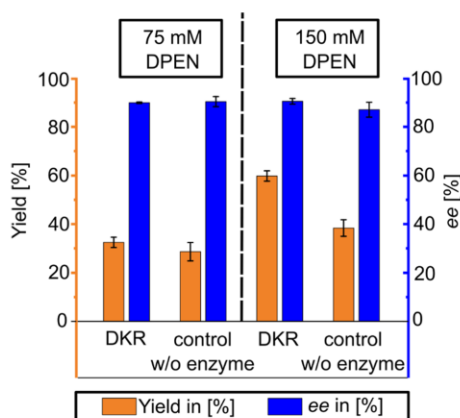


Fig. 2 Left: Yield and enantiomeric excess of DKR-based and CR-based fed-batch experiments after 96 h; 200 mM racemic mandelate, 75 mM (1*R*,2*R*)-DPEN, 10 U ml<sup>-1</sup> mandelate racemase extract (for DKR only), 50 mM HEPES-buffer with 3.3 mM MgCl<sub>2</sub>, pH 7.5, RT (22–23 °C), 96 h, 5 ml. Right: Yield and enantiomeric excess of DKR-based and CR-based fed-batch experiments after 96 h with doubled counterion concentration; 200 mM racemic mandelate, 150 mM (1*R*,2*R*)-DPEN, 10 U ml<sup>-1</sup> mandelate racemase extract (for DKR only), 50 mM HEPES-buffer with 3.3 mM MgCl<sub>2</sub>, pH 7.5, RT (22–23 °C), 96 h, 5 ml. Experiments were performed in triplicates. Substrates and crystallization counteragents were refilled after 24 and 48 h.

significantly to reach slightly over 60% with the DKR-based approaches. For the CR-based controls, the yield reaches nearly 40%, while the *ee* starts to experience a slight decrease towards 87%. XRPD analysis of the harvested product material showed the presence of the monoamine salt as the dominant crystallized solid phase. XRPD results, including mono- and diamine reference salts of both mandelate enantiomers, are provided in the ESI† file (see Fig. S2 and S3). The yields were calculated based on HPLC (showing the mandelic acid remaining in solution) and XRPD investigations.

Compared to the initial crystallization experiments, the *ees* of the product salts were higher with both 75 mM and especially 150 mM (1*R*,2*R*)-DPEN concentrations, with the only difference between the experiments being the time spent stirring (2–3 h vs. 24 h between refills). Thus, it was decided to monitor the change in enantiomeric excess of the formed product salt over time.

For the purpose of simpler monitoring, 72 h long DKR-batches (without refilling) bearing 150 mM of (1*R*,2*R*)-DPEN were done as a triplicate and monitored only for *ee* over the course of 24 h. The progression of the *ee* is shown in Fig. 3. The shown progression explains the discrepancy between the initial crystallization screening and the outcome of DKR- and CR-based batches in terms of enantiomeric excess. A simple waiting period of 24 h elevates *ee* about 10% from 80 to 90% *ee*. However, additional waiting does not significantly contribute to the enantiopurity of the obtained product salt any further.

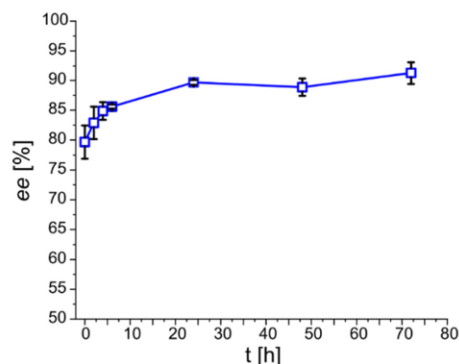


Fig. 3 Enantiomeric excess of the product salt over time in DKR-based 72 h batch with 150 mM (1*R*,2*R*)-DPEN, 200 mM racemic mandelate, 150 mM (1*R*,2*R*)-DPEN, 10 U ml<sup>-1</sup> mandelate racemase extract, 50 mM HEPES-buffer with 3.3 mM MgCl<sub>2</sub>, pH 7.5, RT (22–23 °C), 72 h, 5 ml.

Thus, a DKR-based system for resolution of mandelic acid can be established through the proposed approach on a continuous basis, presenting high yields and a fairly high enantiomeric excess of one product enantiomer. Finally, a proof-of-concept needed to be obtained to evaluate the scalability of the process. Therefore, the system was tested on a preparative scale.

#### Preparative-scale DKR experiment

After the successful initial experiments, the combined racemization-crystallization reaction concept was validated at preparative scale to showcase its synthetic potential. A reaction in the 50 ml format was prepared, operated in a fed-batch mode for 96 h and the reaction progress monitored periodically *via* HPLC (see Fig. 4). The product salt was harvested and its purity was analyzed *via* NMR. The *ee* of this DKR-based approach was determined at 94.9% ((*R*)-mandelic acid), with an overall yield of 60.3% (4.61 g of product salt) determined in accordance with isolated product mass and HPLC analysis. Afterwards, mandelic acid was extracted from the product salt (4.547 g after analytic procedures) to yield 1.78 g (56% overall yield based on racemic mandelic acid) of pure mandelic acid, with a purity of 94% determined *via* NMR, although it has to be noted, that 4.4% of the impurities can be attributed to the spontaneously formed isopropyl ester of the mandelic acid due to residual acid prior to extraction with isopropanol. The counterion was also extracted and yielded 2.24 g with a purity of 98.7%.

## Experimental

### Transformation

Chemocompetent *E. coli* BL21(DE3) cells were thawed on ice in 50 µl aliquots. To the thawed cell suspension on ice, 1 µl of the plasmid solution of pET-52b(+), carrying the gene for

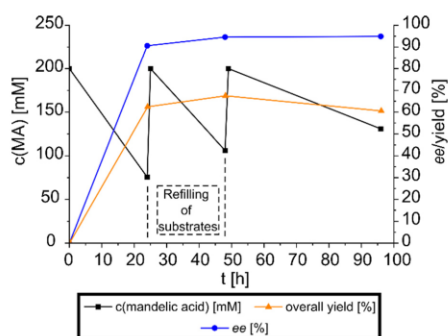


Fig. 4 Monitoring of the preparative DKR fed-batch. The black curve shows the concentration of mandelic acid at the measurement points, while the blue curve shows the enantiomeric excess of the product salt. The overall yield progression is shown as the orange curve. 200 mM racemic mandelate, 150 mM (1*R*,2*R*)-DPEN, 30 U ml<sup>-1</sup> mandelate racemase extract, 50 mM HEPES-buffer with 3.3 mM MgCl<sub>2</sub>, pH 7.5, RT (22–23 °C), 96 h, 50 ml, fed-batch.

the mandelate racemase from *Pseudomonas putida* (N-terminal StrepII-tag and a C-terminal His<sub>10</sub>-tag) and an ampicillin resistance gene,<sup>58</sup> was added. The cell aliquot was incubated for 30 min on ice. After that, a heat shock was applied by placing the cell aliquot into a prewarmed heating block at 42 °C for 30 s. Immediately after, the cells were returned onto the ice and incubated there for another 5 min. 950 µl of sterile LB medium were added to the cells. The cell suspension was incubated at 37 °C and 750 rpm for 1 h and variable volumes were plated onto selective LB-agar plates supplemented with 0.1 mg ml<sup>-1</sup> ampicillin. The plates were incubated at 37 °C overnight.

#### Overnight cultures and Cryostocks

Overnight cultures were prepared in 5 ml of sterile LB medium and supplemented with ampicillin to a final concentration of 0.1 mg ml<sup>-1</sup>. The cultures were inoculated from single colonies from successful transformations or cryostocks and grown overnight at 37 °C and 180 rpm. Cryostocks were prepared by adding 800 µl of an overnight culture to 200 µl of sterile glycerol (resulting in 20% v/v glycerol stocks) and frozen at -80 °C.

#### Protein expression

Expression cultures were grown in 500 ml of LB medium in 2 l cultivation flasks without induction. 1 ml of 50 mg ml<sup>-1</sup> ampicillin stock solution (0.1 mg ml<sup>-1</sup> final concentration) was added. Furthermore, 500 µl of a sterilized 1:10 dilution of antifoam B (by Sigma Aldrich) were added to prevent foaming. The flasks were inoculated to a starting OD<sub>600</sub> of approximately 0.05 from overnight cultures. The resulting cultures were incubated at 37 °C for 4–5 hours under constant shaking at 200 rpm until reaching an OD<sub>600</sub> of

approximately 1. At this point, the cultures were harvested *via* centrifugation at 4000 × *g* for 10 min at 4 °C. The pellets were resuspended in 50 ml of 50 mM HEPES buffer (pH 7.5) containing 3.3 mM MgCl<sub>2</sub> and centrifuged again at 4000 × *g* for 10 min at 4 °C as a washing step, the liquid was discarded. After resuspension in 5 ml of 50 mM HEPES buffer (pH 7.5) containing 3.3 mM MgCl<sub>2</sub>, the pellet suspensions were unified and frozen at -20 °C.

#### Lysis

The frozen harvested cells were thawed on ice. To the thawed suspension, 0.5 ml of a 10 mg ml<sup>-1</sup> lysozyme stock solution (0.25 mg ml<sup>-1</sup> final concentration) and 200 µl of a 1 mg ml<sup>-1</sup> DNase I stock solution (0.1 mg ml<sup>-1</sup> final concentration) were added per 20 ml of suspension. Afterwards, the cells were left on ice for 30 min. As the next step, lysis was performed *via* ultrasonication on a Sonics & Materials Inc. VibraCell VC750 ultrasonic processor equipped with a 3 mm in diameter tapered ultrasonic tip. For the time program, the cell suspension (on ice for cooling) was pulsed for 5 s at an amplitude of 30% and left idle for 10 s. This cycle was repeated, until an overall pulse time of 3 min was reached. After that, the lysed cells were centrifuged at 13 000 rpm and 4 °C for 45 min. The cleared supernatant was unified and shock-frosted with liquid nitrogen. The resulting cell extract was lyophilized overnight. The dried cell extract was then subjected to an activity assay to determine its specific activity.

#### Activity assay for mandelate racemase

For the activity test, the conversion of pure (*R*)-mandelic acid was analyzed over time. For this purpose, a 20 mg ml<sup>-1</sup> stock solution of (*R*)-mandelic acid was prepared in 50 mM HEPES buffer with 3.3 mM MgCl<sub>2</sub> and the pH was adjusted to 7.5. The dried cell extract was also dissolved in the same buffer at pH 7.5 for a stock solution of 2 mg ml<sup>-1</sup>. 500 µl of (*R*)-mandelic acid stock were put in a 2 ml microcentrifuge tube and preheated to 25 °C. To initiate the reaction, 500 µl of the enzyme stock solution were added, resulting into final concentrations of 10 mg ml<sup>-1</sup> (65.7 mM) of (*R*)-mandelic acid and 1 mg ml<sup>-1</sup> enzyme (cell extract) in a final volume of 1 ml. The reactions were incubated at 25 °C and 900 rpm for 15, 30, 45 or 60 s, at which point 100 µl samples were drawn and immediately mixed with 500 µl of acetonitrile to precipitate the protein and hence stop the reaction. The resulting samples were vortexed and then centrifuged at 13000 rpm for 10 min. From the cleared supernatant 200 µl were drawn and mixed with 1300 µl of a 2 mM CuSO<sub>4</sub> solution in ddH<sub>2</sub>O in an HPLC-vial. This sample was then measured in a chiral HPLC set-up for the enantiomeric ratio between (*R*)- and (*S*)-mandelic acid. From the measured percentage and the fixed initial (*R*)-mandelic acid concentration of 65.7 mM the amount of formed (*S*)-mandelic acid in µmol was calculated and plotted against time in min. The plot was linearized to yield an activity of the enzyme in U, which was then divided



by the enzyme concentration of 1 mg ml<sup>-1</sup> (1 ml reactions) in the reaction, resulting in a final specific activity of the analyzed dried cell extracts. For each time point, a triplicate of reactions was performed. If within 15–60 s no clear linear plot could be obtained due to lower activity of the obtained dried cell extract, the measurement points were extended to 1, 2, 4 and 8 min.

#### Preparation of sodium mandelate, (1*R*,2*R*)-DPEN/(*S*)-1PEA hydrochloride salts and amine mandelate salts

To prepare sodium mandelate, 2 g (13.1 mmol) of racemic mandelic acid were dissolved in 50 ml cyclopentyl methyl ether (CPME). To the dissolved mandelate, 500 µl of a saturated NaOH solution was added. The resulting suspension was stirred for 1 h at room temperature, after which the precipitated sodium mandelate was filtered out and dried at room temperature. The purity of the obtained sodium mandelate was analyzed *via* NMR.

(1*R*,2*R*)-DPEN and (*S*)-1PEA hydrochloride salts were prepared in a similar manner. An appropriate amount of the amines, 1–2 g of (1*R*,2*R*)-DPEN (4.7–9.4 mmol) or 1 ml (7.8 mmol) of (*S*)-1PEA, were dissolved in 50 ml of CPME. To this amine solution, 5 ml of a 3 M HCl in CPME solution (Sigma-Aldrich) was added. The resulting suspension was stirred for 1 h at room temperature, after which the precipitated amine hydrochloride (dihydrochloride for (1*R*,2*R*)-DPEN) was filtered out and dried at room temperature.

The amine mandelate salts for the solubility testing were prepared as follows. Separate solutions of (*R*)- or (*S*)-mandelic acid and their amine counterion in CPME were prepared, bearing equimolar concentrations. Thus, equimolar amounts of the stock solutions of mandelate and the amine counterion were unified. For the diamine salts of (1*R*,2*R*)-DPEN, the amount of mandelate was doubled. The resulting suspensions were stirred for 1 hour at room temperature. Monoamine salts of (1*R*,2*R*)-DPEN were prepared from water. Here, equimolar (75 mM) solutions of (*R*)- or (*S*)-mandelic acid and the dihydrochloride of (1*R*,2*R*)-DPEN in water were mixed in equal proportions, the pH was adjusted to 7. To facilitate crystallization, approximately half ((*R*)-salt) to two thirds ((*S*)-salt) of the water volume was evaporated at 40 °C under an argon stream, until first crystals were visible in the remaining aqueous phase. Afterwards, the crystallization was left for 1 h at room temperature (if necessary, the suspension was left for 15 min at 4 °C). The precipitated mandelate salts were filtered out and dried at room temperature.

#### Solubility screening

A small amount (between 10–20 mg) of the chosen mandelate salt was mixed into 1 ml of ddH<sub>2</sub>O. Additional salt was added until saturation was reached, if necessary. pH was kept at 7, adjusted with weak HCl and NaOH solutions, adjusted again after 24 h and afterwards every 48 h. Additional mandelate salt was added, if necessary. The saturated solutions were shaken at 30 °C and 900 rpm for 5 days or until no further

pH changes occurred. After no pH change was observed, the solutions were centrifuged for 10 min at 13 000 rpm and the cleared aqueous supernatant was filtered through 0.25 µm syringe filters to remove traces of crystalline salt. The filtrate was collected into previously weighed vials. Those vials were weighed again filled with the filtrate for the determination of the exact mass of the water. Then, the liquid in the vials was evaporated at 40 °C under a constant argon stream in a Thermo Scientific Pierce ReactiTherm I & ReactiVap I heating and evaporation unit. The evaporated vials were weighed and the solubility of the mandelate salts was calculated. The experiments for each salt were performed in triplicates.

#### Crystallization screening for enantiomeric excess

For resolution testing on small scale, solutions of sodium mandelate and its amine counterion hydrochlorides ((1*R*,2*R*)-DPEN or (*S*)-1PEA) in 50 mM HEPES buffer with 3.3 mM MgCl<sub>2</sub> (pH 7.5) were prepared in double the concentrations, that were meant to be analyzed. The pH was adjusted back to 7.5 with conc. HCl and saturated NaOH solutions.

Afterwards, the solutions were mixed in a 1:1 ratio to obtain 1 ml of final volume (500 µl:500 µl), effectively halving their respective stock solution concentrations. The resulting suspensions were shaken at 750 rpm and room temperature for 3 hours. Then the tubes with the samples were centrifuged for 10 min at 13 000 rpm, the cleared supernatant was discarded. The obtained salt pellet was pressed onto filter paper to remove further liquid and dried for 2 hours at room temperature. The dried pellets were analyzed for enantiomeric excess *via* chiral HPLC according to standard procedure described below. For each analyte ratio, a triplicate was prepared.

#### Batches and fed-batches on a 5 ml scale

Small-scale experiments in the 5 ml format were prepared as follows. A 2.5 ml 400 mM sodium mandelate solution in 50 mM HEPES buffer with 3.3 mM MgCl<sub>2</sub> (pH 7.5) was prepared, the pH was adjusted with conc. HCl and saturated NaOH solutions. An analogous solution of either 150 mM or 300 mM of (1*R*,2*R*)-DPEN dihydrochloride was prepared and pH-adjusted as well, although past the 150 mM mark the hydrochloride yielded rather a suspension than a solution. Both solutions were then mixed to yield a 5 ml reaction with 200 mM of mandelate and either 75 or 150 mM of (1*R*,2*R*)-DPEN. The vial of the (1*R*,2*R*)-DPEN was flushed with the mandelate solution to avoid loss of (1*R*,2*R*)-DPEN. The pH of the formed reaction solution was again adjusted to 7.5. Afterwards, 10 U ml<sup>-1</sup> of the mandelate racemase cell extract was added to the mixture, if the reaction was to be performed in a DKR format, the pH was checked and adjusted to 7.5, if necessary. The reaction was stirred at room temperature and 750 rpm.

For simple batch approaches (*ee* curve), the reactions were stirred for 72 h. 200 µl samples were drawn on certain time points and prepared according to standard procedure (see HPLC method) to measure *ee*. For fed-batch reactions, 200 µl



samples were drawn after 24 h, measuring the mandelate concentration in solution and the respective *ee* (see HPLC method). The mandelate concentration was refilled to its initial value of 200 mM, while (1*R*,2*R*)-DPEN was refilled in a 1:2 ratio (half the molar amount) to the refilled mandelate (all on a scale of 4.8 ml), the pH was adjusted to 7.5. After another 24 h of stirring at room temperature and 750 rpm (48 h mark), the same refilling procedure (4.6 ml scale) was repeated. After refilling, another 10 U ml<sup>-1</sup> of mandelate racemase cell extract was added into DKR-based reactions. The refilled reactions were left stirring for another 48 h (96 h reactions in total) at room temperature and 750 rpm. At the 96 h mark, further HPLC samples were drawn to calculate the yields of the reactions. The product salt was harvested by filtration, the reaction flask was flushed twice with the cleared filtrate to avoid product loss. The harvested salt was pressed into filter paper to remove residual liquid, dried at room temperature and weighed.

#### X-ray powder diffraction (XRPD) analysis

The analysis of a solid phase sample from the reactions and the reference salts was performed using a first-generation Empyrean diffractometer (PANalytical, Almelo, The Netherlands). Data was collected in reflection geometry (Bragg–Brentano) mode using a PIXcel3D 1 × 1 detector. The salt samples were prepared on zero background holders (silicon disks) and the measurements were performed in a 2 $\theta$  range from 4–50° using Cu K $\alpha_{(1+2)}$  radiation. The step size was defined as 0.0131° and the time per step was set to 73.7 s. The setup was controlled using the PANalytical Data Controller software (vers. 5.3). The data was plotted using the Origin software.

#### Preparative scale experiment

On preparative scale, the same approach was chosen, as with the 5 ml reactions. 25 ml of 400 mM sodium mandelate and 25 ml of 300 mM (1*R*,2*R*)-DPEN dihydrochloride solutions in 50 mM HEPES buffer with 3.3 mM MgCl<sub>2</sub> (pH 7.5) were prepared, their pH was adjusted to 7.5 with conc. HCl and saturated NaOH solutions. The solutions were unified in a 100 ml Erlenmeyer flask, briefly stirred and their pH was adjusted. The vial of the (1*R*,2*R*)-DPEN was flushed with the mandelate solution to avoid loss of (1*R*,2*R*)-DPEN. 30 U ml<sup>-1</sup> of the mandelate racemase cell extract were added to the mixture, the pH was checked and adjusted, if necessary. The reaction was stirred at 900 rpm and room temperature for 24 h. 200  $\mu$ l samples were drawn after 24 h, the mandelate concentration in solution and the *ee* were measured (see HPLC method). The reaction was refilled as described for 5 ml fed-batches and stirred for another 24 h. Then, the refilling process was repeated at the 48 h mark, another 30 U ml<sup>-1</sup> of mandelate racemase cell extract were added as well, the pH was adjusted. The reaction was stirred for another 48 h at room temperature and 900 rpm. Afterwards, 96 h HPLC samples were drawn to calculate the final yield from the

residual mandelate concentration in solution. The product salt was harvested by filtration, the reaction flask being flushed twice with the cleared filtrate to avoid product loss. The harvested salt was pressed into filter paper to remove residual liquid and dried at room temperature, weighed and analyzed for enantiomeric excess *via* chiral HPLC and checked for impurities *via* NMR.

The harvested product salt was suspended in 100 ml of ddH<sub>2</sub>O. 25 ml of saturated NaOH were added to the suspension, dissolving the product salt completely and obtaining a yellow precipitate of the (1*R*,2*R*)-DPEN. This solution was then extracted three times with 50 ml of previously dried CPME (24 h, 400 rpm, dried with anhydrous MgSO<sub>4</sub>). The organic phases were unified and evaporated to recover (1*R*,2*R*)-DPEN. To the aqueous phase, 50 ml of a 37% HCl solution were added, the pH was monitored to turn sour. The aqueous phase was then evaporated. The remaining solid was extracted five times with 50 ml of previously dried isopropanol (24 h, 400 rpm, dried with anhydrous MgSO<sub>4</sub>). The extractions were centrifuged to leave the undesired NaCl solid out of the product phase. The extraction phases were evaporated to yield the extracted mandelic acid. The purities of the extracted mandelic acid and (1*R*,2*R*)-DPEN were analyzed *via* NMR.

#### Chiral HPLC

Chiral HPLC analysis was performed on a Shimadzu Nexera series HPLC consisting of the following modules: SCL-40, DGU-405, LC-40D, SIL-40C, CTO-40S, SPD-M40. For separation, a Phenomenex Chirex 3126 column (150 × 4.6 mm; 5  $\mu$ m, 110 Å) was used. The diluent was a mixture of 85% of 2 mM CuSO<sub>4</sub> solution in ddH<sub>2</sub>O (pH ~4) and 15% of HPLC-grade acetonitrile.

For concentration measurements, samples were prepared as follows. From the reaction mixture, 200  $\mu$ l samples were drawn and centrifuged for 10 min at 13 000 rpm. From the cleared liquid phase, 100  $\mu$ l were drawn into another vial. The product salt pellet was pressed onto filter paper and left to dry for 1 hour at room temperature for *ee* monitoring (24 and 48 h samples). To the 100  $\mu$ l of liquid phase, 500  $\mu$ l of acetonitrile was added to precipitate all proteins prior to measurement, the sample was vortexed and then centrifuged for 10 min at 13 000 rpm. 200  $\mu$ l of the cleared supernatant were added to 1300  $\mu$ l of 2 mM CuSO<sub>4</sub> solution, the sample was vortexed. 1 ml of this mixture was drawn into a HPLC-vial. 200  $\mu$ l of a 15 mM solution of D-alanine in 2 mM CuSO<sub>4</sub> was added as an internal standard for normalization. The readied samples were measured, the peak areas of (*R*)- and (*S*)-mandelic acids were normalized by the internal standard and their concentrations were calculated in accordance to an appropriate calibration curve.

For enantiomeric excess measurements of the product solid phase, samples were prepared as follows. For 24 and 48 h samples, the centrifuged pellet of the 200  $\mu$ l samples was used, for the final *ee* measurement, the sample was taken



from the dried harvested product salt. Approximately 3–10 mg of the solid phase (product salt) were dissolved in 500  $\mu\text{l}$  of 2 mM  $\text{CuSO}_4$  with the addition of 10  $\mu\text{l}$  of saturated NaOH solution. 500  $\mu\text{l}$  of acetonitrile were added, the sample was vortexed. Afterwards, the samples were centrifuged for 10 min at 13 000 rpm. 200  $\mu\text{l}$  of the centrifuged sample was added to 1 ml of 2 mM  $\text{CuSO}_4$  to yield the final HPLC sample. The samples pH was adjusted to pH 4 with concentrated HCl (37% w/w). The sample was then briefly centrifuged again, if necessary, to remove possible copper-DPEN complexes precipitates and transferred into a HPLC-vial for measurement. All samples were measured in isocratic mode at a flow rate of 1 ml  $\text{min}^{-1}$  for 60 min. Column temperature was kept at 30  $^\circ\text{C}$ , the detection wavelength was 254 nm.

## Summary and conclusions

This study aims to showcase the synthetic potential of dynamic kinetic resolution towards the preparation of enantiopure mandelic acid, consisting of a diastereomeric crystallization combined with enzymatic racemization using mandelic acid racemase. The presented approach for dynamic kinetic has shown great efficacy and presented a very good enantiomeric excess of the raw product phase. Furthermore, the diastereomeric crystallization was achieved at mild conditions and in a completely aqueous reaction phase, retaining high yields and enantiomeric excesses of the crystalline product salt. The system shows great potential for a continuous approach, including possible gravimetric separation of the product salt and a very good potential for the recyclability of the reaction broth, including the uncrystallized mandelic acid, since it is a racemate due to the racemase in solution, thus it would just need to be refilled to its initial concentration for process continuation. The shown dynamic kinetic resolution system using mandelate racemase may eventually outperform any form of chiral or kinetic resolution as yields of > 50% are obtainable. Investigations of phase diagrams of the product salts of both enantiomers in water would help to determine ideal crystallization conditions and thus maximize possible obtainable yields from the preparative process.

## Data availability

The data supporting this article has been included as part of the ESI†

## Author contributions

Conceptualization: F. B., J. v. L.; data curation: F. B., A. L.; formal analysis: F. B., A. L.; funding acquisition: J. v. L.; investigation: F. B., A. L.; methodology: F. B., A. L., J. v. L.; project administration: J. v. L.; resources: J. v. L.; supervision: J. v. L.; validation: F. B., A. L.; visualization: F. B.; writing – original draft: F. B.; writing – review & editing: F. B., A. L., J. v. L.

## Conflicts of interest

There are no conflicts to declare.

## Acknowledgements

Funding for F. B. and J. v. L. by Central SME Innovation Programme (ZIM, projects 16KN073233 and ZF4402103CR9) and the Heisenberg Programme of the Deutsche Forschungsgemeinschaft (project number 450014604) is gratefully acknowledged. The authors thank Dr. Katja Bettenbrock (Max Planck Institute for Dynamics of Complex Technical Systems, Magdeburg) for providing the plasmid carrying the mandelate racemase gene. The authors also thank Dr. Liane Hilfert and Sabine Hentschel (NMR division, Institute of Chemistry, Otto-von-Guericke University Magdeburg) for their help and fruitful discussions, as well as Ines Sauer (Industrial Chemistry, Institute of Chemistry, Otto-von-Guericke University Magdeburg) for her experimental support in XRPD measurements.

## References

- H. Pellissier, *Eur. J. Org. Chem.*, 2022, **2022**(7), e202101561.
- G. L. Thejashree, E. Doris, E. Gravel and I. N. N. Namboothiri, *Eur. J. Org. Chem.*, 2022, **2022**(44), e202201035.
- H. Pellissier, *Tetrahedron*, 2011, **67**, 3769–3802.
- A. Garg, D. Rendina, H. Bendale, T. Akiyama and I. Ojima, *Front. Chem.*, 2024, **12**, 1398397.
- S. Li, X. Xu, L. Xu, H. Lin, H. Kuang and C. Xu, *Nat. Commun.*, 2024, **15**, 3506.
- G. Han, W. Ren, S. Zhang, Z. Zuo and W. He, *RSC Adv.*, 2024, **14**, 16520–16545.
- Y. Teng, C. Gu, Z. Chen, H. Jiang, Y. Xiong, D. Liu and D. Xiao, *Chirality*, 2022, **34**, 1094–1119.
- S. Mane, *Anal. Methods*, 2016, **8**, 7567–7586.
- H. Lorenz and A. Seidel-Morgenstern, *Angew. Chem., Int. Ed.*, 2014, **53**, 1218–1250.
- M. Hall, *RSC Chem. Biol.*, 2021, **2**, 958–989.
- C. Terazzi, A. Spannenberg, J. von Langemann and T. Werner, *ChemCatChem*, 2023, **15**(19), e202300917.
- E. Forró and F. Fülöp, *Curr. Med. Chem.*, 2022, **29**, 6218–6227.
- S. S. Berry and S. Jones, *Org. Biomol. Chem.*, 2021, **19**, 10493–10515.
- M. M. Musa, F. Hollmann and F. G. Mutti, *Catal. Sci. Technol.*, 2019, **9**, 5487–5503.
- C. José, M. V. Toledo and L. E. Briand, *Crit. Rev. Biotechnol.*, 2016, **36**, 891–903.
- X. Wu, Y. Liu and Z. Jin, in *Dynamic Kinetic Resolution (DKR) and Dynamic Kinetic Asymmetric Transformations (DYKAT)*, ed. J.-E. Bäckvall, Georg Thieme Verlag KG, Stuttgart, 2023.
- R. Gurubrahama, Y.-S. Cheng, W.-Y. Huang and K. Chen, *ChemCatChem*, 2016, **8**, 86–96.



- 18 A. H. Kamaruddin, M. H. Uzir, H. Y. Aboul-Enein and H. N. A. Halim, *Chirality*, 2009, **21**, 449–467.
- 19 L.-C. Yang, H. Deng and H. Renata, *Org. Process Res. Dev.*, 2022, **26**, 1925–1943.
- 20 G. A. Applegate and D. B. Berkowitz, *Adv. Synth. Catal.*, 2015, **357**, 1619–1632.
- 21 C. Femmer, M. Bechtold, T. M. Roberts and S. Panke, *Appl. Microbiol. Biotechnol.*, 2016, **100**, 7423–7436.
- 22 M. M. Musa, *Chirality*, 2020, **32**, 147–157.
- 23 R. V. Singh and K. Sambyal, *Crit. Rev. Biotechnol.*, 2023, **43**, 1226–1235.
- 24 L. Martinková and V. Křen, *Appl. Microbiol. Biotechnol.*, 2018, **102**, 3893–3900.
- 25 X. Chen, Q. Wu and D. Zhu, *Process Biochem.*, 2015, **50**, 759–770.
- 26 S. Wang, T. Shi, Z. Fang, C. Liu, W. He, N. Zhu, Y. Hu, X. Li and K. Guo, *J. Flow Chem.*, 2022, **12**, 227–235.
- 27 S. Chen, F. Liu, K. Zhang, H. Huang, H. Wang, J. Zhou, J. Zhang, Y. Gong, D. Zhang, Y. Chen, C. Lin and B. Wang, *Tetrahedron Lett.*, 2016, **57**, 5312–5314.
- 28 Y. Cao, S. Wu, J. Li, B. Wu and B. He, *J. Mol. Catal. B: Enzym.*, 2014, **99**, 108–113.
- 29 D. Yıldırım and S. S. Tükel, *Biocatal. Biotransform.*, 2014, **32**, 251–258.
- 30 C. Yao, Y. Cao, S. Wu, S. Li and B. He, *J. Mol. Catal. B: Enzym.*, 2013, **85–86**, 105–110.
- 31 U. T. Strauss and K. Faber, *Tetrahedron: Asymmetry*, 1999, **10**, 4079–4081.
- 32 M. E. Scott, X. Wang, L. D. Humphreys, M. J. Geier, B. Kannan, J. Chan, G. Brown, D. F. A. R. Dourado, D. Gray, S. Mix and A. Pukin, *Org. Process Res. Dev.*, 2022, **26**, 849–858.
- 33 X. Zhang, F. Chang, F. Zhu, T. Xu and Y. Zhang, *J. Chem. Res.*, 2022, **46**(4), 17475198221109155.
- 34 X.-H. Zhang, C.-Y. Wang, X. Cai, Y.-P. Xue, Z.-Q. Liu and Y.-G. Zheng, *Bioprocess Biosyst. Eng.*, 2020, **43**, 1299–1307.
- 35 L. Martinková, L. Rucká, J. Nešvera and M. Pátek, *World J. Microbiol. Biotechnol.*, 2017, **33**, 8.
- 36 P. Kaul, A. Banerjee, S. Mayilraj and U. C. Banerjee, *Tetrahedron: Asymmetry*, 2004, **15**, 207–211.
- 37 T. Yuthalekha, C. Wattanakit, V. Lapeyre, S. Nokbin, C. Warakulwit, J. Limtrakul and A. Kuhn, *Nat. Commun.*, 2016, **7**, 12678.
- 38 X.-P. Jiang, T.-T. Lu, C.-H. Liu, X.-M. Ling, M.-Y. Zhuang, J.-X. Zhang and Y.-W. Zhang, *Int. J. Biol. Macromol.*, 2016, **88**, 9–17.
- 39 P.-C. Yan, J.-H. Xie, X.-D. Zhang, K. Chen, Y.-Q. Li, Q.-L. Zhou and D.-Q. Che, *Chem. Commun.*, 2014, **50**, 15987–15990.
- 40 T. Lerdwiriyanupap, R. Cedeno, P. Nalaoh, S. Bureekaew, V. Promarak and A. E. Flood, *Cryst. Growth Des.*, 2023, **23**, 2001–2010.
- 41 M. H. T. Kwan, J. Breen, M. Bowden, L. Conway, B. Crossley, M. F. Jones, R. Munday, N. P. B. Pokar, T. Screen and A. J. Blacker, *J. Org. Chem.*, 2021, **86**, 2458–2473.
- 42 S. K. Tulashie, J. von Langermann, H. Lorenz and A. Seidel-Morgenstern, *Cryst. Growth Des.*, 2011, **11**, 240–246.
- 43 Z. Szeleczky, P. Bagi, E. Pálovics, F. Faigl and E. Fogassy, *J. Chem. Res.*, 2016, **40**, 21–25.
- 44 X.-H. Pham, J.-M. Kim, S.-M. Chang, I. Kim and W.-S. Kim, *J. Mol. Catal. B: Enzym.*, 2009, **60**, 87–92.
- 45 K. Kodama, K. Kawasaki, M. Yi, K. Tsukamoto, H. Shitara and T. Hirose, *Cryst. Growth Des.*, 2019, **19**, 7153–7159.
- 46 K. Kodama, H. Shitara and T. Hirose, *Cryst. Growth Des.*, 2014, **14**, 3549–3556.
- 47 H. Shitara, T. Shintani, K. Kodama and T. Hirose, *J. Org. Chem.*, 2013, **78**, 9309–9316.
- 48 J. Wang and Y. Peng, *Molecules*, 2021, **26**(18), 5536.
- 49 X. Buol, C. Caro Garrido, K. Robeyns, N. Tumanov, L. Collard, J. Wouters and T. Leyssens, *Cryst. Growth Des.*, 2020, **20**, 7979–7988.
- 50 Z. Szeleczky, P. Bagi, E. Pálovics and E. Fogassy, *Tetrahedron: Asymmetry*, 2014, **25**, 1095–1099.
- 51 D. Li, Z. Zeng, J. Yang, P. Wang, L. Jiang, J. Feng and C. Yang, *Biosci., Biotechnol., Biochem.*, 2013, **77**, 1236–1239.
- 52 W. J. Choi, K. Y. Lee, S. H. Kang and S. B. Lee, *Sep. Purif. Technol.*, 2007, **53**, 178–182.
- 53 N. Kaftzik, *J. Mol. Catal. A: Chem.*, 2004, **214**, 107–112.
- 54 K. Wrzosek, M. A. G. Rivera, K. Bettenbrock and A. Seidel-Morgenstern, *Biotechnol. J.*, 2016, **11**, 453–463.
- 55 K. Wrzosek, I. Harriehausen and A. Seidel-Morgenstern, *Org. Process Res. Dev.*, 2018, **22**, 1761–1771.
- 56 I. Harriehausen, K. Wrzosek, H. Lorenz and A. Seidel-Morgenstern, *Adsorption*, 2020, **26**, 1199–1213.
- 57 M. Pogorevc, H. Stecher and K. Faber, *Biotechnol. Lett.*, 2002, **24**, 857–860.
- 58 A. Narmandakh and S. L. Bearne, *Protein Expression Purif.*, 2010, **69**, 39–46.



## Ehrenerklärung

Ich versichere hiermit, dass ich die vorliegende Arbeit vollständig ohne unzulässige Hilfe Dritter und ohne Benutzung anderer als der angegebenen Hilfsmittel angefertigt habe.

Alle verwendeten fremden und eigenen Quellen sind als solche kenntlich gemacht und im Falle einer Ko-Autorenschaft, insbesondere im Rahmen einer kumulativen Dissertation, ist der Eigenanteil richtig und vollständig ausgewiesen. Insbesondere habe ich nicht die Hilfe einer kommerziellen Promotionsberaterin/eines kommerziellen Promotionsberaters in Anspruch genommen. Dritte haben von mir weder unmittelbar noch mittelbar geldwerte Leistungen für Arbeiten erhalten, die im Zusammenhang mit dem Inhalt der vorgelegten Dissertation stehen. Ich habe bei der Anfertigung der vorliegenden Arbeit keine KI-basierte Tools verwendet.

Ich habe insbesondere nicht wissentlich:

- Ergebnisse erfunden oder widersprüchliche Ergebnisse verschwiegen,
- statistische Verfahren absichtlich missbraucht, um Daten in ungerechtfertigter Weise zu interpretieren,
- fremde Ergebnisse oder Veröffentlichungen plagiiert,
- fremde Forschungsergebnisse verzerrt wiedergegeben.

Mir ist bekannt, dass Verstöße gegen das Urheberrecht Unterlassungs- und Schadensersatzansprüche der Urheberin/des Urhebers sowie eine strafrechtliche Ahndung durch die Strafverfolgungsbehörden begründen können.

Ich erkläre mich damit einverstanden, dass die Dissertation ggf. mit Mitteln der elektronischen Datenverarbeitung auf Plagiate überprüft werden kann.

Die Arbeit wurde bisher weder im Inland noch im Ausland in gleicher oder ähnlicher Form als Dissertation eingereicht und ist als Ganzes auch noch nicht veröffentlicht.

Magdeburg, den 26.02.2025

Feodor Belov

## Declaration of Honor

I hereby declare that I produced this thesis without prohibited external assistance and that none other than the listed references and tools have been used.

In the case of co-authorship, especially in the context of a cumulative dissertation, the own contribution is correctly and completely stated. I did not make use of any commercial consultant concerning graduation. A third party did not receive any nonmonetary perquisites neither directly nor indirectly for activities which are connected with the contents of the presented thesis. All sources of information are clearly marked, including my own publications. I did not use AI-based tools during the work on this thesis.

In particular I have not consciously:

- Fabricated data or rejected undesired results
- Misused statistical methods with the aim of drawing other conclusions than those warranted by the available data
- Plagiarized data or publications
- Presented the results of other researchers in a distorted way

I do know that violations of copyright may lead to injunction and damage claims of the author and also to prosecution by the law enforcement authorities.

I hereby agree that the thesis may need to be reviewed with an electronic data processing for plagiarism.

This work has not yet been submitted as a doctoral thesis in the same or a similar form in Germany or in any other country. It has not yet been published as a whole.

Magdeburg, 26.02.2025

Feodor Belov